



<https://theses.gla.ac.uk/>

Theses Digitisation:

<https://www.gla.ac.uk/myglasgow/research/enlighten/theses/digitisation/>

This is a digitised version of the original print thesis.

Copyright and moral rights for this work are retained by the author

A copy can be downloaded for personal non-commercial research or study, without prior permission or charge

This work cannot be reproduced or quoted extensively from without first obtaining permission in writing from the author

The content must not be changed in any way or sold commercially in any format or medium without the formal permission of the author

When referring to this work, full bibliographic details including the author, title, awarding institution and date of the thesis must be given

Enlighten: Theses

<https://theses.gla.ac.uk/>
research-enlighten@glasgow.ac.uk

VOLUME I

MICROSTRUCTURE OF METALLURGICAL COKES

BY

MARTIN JOHN FRANCIS SHEVLIN

being a thesis submitted for the degree of Doctor of
Philosophy in the Chemistry Department of the University of
Glasgow.

MAY 1987

VOLUME I Text & Figures

VOLUME II Plates

© MARTIN J.F. SHEVLIN 28th MAY 1987

ProQuest Number: 10995569

All rights reserved

INFORMATION TO ALL USERS

The quality of this reproduction is dependent upon the quality of the copy submitted.

In the unlikely event that the author did not send a complete manuscript and there are missing pages, these will be noted. Also, if material had to be removed, a note will indicate the deletion.



ProQuest 10995569

Published by ProQuest LLC (2018). Copyright of the Dissertation is held by the Author.

All rights reserved.

This work is protected against unauthorized copying under Title 17, United States Code
Microform Edition © ProQuest LLC.

ProQuest LLC.
789 East Eisenhower Parkway
P.O. Box 1346
Ann Arbor, MI 48106 – 1346

CONTENTS

	<u>Page</u>
Summary	(i)
<u>Chapter 1</u> INTRODUCTION	1
1.1 Formation of Metallurgical Coke	1
1.1.1 Carbonisation	1
1.1.2 Industrial Carbonisation	3
1.2 Factors Affecting Coke Quality	11
1.2.1 Coal Type	11
1.2.2 Coal Blending	17
1.2.3 Precharging Treatments	19
1.3 Coke and the Blast Furnace	21
1.4 Coke Quality Analysis	24
1.4.1 Assessment of Coke Strength	24
1.4.2 Porosity	29
1.4.3 Coke Reactivity Assessment	35
1.4.4 Chemical Analysis	38
1.5 Graphite Structure	41
1.5.1 Ideal Lattice	41
1.5.2 Non-ideal Crystal Structure	43
1.5.3 Electronic Structure of Graphite	45
1.6 Coke Structure	46
1.6.1 Structure of Disordered Carbons	46
1.7 Graphitisation	53
1.8 Alkali Interactions	56
1.8.1 Catalytic Gasification	60

	<u>Page</u>
1.8.2 Intercalation Compounds	82
1.9 Aim of the Present Work	100
<u>Chapter 2</u> ELECTRON MICROSCOPY	103
2.1 History and Development	103
2.2 Electron Scattering by the Specimen	105
2.3 Contrast Transfer and Retrieval of High Resolution Information	108
2.4 Limitations to Retrieval of High Resolution Information	118
2.4.1 Astigmatism	118
2.4.2 Specimen Contamination	119
2.4.3 Specimen Stability	120
2.4.4 Mechanical Stability	121
2.5 Optical Processing	121
2.6 Electron Diffraction	122
2.7 Special Operational Modes	127
2.7.1 Dark Field	127
2.7.2 Tilted Bright Field	128
2.7.3 High Voltage Microscopy	128
2.8 Scanning Electron Microscopy	130
2.8.1 Electron Emmission from Solids	130
2.8.2 Principle of Scanning Electron Microscopy	130

<u>Chapter 3</u>	EXPERIMENTAL	134
3.1	Materials	134
3.1.1	Coke	134
3.1.2	Gases	135
3.1.3	Reagents	135
3.2	Sample Preparation	135
3.2.1	Sample Preparation for TEM	136
3.2.2	Sample Preparation for SEM	137
3.3	Energy Dispersive X-ray Analysis	138
3.4	Preparation of Holey Carbon Films	139
3.5	Sample Preparation for XRD	140
3.6	Sample Preparation for TGA	141
3.7	Furnace Construction	142
3.8	Furnace Operation	143
3.9	Effects of Inert Carrier Gases	146
3.10	Structural Changes Effected by Heating	147
3.10.1	High Temperature Treatment	147
3.10.2	Reaction of Feed Cokes at Below Carbonisation Temperature	147
3.11	Infrared Analysis	148
3.12	Density	149
3.13	Temperature Programmed Reduction	149
3.14	Detection of Potassium Penetration	150
3.15	Graphite / Potassium Reactions	152
3.15.1	Graphite / Metal Reactions	152
3.15.2	Graphite / Potassium Carbonate Reactions	153
3.16	Microporous Structure Determinations	154

	<u>Page</u>
<u>Chapter 4</u> RESULTS	155
4.1 Analysis of Feed Cokes	159
4.2 Analysis of Ex-tuyere Cokes	164
4.3 Graphite / Potassium Reactions	169
4.4 Analysis of Reacted Feed Coke Samples	170
4.(a) Microporous Structure of Cokes	177
4.5 Effect of Temperature on Coke Structure	177
4.6 Reaction of Feed Cokes Below Carbonisation Temperature	183
4.7 Analysis of Reacted Ex-tuyere Cokes	190
4.8 Effects of Inert Carrier Gases	194
 <u>Chapter 5</u> DISCUSSION	 197
5.1 Macrostructure of Cokes	197
5.2 Energy Dispersive X-ray Analysis	200
5.3 Chemical Analysis	205
5.4 Penetration of Potassium	217
5.5 Transmission Electron Microscopy	218
5.6 Microstructural Analysis of Feed Cokes	219
5.7 Microstructural Analysis of Ex-tuyere Cokes	223
5.7.1 Intercalated Potassium	225
5.7.2 Structural Ordering	230
5.8 Microstructural Analysis of Reacted Feed Cokes	234
5.9 Effect of Temperature on Feed Cokes	237
5.10 Ex-tuyere Cokes Reacted with Potassium Vapour	239

	<u>Page</u>
5.12 General Discussion	241
Future Work	245
Conclusions	248
References	250
List of Tables	
List of Figures	
List of Plates	

ACKNOWLEDGEMENTS

I would like to thank my supervisors, Dr. Tom Baird and Dr. John Fryer, for their help and guidance throughout my degree studies.

I would also like to thank the many members of the electron microscopy section, past and present, for their inspirational discussions and in particular David Thom for his valuable technical assistance.

Last but certainly not least I wish to thank my family for their moral support during the writing of this thesis and my fiancée, Angela, who uncomplainingly proof read and assisted with the production of this manuscript.

I also acknowledge the financial support given to me by the National Coal Board (British Coal) and also for providing industrial samples for analysis along with relevant data pertaining to these samples.

SUMMARY

Coke ovens are the second largest consumer of coal in Britain today, accounting for around ten percent of the UK's yearly coal output. Iron and steel making are the main users of coke (metallurgical coke), where it is of major importance in the production of millions of tons of steel per annum.

It is generally accepted that coke fulfills three roles in the blast furnace. It provides a source of reducing gas, vital for the high temperature stages of iron oxide reduction. Second, it is the main source of heat in the furnace, to melt the iron and slag materials. Finally, it provides a matrix of permeable material, particularly in the lower regions of the furnace where it is the only solid constituent present, through which the gases may ascend and the molten materials percolate to hearth. The performance of coke in this third role is of vital importance in determining the output and fuel efficiency of the furnace. A lack of permeability will restrict blowing rates, lead to poor gas distribution within the shaft and will cause a considerable pressure drop within the furnace. The breakdown of coke, in the blast furnace, reduces the mean size and also decreases the voidage by altering the size distribution of the material. The present research has therefore been targeted at investigating the factors influencing the breakdown of metallurgical coke.

Conditions in modern blast furnaces subject coke to severe

chemical, thermal and mechanical stresses. In this context, it is believed that recirculating alkali vapour (in particular potassium) is a major influence in the degradation of metallurgical coke lumps.

The microstructure of metallurgical cokes has been investigated using high resolution electron microscopy (HREM) and complementary techniques. The object of the study was to evaluate the role of recirculating alkali, present in blast furnaces, in the weakening and subsequent degradation of the coke. It is shown that the feed coke's microstructure (cokes charged to the furnace) markedly differs from samples removed from the high temperature regions of the furnace (ex-tuyere cokes). The feed cokes exhibited a turbostratic structure of short range order, whereas the ex-tuyere cokes show two distinct, additional microstructural species, viz. an intercalated material, retaining the turbostratic disorder and an extensively ordered carbon structure. It has also been found that the nature and distribution of the mineral matter, inherent in metallurgical cokes, is that of randomly dispersed aluminosilicates. Successful replication of the ex-tuyere microstructural forms has been achieved by reaction of the feed cokes, with potassium carbonate, in laboratory experiments.

It has been shown that both potassium vapour and thermal treatment cause localised ordering of the carbon structure. However, the greatest amount of structural ordering occurs in the cokes when these two major influencing factors are

combined. It is postulated that the intercalated material formed is an intermediate in the changes in coke structure, from a turbostratic structure to a more ordered arrangement of the carbon layers. The observed structural changes appear to be independent of the inert carrier gas employed in the laboratory reaction of feed coke samples.

It is believed that the mechanical weakening of metallurgical coke arises primarily from changes occurring at the molecular level which consequently alter the macrostructure of the material, leading to a decrease in the lump strength of metallurgical coke.

INTRODUCTION

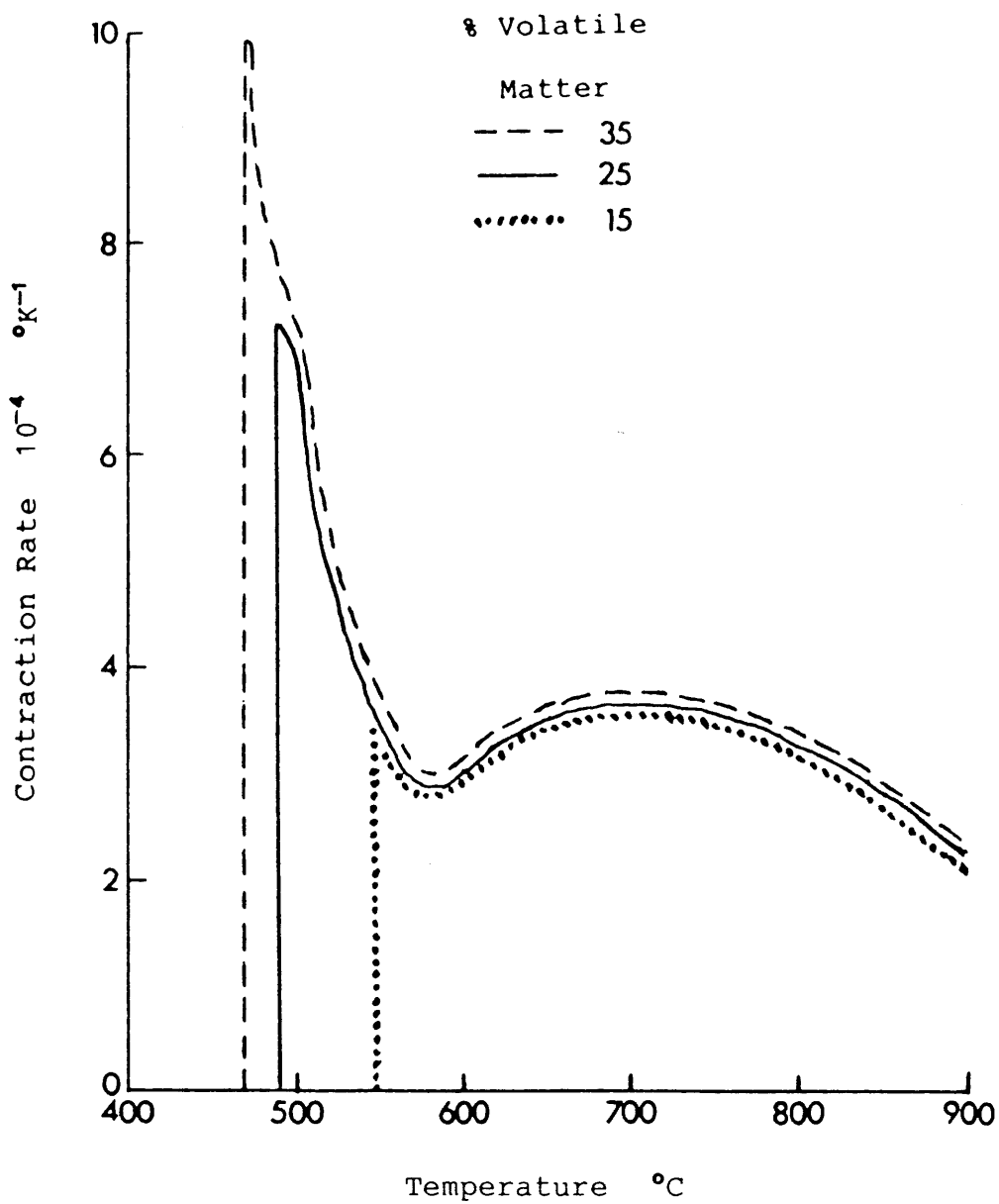
1.1 Formation of Metallurgical Coke

1.1.1 Carbonisation

Carbonisation is a process of formation of carbon from organic material by pyrolysis. Pure carbon is obtained at temperatures of around 1600°C . Higher temperatures do not increase purity but cause crystal ordering to graphite or near graphite structures (Oberlin, 1975 (a)).

Coal carbonisation involves the heating of the material in the absence of air, resulting in the removal of volatile matter. These volatiles are higher in hydrogen content than the feed coal units, from which they are composed, and consequently the coal's carbon content is increased.

Analysis of coke formation using dilatometry methods shows an initial volume loss (fig. 1) in the region of $300 - 400^{\circ}\text{C}$. This is caused by compaction of the coal as it starts to become plastic (Grainger and Gibson, 1981). However, in the temperature region $400 - 475^{\circ}\text{C}$ a large increase in the volume occurs due to the release of volatile matter. The temperature and degree of swelling is very much dependent on the nature and volume of the volatiles released, as does the porosity of the formed coke. Further heating above 500°C results in a decrease in the volume, as the loss of volatile matter is accommodated (Grainger and Gibson, 1981).



Variation of Contraction Rates
with Temperature

FIGURE 1

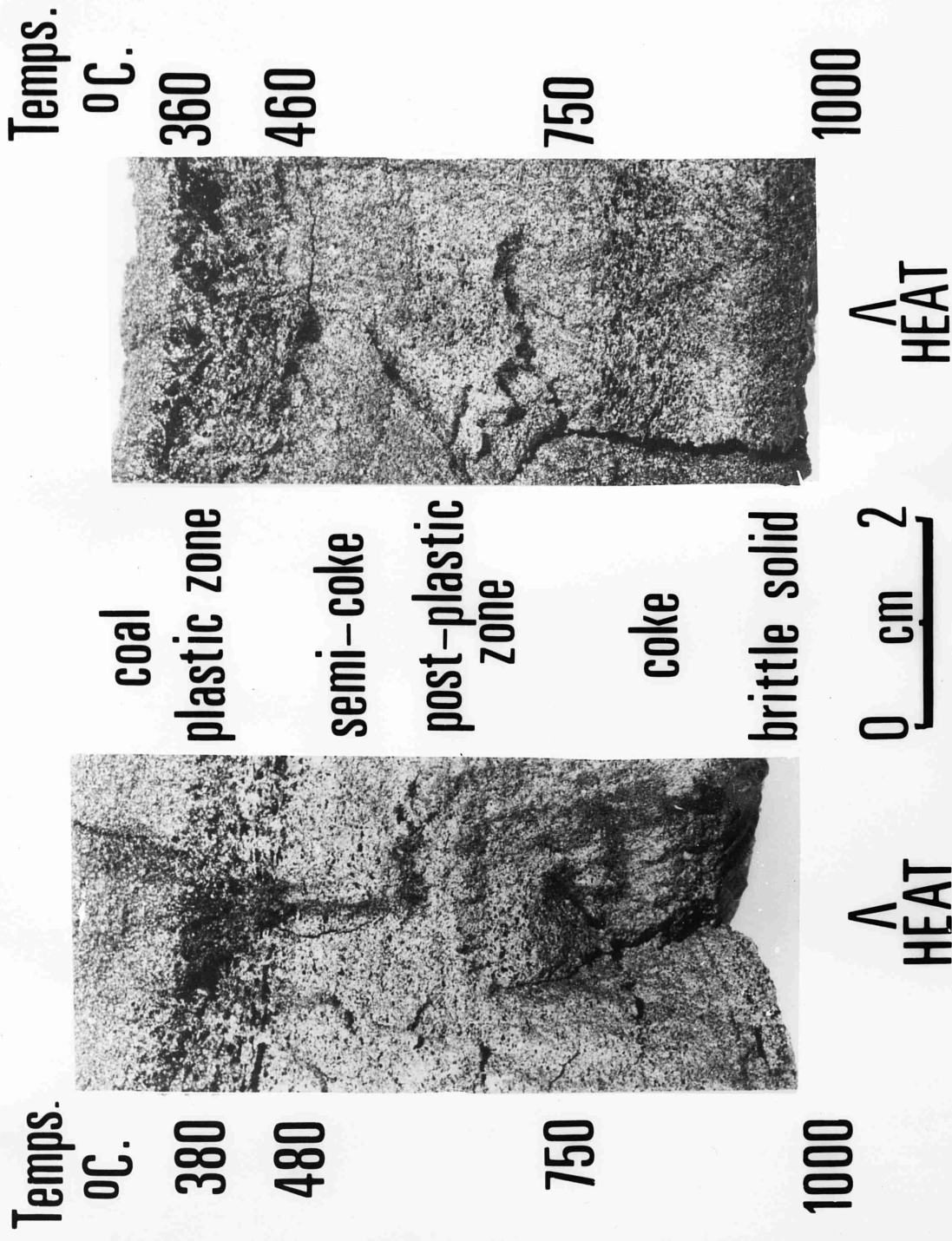
Contraction first occurs around 500°C and this is attributable to a continued loss of mass soon after resolidification. At 700°C further contraction occurs due to ordering of the carbon structure, with a corresponding increase in the density of the coke. It has been shown (Gibson, 1979) that only the first contraction is sensitive to volatile matter content and that the increase in density from the second contraction is associated with an increase in the mean atomic weight of the coke, caused by the loss of hydrogen atoms. The process of carbonisation is summarised in plate 1.

Carbonisation chemistry is extremely complex, indeed Marsh and Walker (1979) stated that "...it is not possible to ever know in detail, the chemistry of all the pyrolytic reactions of carbonisation". However, the general reaction scheme, of polymerisation (Lewis, 1982), has been identified. Carbonisation is believed to take place via a free radical condensation mechanism (Grainger and Gibson, 1981). As the coal is heated cross linkages in the reactive component, vitrinite, are broken (fig. 2). These linkages between aromatic groups can further break down (van Krevelen (1961); Fitzer et al., 1984) to give rise to gaseous products such as methane and other hydrocarbons of low molecular weight (the volatile matter) together with the complex mixtures of organic material found in coal tar (e.g. Phenols, Xylenols and Naphthalenes). The remaining heavier units then form semi-coke on resolidification. Hydrogen is the major gaseous product in the condensation of the larger units; its formation and removal, and the

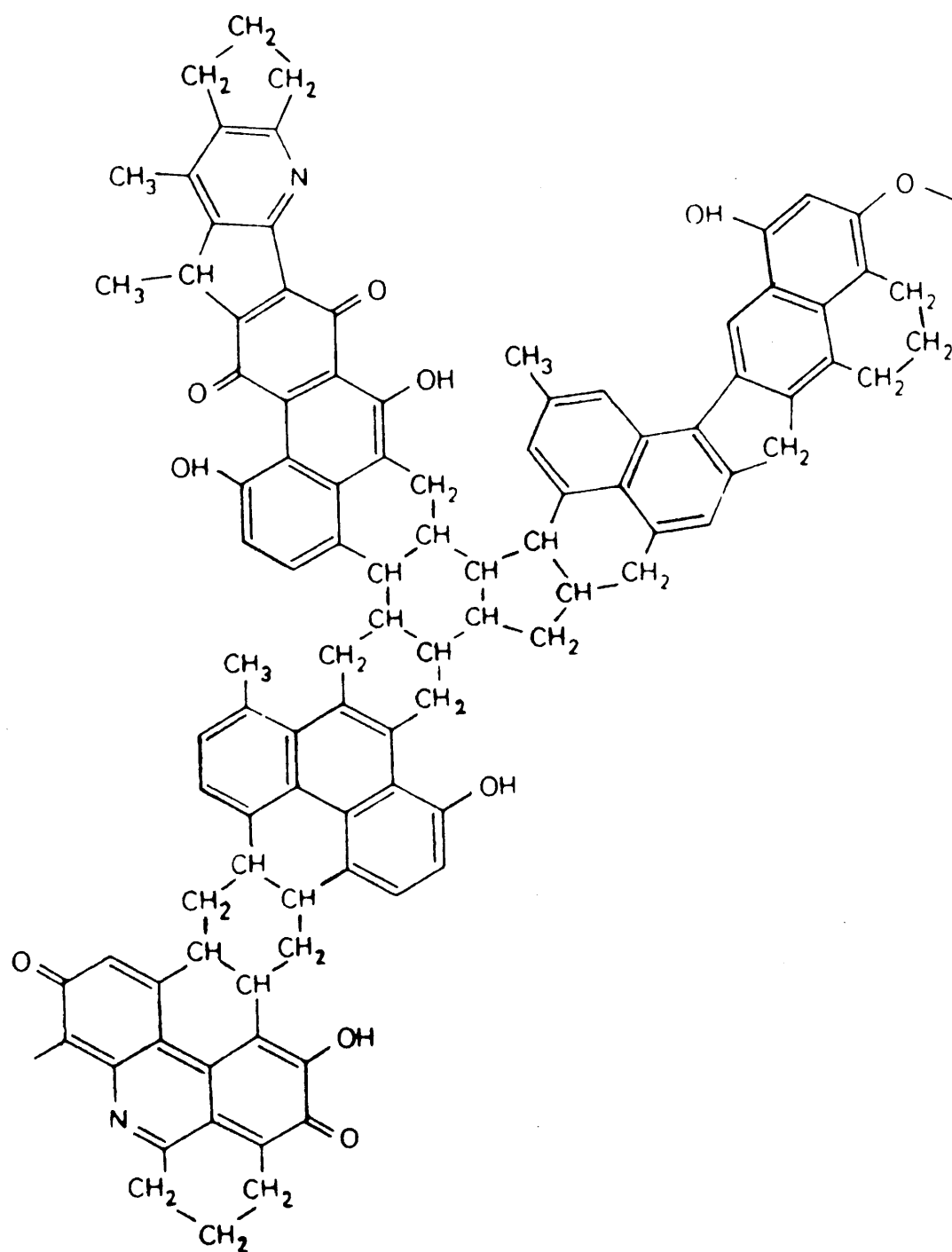
PLATE 1

"From Coal to Coke"

The process of carbonisation.



Sequence of phase changes in conversion of coal to coke



Proposed Model of an 82 % Carbon Vitrinite

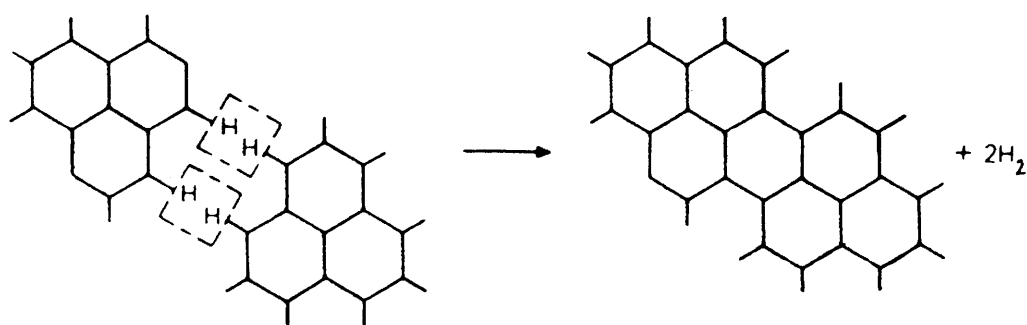
subsequent condensation of neighbouring aromatic units is outlined in fig. 3.

1.1.2 Industrial Carbonisation

1.1.2 (a) History and Development

Early methods of coal carbonisation were extremely primitive (King, 1948; Finney and Mitchell, 1961; Barritt and Robinson, 1961). These methods evolved from those used in the production of charcoal- the reducing agent and heat source which coke was replacing in the iron and steel industry. Essentially coking coal was piled in an open yard and ignited using wood or burning coal. Once coking had been initiated the coal mass was covered with earth, wet coke dust and leaves, with crude flue arrangements to aid burning, and left until the coking process was complete. After a period of five to eight days, depending on the weather, small amounts of water were poured down the flues to stop the coking process. This was known as pile or "open air" coking.

This highly inefficient method of coke production was subsequently replaced by the beehive oven, which developed in the mid 19th century and persisted well into the 20th century (Bennit, 1939). The beehive oven was essentially a brick structure in which the coal was charged through the top and levelled off through the side door. Holes in the side door provided air so that the combustion took place from the top of the charge downwards as opposed to the



Hypothetical Condensation Process

FIGURE 3

"open air" method in which the reverse was the case.

There are two main consequences of coke production by the pyrolysis of coal. First, the creation of a strong porous material, with a high calorific power, for use in the iron and steel industry and second the production of vast amounts of volatile organic materials which have a variety of uses. The former is the major economic factor in modern-day coke production, but around the start of the 20th century the latter was the more profitable side of the industry.

The beehive oven, whilst an improvement on the "open air" furnace, was still highly inefficient. These ovens lost all the volatile matter present in the coal. Also lost was the heat energy present in the unburned portions of this volatile material as well as the heat which these gases themselves contained. Thus it was these financial losses which led to the development of the waste - heat - recovery beehive oven around the turn of the 19th century. These ovens incorporated a waste heat flue, supplied by a duct adjacent to the charging hole, which carried the hot gases to a waste-heat boiler.

However, this design of oven generated its own type of problems. Only high grade coking-coals could be used, leaving behind coals of inferior quality. Inventors, constantly striving to make improvements in the process, added flues vertically adjacent to the ovens. The hot gases driven off were mixed with air and combustion took

place in the flues. Thus heat was supplied to the coal mass through the oven walls instead of directly from a burning flame. This more efficient method of coking was termed "by-product coking" and has been developed from its basics to modern-day coking practices in large slot ovens.

1.1.2 (b) Modern-day Coking Practice

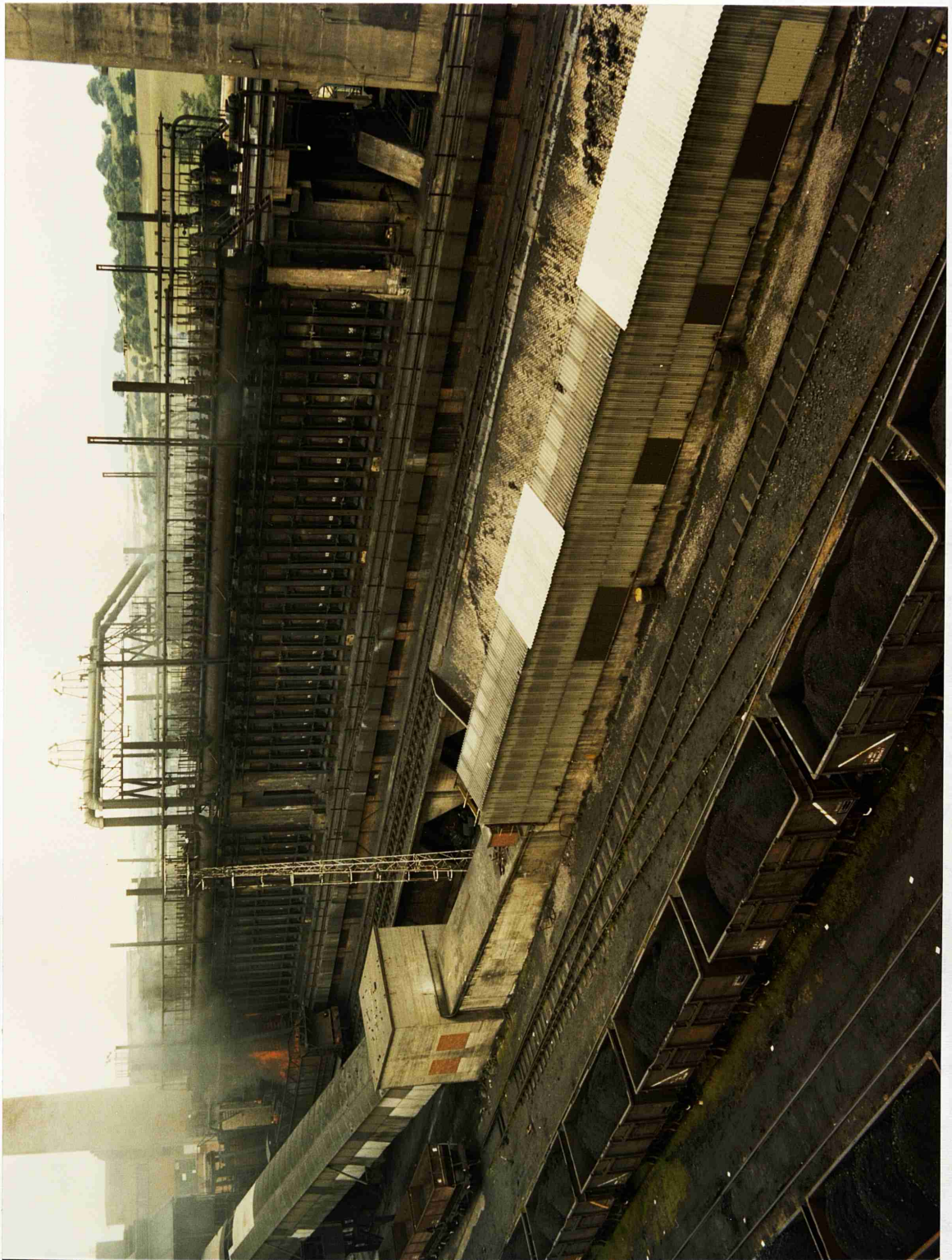
Large scale coking in a modern-day plant requires the successful integration of several processes (fig. 4) in order for the plant to function efficiently and be economically viable (Denig, 1945). Coal selection, blending, pretreatment and coking process all combine to determine the characteristics of the coke produced.

Once suitable coals have been selected they are shipped to the coke works where the first process is to pulverise them into pieces of less than one inch in size. This is usually done using jaw crushers and swing hammer mills, and is necessary to obtain maximum bulk density of the coal. Some plants pulverise to a greater extent than this, in order to achieve better weight of coal per cubic foot, better mixing and better overall quality, but this can also lead to a greater amount of coke dust being carried out of the coke oven and settling in the coal tar.

Once pulverised the coal is transferred to large blending bunkers, each bin containing a specific crushed coal. Gravity feeding is used to mix the coals (in predetermined proportions) on moving belts. These belts convey the

FIGURE 4

Essential Units Comprising a Modern Coking Plant

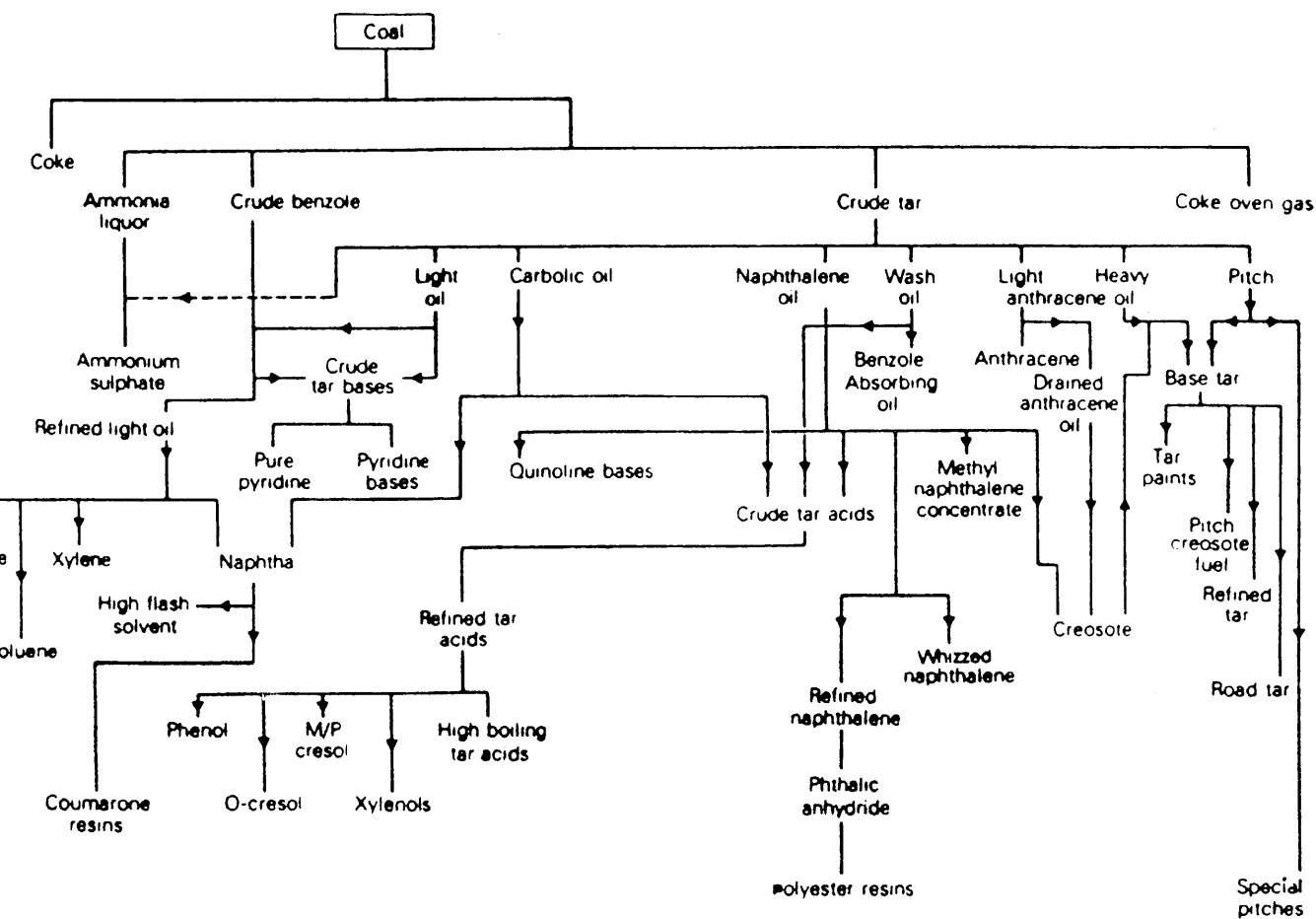


charging, help level the coal and prevent localised packing. Once charging has been completed the pusher machine is aligned with the oven and a leveller-bar is inserted through an opening in the door. The leveller-bar pushes and pulls the coal along the length of the oven until an even charge is obtained. The leveller-bar is then removed, the charging hole lids replaced and the oven is connected to the gas collecting main, which carries the gases produced to the by-product house.

The coking process begins as soon as the coal is charged to the oven. Production of volatile matter continues until almost all has been expelled- in practice up to three per cent is left in the coke, as pushed, in order to gain the maximum metallurgical value from the product.

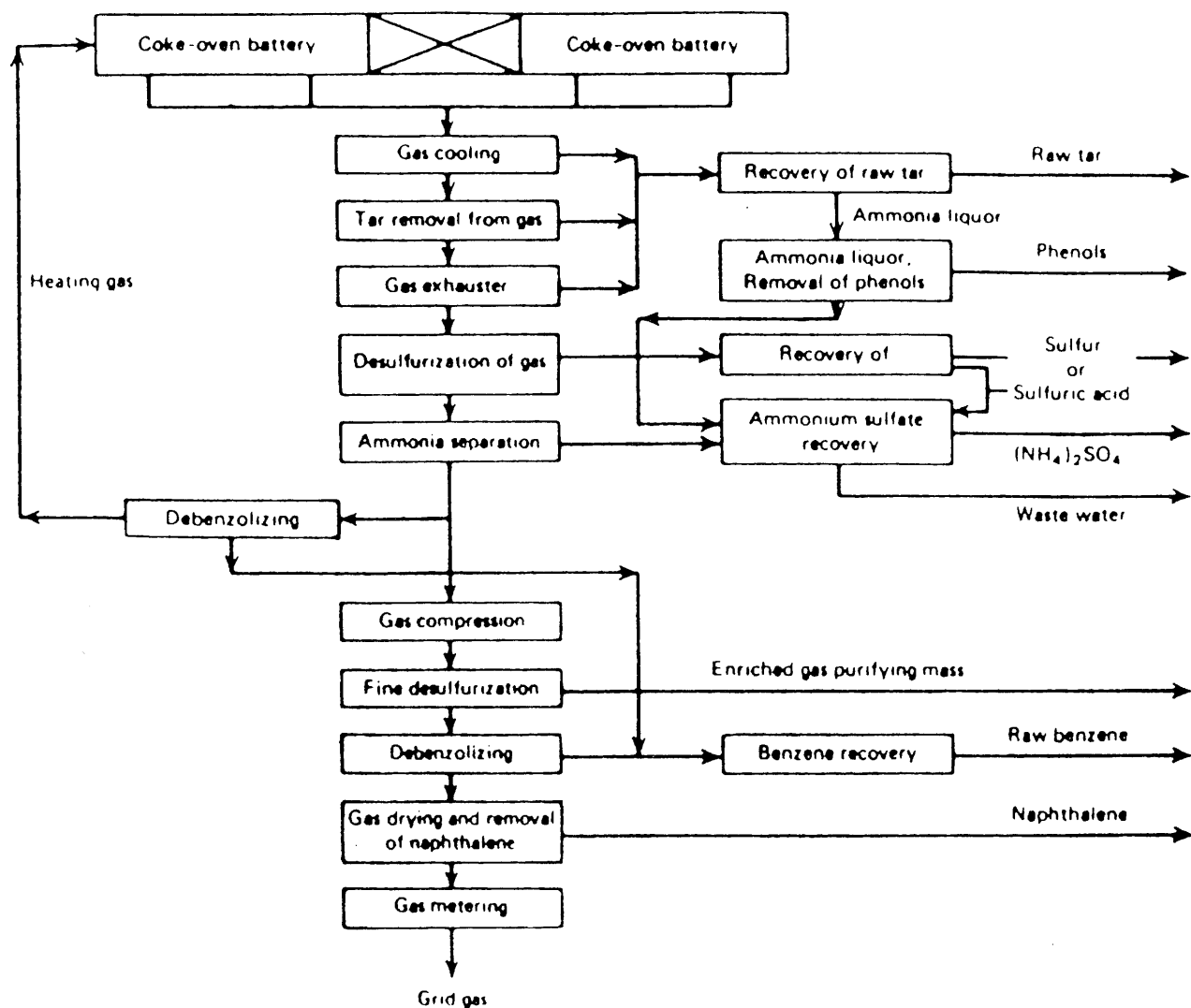
The volatile matter is passed- via the collecting main- to the by-product house. Here the gases are stripped by condensers and scrubbers of all useful components (e.g. ammonia and tar) and returned to the ovens to be burned, to supply the heat required for carbonisation. The useful components from the gases are processed on the coking plant to give products such as ammonium sulphate fertiliser, tar pitch and sulphuric acid among many others (figs. 5 and 6).

The coke oven gas and air enter their respective regenerators at the same time. After passage through the regenerator system (where the air is preheated) the gas and air combine at the bottom of vertical flues. Combustion commences here and the design of the flues is such that the



Compounds taken from the by-products of coal carbonisation

FIGURE 5



Flow Diagram of the Treatment of Coke-Oven Gas.

gas and air combine with a streamline effect, so that combustion of the gas is distributed throughout the entire length of the flues, thus giving even heating of the ovens. Combustion products are collected from the vertical flues and carried over the top of the oven by means of crossover flues. From these crossover flues the waste gases pass down the vertical flues on the other side of the oven, directly opposite those in which they have been produced. The waste gases then pass into regenerators, where they transfer their heat.

Upon reversal of the valves, which is automatically controlled and occurs at around thirty minute intervals, the coke oven gas and air travel up, through the regenerators which the waste gases have previously passed, to the combustion point at the vertical flues above. This alternating cycle is continued throughout the carbonisation period, thus keeping the oven walls at the temperatures required for coking. To compensate for the increased oven width, on the side from which the coke emerges, the gas and air ports are varied in width throughout the oven. This gradation of port width ensures that the whole of the oven charge is equally carbonised.

Carbonisation times vary, depending on the nature of the coal and the quality of the coke required, but are normally around eighteen to thirty hours. The centre of the charge reaches 900 - 950°C within a period of about twelve to fourteen hours and remains at this temperature for the remainder of the carbonisation period (plate 3).

Once a sufficient degree of carbonisation has been achieved the coke mass is ready for removal from the oven, this is known as "pushing" the oven. On the pusher side the pushing machine (which can travel the entire length of a battery) is aligned with the designated oven. At the same time the coke guide machine is aligned with the oven on the coke side. Both machines then remove their respective oven doors and the coke guide is placed in front of the oven. The guide has a steel framework with strips of steel three to four inches apart, to prevent warping, and can also travel the whole length of the battery. Once the guide is in place, the pusher starts to remove the formed coke. The pusher is essentially a ram, the head of which has roughly the same cross-sectional area as that of the oven door. Attached to the head is a steel beam which is racked forward into the oven such that the coke is removed horizontally from the oven. The hot coke emerges on the coke side and is directed into a steel collecting car by the coke guide (plate 4).

Ovens are charged and pushed in series. If adjacent ovens were pushed the drop in temperature of the intermediate heating wall would be severe. The temperatures of the oven walls must not drop sharply or else they would crack and the oven would have to be shut down for repair. As every oven supplies heat to the adjacent ovens these too would be affected by the shut down and thus the plant's effective output would be drastically altered. Such temperature drops are avoided by using well defined pushing schedules. The most frequently used is the cycle developed by Koppers

PLATE 3

Coke Oven During Carbonisation.

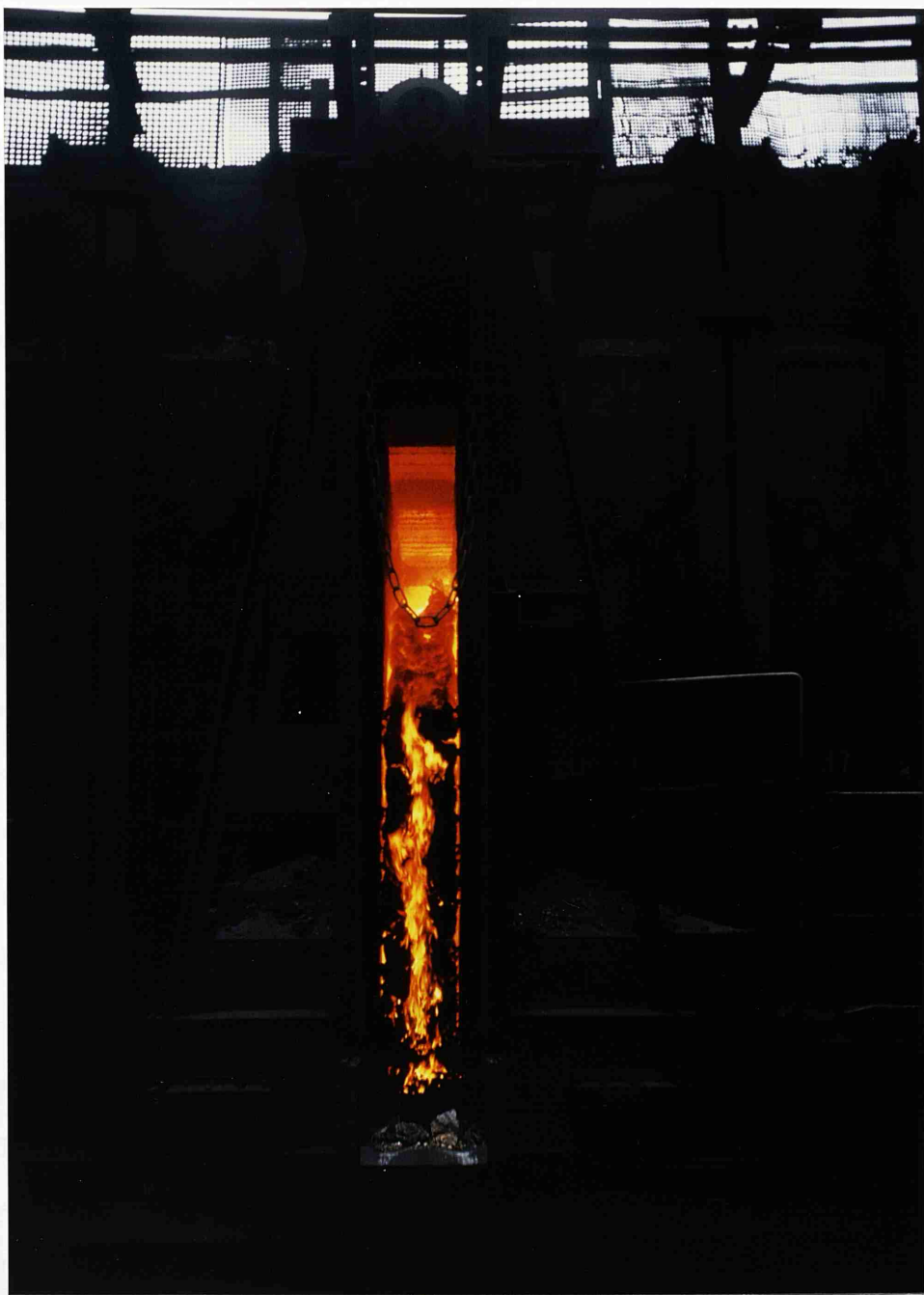


PLATE 4

Pushing Hot Coke from the Coke Oven.

(Doris, 1949). Marguard (1919) proposed a mathematical model for a pushing cycle, but many operators use their own methods. All pushing schedules though have the same basic principles behind them; (a) to maintain uniform



(Denig, 1945). Marquard (1919) proposed a mathematical model for a pushing cycle, but many operators use their own schemes. All pushing schedules though have the same basic principles behind them; (a) to maintain uniform heats (b) to have ovens approximately the same age on either side of the oven to be pushed (c) to have the age of ovens such that any wall movement caused by the charging of mildly expanding coals would be constrained.

Having removed the coke mass from the oven the coke guide and pusher machines are removed. The doors are then replaced and the oven is once again ready to be charged. The collecting car carries the hot coke first to the quenching tower. Here around ten thousand gallons of water are sprayed on to the coke within a couple of minutes. The water sprayed is hot in order to minimise the moisture content of the coke after draining. The collecting car then carries the coke to the coke wharf, into which it is emptied.

From the coke wharf the coke is taken to the screening plant, where it is sized by a series of mechanical screens. Oversize coke is removed, transferred to the coke cutter and then returned to the screening plant, undersize coke is also removed. From the screening plant the coke is transferred to hoppers from which it is loaded for shipment.

Therefore, to summarise the essential features of this process, coal is heated to $900 - 1200^{\circ}\text{C}$ in a reducing

atmosphere, composed largely of volatile hydrocarbons present in the original coal. The duration of exposure is eighteen to thirty-six hours and the residual coke contains up to three per cent of the original volatile matter.

1.2. Factors Affecting Coke Quality

1.2.1 Coal Type

There are a large and varied number of types of coal and as such it is necessary to be able to distinguish those which are suitable for coke production from those which are not. There have been many types of classification systems applied to coal over the last century, using almost every characteristic of the material. They have been classified in a variety of ways, depending on the needs and the viewpoint of those requiring the system, and also due to the widespread occurrence and variety of coals.

The coal deposits of most interest to coke manufacturers were formed during later Paleozoic and Mesozoic time, beginning in the Carboniferous and extending through the Cretaceous Periods (Janssen, 1948; Francis, 1961). The degree of metamorphism of the plant material determines the rank (degree of coalification of the coal), whereas the original species of plant material determines the type or variety of the coal. Theisen and Sprunk (1941) showed in a summary of coal paleobotany that there are three types of plants easily recognisable in coal, namely: coniferous-like, cycadophyte or fernlike and lycopods (which were

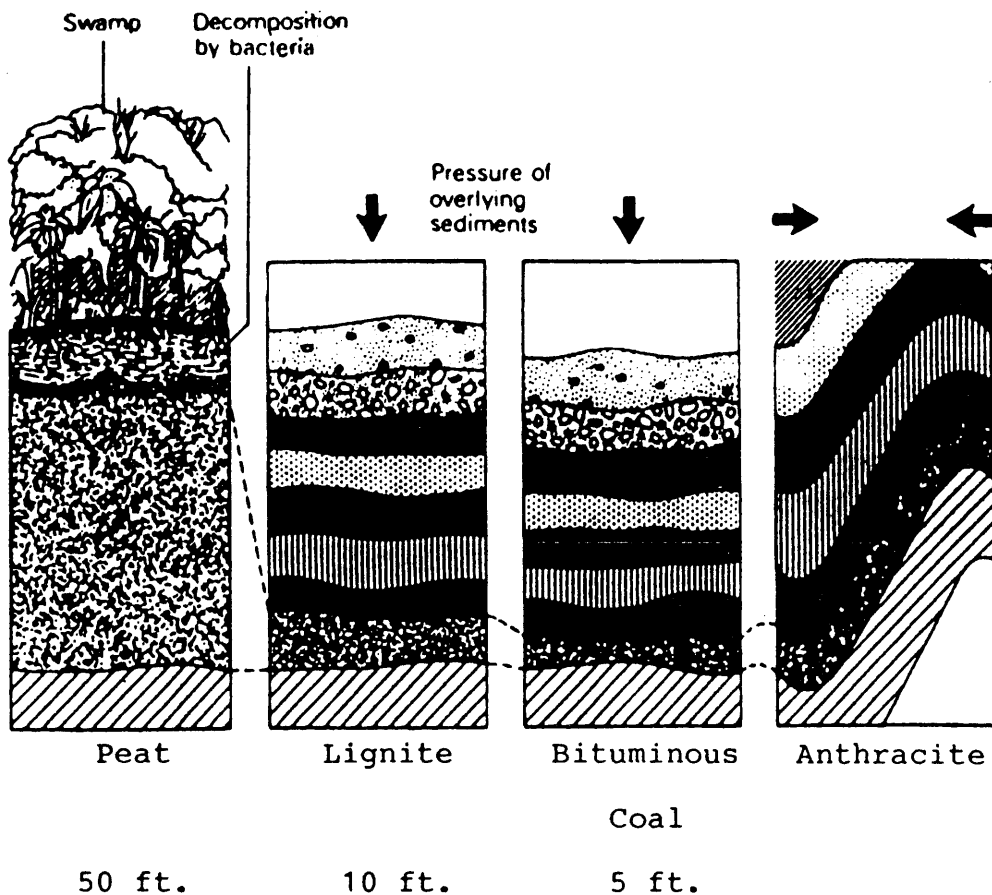
trees related to present day club mosses). These are not mixed evenly throughout the coal but are aggregated separately with usually one class of plant being predominant in a specific coal bed or layer thus giving rise to differing types of coal even within a single mine.

Geologic age is one of the oldest means of describing coal type and is always quoted in a comprehensive classification of the material.

The classification system used must, at minimum, give a general indication of rank, for example; lignite, sub-bituminous coal, bituminous coal, anthracite. As rank increases from peat to bituminous coal to anthracite, the carbon, hydrogen, oxygen and volatile matter contents alter by becoming richer in carbon, through the elimination of hydrogen, oxygen and water through the compaction of the plant material (figs. 7 (a) and (b)).

Seyler in 1899 published probably the most famous classification system, in which he used the parameters of carbon and hydrogen content or volatile matter content and calorific value in describing the material. However, this system is too complicated for most purposes and other methods of classification such as banded structure, ultimate analysis, proximate analysis (in which only some of the elements are defined), and chemical activity have been developed.

The most generally used classification system in Britain



Process of Decomposition, Subsidence and Pressure by which the Progressive Ranks of Coal are Formed, Anthracite being the Highest of all.

FIGURE 7 (a)

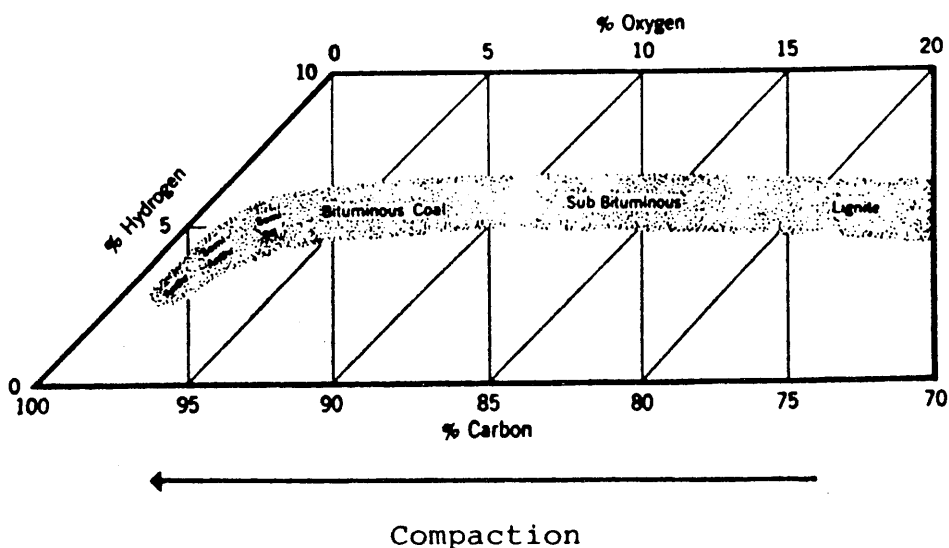


FIGURE 7 (b)

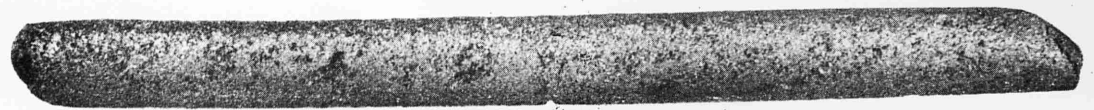
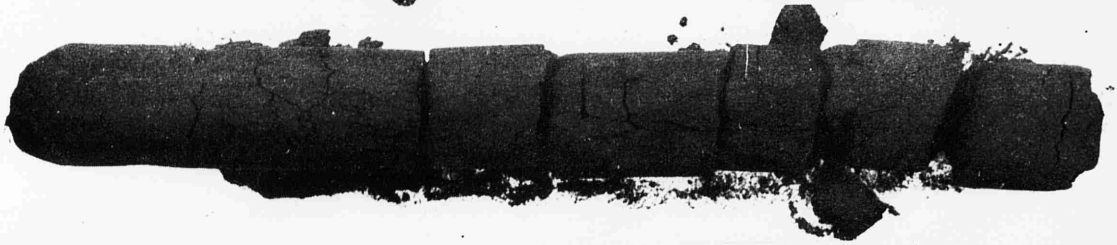
today is a relationship between the swelling properties of the coal and its volatile matter content (ASTM index is used in the USA and Vitrinite reflectance in Russia). Substantial differences in swelling properties have been recognised in samples taken from different parts of a mine or different levels vertically across a given coal seam, thus giving rise to the development of a classification system incorporating a Gray-King swelling index.

Gray-King swelling indices are measured (British Standard 1016, part 12, 1980) by heating finely divided coal to six-hundred degrees centigrade in a retort. The swelling of the coal is then measured by comparison with photographs of standard profiles (fig. 8). The letters A to G are used progressively to designate coals which vary from non-coking to those which give a strong coke of the original volume. Coals of greater swelling power than G coals are given subscripts (G1, G2, etc.) to denote the number of parts of electrode coke (inert) required to one part of the coal to reduce the swelling to the standard G level.

Volatile matter content of the coal is measured on a dry, mineral-matter-free basis. This is in order to classify coals as nearly as possible as a pure coal substance, calculated free from variable and accidental mineral impurities, with several techniques having been developed to account for ash content, sulphur and other impurities (Turner and Anderson, 1932; Fieldner, 1933; Simek et al., 1935; ASTM, 1939).

FIGURE 8

Gray-King Swelling Profiles

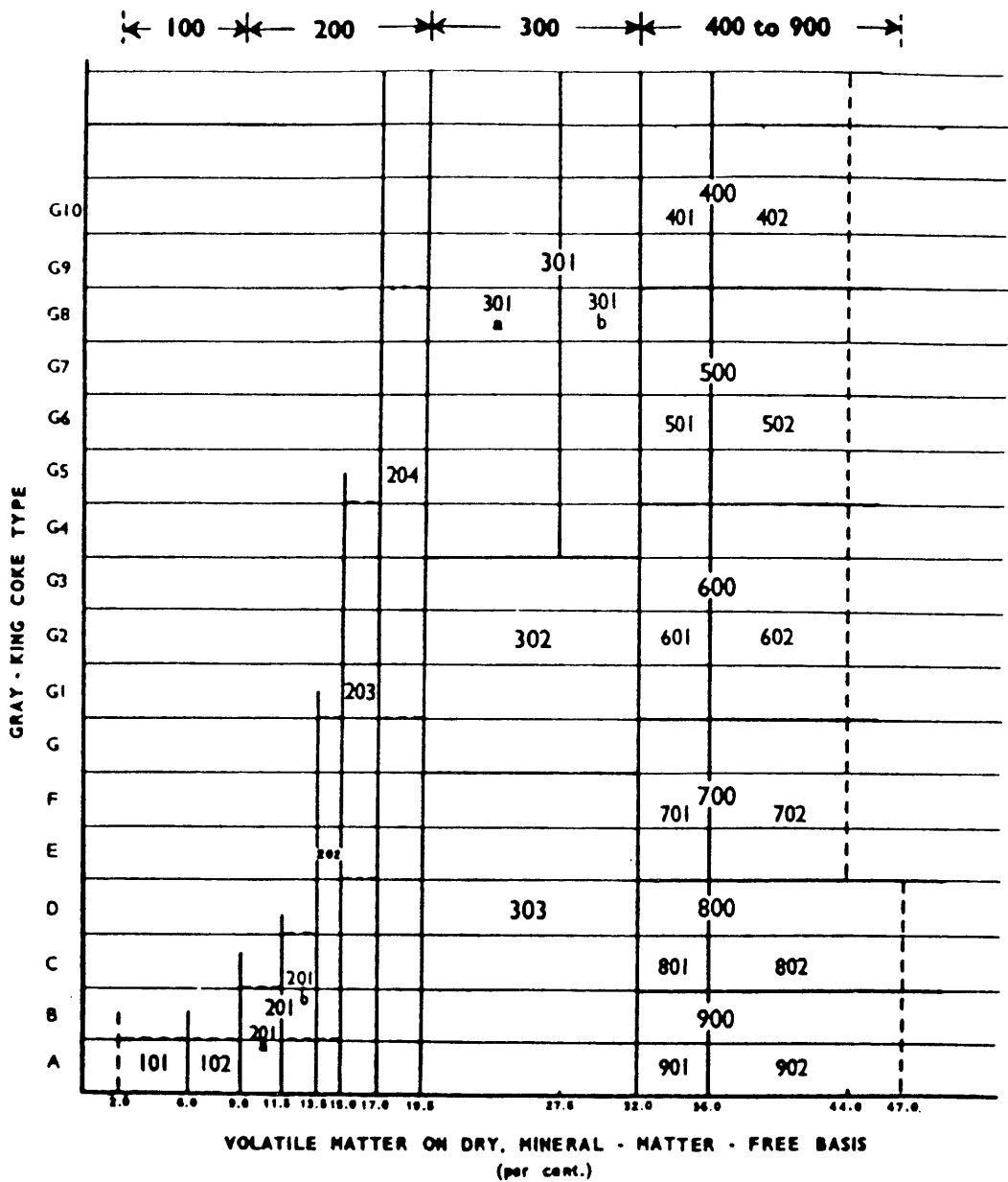


The classification system commonly used by the National Coal Board (British Coal) is shown in figures 9 and 10. However, it should be stressed that the purpose of this system is to describe the rank, or degree of coalification, of the coal substance of any coal. Other properties of the coal, as used or as sold, such as its ash or sulphur content, require to be specified additionally and should not be confused with the fundamental nature of the coal substance.

The prime coking-coals are those of rank 301a and 301b- the medium volatile bituminous coals, with a 20 - 25% volatile matter content. The coals of this rank have a greater ability to soften and swell upon heating to yield a coherent distended coke than any of the others. They also show a lower moisture content than those of higher or lower rank. The porosity and "internal surface" area is at a minimum between 15 and 25% volatile matter- which is equivalent to about 88 - 90% total carbon (King and Wilkins, 1944; Perch and Russell, 1949; Dryden, 1957; Berkowitz, 1960). Other coal properties such as hardness, strength and density exhibit a minimum in the low to medium volatile bituminous rank (Yancey and Geer, 1945; Brown and Hiorns, 1963; Tschamler and de Ruiter, 1963). Conversely the grindability index, the ease of grinding or pulverisation of the coal, passes through a maximum in this rank (Yancey and Geer, 1945; Brown and Hiorns, 1963). Structural and tectonic factors also alter the strength and friability of the coal (Stutzer and Noe, 1940; Hendricks, 1945).

COAL CLASSIFICATION SYSTEM USED BY N.C.B.

(Revision of 1964)



----- Defines a general limit as found in practice, although not a boundary for classification purposes.
———— Defines a classification boundary.

NOTES

- 1. Coals that have been affected by igneous intrusions ('heat-altered' coals) occur mainly in classes 100, 200 and 300, and when recognized should be distinguished by adding the suffix H to the coal rank code, e.g. 102H, 201bH.
- 2. Coals that have been oxidized by weathering may occur in any class, and when recognized should be distinguished by adding the suffix W to the coal rank code, e.g. 801W.

FIGURE 9

THE COAL CLASSIFICATION SYSTEM USED BY THE NATIONAL COAL BOARD

(Revision of 1964)

Coals with ash of over 10 per cent. must be cleaned before analysis for classification to give a maximum yield of coal with ash of 10 per cent. or less.

Coal Rank Code			Volatile Matter (d.m.f.) (per cent.)	Gray-King Coke Type*	General Description
Main Class(es)	Class	Sub-class			
100	101† 102†		Under 9.1 Under 6.1 6.1-9.0	A A	Anthracites
200	201	201a 201b	9.1-19.5 9.1-13.5 9.1-11.5 11.6-13.5	A-G8 A-C A-B B-C	Low-volatile steam coals
	202 203 204		13.6-15.0 15.1-17.0 17.1-19.5	B-G E-G4 G1-G8	Dry steam coals Coking steam coals
300	301	301a 301b	19.6-32.0 19.6-32.0 19.6-27.5 27.6-32.0	A-G9 and over G4 and over G4 and over	Medium-volatile coals Prime coking coals
	302		19.6-32.0	G-G3	Medium-volatile, medium-caking or weakly caking coals
	303		19.6-32.0	A-F	Medium-volatile, weakly caking to non-caking coals
400 to 900:-			Over 32.0	A-G9 and over	High-volatile coals
400	401 402		Over 32.0 32.1-36.0 Over 36.0	G9 and over G9 and over	High-volatile, very strongly caking coals
500	501 502		Over 32.0 32.1-36.0 Over 36.0	G5-G8 G5-G8	High-volatile, strongly caking coals
600	601 602		Over 32.0 32.1-36.0 Over 36.0	G1-G4 G1-G4	High-volatile, medium- caking coals
700	701 702		Over 32.0 32.1-36.0 Over 36.0	E-G E-G	High-volatile, weakly caking coals
800	801 802		Over 32.0 32.1-36.0 Over 36.0	C-D C-D	High-volatile, very weakly caking coals
900	901 902		Over 32.0 32.1-36.0 Over 36.0	A-B A-B	High-volatile, non-caking coals

*Coals with volatile matter of under 19.6 per cent. are classified by using the parameter of volatile matter alone; the Gray-King coke types quoted for these coals indicate the general ranges found in practice, and are not criteria for classification.

†In order to divide anthracites into two classes, it is sometimes convenient to use a hydrogen content of 3.35 per cent. (d.m.f.) instead of a volatile matter of 6.0 per cent. as the limiting criterion. In the original Coal Survey rank coding system the anthracites were divided into four classes (then designated 101, 102, 103 and 104). Although the present division into two classes satisfies most requirements it may sometimes be necessary to recognize more than two classes.

NOTES

1. Coals that have been affected by igneous intrusions ('heat-altered' coals) occur mainly in classes 100, 200 and 300, and when recognized should be distinguished by adding the suffix H to the coal rank code, e.g. 102H, 201bH.
2. Coals that have been oxidized by weathering may occur in any class, and when recognized should be distinguished by adding the suffix W to the coal rank code, e.g. 801W.

FIGURE 10

Generally, lower volatile coking-coals are easier to pulverise, more friable and generate more fines on grinding than the higher volatile coking-coals. Consequently steps must be taken during the coking process to achieve optimum size of pulverisation without generating excessive fines (Leonard and Clendinin, 1961; Beimann et al., 1963). Analysis has also shown that the strength of the produced coke (Russell and Perch, 1943), coking power index (Loison, et al., 1963; Kovalik et al., 1964) and fluidity (Perch and Russell, 1949) of the coke plastic stage pass through a maximum in the range of 15 to 25% volatile matter.

Thus it can be seen that virtually all the characteristics of the 301a and 301b rank coals make them ideal for use in the formation of metallurgical coke.

Another method of coal analysis, which is perhaps worth a more detailed description due to its increase in popularity (especially in determining blend formulations), is coal petrology.

Early work in this field relied on distinguishing different components (macerals) of the coal material using sections thin enough to be translucent, and a microscope using transmitted light. However, preparation of these thin sections is very laborious and can only be carried out on particles above a certain size. Modern-day coal petrology uses samples which are crushed, mounted in resin and polished, for examination by reflected light microscopy. Colour differences which show up in transmitted light are

then lost but macerals can still be identified by differences in form and reflectance.

Dr. Marie Stopes pioneered the work on reflectance in 1919 and developed her initial work into the widely used Stopes-Harleen petrology system (Rose, 1945; Harrison, 1961; Parks, 1963). Four rock types or lithotypes (coal is a rock not a mineral) were originally distinguished in banded bituminous coal- vitrain, clarain, durain and fusain- by gross observation:

Vitrain: bright, black, usually brittle, frequently with fissures.

Clarain: semi-bright, black, very finely stratified.

Durain : dull, black or grey-black, hard rough surface.

Fusain : silky lustre, black, fibrous, soft, quite friable.

The four lithotypes can be further divided into microlithotypes and maceral groups (tables 1 and 2). In addition to determining the relative amounts of each maceral in the coal, the rank of the coal can be measured by the amount of vitrinite reflectance. Vitrinite composes more than 60% of the coal and therefore is the principal species determining the rank and the coal's plastic properties. Hoffman and Jenkner (1932) used reflected light microscopy with a microphotometer to observe vitrain and concluded that the degree of reflection was directly proportional to the degree of coalification. Using polarised light, coal sections of increasing rank exhibited an increasing anisotropy. Detection of durain using

LithotypeMicrolithotype

Vitrain

Vitrite

Clarite (where $V > E$)

Durain

Clarite (where $V < E$)

Durite

Trimacerite

Fusain

Inertite (semi-fusinite
and fusinite)

Clarain

may contain elements of
any microlithotype or
maceral group

Relation of macro- and micro- structures

TABLE 1

	<u>Microlithotype</u>	<u>Maceral groups</u>
Monomaceral	Vitrite	Vitrinite / Humanite
	liptite	Exinite / Liptinite
	inertite	Inertinite
Bimaceral	Clarite	$V + E$
	Durite	$I + E$
	Vitinerite	$V + I$
Trimaceral	Duroclarite	$V > I + E$
	Clarodurite	$I > V + E$
	Vitrinertoliptite	$E > I + V$

Microlithotype and Maceral groups

TABLE 2

polarised light has also been shown to be advantageous and coal lustre to increase with decreasing volatile matter content (Zhemchuzhnikov, 1935). As with other systems for rank classification, however, other properties of the coal such as moisture, ash and sulphur content have to be stated separately.

1.2.2 Coal Blending

The shortage of prime coking-coals has led to the carbonisation of poorer quality coking-coals (marginal coals) for use in the blast furnace. The blending of marginal coals to give mixtures which behave as prime coking-coals (i.e. a strong coke of good quality) has been increasing since the mid-sixties. In the United Kingdom prime coking-coals make up only about 25% of the total coal carbonised. A large proportion of metallurgical coke is in fact produced from blends of coals containing none of the prime coking type.

The essential point in coal blending is to obtain uniform, strong textured coke as a composite material by optimum combination of various grades of coal which have different heating properties (thermal transformation temperatures).

A major requirement in coal blending is that the mixture must give adequate fusion between particles during the swelling period. Under normal charging conditions it has been shown that a minimum dilation of 40 - 50% is required to obtain this fusion pressure.

Another major factor in achieving a good metallurgical coke from blended coals is considered to be directly related to the post-swelling contraction behaviour. The first contraction peak coefficient gives rise to fissuring within the coke due to differential stresses set up by the high temperature gradients across the coke mass. This determines the size distribution of the pieces of coke and also the bulk strength which is closely related to macrofissuring within the coke. Volatile matter (as stated previously) has no real effect on the second contraction peak coefficient; the effect of adding small, inert, non-contracting particles to the mass mitigates to some extent its effect- which is obvious in increased abrasion resistance of cokes thus produced. The naturally occurring mineral matter in the coal contributes to this effect, but often additions of finely ground coke breeze (fine coke dust), anthracite fines, graphite or sand are made to give more control over the second contraction peak.

Lastly, although a mixture of coals may have a suitable average volatile matter content for producing a good metallurgical coke, the swelling zones would be required to overlap. If coals of widely differing rank were used in the blend then one component might remain solid as the other swells and fuses and may well even inhibit this fusion. Addition of a "bridging coal" and / or fluxing agent is usually used to overcome these problems. These "bridging coals" are often small amounts of prime coking-coals and the fluxing agent is usually pitch, both

of which must be compatible with the coals to be blended and give rise to a homogeneous softening of the charge.

Blending of coals is never successful however, unless the varying coal components of the blend are intimately mixed and charged at the correct density.

1.2.3 Precharging Treatments

Precharging treatments are mainly concerned with cleaning and densification of the oven charge.

Cleaning of the coal is generally orientated towards the reduction of the ash and sulphur content. Ash content is normally reduced by washing and froth flotation methods. Sulphur is reduced by the addition of compounds to the coal before coking, treatment of the hot coke by the passage of various gases through it and the treatment of the hot coke with either hot or cold liquid reagents. Some of the various methods used for the desulphurisation of coke have been reviewed by Powell and Thompson (1923) and by Simmersbach and Schneider (1930).

Densification of the charge is probably the most important of the pretreatments and is carried out using a variety of methods. As described previously, the degree of pulverisation markedly affects the charge density. The coal must be crushed to the extent where sufficient fusion pressure will be generated between particles, without the pulverisation creating excessive fines (powdered coal),

which are detrimental to the carbonisation process.

Stamp charging and partial briquetting are also used to densify the charge. Stamp charging involves mechanical pressing of the coal to form a cake which is then charged as a whole to the oven. However, labour and environmental problems have severely restricted this practice. Partial briquetting is used fairly extensively and successfully, (especially in Japan) and involves charging the coke oven with a mixture of crushed coal and coal compressed into small briquettes.

The most widely used practice however, in the pretreatment of coal for carbonisation is preheating the coal. The initial objective of preheating coal was to reduce its moisture content, which would thus cut down on the oven heating load, consequently reducing the time of the carbonisation cycle. Investigations of coal heated to around 250 °C showed several additional advantages. It was found that coal treated in this manner has a higher bulk density and better heat transfer properties than coal which has not been preheated. The coal also flowed more easily when hot and required virtually no levelling within the oven. The capacity of the coke oven is increased, as is the economy of the carbonisation process when the coke is preheated in separate equipment from the coking oven. It reduces the volume of liquor as a troublesome effluent to be disposed of. The yields of tar, gas and most importantly coke are not significantly affected when preheating practices are used. The strength and structure

of the produced coke should have a cell structure more uniform in nature with improved impact and abrasion resistance, thus giving rise to a coke of improved quality.

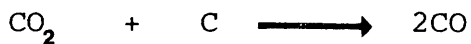
Charging hot, dry, pulverised coal creates serious hazards, if the coal is exposed to air. The two systems used commonly in industry are the flash entrainment drier and a hybrid fluidised bed / entrainment drier. The hot coal is removed from the drier by cyclones and stored in sealed bunkers.

Factors also important in coke production are the final carbonisation temperature and the rate of carbonisation. The final temperature of carbonisation (the maximum temperature attained) determines, along with the time spent at this temperature, the residual amount of volatile matter retained in the coke structure. This is often measured by the flue temperature although this is not as accurate as a measurement of the oven wall temperature. The rate of carbonisation determines the size and strength of the coke produced. Rapid carbonisation leads to high stresses, which give rise to a large degree of fissuring in the coke structure. A lower heating rate, particularly in the very important plastic range of carbonisation, will reduce these stresses and lead to the production of a larger and stronger coke.

1.3. Coke and the Blast Furnace

Coke is generally regarded having three main roles in the

blast furnace. First, as a source of heat to melt the iron and slag materials. It contributes approximately 65% of the total energy requirements of an integrated steel works. The heat supplied by the coke is achieved by reaction of the carbon with the hot blast driven into the lower regions of the furnace through a series of holes known as the "tuyeres". Second, it is a source of reducing gas- either by direct reaction with the heamatite, or more commonly by the production of carbon monoxide:-



carbon monoxide being the major reducing gas within the furnace, regenerating carbon dioxide as a result of the final high temperature stages of iron oxide reduction.

Coke occupies approximately 50% of the furnace volume, thus giving it a third important function in the furnace. Due to the coke's high level of porosity it provides a matrix of permeable material, especially in the lower regions of the furnace where it is the only solid constituent of the burden, through which the gases produced may ascend to the top of the furnace and the molten iron and slag materials percolate to hearth. The performance of coke in this third role is considered to be of prime importance in determining the output and fuel efficiency (often termed the "coking rate") of the furnace. A lack of matrix permeability will restrict blowing rates, lead to poor gas distribution in

the shaft and cause a considerable and serious pressure drop within the furnace.

Thus as a fuel and a reducer the coke's calorific power and carbon content must be of a high level and as a permeability agent, it must be refractory and strong enough to ensure a high void volume.

Fluid flow through a packed bed is a complex problem, though mean particle size and bed voidage strongly influence it (Ergun, 1952). The overriding factor in determining permeability is the strength of the coke comprising the burden matrix.

From the coke oven to the point of combustion at the tuyeres the coke is subjected to several different degradation forces. The many physical transfers of stacking, reclaiming, loading and unloading lead to degradation by volumetric breakage, abrasion, freezing and weathering. Once charged to the blast furnace the coke undergoes further degradation by abrasion and crushing as well as a consequence of the many complex chemical and thermal reactions occurring within the furnace. The coke must not suffer any substantial reduction in its physical strength until the iron melts. Thus stringent rules have been laid down governing the quality of metallurgical coke supplied to the blast furnace and careful analysis of the material is required to ensure that these conditions are met.

1.4. Coke Quality Analysis

Samples of coke analysed must be representative of the bulk. Care must be taken to ensure that the heterogeneity of the material is maintained in the sample taken (c.f. experimental section).

1.4.1 Assessment of Coke Strength

A prime property in the assessment of coke quality is coke strength. Measuring coke strength in terms of resistance to abrasion and fracturing is of fundamental importance.

Standard tests of coke strength generally involve the imposition of breaking stresses followed by analysis and screening. The results of these tests are largely based on the extent of size reduction and are expressed in the form of various indices. The tests are of two types: drop tests in which the breakage of the coke is by impact alone and drum tests, in which degradation of the coke takes place both by impact and abrasion.

1.4.1 (a) Drop Tests

The specifications for this test state that a 25 Kg, representative coke sample is dropped four times from a height of 1.83 metres (British Standard 1016, part 13, 1980). The shattered coke is then analysed for size and the shatter index is reported as the percentage by weight of the original material remaining above the specified

sieve size of fifty millimetres.

1.4.1 (b) Drum Tests

These are by far the most common of the strength tests (British Standard Method 1016, part 13, 1980). Two breakage processes occur during the tests: impact breakage, which occurs during the early part of the test, where the coke is broken along large natural fissures and reduction in size due to abrasion, which is most pronounced during the latter stages of the test. The initial size of the sample is important in relation to the magnitude of the test results and the degree of coke breakage. Degradation occurring by both processes leads to the material having a bimodal size distribution.

In the drum tests a prescreened 5 Kg (dependent on the drum size) representative coke sample is used. This is rotated for one hundred revolutions in a drum with internal vanes (usually at an angle of 1.5°) such that the sample suffers a series of drops and self abrasion. The M40 index is then taken to be a measure of the impact strength, that is the percentage of the original sample remaining on a 40mm sieve screen after the test. The M10 index represents the percentage of the original coke passing through a 10mm sieve screen after the test. The M10 index is taken to be a measure of the degree of abrasion having occurred. The drum tests may also be extended by increasing the number of revolutions, or elaborated on, to study breakage mechanisms, factors affecting the coke strength, and to

obtain the fissure-free size, the point at which no further impact breakage occurs along natural major fissures.

In recent years more emphasis has been placed on evaluating coke strength at temperatures elevated to those to which the coke is subjected in the blast furnace, as opposed to tests carried out at ambient temperature. These tests are often referred to as the thermal stability of the coke. Initial evidence from these tests has shown (Echterhoff 1961, Bradshaw and Wilkinson 1969, Wasa et. al. 1974):

(i) Coke strength is reduced and abrasion increased when coke is heated to above its carbonisation temperature.

(ii) Strength at elevated temperatures is not related to strength at ambient temperature. In some cases cokes with identical properties at ambient temperature showed significantly different properties when tested at elevated temperatures.

(iii) Annealing of the coke appears to occur at temperatures between 600°C and 1000°C , leading to increased coke strength.

Thus it is clear that the thermal behaviour of the coke cannot be inferred from tests carried out at ambient temperature. However, due to the complex nature of tests carried out at elevated temperatures no attempt has yet been made to formulate a standard test for the thermal stability of coke.

Other physical tests commonly carried out to evaluate coke quality are tensile strength, compressive strength, Young's modulus (both static and dynamic), apparent and true densities, bulk density and porosity measurements.

1.4.1 (c) Apparent and True Densities

Methods for measuring apparent density are given in the British Standard Method 1016, part 13 (1980). The principle of the test is the weight difference between a dry sample of 40 - 60mm coke and the weight of the same sample submerged in a water bath. This weight difference gives the upthrust of the submerged coke and hence the volume of the coke and the pores.

True density tests are an extension of those used for apparent density and are described in the same British Standard Method reference.

1.4.1 (d) Bulk Density

This test is often used in the determination of coke supplied on an industrial scale. The method is outlined in British Standard Method 1016, part 13 (1980) but is essentially just a known weight in a known volume eg. a blast furnace charging car. The test is accurate enough on this scale and the main problem is obtaining a level surface of coke such that the projections above the level balance the depressions in the mass below the plane, such that a reasonably accurate measure of the volume of the coke is obtained.

1.4.1 (e) Young's Modulus

The Young's modulus of elasticity is derived from the stress- strain relationship when the stress is applied relatively slowly (static test), or calculated from the resonant frequency of vibrational waves generated when stress is applied.

Patrick and Stacey (1972) showed that industrial coke conformed to the typical stress- strain relationship of an elastic material. Dynamic tests are far more useful for measurements at elevated temperatures. Billyeald and Patrick (1975) developed a method suitable for dynamic measurements on industrial coke.

1.4.1 (f) Compressive Strength

These measurements are of a comparative nature and can be used at ambient or elevated temperatures (Holowaty and Squarcy, 1957; Zorena et al., 1960). Essentially a cylinder of coke is placed between steel plates and a load supplied. The variation in compression with load applied is plotted and breakage of the coke cylinder is deemed to have occurred when a sudden drop in the load supplied is observed.

1.4.1 (g) Tensile Strength

Due to the heterogeneous nature of coke and that it is a highly porous, brittle material, direct tensile strength

measurements are difficult to perform due to complications in preparing suitable samples.

Patrick et.al. (1972, 1973) developed an indirect method of measurement in which a compressive stress is applied across the diameter of a thin disc of coke with breakage occurring due to the tensile stress which is developed at right angles to the applied load. The developed tensile stress (P) is then related to the applied load (W) by the equation:-

$$P = 2W / \pi td$$

where (t) is the thickness and (d) is the diameter of the specimen. The relationship between this measurement and those by the direct method is not known. The results can only be considered comparative as the requirements for an isotropic, homogeneous material behaving elastically under line loading are not fully met. A statistical approach is required when coke is used, due to its heterogeneous nature. The average strength is calculated from a minimum of fifty tests. The median value (used due to a skewed distribution of values) of industrial cokes is typically 2 - 4.5 MN/m². The test can be readily adapted for samples at elevated temperatures by the incorporation of a suitable furnace.

1.4.2 Porosity

Coke is a sponge like material, consisting of the material

and a network of pores of different shapes and sizes. The majority of the pores are interconnected, while some are closed. The pores can be any shape and range in size from less than 2nm (microporosity involved in gas adsorption) through the mesopore range (2 - 50 nm) to the macropores (greater than 50 nm), many of which can be seen with the naked eye.

There is no single method which can be employed to measure the porosity over this vast range. Several indirect methods have to be used including mercury porosimetry, molecular probes, gas capillary condensation, density measurements and microscopy.

1.4.2 (a) Density Measurements

Apparent and true density measurements can be combined, using the equation:-

$$\% \text{ porosity} = 100(1 - \text{apparent density} / \text{true density})$$

to give the volume porosity of the sample.

1.4.2 (b) Mercury Porosimetry

Values for the porosity are obtained using this method by forcing mercury under pressure into the pores. The volume of mercury penetrating the pores is then measured as a function of the applied pressure. A pore size distribution can then be found by assuming pores with a circular cross

section and applying the formula:

$$r = 750000 / p$$

where r is the pore radius (nm) and p is the applied pressure (Kg / cm^2). This gives a size distribution for the pores in the range of 2 nm - 0.25 mm.

However, only open porosity is measured by any fluid penetration method and no values for the closed porosity can be obtained. The equation assumes a value for the surface tension and angle of contact as well as the occurrence of only cylindrically shaped pores. Uncertainty arises about the true values for surface tension and angle of contact, as these can both be severely affected by contamination of the mercury. Coke crushing has been shown to have a relatively small effect, in the case of industrial coke, on values obtained by mercury porosimetry (Jüntgen and Schwuger, 1966). The technique, despite its assumptions, does give a relative measure of a wide range of pore sizes which lie between the coke's microporosity and the macroporosity as obtained by optical microscopy.

1.4.2 (c) Optical Microscopy Techniques

Analysis of coke porosity by optical microscopy can be carried out in two ways. Lineal analysis measures the width of pores and pore walls in a straight line traverse. The sum of the pore sizes as a fraction of the total giving the porosity as described by Abramski and Mackowsky (1952).

In the the point counting method the specimen is traversed in a series of defined steps, recording the nature of the material (pore or pore wall) at each individual step, though many points are required to give an accurate result.

The coke samples are prepared by embedding in an epoxy resin, such that all the pores are filled, and polishing until a flat surface is obtained. Many fields of view must be examined due to the heterogeneity of the coke and the porosity values obtained are resolution dependent. That is to say, the higher the resolution, which in this case is closely linked to the magnification, the smaller will be the pores incorporated in the porosity measurement.

Manual counting methods are very accurate but they are slow and tedious and do not lend themselves to routine analysis. Coupling of the microscope to a computerised automatic image analyser (e.g. Quantamet 720) vastly speeds up the analysis and gives more detailed information on the porosity, such as the derivation of pore shape factors as well as giving total porosity, total pore circumference, number of pores and pore wall and pore intercepts.

Also possible by optical microscopy is the examination of the effects of inerts (coke breeze etc.) on crack propagation and the determination of the optical anisotropy of the coke which acts as a classification, either by composition or unit size of the coke.

1.4.2 (d) Gas Adsorption Methods

These methods rely on the application of a suitable isotherm describing the material to be analysed. The most commonly used isotherms in studies of carbons are the Brunauer, Emmett and Teller (B.E.T.) and the Dubinin / Raduskevich isotherms.

The B.E.T. isotherm (1938) takes into account multilayer adsorption of gases, with the assumption that no interaction occurs between adjacently adsorbed molecules and that only one molecule is adsorbed per site on a surface composed of an array of uniform reactive sites. Emmett and Brunauer (1937) also interpreted that, in classical adsorption curves, the end of the near linear portion corresponded to completion of monolayer adsorption. The B.E.T. isotherm takes the form:-

$$X / v(1-X) = 1 / V_m C + (C-1)X / V_m C$$

where $X = P / P_0$, P = equilibrium pressure, P_0 = saturated liquid vapour pressure, v = amount sorbed at $P / P_0 = X$, V = monolayer capacity, C is a constant and represents $a_1 b_2 \exp (E_1 - E_i) / a_2 b_1 RT$, E_i = energy of liquifaction, E_1 = energy of adsorption between sorbate sorbent in the monolayer and $a_1 b_2 / a_2 b_1$ are a group of kinetic constants which are usually taken to have the approximate value of unity.

However, the B.E.T. isotherm assumes the occurrence of only

cylindrically shaped pores. The Dubinin / Raduskevich isotherm (1947) more realistically also takes into account the occurrence of slit-shaped pores. The Dubinin / Raduskevich isotherm takes the form:-

$$W = W_0 \exp[-B(T / \beta)^2 \log^2 (P_0 / P)]$$

where W = volume of adsorbate condensed in the micropores at temperature (T) and relative pressure (P / P₀), W₀ = the total volume of the micropores, β = affinity coefficient and is a shifting factor depending on adsorptive only, B = structural constant and also reflects the average micropore size.

The techniques of gas adsorption are used along with electron microscopy for the analysis of the coke's microporous system and can account for pores in the size range of 0.2 - 2 nm (Fryer, 1978).

1.4.2 (e) Molecular Probes

This technique is one in which molecules of various sizes are used to determine the size of the pores (Spencer, 1967). The pore size is defined by the maximum size of molecule which will penetrate the pore. This method of pore analysis covers the size range of around 1 nm.

It must be stressed however, that the strength and size of coke required for optimum operation of the blast furnace is related to the furnace diameter, height and operating

conditions. There has been a growing awareness in recent years that although the standard physical tests provide good guidelines of coke quality they do not adequately describe information relevant to iron production in the blast furnace. Instances have been recorded where cokes which have performed identically in strength tests have led to different rates of iron production in blast furnaces, working under almost identical conditions (Mukherjee, 1965). It must therefore be concluded that the standard physical tests do not provide information directly relevant to coke degradation in the blast furnace.

1.4.3 Coke Reactivity Assessment

Advanced blast furnace technology has shown that the stability factor is deficient in defining the quality of coke required. It has long been the aim to correlate the performance of the blast furnace with the quality of coke supplied and in this respect the measurement of the coke's reactivity and the relative importance of this factor has been a matter of discussion for many years.

Reactivity is an important characteristic of blast furnace coke, governing the fuel consumption of the process. The higher the reactivity, the greater is the extent to which the coke reacts with carbon dioxide, which is formed during the reduction process. The reactivity determines the size of the active combustion zone, of the coke which in turn determines how smoothly the burden descends the furnace towards the high temperature zone (Syskov, 1943, 1949).

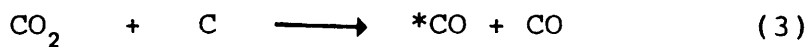
In order to understand the reactivity of the coke it is necessary to appreciate the nature of the reactions which it undergoes. The reduction of the iron ore is governed by its reaction with carbon monoxide, generated by direct combustion of the coke or by the reaction of carbon dioxide with the coke according to the Boudouard (solution loss) reaction (Boudouard, 1899, 1901 (a) and (b)):-



The rate at which this reaction occurs determines the reactivity of coke. Too low a reactivity will not produce sufficient quantities of carbon monoxide and will reduce the efficiency of the operation. Too high a reactivity may give rise to excess carbon monoxide which will thus increase the coking rate and again decrease the furnace efficiency; though the endothermic nature of the solution loss reaction and the stack temperature would tend to minimise excess carbon monoxide production. The solution loss reaction is accepted as the rate determining step in the reduction of the iron ore:-



Reactivity tests should be designed with consideration of the kinetics of the solution loss reaction. The currently accepted reaction sequence is (Marsh, 1973 (a)):-



*CO is a surface oxide

The rate determining step has been shown to be reaction (4), - the decomposition of the surface oxide.

Mathematical treatments of the solution loss reaction (Hedden and Wicke, 1957; von Bogandy and Engel, 1971) have identified different rate determining mechanisms depending on the temperature region.

<u>Temperature</u>	<u>Rate Determining Mechanism</u>
1000 - 1100 °C	Chemical reaction (temperature dependence is high)
1100 - 1400 °C	Porous gaseous diffusion
+1400 °C	Diffusion in gaseous boundary layer around carbon particles

The energy of activation for the solution loss reaction has been taken as 362.06 kJ / mole, although this is dependent on the particular type of carbon used and varies between

324.17 and 395.74 kJ / mole (Okstad and Hoy, 1965). However, Fryer (1974) has shown by considering the different rates of oxidation of graphite at low oxygen pressures, the difference in activation energies is a difference in pre-exponential factors and not in the actual activation energies.

The coke reaction with carbon dioxide is surface dependent and as such the reactivity index is a function of particle size and time. It is also dependent on the temperature, gas composition, porosity and alkali content (either from mineral matter inherent in the coke or supplied externally) as alkalis may catalyse the reaction. Thus, the parameters on which the solution loss reaction depends are too numerous and varied to make correlation of reactivity with furnace performance viable, or even to describe coke quality. The solution loss reaction though is important but its relative importance in the degradation of blast furnace coke is still a matter for discussion. Many authors describe it as probably the most important factor in coke breakdown (Kojima et al., 1977; Tate et al., 1979; Benedict and Thompson, 1980 and Hatano et al., 1982), while others argue the importance of different influencing factors (Botham et al., 1974; British Steel Corp., 1983; Goleczka et al., 1982).

1.4.4 Chemical Analysis

Analysis of blast furnace coke must also take into account factors other than the material's physical strength.

Moisture, sulphur and ash are the main components of coke which affect furnace performance and reduce the coke's value as a source of carbon.

Ash content alters slag chemistry and increases slag volume, thus reducing the cost effectiveness of the process. Moisture also affects blast furnace economics, as excess moisture requires additional heat to be driven off. Sulphur however, is the main problem for furnace operators. The distribution of the sulphur between the iron and slag products depends on its concentration within the coke, as the majority of sulphur in the furnace arises from the coke. Sulphur is detrimental to the strength of the iron (and finished steel products) and removal after incorporation in the metal is costly and reduces productivity.

Industrial analysis of coke often takes the form of "proximate analysis" in which only the major influencing components such as ash, moisture, volatile matter and sulphur are analysed for.

Moisture content is analysed by drying the coke at 105°C and determining the weight loss. However, Wilkinson (1965) reported that this method of analysis does not represent the total moisture present as further amounts are released at the higher temperatures involved in determining volatile matter content. Hence, many determinations of volatile matter content record non-accurate values which are too high due to insufficient correction for moisture content.

Volatile matter content is analysed for by heating the coke to around its carbonisation temperature and measuring the weight loss. This gives a value for a degree of carbonisation and hence carbon content. More accurate values for degree of carbonisation are obtained from the hydrogen content and this can be determined simultaneously with carbon as described by Mott and Wilkinson (1957). This method does not require the incorrect assumption that the percentage "fixed carbon" (amount remaining in the coke) can be determined by subtracting the moisture, ash and volatile matter from 100 %.

Ash is determined straight forwardly by ashing the sample and the sulphur content can be analysed in a variety of standard practices.

Industrially, there is less awareness of the importance of the minor components in coke such as chlorine, nitrogen and phosphorus and little appreciation of the possible effects of substances present in even smaller amounts, such as alkalies. Tests for these minor components are readily available if necessary but are not normally included in the industrial practice of proximate analysis.

The chemical properties of coke are probably of less importance than the physical properties in relation to efficient and smooth operation of the blast furnace. Although once charged to the furnace the chemical properties may significantly alter the physical properties.

Of the physical properties, strength is of prime importance in maintaining burden permeability. The strength of coke is largely governed by its structural characteristics.

Coke Structure

Metallurgical coke consists of approximately 80% carbon. Thus, in order to understand the coke structure, it is necessary to first be aware of the structure of the carbon portion of the material.

The element carbon exists in basically two allotropic forms: diamond and graphite. However, extreme conditions are required for the formation of diamond (Hall, 1959) and thus graphite is by far the most commonly occurring elemental form of carbon. All carbons, other than diamond, including metallurgical cokes, possess "graphite" units.

1.5. Graphite Structure

1.5.1 Ideal Lattice

The crystal structure of graphite has been extensively studied since the early work of Ewald (1914), by authors such as Debeye and Scherrer (1917); Hassel and Mark (1924) and Bernal (1924), having been one of the first structures to be studied by X-ray diffraction, and it is described as a regular layer structure. The layers are infinitely large and are composed of planar hexagonal net-works of carbon atoms. The carbon atoms in the layer planes are joined to

their nearest neighbours by three sp^2 hybrid orbitals, angled at 120° to each other, with a C - C distance of 0.1421 nm. The fourth valence electron is delocalised over the whole plane, giving the layers an aromatic character. Franklin (1951 (a)) reported the planes to be arranged in parallel, with the distance between successive layer planes as 0.33538 nm, for well orientated graphite, the magnitude of this distance making bonding between the layer planes of the weak van der Waals type. Franklin also stated that, in graphite with a lesser degree of orientation, the interplanar distance (measured by experimental methods) is of an average value depending on the relative proportion of oriented layers, having an interlayer spacing of 0.33538 nm and disorientated layers with spacings of 0.344 nm.

Two main types of stacking sequence occur for the carbon planes: hexagonal (Bernal, 1924) and rhombohedral (Laidler and Taylor, 1940; Lipson and Stokes, 1942 (a) and (b)). The hexagonal form has the carbon atoms in one layer displaced relative to its nearest neighbour in an ABAB... stacking sequence, such that each atom in every alternate layer is in perfect coincidence, as shown in figure 11. The unit cell dimensions of this hexagonal structure were evaluated by Trzebistowski (1937) to be $a = 0.2456$ nm and $c = 0.6696$ nm. Four reference axes are used to define the crystal structure, three of which are in the layer plane (at 120° relative to each other) denoted as a_1 , a_2 , and a_3 , with the fourth perpendicular to the plane, denoted as c . The appropriate Miller indices are $(h, k, h+k, l)$,

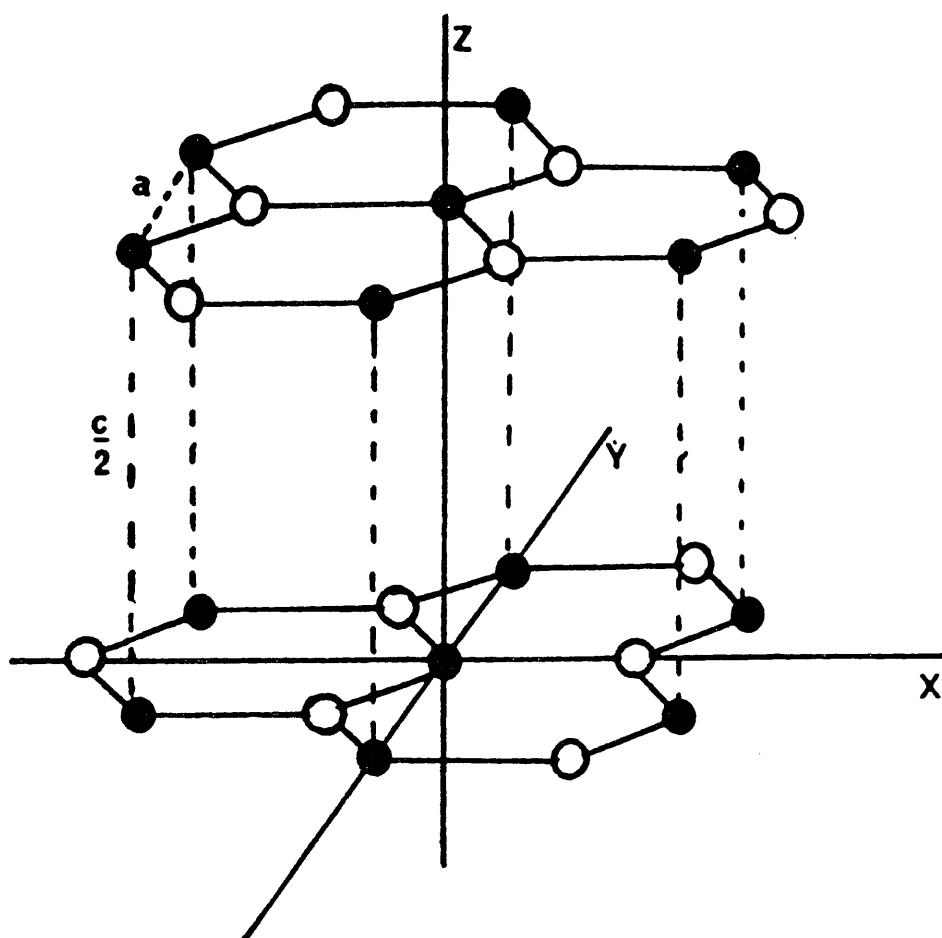


FIGURE 11

Hexagonal Form of Graphite

with the third index used to clarify some of the symmetry relationships present in graphite. The unit length in the carbon plane is described as one side of a carbon hexagon, with the 1 unit length being twice the distance between a pair of layer planes. The unit cell projection on the basal plane is shown in figure 12. The rhombohedral form involves a third layer, and a stacking system of ABCABC..., in which the third layer has the same relative position to the second layer as the second layer has to the first (figure 13).

Both types of stacking structure are to be found in natural graphite, as described by Finch and Wilman (1936); Boehm and Hofmann (1955). It has been shown that mechanical treatment (Bacon, 1952 (a)), heat (Boehm and Hofmann, 1955) and chemical treatment (Laidler and Taylor, 1940; Lukesh, 1951 (a) and (b)) can be used to convert the rhombohedral form to the more stable hexagonal structure, presumably by the layers sliding over each other, due to the low stacking fault energy of $0.51 \times 10^{-7} \text{ J / cm}^2$ (Baker et al., 1961).

1.5.2 Non-ideal Crystal Structure

1.5.2 (a) Discontinuity of the Bulk Structure

Even the purest of graphites do not conform to the idealised lattice structure, and good three dimensional crystals of appreciable size are rare. This property of restricted crystalline order is even more obvious in synthetic graphites, as shown by Dawson and Follett (1959).

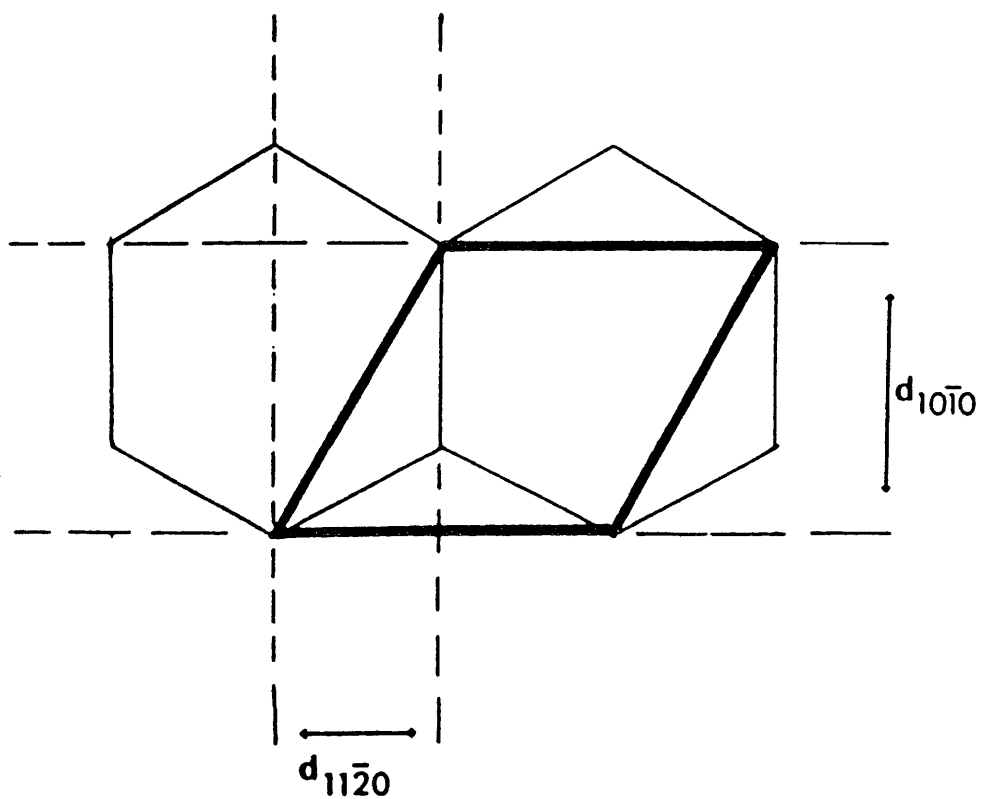
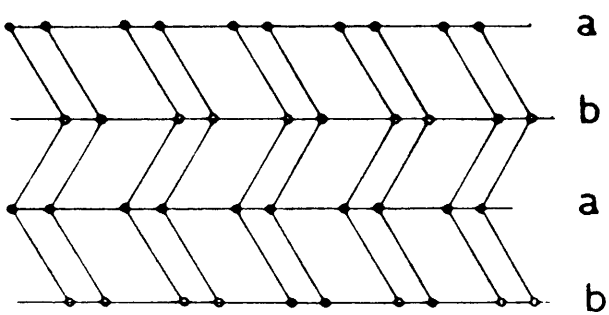


FIGURE 12

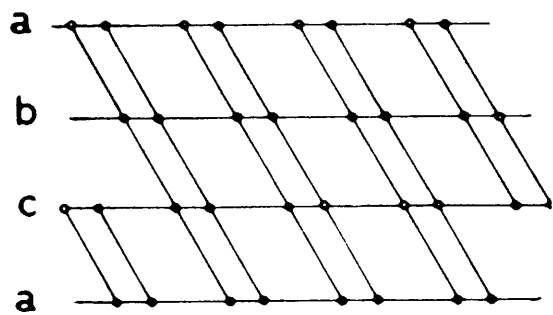
Graphite Unit Cell Basal Plane Projection

Hexagonal.



(a)

Rhombohedral.



(b)

(a) Cross section of hexagonal graphite.

(b) Cross section of rhombohedral graphite

Restricted crystalline order can to some extent be attributed to voids or micropores within the bulk sample, the presence of which is confirmed by comparison of the theoretical density of graphite (Hofmann and Wilm, 1936) with that found by liquid and gas displacement density measurements.

The porosity of the material can be classed as "open" or "closed" porosity, closed porosity being those pores inaccessible to liquid or gas. Around 20% of the total pore volume is inaccessible (although this can be opened up by chemical and mechanical treatments) and has been shown by Loch and Austin (1956) to be associated with the small separations between adjacent crystallites (short range crystal structures) in the bulk carbon.

Crystallographic Defects

Two common types of defect are found in graphite crystals. The first is a disorder of the stacking sequence, which may arise from a shift in the relative positions of the carbon layers. The second type of defect is caused by a disturbance in the carbon plane.

1.5.2 (b) Stacking Disorder

The relative interplanar spacings in graphite are dependent on the degree of stacking disorder present, as has been previously mentioned (Bacon, 1950, 1951, 1952 (a), 1958; Franklin, 1951 (a)). If the carbon planes are shifted

relative to one another, so as they no longer form an ABAB... or ABCABC... sequence, then this is a stacking disorder (often referred to as "turbostratic" disorder). Perfect dislocations dissociated into partials, with fractional Burgers vectors, also cause turbostratic disorder between the partials (Read, 1953 and Friedel, 1964).

1.5.2 (c) Layer Defects

Disruption of the planar aromatic carbon structure constitutes the second major type of defect in graphite, and is referred to as "layer defects". This disruption can be caused by the formation of a hole defect (Ubbelohde, 1957; Ubbelohde and Lewis, 1960) as a result of irradiation of the sample, which causes a displacement of atoms to form interstitials (Bollmann, 1960, 1961 (a), (b) and (c)) or the occurrence of twin planes, produced by tilting of the layer planes (Lukesh, 1950 and Baker et al. , 1965). These defects can also be produced by forming bonds with impurity atoms, and by the presence of intercalated atoms (Heerschap et al., 1964).

1.5.3 Electronic Structure of Graphite

As previously described, the carbon atoms in graphite are joined to their neighbours by sp^2 hybrid orbitals, with the fourth valence electron being delocalised (in the π orbital) over the carbon plane.

Due to the distance between layer planes, in relation to

carbon - carbon planar distances, interplanar interactions are normally disregarded and the electronic structure of graphite is treated as a problem in two dimensions. Coulson (1947) and Wallace (1947) initially postulated that the π band could be regarded as a filled valence band and an empty conduction band. Coulson and Taylor (1952) and McClure (1959) later described the conduction and the valence bands as marginally overlapping or touching, at the corners of the Brillouin zones.

Graphite is now regarded as a semi-metal, composed of small discrete pockets of electrons in the conduction band and an equal number of pockets of holes in the valence band. This model of graphite being due to the work of Slonczewski and Weiss (1958), who in deducing this structure included in their calculations the perturbation of interlayer interactions. The high electronic conduction of graphite is due to its semimetal characteristics, which unlike a semiconductor has a marginal, finite overlap between the valence and the conduction bands. Graphite's electronic structure and Fermi surface have been extensively studied and reviewed in papers by Haering and Mrozowski (1960) and by Cracknell (1969).

1.6. Coke Structure

1.6.1 Structure of Disordered Carbons

The structure of metallurgical coke can be described by the general consideration of the structure of disordered carbons.

X-ray diffraction spectra of disordered carbons reveals two major features. First, peaks of the type (001), which arise from parallel layer plane stacks and second peaks arising from regular structure within individual layer plane segments. This second feature can be described as two dimensional (h,k) peaks (Fischbach, 1971). The absence of (h k l) peaks, present in graphite, demonstrates that there is virtually no stacking order of parallel layers in the stacking segments.

All non - graphitised carbons possess this disordered or "turbostratic" structure, in other words, although they are all composed of elementary layers identical to graphite, the arrangement of these layers with respect to each other is much more disorganised than in graphite. Turbostratic carbon consists of stacks of the parallel planes which are disorientated to each other by rotations around a common axis which is perpendicular to the layer planes. The layer planes can be displaced from the ABAB... relationship with their nearest neighbours by translations or rotations about the c-axis (normal to the plane). Warren (1941) formulated this turbostratic model and it remains, with modifications, one of the best methods for describing disordered carbon structures.

This displacement from the equilibrium relationship (ABAB...) leads to an increase in the mean interlayer spacing is due to a reduction of the van der Waals forces of attraction between layers, due to the stacking faults.

This turbostratic model has subsequently been revised (Biscoe and Warren, 1942; Houska and Warren, 1954; Warren, 1956; Warren and Bodenstein, 1965, 1966; Franklin, 1950, 1951 (a) and (b); Bacon, 1950, 1951, 1952, 1954, 1958).

As the model has been revised it has become clear that layer plane defects as well as stacking disorders must be invoked in order to understand the structures of disordered carbons.

Mering and Maire demonstrated some of the short falls of the turbostratic model. They proposed the presence of "interstitial" carbon atoms firmly attached to each side of the layer planes (Maire and Mering, 1970). These atoms are then assumed to cause lattice distortion and hence increased interlayer spacings in the carbons. Variations in graphitisation behaviour of carbons having the same amount of structural disorder are attributed to concentration variances of these interstitial atoms (Schiller et al., 1967 (a) and (b)). During graphitisation the structure undergoes an initial transition of these interstitials from a disordered to an ordered arrangement relative to the hexagonal layers to which they are attached (Schiller and Méring, 1967), followed by removal of the defects from first one side and then the other. Four phases are then assumed to span the differences between the ordered graphite structure and highly disordered carbon. Thus the loss of the interstitial imperfections allows the formation of the ordered ABAB... stacking sequence. Although Mering and co-workers have provided physical,

structural and chemical data supporting this model, it is unlikely that this model is sufficient for describing structural disorder in carbons. The complex nature of highly disordered carbons and their graphitisation is unlikely to be described by such a simple model as this. Maire and Mering's model assumes the presence of only one specific imperfection in the structure. Also, the model is based on polyvinyl chloride samples and conventional pitch cokes, no work has been done on a wider range of carbons. Mering also noted that the assumed "bound" interstitial differs from the interstitial, described by Wallace (1966), formed by radiation damage. However, Maire and Mering's model does successfully describe many features relevant to real carbons.

It is generally accepted that the bonds within the carbon layer plane are identical (three equally distributed single bonds and one resonating bond per atom). Pauling has proposed that this is the nature of the bonds present in turbostratic carbon. However, he proposed a quinoid structure for graphite, in which two of the bonds are single and the third double, producing a large and out of plane bulge for the double bond. Regular arrangement of such bonds in the ABAB... stacking sequence would stabilise the structure by enhancement of the van der Waals bonding between layers, by coincidence of these bulges with the open hexagon centres in the adjacent layers. It is then assumed that graphitisation occurs by a transformation of the resonance bond to the quinoid structure. Pauling also noted that X-ray diffraction, magnetic susceptibility and

layer plane compressibility are consistent with this proposed model.

However, the quinoid structure would result in an orthorhombic crystal structure with two values for the interplanar distance instead of one and a relative displacement of the A and B, layers different from the hexagonal structure. Ergun (1968 (a)) argued several points against Pauling's model but concluded that the evidence was inconclusive on a quinoid structure in graphite. Ergun has also reviewed the inadequacies of the turbostratic model in several papers (Ergun, 1968 (a) and (b); Ergun and Gifford, 1968, 1969).

The probability of the occurrence of interstitial carbon atoms (both individual and clusters), as well as "cross - link" or distorted carbon - carbon bonds and holes in layer planes has been described by a number of authors (Ruland, 1964, 1965 (a) and (b), 1967 (a) and (b), 1968; Perret and Ruland, 1968 (a) and (b); Strong, 1969). The importance of layer curvature has also been described by Woodruff (1969).

Ruland has shown that a good linear relationship exists, with relatively little scatter, between the mean interlayer spacing and the r.m.s. displacement of adjacent layers parallel to the layers. Second, the r.m.s. displacement of adjacent layers normal to the layers decreases with decreasing values of the mean interplanar distance, although the scatter band is broad and the r.m.s. displacement values of adjacent layers normal to the layers

are in general significantly larger than the difference between the mean and minimum interplanar distance. Third, the incidence of rhombohedral stacking drops sharply as the mean interplanar spacing falls below 0.338 nm, but is still significant in moderately well graphitised samples.

The first of the points made by Ruland shows that there is no fundamental basis for the mean interplanar spacing of 0.344 nm traditionally associated with random parallel stacking. However there is evidence for differences in the defect structure of different carbons with the same mean interplanar value, and the increased mean interplanar values of disordered carbons must largely result from defects rather than stacking disorders. Ruland acknowledged the importance of a variety of defect types, both within and between the layers, and his model assumes that graphitisation takes place by an annealing out of the defects, similar to Maire and Mering's model.

The mean interplanar spacing appears to be the only traditional parameter describing turbostratic carbon to have come through the many reviews of this structure unscathed. However it now seems likely (Maire et al., 1968) that a significant portion of the interlayer spacing increase in disordered carbons arises from defects between the layers.

The parameters L_a and L_c have been questioned and / or replaced by other parameters during these reviews. The

interpretation of L_a (the apparent layer diameter) values appears to be particularly important due to the numerous correlations between L_a and other structural or physical properties, which have been observed. The accuracy of the measured L_a value with the actual dimensions of the layer structure have been questioned for some time. It is now fairly well accepted that the measured L_a distance is generally appreciably smaller than the average diameter of the layer planes. This phenomenon arises due to L_a being effectively a measure of the average size of planar, defect free regions. Thus smaller L_a values are obtained for layers which are bent or have holes in them, while the extent of the imperfect layer structure is large. A variety of X-ray diffraction techniques have been developed in the hope of accounting for these defects. However, these techniques (Bourauoi and Mering, 1964; Short and Walker, 1963; Eeles and Wilson, 1965) are extremely complex to employ.

Kinetic studies and mechanism of graphitisation often give L_a values. These are probably best interpreted as an indication of relative flatness and perfection rather than as true crystallite diameters. The actual extent of the defective layer structure is however very important and may be the fundamental basis in distinguishing between non-graphitising and graphitising carbons. Non-graphitising carbons appear to have small layer segments (Perret and Ruland, 1968; Schiller et al., 1967) as opposed to graphitising carbons in which the layer structure appears to be extensively developed (Ergun, 1968 (a)).

1.7 Graphitisation

Many reviews of the process of graphitisation of carbons have been made (Maire and Méring, 1970; Fischbach, 1971; Pacault, 1971; Robert et al., 1973).

Franklin (1951 (a)) described the transformation of certain carbons (known as soft, or graphitisable carbons) to the structure of graphite by heat treatment. Thus, the definition of graphitisation is attainment of the stable graphite structure, as described by Bernal (1924).

Oberlin (1984) has described graphitisation as occurring in various stages. First, before the semi - coke stage of carbonisation, bulk mesophases composed of basic structural units are formed. These misorientated basic structural units then coalesce into stacks of distorted layers, as heat treatment temperature (HTT) increases. At even higher temperatures the wrinkling of the layers decreases which become stiff and perfect as the graphite structure is obtained. This process is summarised in figure 14.

Maire and Mering (1970) described the degree of graphitisation by the equation:-

$$\bar{g} = \frac{3.44 - \bar{d}_{002}}{3.44 - 3.354} = \frac{3.44 - \bar{d}_{002}}{0.086}$$

where: \bar{g} is the degree of graphitisation.
 \bar{d}_{002} is the measured average interlayer
spacing.
0.344 nm is the interlayer spacing in
pregraphitic layers.
0.3354 nm is the interlayer spacing in
graphite.

These authors have also shown experimentally that the relationship:-

$$P_1 = g^2$$

is observed, where (P_1) is the probability that two adjacent layers in the carbon are in the graphitic stacking sequence.

The nature of a carbon material, whether graphitising or non - graphitising, appears to be determined during the mesophase stage of carbonisation. The formation of mesophase spheres, as reported by Brooks and Taylor (1968), gives rise to parallel preferred orientations of polyaromatic molecules. This "embryonic" structure can then develop at higher temperatures. Non - graphitising carbons do not possess this "embryonic" preferred orientation, and will not graphitise even on heating to 3000°C. Non - graphitising, or "hard", carbons have a poor preferred orientation of the elementary stacks, compared with the "soft" carbons and consequently graphitisation becomes sterically impossible. Thus geometric factors

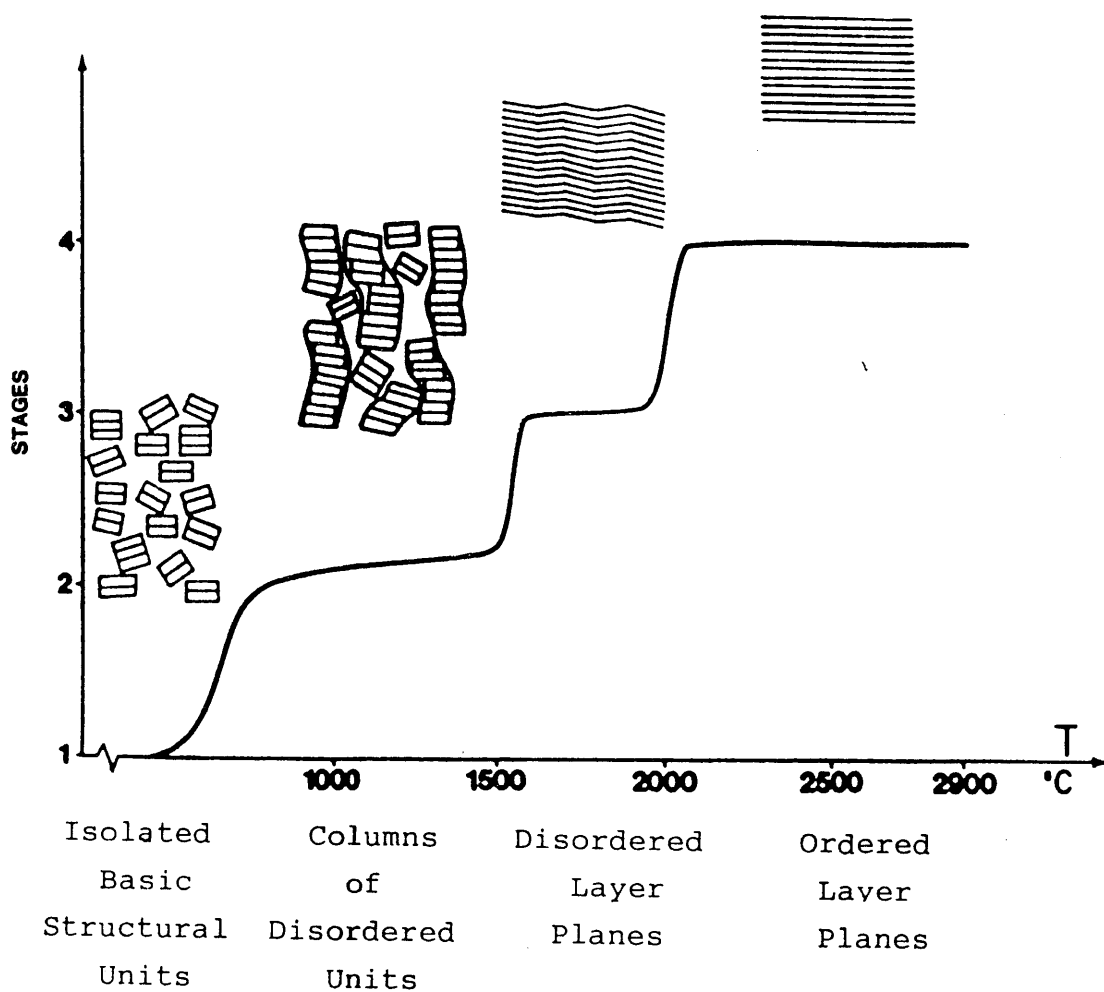


FIGURE 14

Stages of Graphitisation

prevent crystal growth in non - graphitised carbons (Oberlin et al., 1975 (b)).

General conclusions can thus be made on the graphitisation of carbons. The rate of graphitisation increases with increasing heat treatment temperature (HTT), pressure and stress. The kinetics of the process cannot be represented by any simple law, and the leading parameter for the early stages of the process is the zig - zag texture formed, which allows for defect mobility, either in plane defects or interstitial defects with a minimum energy.

Marsh et al. (1973 (b)) has drawn some general conclusions as to the importance of liquid crystal development for metallurgical coke production. First, the lower rank coals exhibit relatively small liquid crystal units. This may be a consequence of a heterogeneity of molecular properties in the plastic phase of carbonisation; liquid crystals can grow from an isotropic melt but their size is limited if an isotropic carbon is formed during an early stage of carbonisation. The growth process of the liquid crystal is restricted if the isotropic plastic phase contains various molecular systems capable of forming liquid crystals but at temperatures differing by around 40°C. Second, inert inclusions, of around 10 to 50 nm in size, disrupt liquid crystal growth, by adhering to the surfaces of the growing crystals. However, inerts of larger surface area may promote crystal growth by providing a larger surface for coalescence into larger anisotropic units, thus affecting the properties of the formed cokes. Third, the liquid

crystals can accomodate in their structure units which would otherwise be isotropic i.e. there is forced anisotropy. This suggests a mechanism for maintaining anisotropy, while blending coals, which is important in metallurgical coke formation. Also, the coking coals represent an optimum in the facility of liquid crystal formation while maintaining a balance in the inert material (mineral matter etc.).

The inert material in the metallurgical coke arises from the parent coals (used in the coke's production), which contained inorganic impurities in the vegetation and also in impurities deposited during coalification. The major mineral components of coal include clays, metallic sulfides, oxides, alkaline carbonates and quartz. However, minor and trace impurities in coal include almost every element known (Berkowitz, 1979). These inerts are incorporated into the coke structure during the carbonisation process.

Thus coke structure can be understood by a consideration of the above factors along with a development of the porous structure of the material. The vast majority of the coke's porosity arises from escape of volatile material during coke formation.

1.8 Alkali Interactions

As previously mentioned the conditions within the modern day blast furnaces are extreme and complicated.

However, of the many complex chemical reactions occurring in the blast furnace a discussion of the role of alkali, with respect to metallurgical coke, is of vital importance.

The methods of alkali generation within the furnace have been discussed by many authors (eg. Abraham and Staffanson, 1975; Davies et al., 1978; Kondoh, 1981; Lu and Holditch, 1982). The alkali enters the furnace in the mineral matter inherent in the coke and also in the iron ore, in the form of complex alumino - silicates. These alumino - silicates subsequently react with the lime (which is added to separate out the slag materials) to give rise to potassium vapour. The potassium vapour then reacts with the carbon in the coke and nitrogen (in the air blown in through the tuyeres) to form potassium cyanide. The potassium cyanide rises through the coke bed and condenses out in the cooler regions of the furnace, where in a more oxidising atmosphere it is converted to the carbonate species. It should be pointed out that the cyanides themselves are unstable in the low temperature regions of the stack relative to the carbonate but because of the non - equilibrium conditions in the furnace, the cyanides are found in the stack gases and thus some are condensed on the burden along with the carbonates. The lack of equilibrium results from the rapid passage of gases through the furnace not allowing attainment of equilibrium pressures. As the coke bed progressively moves towards the high temperature regions of the furnace the carbonate decomposes, giving rise to potassium vapour again. The potassium vapour repeats the reactions mentioned above and thus the

potassium level in the furnace increases. This cycling method of alkali (in particular potassium, although it is presumed that sodium undergoes similar reactions) has been recognised to occur in the blast furnace for many years (Davies et al., 1978; Kondoh et al., 1981; Lu and Holditch, 1982; Goleczka et al., 1982). This method of cyclisation is shown in figure 15.

It has been reported (Hawkins et al., 1974) that only around one tenth of the amount of alkali metal which enters the blast furnace is eventually removed in the slag material. The rest is carried up with the gases and is deposited on the burden, the refractories or is removed in the flue gases. The removal of alkali is dependent on the operational parameters of each individual furnace. The fraction removed in the slag is dependant on slag volume, basicity, viscosity, temperature and partial pressure of alkali in the bosh region of the furnace. The alkali levels in the slag are inversely related to the thermal state of the furnace and are higher at low basicity levels (Nanavati and Cohen, 1972). Fractional removal of alkali in the flue gases depends on the CO / CO_2 ratio and top gas temperature.

The conditions for optimum slag removal of alkalies are unfortunately the opposite to those required for low metal sulphur content. Thus lowering the slag basicity increases the levels of sulphur in the metal, which results in costly external desulphurisation of the metal. The only condition for increased alkali removal without increasing the

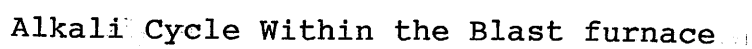


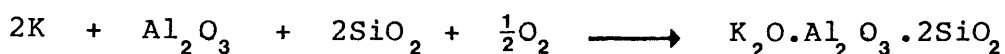
FIGURE 15

sulphur / metal ratio is to raise the slag volume, but this again decreases the cost efficiency of the process.

It has long been appreciated that alkalis are detrimental to the smooth running of the blast furnace (Armatorio, et al., 1971; George and Peart, 1973).

This decrease in furnace efficiency, resulting from high alkali content has been mainly due to alkali attack on the metallurgical coke and carbon refractories of the furnace (Snow and Shapland, 1962; Hatano et al., 1980; Narita et al., 1981). The mode of alkali attack is therefore of great importance in determining the degradation mechanism in metallurgical coke.

Hawkins et al. (1974) have discussed the mode of alkali attack in the blast furnace on refractory carbons. They have described the method of attack on the ash content of the carbons as a mixture of:-



However they concluded from other experimental evidence that the effect of potassium on the carbon was more important than its action on residuals and thus, that the ash content of the carbon does not have a significant role

in the attack process.

It would be expected that these results would also hold for the metallurgical coke portion of the furnace burden (van Niererk et al., 1986). As such, the method of potassium attack on the carbon portion of the coke requires investigation.

The interaction of carbon with alkalies is complex, resulting in a wide variety of chemical reactions. First, and most obviously is the catalytic effect of the alkalies on the carbon and second, the formation of lamellar intercalates of various kinds.

1.8.1 Catalytic Gasification

Carbon gasification encompasses a wide range of reactions and can in general be described as the combustion of carbonaceous material. The combustion of this material is very probably one of the first and most important chemical reactions employed by mankind, with patents for the combustion of coal dating back to 1884 (Green, 1928). However, although the process has been in existence for many thousands of years it is only in recent times that progress in understanding the processes involved in carbon gasification (largely due to the fact that the majority of the world's energy is thus produced) has been made. The problems of explaining the processes involved are many including constantly changing heterogeneous surfaces, complex chemical structures, the gaseous

environments and the presence of inorganic impurities.

Considering these problems it is not surprising to find that there are contradicting reports on catalytic effectiveness, in the literature. For example, discrepancies are found in comparisons of the effectiveness of alkali metal chlorides (eg. NaCl, KCl) and alkali metal carbonates (eg. Na_2CO_3 , K_2CO_3) as catalysts (Kislykh and Shishakov, 1960; Haynes et al., 1973; Veraa and Bell, 1978).

The increased knowledge of the gasification reactions has been made possible by use of more refined experimental techniques to investigate extremely pure carbons with a highly crystalline structure. The reactions of these "pure" carbons with impurities of well defined chemical composition has allowed theoretical treatments of the reactions to be made.

As a material for fundamental studies, graphite has many advantages. It is easily cleaved to give clean surfaces, easily purified and can have an extensive structure, as large single crystals. Graphite powder is normally nonporous and as such can be studied without the problems which arise from mass transport effects in porous substances.

The observation of these simpler reactions can then to some degree be used to explain observations made on more complex and generally used carbon systems. However, graphite is

not coal or coke and thus caution is required when extrapolating data from graphite observations to explain coal or coke reactions. It would appear though, that the chemical behaviour of coals of high rank and to an extent coke formed from these coals is more similar to that of graphite than low rank coals. Thus graphite can be treated very loosely as the highest rank member of the coal series.

The major factors (McKee, 1981) which appear to determine rates of gasification reactions of carbon (with carbon dioxide, water vapour, oxygen and hydrogen) are;

- 1) The presence of inorganic impurities.
- 2) The crystallinity and structure of the carbon material.
- 3) The concentration of active sites for gasification on the carbon surface.
- 4) The diffusion of gases to the reactive sites, to participate in gasification.

Early work on carbon gasification has been reviewed by many authors (Kroger and Angew, 1939; Walker et al., 1959; Walker et al., 1968; Lewis, 1970).

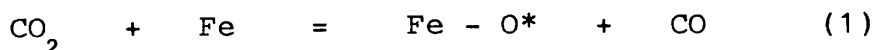
There are a wide variety of catalysts which promote the rate of gasification of carbon, many of which are present in metallurgical coke. However, only the action of alkali metal oxides and salts, along with iron and its oxides, will be considered here, as these elements appear to be the most important in metallurgical coke degradation.

1.8.1 (a) Catalytic Role of Iron and Iron Oxides

King and Jones (1931) studied the effects of iron and its oxides on the gasification of a coke made from coal. They observed that the initial increase in gasification rate in carbon dioxide of the coke dropped off as a change in the oxidation state of the iron occurred. They concluded that during the contact, of the iron-containing coke, with carbon dioxide the "reducible iron" was gradually oxidised and a resulting decrease in catalytic activity took place. Walker et al. (1968) demonstrated a similar effect, by examination of magnetic susceptibilities, during the iron catalysed gasification of graphite in carbon dioxide. They concluded that the metal was the most active catalyst and that catalytic activity decreased as the iron was progressively oxidised to wüstite ($\text{Fe}_{0.95}\text{O}$), which was less active, and magnetite (Fe_3O_4) which was completely inactive catalytically.

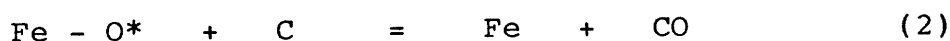
The authors proposed a mechanism for the catalytic action of Fe in the Boudouard reaction. This mechanism proposed was that of a cyclic oxidation - reduction process, the initial step being the dissociative chemisorption of CO_2 at the surface of the iron, to produce a labile chemisorbed oxygen atom. The dissociative chemisorption of CO_2 on iron surfaces was previously reported by Blyholder and Neff (1962) and the labile chemisorbed oxygen atom (at elevated temperatures) by Melmed (1966).

The postulated mechanism (Walker et al.) was:-

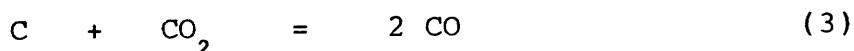


where * represents an
adsorbed species

The oxygen atom may then diffuse to the carbon metal interface, where it can react to give rise to CO_2 .



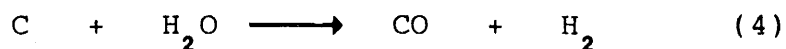
giving an overall reaction:-



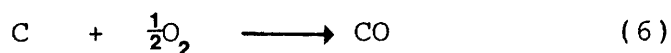
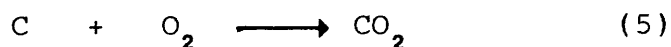
This mechanism implies localised gasification of the carbon, near the carbon / iron interface. This would infer the pitting and channeling of the carbon surface near to the metal particle. These topographical features have been reported during further studies of the catalysed Boudouard reaction (Adair et al., 1971; Marsh and Rand, 1971; Skowronski, 1977).

Studies on the stability of the iron catalyst (King and Jones, 1931; Grabke, 1972) have shown that when the CO concentration is high the metal is the stable phase ($> 74\%$ CO), wüstite is the stable phase between 20 and 74% CO and magnetite becomes the stable phase at carbon monoxide concentrations of less than 20%. This implies that if the carbon monoxide concentration falls below 20% iron will become an inactive catalyst for the Boudouard reaction.

Lothe and Melson (1965) found that gasification reaction of graphite with steam:-



could be catalysed by iron, although catalytic activity was significantly reduced at high water pressures. This is consistent with findings for the Boudouard reaction in which the metal is active and the metal oxides are less active catalysts. Lothe and Melson also found that the presence of sufficient concentrations of hydrogen maintained the catalytic activity, by maintaining the reduced state of the catalyst. Again, a similar effect was found for catalysis, by iron, of C / O₂ gasification.



in which high oxygen concentrations severely reduced catalytic activity (Thomas and Walker, 1965).

Thus it would appear that, in the case of iron, the reduced metal is the most active catalyst in the majority of carbon gasification reactions, The catalytic activity, for these reactions falls dramatically as higher oxides are formed.

1.8.1 (b) Alkali Metal Oxides and Salts

The alkali metal salts are amongst the oldest known catalysts of carbonaceous materials. They catalyse a wide

variety of reactions eg. combustion of neutron irradiated graphite (Harker et al., 1970), the Kellogg process (Cover et al., 1973; Kohl et al., 1978), the COED char - steam reaction (Starkovich et al., 1977) and the combustion of coke (Patrick and Shaw, 1972).

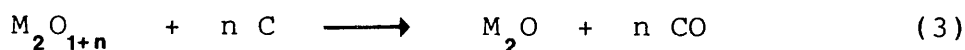
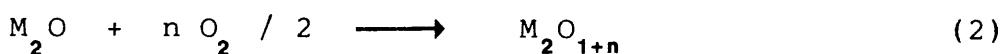
However, of all the reactions which these compounds catalyse only those involving the gasification of carbon in the presence of carbon dioxide, oxygen and water vapour will be considered in this discussion. These are the reactions most likely to be encountered in the blast furnace environment, although catalytic gasification of the Boudouard reaction is by far the most important of the three.

When the alkali metal is added to the carbon in the form of different salts, variations in activity are observed. These are attributed to the effect of the anion in the salt. A spectrum of activities is found for the salts of alkali metals, the highest catalytic activity is observed with the carbonate and the lowest with the metaphosphate.

The catalytic activity is greatest for the alkali metal carbonate and this according to the alkali cycle is the most important salt involved in coke degradation, in the blast furnace. Due to these considerations the carbonate species will mainly be dealt with in the following discussion of the catalysis of carbonaceous materials by alkali metal oxides and salts.

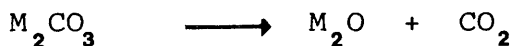
Catalytic Gasification of Carbon - O₂ Reaction

The catalytic action of alkali metal oxides and carbonates on the graphite - O₂ reaction has been described by McKee and Chatterji (1975). They concluded that the action of these catalysts involved the intermediate formation of a peroxide or higher oxide, by the following mechanism:-



They noticed that catalytic channeling, by the liquid droplets, occurred during the Na₂CO₃ catalytic oxidation of graphite crystals and suggested that these droplets resulted from the formation of Na₂O₂ on the graphite surface during oxidation. It was also noted that gasification rates accelerated at temperatures around the melting point of the peroxide, not the carbonate.

Reaction (1) was proposed as thermal dissociation of most alkali metal carbonates to produce the corresponding oxides:-



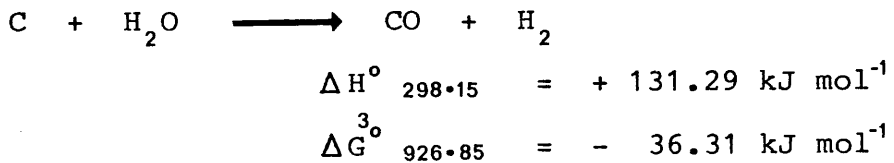
This reaction would only occur at around the carbonate's melting temperature (or at lower temperature in the presence of exceptionally low CO₂ pressures). However, the reaction:-



provides a sufficient thermodynamic driving force to make reaction (1) feasible. It is suggested that reaction (1) would be the rate determining step in this type of catalytic gasification as both reactions (2) and (3) are thermodynamically favourable for most M_2O species of relevance (negative ΔG° values).

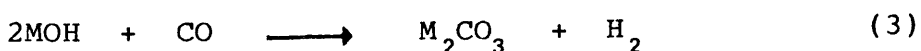
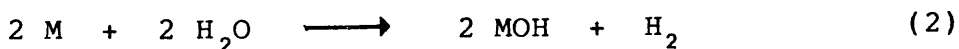
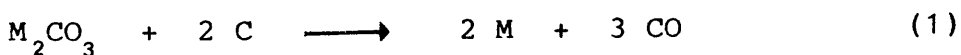
Catalytic Enhancement of the Carbon - Steam Reaction

The endothermic reaction between carbon and steam (water vapour):-

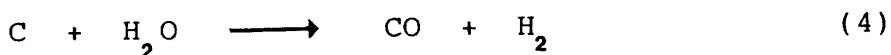


is favoured by elevated temperatures and reduced pressures, occurring very slowly below 1000°C in the absence of a catalyst.

McKee and Chatterji (1978) suggested a plausible mechanism for the catalytic action of alkali metal carbonates on the carbon - steam reaction:-



giving an overall reaction:-



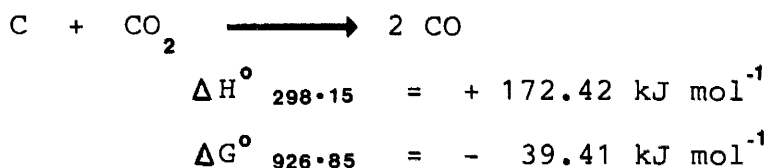
The alkali metal hydroxides probably act as unstable intermediates as LiOH and KOH would be unstable in an atmosphere of CO. The rate determining step in the catalysis sequence is probably (1), as this is the slowest reaction. The overall gasification rate will be dependant on the salt - carbon interfacial contact area, which rapidly increases as the salt melts and wets the carbon surface.

A careful study by Veraa and Bell (1976, 1978) on steam gasification of char produced from a sub-bituminous coal led to a proposal of a similar cycle to McKee and Chatterji's for the catalytic enhancement of this reaction.

Catalysed Carbon - CO₂ Reactions (Boudouard Reaction)

The catalytic gasification of carbon, in the presence of carbon dioxide, is the most important gasification reaction with respect to blast furnace chemical conditions. The volume of CO₂ and high levels of recirculating alkali metal species make it inevitable that some measure of coke degradation occurs via this process.

The Boudouard reaction is endothermic:-



The carbonates and oxides of the group IA metals have long been known to significantly catalyse the Boudouard reaction, with the salts of lithium being the most active.

McKee and Chatterji (1975) carried out an extensive study of catalysis of this reaction using alkali metal carbonates. They observed that gasification rates became accelerated at temperatures close to the melting points of the carbonate phase. Alkali metal was observed to have sublimed onto the quartz envelope of the thermobalance employed. This suggested that vapour phase alkali metal in a catalytic oxidation / reduction cycle might be involved.

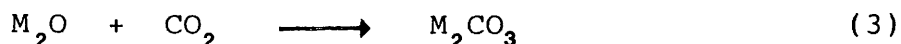
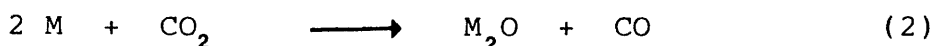
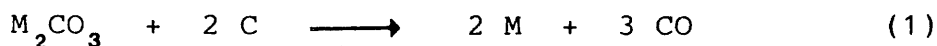
Vapourisation of alkali during catalysed C / CO₂ reaction had been previously reported by Fox and White (1931), although even after extensive outgassing in vacuum at 900°C enough alkali salt was retained to exert a strong catalytic effect on subsequent heating in carbon dioxide.

Observation of graphite flakes with particles of alkali metal carbonate dispersed on their basal planes (on a microscope hot stage) failed to show any catalytic channeling or particle mobility at temperatures of up to 1000°C. At temperatures above the melting points of the

carbonates, droplets of the molten salts remained motionless on the basal planes of the graphite (McKee and Chatterji, 1975). This proved that the catalytic mechanism employed in the case of the Boudouard reaction differed from that of catalytic gasification of carbon in an oxygen atmosphere.

There was no evidence of a stable existence of metal oxides, as these would readily have been converted to the carbonate species in the presence of carbon monoxide, even at relatively low temperatures. Jalan and Rao (1978) found, during a study on carbon black, that the kinetics of the catalytic gasification were similar whether the alkali metal oxide or alkali metal carbonate was added to the system initially.

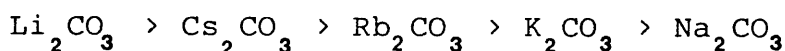
McKee and Chatterji (1975) considered that vapourisation of the alkali metal might suggest that the formation of free alkali metal would be an intermediate in the gasification reaction. They consequently proposed a reaction mechanism:-



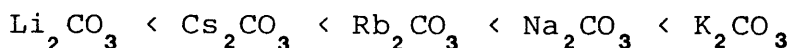
for the catalysed Boudouard reaction. Step (1) is likely to be the rate determining step. This would be consistent with the observation that the reaction proceeds slowly below, but rapidly above the carbonate melting temperature.

The authors further suggested that although reaction (1) has a positive ΔG° value in the normal gasification temperature range, sufficient pressures of alkali metal vapour might exist in the system for the catalytic gasification to occur, depending on the ambient pressure of carbon monoxide.

McKee and Chatterji also found during this study that the decreasing order of catalytic activity, for the alkali metal carbonates at a given temperature, was:-



while the melting points increased in the order:-



This explanation of increasing catalytic activity, based on the melting points of the materials, is convincing but seems incomplete when the reversal of K_2CO_3 and Na_2CO_3 are examined.

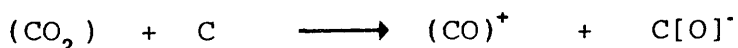
The formation of free alkali metal vapour is certainly important in the catalysed Boudouard reaction, but it may also involve other processes, such as the formation of solid - phase complexes of the alkali metal with the carbon, as suggested by Wen (1980).

The above discussion of catalytic gasification has approached the subject by assuming an oxygen transfer

mechanism. This system regards active catalysts, for carbon gasification, to be oxygen carriers which undergo oxidation / reduction cycles on the surface of the carbon. However, another general mechanism has also been proposed for catalytic gasification, which can broadly be classified as the electron transfer mechanism.

Long and Sykes (1950, 1952) attempted to formulate an electron transfer mechanism. This theory was based on the observation that many of the catalytically active substances have unfilled energy bands capable of accepting electrons from the carbon matrix, or alternatively can donate labile electrons to the matrix. The theory assumed a weakening of the carbon - carbon bonds at edge sites of the graphite sheets studied. Also assumed was a redistribution of the π - electrons and an increase in the carbon - oxygen bond strength, during the catalysed oxidation. This mechanism would therefore have implications for CO desorption which has often been cited as the rate determining step in carbon oxidations (Barton et al., 1973).

Hedden et al. (1959) modified the Long and Sykes model and introduced negatively and positively charged surface units.



representing the formation of a strongly chemisorbed oxygen atom and a weakly chemisorbed CO molecule. The oxygen atom is a strong acceptor and is able to find excess π -electrons

from the carbon lattice, the limiting factor therefore being the formation of the positively charged $(CO)^+$ groups. Hedden et al. suggested that electron donors at low concentrations would act as catalysts and electron acceptors as inhibitors.

Harker (1959) rationalised the catalytic effect of alkali metals, in the Boudouard reaction, by the same presumptions of electron transfer, although the interpretation was the opposite to that of Hedden et al.. Harker stated that the depletion of the π -electrons of the carbon upon oxygen adsorption and the concomitant formation of acceptor levels in the carbon were assumed to be the initial controlling factors in the process. The alkali metal's function was then in their ability to remove these additional acceptor levels.

Heuchamps (1960) discussed the electronic theory of catalysis. This discussion proposed that the chemisorption of oxygen is controlled by a double electrical layer of charge at the prismatic surface of the carbon. Impurities influencing the kinetics of carbon oxidation were then divided into three classes:-

- (1) Electron donors such as alkali metals, which form positive ions at the carbon surface, decrease the barrier of potential energy towards chemisorption of oxygen and cause increased oxidation of the carbon.

- (2) Electron acceptors, such as halogens, which form negative ions at the carbon surface, increase the potential energy to oxygen chemisorption and cause a decrease in carbon oxidation (inhibitors).
- (3) Transition metals which accept electrons into their unfilled d - shells thereby increasing carbon oxidation by the production of active sites of the carbon surface.

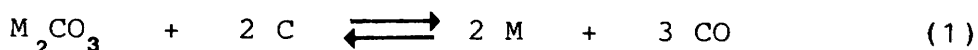
However, there has been limited success in tying together catalytic activity and properties such as ionisation and lattice energies. An earlier correlation thought to occur between the lattice energies of transition metal monoxides with the activation energy for catalytic oxidation of carbon (Heintz and Parker, 1966) has been disputed by Harris (1972).

Franke and Meraikib (1970) have described a variation of the electron transfer mechanism to account for the catalytic effects of alkali metal carbonates in both the C / O_2 and C / CO_2 reactions, by the formation of intercalation compounds between the alkali metal and the carbon matrix.

Wen (1980) has subsequently taken the idea of alkali metal lamellar compounds, with carbon, in conjunction with the cycles postulated by McKee and Chatterji to try to further explain alkali metal carbonate catalytic gasification of carbon.

The formation of lamellar compounds of alkali metals with carbon along with methods for their detection will be described later. It will suffice for the present discussion to state that insertion of alkali metals between the carbon layer planes creates charge transfer (CT) compounds, often referred to as electron donor - acceptor (EDA) compounds.

Wen states that the crucial step, in this method of catalytic gasification, using alkali metal carbonates is the primary formation of free alkali metal.

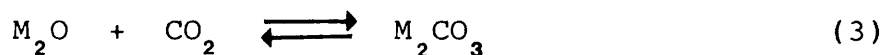
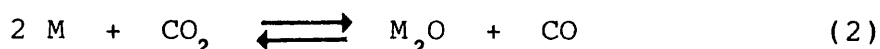
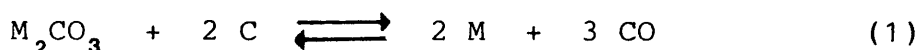


Once sufficient alkali metal is generated it can complex with aromatic carbons, graphite, soft carbons etc. to give rise to EDA complexes which proceed to catalyse the reactions of the surrounding carbonaceous materials with various gases.

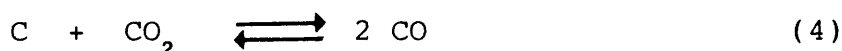
In an inert atmosphere, the heating of alkali metal carbonates with carbon will give rise to reaction (1). In the absence of carbon very little K_2CO_3 would thermally decompose when heated to $1000^\circ C$ at a pressure of one atmosphere of argon gas. However, when carbon is introduced to the system K_2CO_3 begins to react at temperatures as low as $800^\circ C$, with condensation of alkali metal having been observed on cooler parts of the reaction vessel (Fox and White, 1931; McKee and Chatterji, 1975, 1978). It is important to emphasise this mutual catalysis

as it implies the formation of low energy intermediates which Wen states can be identified as EDA complexes.

McKee and Chatterji (1975) postulated the series of reactions for catalytic gasification, by CO_2 , using alkali metal carbonates:-

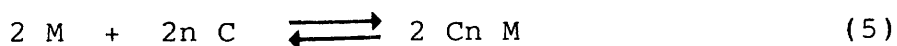


giving an overall reaction:-

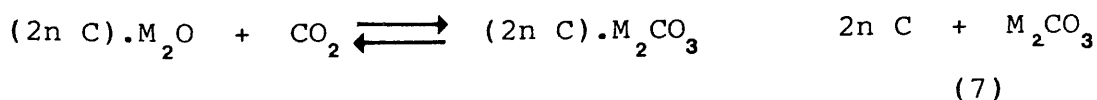
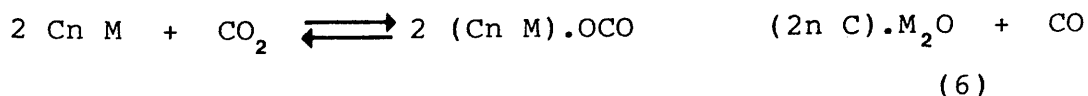


where $\text{M} = \text{Li}, \text{Na}, \text{K}, \text{Rb}, \text{Cs}$

Wen suggests that as soon as reaction (1) takes place and enough alkali metal is formed it will react with the carbon matrix to give rise to EDA complexes:-

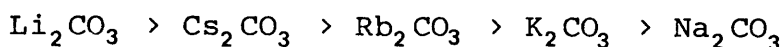


These EDA complexes will subsequently catalyse the carbon gasification with CO_2 :-

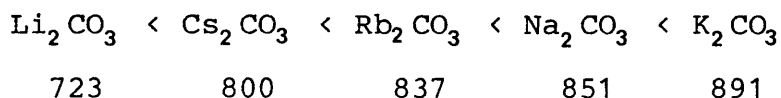


where $n =$ 6, 12, 18 for Li
 $n =$ 64 for Na
 $n =$ 8, 24, 36, 48, 60 for K, Rb, Cs.

As previously mentioned McKee and Chatterji (1975) found the decreasing order of catalytic activity for this reaction to be:-



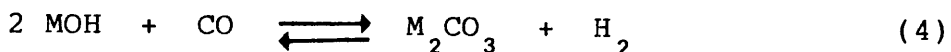
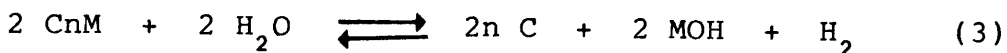
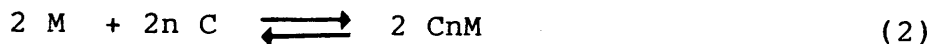
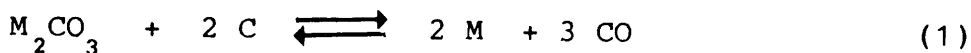
and that the increasing order of melting points to be:-



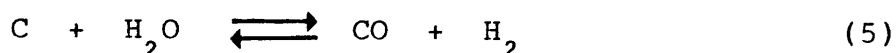
(melting points given in degrees centigrade).

Thus explaining to some extent the order of catalytic activity, apart from the anomaly of the reversed order of K_2CO_3 and Na_2CO_3 . However, the ionisation potential for graphite is 4.39 eV while those of sodium and potassium are 5.14 eV and 4.34 eV respectively. The fact that the ionisation potential of sodium is greater than that of graphite, while that of potassium is smaller, may explain why sodium does not form many of the intercalates formed by potassium. Thus the order of catalytic activity of the metal - graphite complexes is $\text{K} > \text{Na}$ and this apparently dominates over the melting temperature for these two carbonates.

Wen has also proposed a similar mechanism for, alkali metal carbonate, catalysed steam gasification of carbon:-



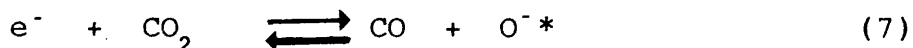
giving an overall reaction:-



Franke and Meraikib (1970) suggested that the doping of the graphite crystals with an electron donor would enhance the chemisorption and dissociation states:-



and

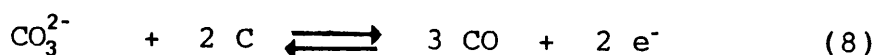


where * indicates an adsorbed species.

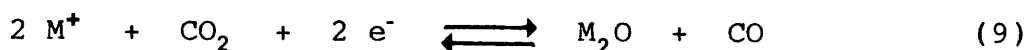
thereby accelerating the overall gasification rate.

Jalan and Rao (1978) have published an "electrochemical" mechanism for alkali metal carbonate catalysis of the Boudouard reaction. Their mechanism suggests that the alkali metal carbonate, above its melting temperature, will form a thin layer of electrolyte over the carbon surface. Carbonate ions then react to give CO at the anodic sites on

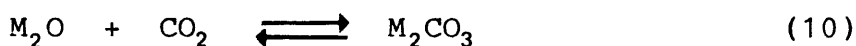
the surface:-



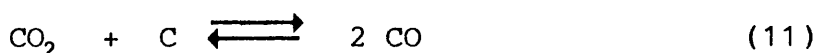
The alkali metal cations migrate through the melt and electrons are transferred through the carbon substrate to neighbouring cathodic sites, to facilitate CO reduction:-



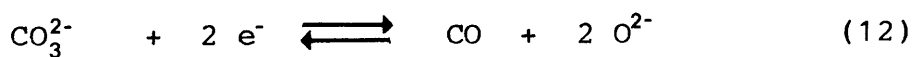
The resulting M_2O being converted to M_2CO_3 with ambient CO_2 :-



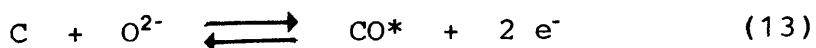
giving an overall reaction:-



Thus two separate types of reaction sites (anodic and cathodic) on the carbon surface are assumed to occur separately. Wagner (unpublished) proposed the simultaneous electrochemical reaction:-



(cathodic)



(anodic)

with desorption following:-



where * represents an adsorbed species.

However, it must be stated that at this stage there is not enough evidence to unambiguously decide which mechanism is the "true" mechanism for catalytic gasification of carbonaceous materials, each mechanism having its own merits.

The mechanisms of catalytic gasification of coal and coke are much more complex than those of graphite, due to the inhomogeneity and more complex structure of these materials. For example, the presence of various inorganic materials may catalyse the gasification of coal and coke in a variety of ways, In contrast the cross linkages, in coal and coke, hinder gasification as does the occurrence of sulphur, which can poison the metal catalysts. The presence of silica minerals may also hinder gasification by binding alkali and other metals, converting them to silicates and thus restricting the recirculation of the metal catalysts. Thus, it would be expected that higher levels of catalyst would be required, for coal and coke, in order to obtain similar rates of gasification to those of graphite.

Although of obvious importance, gasification is not the only way in which alkali may react with carbonaceous materials.

1.8.2 Intercalation Compounds

The highly anisotropic nature of graphite, with strong bonding within each layer and relatively weak van der Waals bonding between layers, makes it possible for certain chemical species to penetrate between the carbon layers, forming what are referred to as intercalation compounds.

Intercalation compounds of carbon have been known since 1841, when Schafhaeütl reacted graphite with bisulphate. The first alkali metal compounds were discovered by Fredenhagen and Cadenbach (1926) and Fredenhagen and Suck (1929). These compounds are amongst the oldest lamellar compounds known.

The penetration of guest species between the carbon layers results in expansion of the carbon material, in the c-axis direction. Intercalation is normally a stage process, where the region between the expanded carbon layer planes is called a gallery.

Since these earlier studies, much work has been carried out on the formation of intercalates and characterisation of them. There have been a number of recent reviews of the subject by researchers, such as Riley (1945), Hennig (1959), Croft (1960), Ubbelhode and Lewis (1960), Novikov et al. (1971), Ebert (1976) and Selig and Ebert (1980). Three main classes have been distinguished; non-conducting, lamellar and residue compounds.

1.8.2 (a) Non - Conducting Compounds

These type of compounds have sp^2 hybridised carbon which forms a covalent bond with the intercalate. In this manner the aromatic character of the graphite planes is destroyed and the planes become puckered, thus leading to a loss in conducting ability compared with the original graphite. One of the best known of these type of compounds is $(CF)_n$ (Ruff and Brettsneider (1934); Rudorff and Rudorff (1947), where n is an integer.

1.8.2 (b) Residue Compounds

Residue compounds are formed when a lamellar type intercalation compound (see subsequent section) decomposes. Due to the highly reactive nature of the lamellar compounds they readily degrade when exposed to water, air, heat, mechanical stress and even vacuum, to give rise to residue compounds. When the lamellar type compound decomposes it loses most of the intercalated material. However, a definite proportion of intercalate remains within the carbon and it is this which constitutes the residue compound.

The structure of these residue compounds was proposed by Hennig (1952) and Ubbelohde (1957), to be the remaining intercalate trapped at crystal imperfections. However, Maire and Mering (1959) proposed that single layers of intercalate were present between perfect and imperfect layer planes, having observed the X-ray structure of a

bromine residue compound.

The amount of intercalate retained in the residue compound appears to be dependent on the nature of the parent lamellar compound, which is in turn likely to be dependent on the original carbon. However, given a fully intercalated compound, it would appear that the amount of remaining intercalate in the residue compound is fairly constant.

Daumas and Hérold (1971), in considering the bent layer model, proposed that the residue compound was composed of a mixture of graphite and very dilute intercalation compounds. However, studies by electron microscopy (Heerschap and Delavignette, 1967) have indicated that residue compounds are in the form of small isolated loops (islands) of intercalation compound pinned at crystal imperfections.

1.8.2 (c) Lamellar Compounds

These types of compounds arise when the intercalate assumes an ordered arrangement within the graphite lattice, occupying in the most concentrated case every interplanar spacing. In less concentrated compounds the intercalate will occupy every second, third or more interplanar space thus giving rise to the various stages or degree of intercalation. It should be noted that the inserted reagents are partly ionised (Rudorff and Hoffman, 1938), which implies that the carbon layer is able to give or

receive electrons. The separation of the carbon layers in order to form a lamellar compound involves energy. The formation of such a compound also commonly involves a reduction in entropy. This can be considerable in the case where the material to be inserted between the layers is in the gaseous state and becomes a guest species in a highly ordered arrangement. Two types of lamellar compounds can then be distinguished, dependent on whether or not the carbon layers are positively or negatively charged in the intercalated compound which is formed.

Typical electron acceptors are halogens and bisulphate and common electron donors are alkali metals. These reagents interact with the conduction band of graphite by accepting or donating electrons and thus altering the electrical and magnetic properties of graphite (McDonnell et al. 1951; Hennig and McClelland, 1955; Hennig, 1956, 1960; Ubbelohde, 1961). The resulting intercalation compounds have been described (Dzurus and Hennig, 1957; Robert et al. 1973) using the nomenclature of semiconductors, p-type compounds (positive) are those in which the carbon layers have given up electrons to the inserted reagent and n-type (negative) in which the carbon layers have become negatively charged through acceptance of electrons from the intercalated material.

The formation of an intercalated compound is often accompanied by a change in colour and always by a macroscopic swelling of the carbon. The swelling property is readily confirmed by X-ray evidence and is easily

explained by the fact that the carbon layers must move apart to make room for the inserted reagent layers. The metallic type colour change (some are steel blue and some have a copper tint) implies a change in the electronic state of graphite, which is confirmed by electrical conductivity measurements made after insertion. Often the intercalated lamellar complexes exhibit a ten to twenty fold increase in conductivity after intercalation has taken place.

1.8.2.(d) Electronic Structure of Graphite

The highly anisotropic nature of graphite makes it possible to distinguish between the sigma electrons, which provide the bonds within the carbon layer, and the pi electrons, which are alone responsible for the lamellar and electronic properties. The energy levels of the pi electrons form a continuous series which constitutes a valence band for the ground state of graphite and a conduction band for excited states.

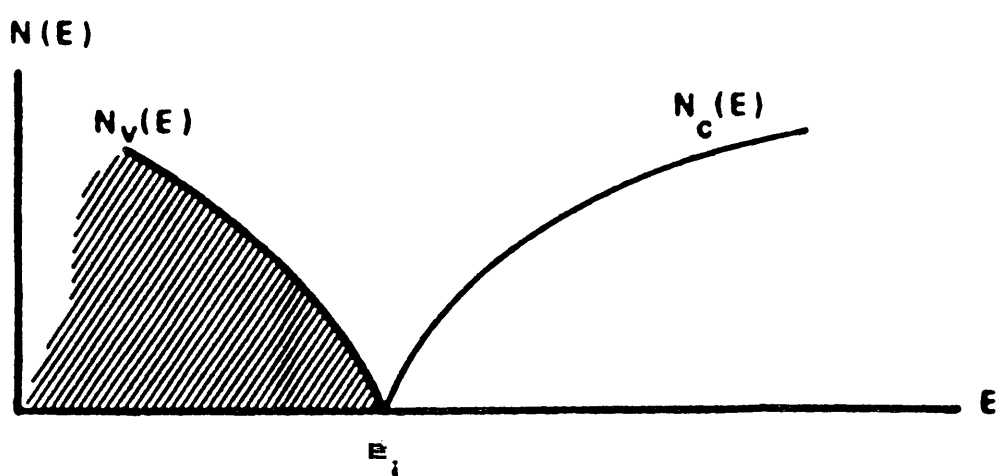
The bonding of the planar sigma bonded layer (ab plane) is enhanced by the pi bonding derived from a combination of the pz orbitals of each carbon atom. The carbon layers are chemically and physically robust and do not appear to be markedly changed on reduction or oxidation. The removal of electrons from the valence band (pi orbitals) or addition of electrons to the conduction band (antibonding pi orbitals) decreases the strength of the bonding in the layers. This intercalation does effect small changes in

the ab plane dimensions. The effective van der Waals thickness (0.335nm for pure graphite) does not however appear to be markedly changed by oxidation or reduction.

Since in most circumstances intercalation does not lead to gross changes in the carbon layers, it is useful to use the band structure of graphite to understand the electronic properties of graphite intercalation compounds. In view of the weak interlayer bonding in graphite it is sufficient to treat the band structure of the material as that of an isolated layer, that is to deal with it simply as a two dimensional model.

Figure 16 illustrates schematically the density of states $N(E)$ of the electrons in graphite as a function of their energy and shows the highly characteristic structure of these bands. E_i is the point at which the conduction band $N_c(E)$ and the valence band $N_v(E)$ meet. The valence band is completely filled and the conduction band completely empty for pure graphite. This results in the Fermi level (highest energy level occupied, E_f) coinciding with E_i . This is strictly only true at absolute zero. Above this point electrons pass from the valence band to the conduction band (increasing with rising temperature). For practical purposes though, E_i can be equated with E_f for pure graphite. The Fermi level can be derived from the electronic work function and is found to be 4.39 eV for pure graphite.

The semi-metallic nature of graphite means that it can



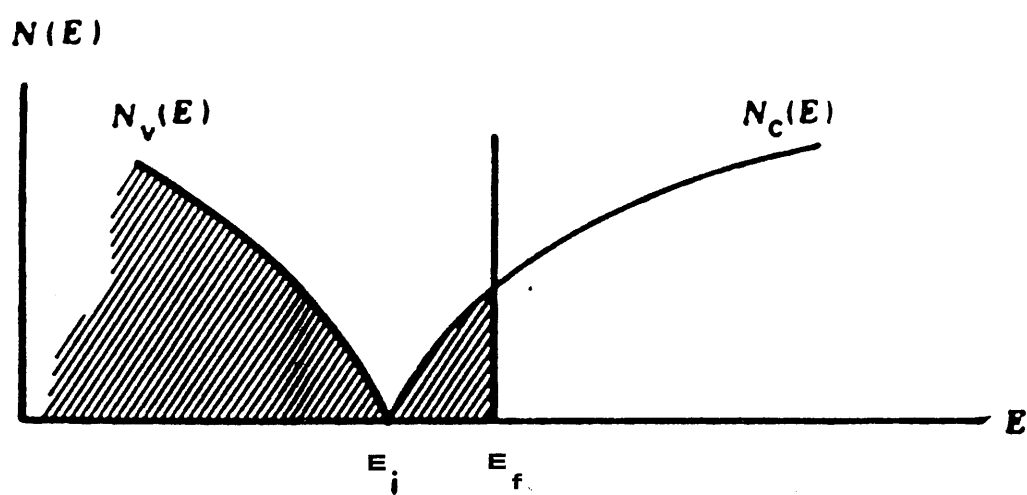
The density of states, $N(E)$, of electrons as a function of their energy on a basis of a two-dimensional model.

FIGURE 16

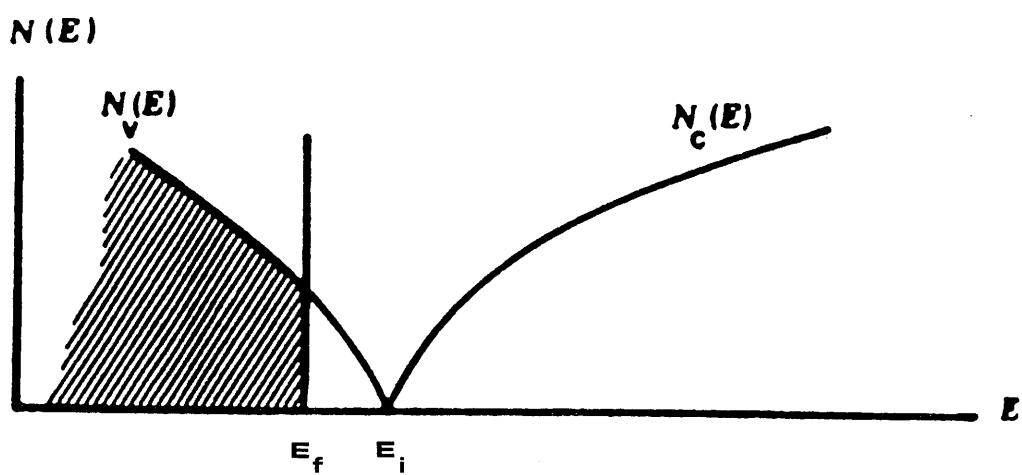
either be a donor or an acceptor of electrons and thus the work function corresponds both to the ionisation potential and electron affinity of graphite. Addition or removal of electrons results in a population of the valence band or a depopulation of the conduction band respectively.

Figure 17 illustrates the band structure situation for n-type compounds, of which the alkali metals are an example. The intercalating alkali metal is partially positively ionised. This ionisation is due to a transfer of electrons to the graphite from the alkali metal, thus partially filling the conduction band. In this case E_f is greater than E_i and E_f marks the position of the highest energy level populated after insertion of the metal. As a consequence there is a marked increase in the conducting properties of the graphite, after intercalation has taken place.

Figure 18 illustrates the band structure situation for p-type intercalation compounds, of which the halogens are an example. Here the inserted layer is partially negatively charged due to a transfer of electrons from the carbon layers to the inserted material. This results in a depopulation of the valence band. Once again E_f marks the highest energy level populated but in this case E_f is less than E_i . The observed high electrical conductivity of these compounds is a result of the appearance of new charge carriers, which are the vacancies created in the valence band by the removal of electrons, and are therefore positive.



Electronic Structure of n-type Compounds



Electronic Structure of p-type Compounds

The representation of the electronic band structure of graphite has been confirmed by analysis of a number of properties including electrical conductivity, magnetic susceptibility and determination of the sign of the Hall effect coefficient.

However it must be remembered that the three dimensional structure of graphite gives rise to a more complex situation than the one described above. The major difference is that in the three dimensional case the layer-layer interactions, although merely van der Waals, results in overlap of the valence band and the conduction band. This overlap means that the conduction band contains some electrons and the valence band some holes.

The two dimensional model for the band structure may be satisfactory for first stage graphite compounds, when the intercalates are large closed shell species, which provide no effective overlap of orbitals with the P_z orbitals of graphite. Where the graphite compounds contain intercalants which possess partially filled or vacant orbitals, the resulting overlap with the carbon layer P_z orbitals would result in chemical bonding. It is therefore unlikely that the two dimensional model is accurate in these cases.

The simple model as such is unlikely to be totally satisfactory for describing the situation of intercalation of alkali metal and alkaline earth metal intercalates in graphite. The observed increase in c-axis electrical

conductivity of these compounds, relative to pristine graphite (they approach three dimensional metallic behaviour), appears to point to overlap of the valence orbitals of the intercalant with the Pz orbitals of the carbon (Bartlett and McQuillan, 1982).

As the main interest of this thesis is in the effects of alkali metals on the structure of metallurgical coke, further discussion of intercalation compounds will be restricted to insertion of alkali metals into the carbon matrix.

There are generally five main methods of preparation of intercalation compounds of potassium.

1. The preparation employed by Fredenhagen and Cadenbach (1926). This involved direct heating of a mixture of graphite and potassium, in a sealed ampoule, to between 300°C and 400°C . This produced C_8K and C_{16}K compounds.
2. Fredenhagen and Suck (1929) prepared C_9K and C_{18}K compounds by maintaining the graphite at a fixed temperature (400°C - 500°C), while varying the temperature of the potassium from 200°C to 400°C or 500°C .
3. Hérolld (1951, 1955) reported the formation of C_8K , C_{24}K and C_{40}K compounds. These were prepared by maintaining the potassium at around 250°C while changing the temperature of the graphite from 250°C to 600°C .

4. Rudorff et al. (1954 (a), 1955, 1959) prepared a large number of graphite compounds by reacting the graphite with solutions of alkali metals in ammonia, methylamine and pyridine at temperatures between -100°C and -50°C . Liquid ammonia produced a ternary lamellar graphite compound. In the case of the C_8K compound some of the potassium enters into solution with the ammonia to form $\text{C}_{12.5}\text{K}(\text{NH}_3)_2$ whereas in the case of C_{24}K hardly any of the potassium is removed from the graphite. The compound formed is $\text{C}_{28}\text{K}(\text{NH}_3)_{2.8}$.

5. Stein et al., (1965, 1967), prepared alkali metal lamellar compounds by exchange between graphite and aromatic radical-ions such as sodium naphthalene in tetrahydrofuran. The equilibrium quantity of potassium intercalated in this reaction is independent of the radical anion but the rate of reaction is dependent on the radical anion.

Also found was that 80% of the potassium penetration in this reaction takes place in the first five hours. It also appears that the reaction reaches completion after a further thirty-five to forty hours (Scott et al., 1934; Paul et al., 1956; Haijitink et al., 1956), based on the reaction of alkali metals with aromatic hydrocarbons.

The thermal decomposition of these compounds was studied by Nominé and Bonnetain (1967) who showed that both lithium and sodium formed various phases with the solvent depending on the degree of solvation, although potassium graphite has only one phase at room temperature and will eventually lose

its intercalated solvent.

The synthetic methods employed in the formation of alkali metal intercalates distinguish two separate classes of alkali metal. Potassium, rubidium and caesium all react readily with graphite when a standard two bulb technique is employed. Lithium only reacts with graphite in this manner at much higher temperatures or pressures and lithium carbide is a common impurity in the product formed. The sodium compound is extremely difficult to prepare and is relatively poorly characterised. This has led to speculation that the ionisation potentials of the elements are involved. The ionisation potentials of K, Rb and Cs lie below the electron affinity of graphite, whilst those of Li and Na lie above. More accurately a sum of the ionisation potential and sublimation energy of the element has more meaning than purely the ionisation potential. However, the sum of these two properties leads to generally the same conclusions (c.f. previous section on catalytic gasification).

With respect to sodium it is possible to distinguish two classes of carbon. Generally sodium can be said not to form intercalation compounds with graphite. However several reports have been made of sodium intercalation with non-graphitised carbons (Roberts et al., 1973; Berger et al., 1975). It has been suggested (Bartlett and McQuillan, 1982) that for reducing intercalants, such as the alkali metals, interlayer cross-linking aids intercalation, due to a lowering of the Fermi level by the cross-linkages.

However, with respect to potassium this does not necessarily imply that it should intercalate into more readily non-graphitised carbon than graphite. The ease of intercalation will be determined by the potential of the material to intercalate (ionisation potential of the intercalant compared with the electron affinity of carbon) and also the mechanism of intercalation, in particular the accessibility of the graphite basal planes to the intercalant.

1.8.2 (e) Mechanism of Intercalation

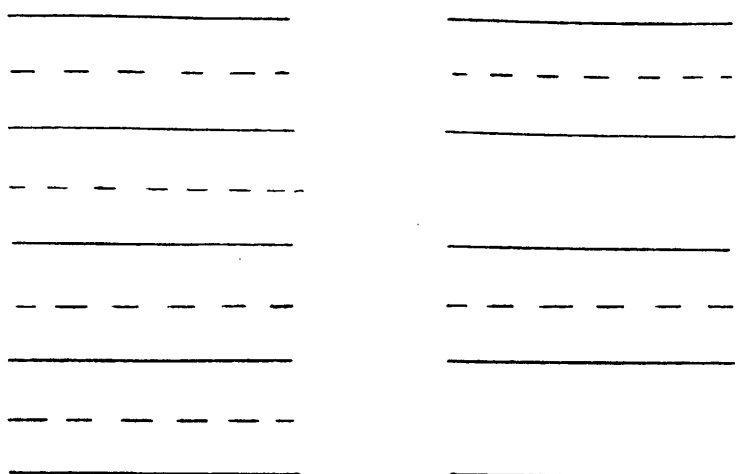
Mechanistic studies of the intercalation have only been carried out on a relatively small number of systems. Hooley (1977) was the first to demonstrate that bromine intercalation (Br_2) is determined by basal plane adsorption. This was determined by observing that no Br_2 insertion into graphite occurred if the basal planes were coated with wax. These experiments also demonstrated that the regions nearest the basal planes open first. The stage of the intercalate obtained was dependent on the partial pressure of the intercalant with a first stage compound being formed at the highest activity.

It would seem quite likely that intercalation of a variety of materials into graphite occurs in a similar manner to that of Br_2 . That is, the process involves adsorption of the guest species onto the basal (001) plane of graphite followed by electron transfer between the intercalant and graphite and subsequent opening of galleries.

Many turbostratic carbons also seem to be able to produce intercalation compounds similar to graphite. A large proportion of these turbostratic carbons possess a considerable ultramicroporosity. It therefore seems illusory to attempt to distinguish in these structures between condensation of a metal in this porosity (where the walls are to a great extent graphitic layers) from intercalation.

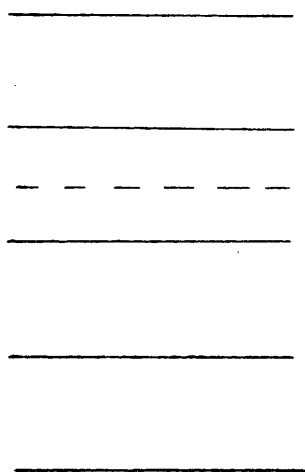
1.8.2 (f) Structure of Intercalate

Information on the structure of the potassium graphite compound has been obtained mostly using X-ray methods (Vol'pin et al., 1971). The studies carried out by Schleede and Wellman (1932), Rudorff and Schultz (1954(b)) and by Hérolld (1955) enabled a model for the structure of these compounds to be proposed. The compound can be formed in a number of stages (Figure 19). In the stage I compound (C_8K) every interplanar space in graphite is occupied by potassium. In the Stage II compound ($C_{24}K$) every second interplanar space is occupied by potassium. Several stages have been formed. In 1962 Matayuma obtained a range of compounds up to stage XI, Salzano and Aronson (1967) reported the occurrence of $C_{10}K$ and Hérolld and Carton (1972) demonstrated the presence of a non-stoichiometric phase present between C_8K and $C_{24}K$, which is thought to be a first stage compound in which the metal atoms are disordered. It appears that the filled layer, in the intercalated compound, has a constant thickness for a given intercalate and that the unfilled layers have a constant



STAGE I

STAGE II



STAGE III

——— CARBON LAYER
 ----- POTASSIUM LAYER

Simple Intercalation Model

FIGURE 19

thickness identical to that of the original graphite. X-ray techniques have also shown that there is order within the potassium layer, and that the potassium atoms are arranged in a triangular pattern in the most concentrated compound C_8K (figure 20). In the higher stage compounds the potassium rearranges to form a hexagonal pattern which would result from movement of atom A out of the lattice. Another phenomenon discovered by X-ray analysis is the superposition of graphite layers adjacent to the intercalate. The stacking sequence in graphite then becomes A/A or B/B etc., where / denotes the presence of the intercalated species.

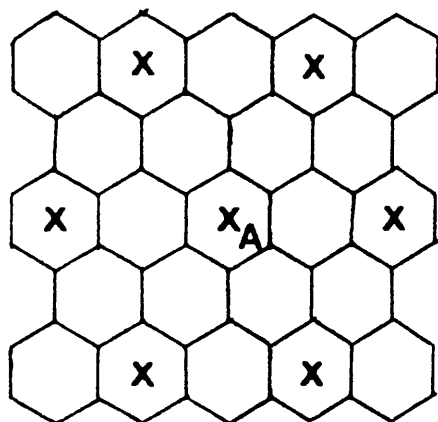
The potassium intercalate not only possesses long range order within the layer but also long range order down through the graphite layer planes. In fact the potassium atoms lie on well defined sites above the graphite planes, giving rise to a superlattice.

Parry and Nixon (1968) reported that the carbon networks remote from the potassium may undergo particle displacement unlike those layers directly adjacent to the metal intercalate, which undergo complete displacement. These workers also suggested that for the stages the arrangement would be;

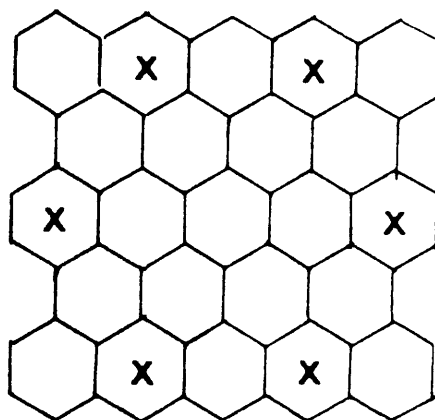
Stage II	AB	K	BC	K	CA	KA
----------	----	---	----	---	----	----

Stage III	ABA	KA	CA	KA
-----------	-----	----	----	----

Stage IV	AB	ABK	BC	BC	K	CACA	KA
----------	----	-----	----	----	---	------	----



(a)



(b)

X Potassium

(a) Arrangement of potassium in graphite c-plane for C_8K .

(b) Arrangement of potassium in graphite c-plane for $C_{24}K$.

Hérolld's Model

Daumas and Hérolld (1971) proposed another model for the structure of lamellar compounds, to explain the results of their studies of the chemical reactions between oxygen and other volatile oxides, with potassium / graphite intercalation compounds. Their experiments demonstrated that the lamellar compounds rapidly transformed from one stage to another, as the reaction proceeded. They found that these observations were hard to equate with the stage model as proposed by Robert and Schultz and thus formulated the "bent layer" model.

The bent layer model has received experimental support from direct imaging studies of the graphite / FeCl_3 system (Thomas et al., 1980) and although different in structural aspects from the stage model in no way would alter the compound's characteristics, with respect to its other physical and chemical properties. The first stage of the bent layer model agrees with that of the stage model, as a compound composed of alternating carbon and potassium layers with a C:K ratio of 8:1. However in the second and subsequent stages the two models differ (Figure 21). The stage model suggests that a change from a stage I to a stage II compound not only involves a redistribution of the alkali metal to a dodecahedral structure but also involves the complete removal of every second layer of potassium. With the new model, all the interlayer spacings are occupied by equal quantities of the intercalate no matter what the stage of the compound and each interplanar space

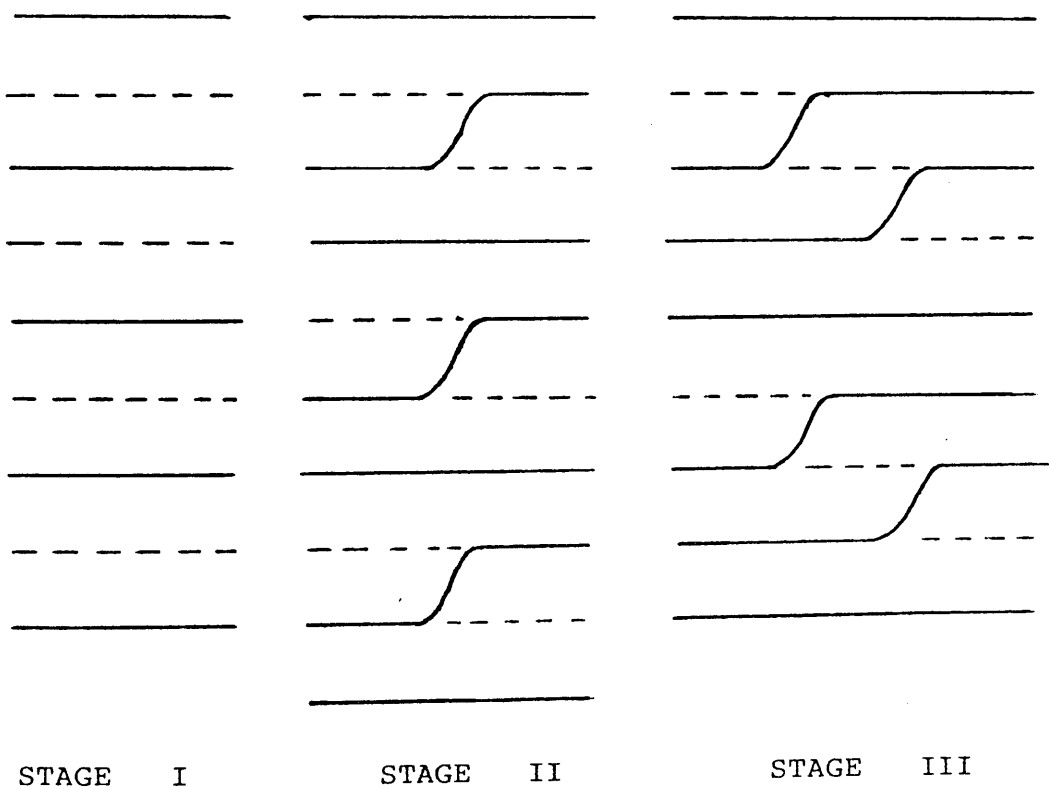
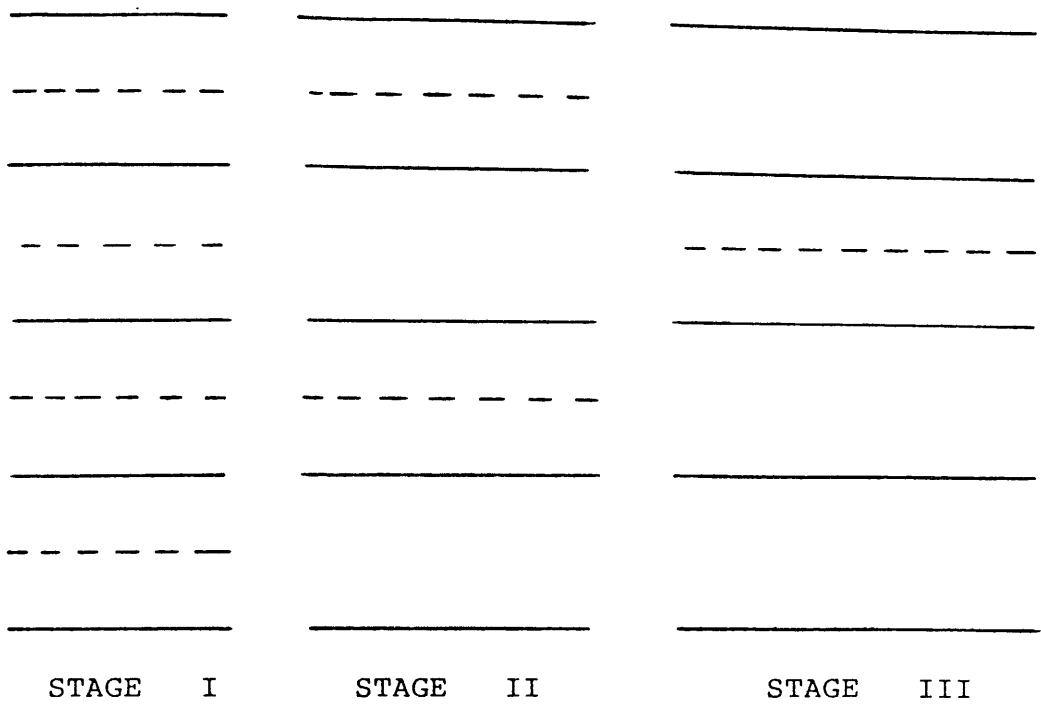


FIGURE 21

Herolds Bent Layer model

is portioned into domains occupied by one layer of metal, which expands the c-axis spacing and empty domains where the original c-axis spacing is conserved. Superposition of the full and empty zones preserves the characteristic stacking sequence. Thus changing from a stage I to stage II compound, or a higher stage, involves just an increase in the areas unoccupied within a layer.

1.8.2 (g) Characterisation of Intercalates

Detection of graphite intercalates can be accompanied by a comparison of the electrical conductivity and magnetic properties of the product compounds with the original carbon material. However, the characterisation of the guest species and the compounds in general prove a major experimental challenge. The use of longer wavelength electromagnetic radiation is limited, as it ordinarily does not penetrate beyond the surface layers. Infrared spectroscopy usually samples the surface of the material whilst the shorter wavelength, Raman spectroscopy, can excite depths of up to 100 nm. Similar difficulties can arise with NMR spectroscopy and ESR measurements have not entirely proved unambiguous. Highly penetrating hard X-rays can measure bulk structural features and is a very useful technique, often applied, in structural studies of these compounds. Detailed structural information on residue compounds is often difficult to obtain by conventional X-ray diffraction techniques, as the data is collected from a relatively large volume of sample and thus produces only an averaged structure.

The availability of high resolution electron microscopy (HREM), which can resolve particular lattice planes of the sample, provides the ideal tool for obtaining structural information. Thus the nature and occurrence of intercalation compounds and residue compounds, which have been formed from the decomposition of the parent intercalated material, can be inferred directly from imaging studies using HREM.

1.8.2 (h) Electron Microscopy of Carbon Intercalation

Compounds

Interlamellar compounds of graphite with bromine and iodine were studied by Eeles and Turnbull (1963, 1965), using electron microscopy, electron diffraction and X-ray diffraction. It was found that the bromine was highly ordered and that a residue compound ($C_{28}Br$) with a two dimensional structure, consisting of bromine molecules orientated with respect to the graphite layer planes. It was also found that the structure was independent of the graphite used. Transmission electron microscopy showed the presence of loop and line defects, which moved rapidly due to the heating effect of the electron beam. These defects were similar to those found by Heerschap et al., (1964) in the residue compounds of bromine and iodine monochloride and were interpreted as dislocations with stacking fault contrast on one side which formed boundaries of intercalated areas. It was also found that the carbon layers on either side of the intercalant had shifted to an AA stacking sequence. A proposed mechanism for the

production of residue compounds involved movement of boundary dislocations, which would leave behind areas of occluded reactant on their way through the crystal.

In the graphite / ferrric chloride case it was found that the direction of the burgers vector for the boundary dislocations was perpendicular to the c-planes and therefore the graphite had altered the ABAB... stacking sequence. Dislocation loops of ferric chloride were found (Heerschap et al., 1964; Heerschap and Delavignette, 1967). The formation of the residue compound of ferric chloride / graphite was shown to proceed by dissociation of the intercalated compound into free graphite and a ferric chloride inclusion.

The concentrated potassium / graphite and the residue compounds of sodium and potassium have been studied by Haplin and Jenkins (1971). It was found that both sodium and potassium remained in the graphite in the form of intercalated rafts, even after heating to 1100°C . It was also found that there was AA stacking in the intercalated areas. Some heavily doped material gave a diffraction pattern which was ascribed to a thin epitaxial layer on the surface of the graphite. The authors also found a diffraction pattern which they attributed to a potassium superlattice, with a spacing of 0.426 nm and which they reported as corresponding to a C_{10}K structure. The characteristic features of the heavily doped material included dot moire patterns, ring defects line moire patterns and bright discs. They proposed that the ring

defects or contoured areas were moire patterns caused by tilted lenticular defects. The bright discs were shown to arise from electron absorption and probably indicate a gap in the intercalated potassium.

Evans and Thomas (1975) studied potassium / graphite, graphite / bromine, graphite / ferric chloride and the ternary compounds of graphite / ferric chloride by high resolution electron microscopy. The electron diffraction pattern for the graphite / potassium compound corresponded to the pattern obtained by Halpin and Jenkins (1971) for the surface epitaxial potassium film on the heavily doped complex. Also in agreement with Halpin and Jenkins they also found potassium in hexagonal islands with orientated edges. When powdered SP1 graphite was used for intercalation it was shown, from interplanar spacings, that the potassium was intercalated at random in the residue compound.

Several other authors have made important contributions to the understanding of carbons and their intercalated compounds by HREM including Carr, 1965; Saunders, 1978; Millward and Jefferson, 1978.

1.9 Aim of Present Work

One of the most important roles which metallurgical coke fulfils is the formation of a permeable matrix within the blast furnace. This matrix, of coke lumps, allows the gases to ascend and molten material to percolate to hearth.

In order that furnace efficiency is kept at a high level the permeability of this matrix must also remain at a high level. Metallurgical coke is the only solid constituent in the high temperature regions of the blast furnace and small changes in the properties of the material, in this environment, can have profound effects on the matrix voidage, by reduction of coke strength.

The object of the present work has been to elucidate the effects of the modern blast furnace on the metallurgical coke employed in the process of iron ore reduction. This has been in the hope that factors detrimental to coke strength may be identified and subsequently removed or at least have their effects mitigated.

To this end a comparison of the microstructure of coke entering the furnace with coke removed from the high temperature regions of the furnace has been made. The majority of this work has involved analysis of the microstructural aspects of the coke and the changes induced therein. The most suitable tool for this type of work is the high resolution transmission electron microscope. Thus the majority of coke analysis was carried out using HREM with a variety of other analytical techniques being used to complement HREM results and to investigate properties not suitable for analysis by HREM.

Comparisons having been made between the feed and ex-tuyere cokes, the objective was to induce, in the laboratory, any structural effects which had been observed to have occurred

during the coke's passage through the furnace. Successful replication of any structural changes would identify the parameters involved in inducing these changes.

Analysis of these laboratory reacted samples was carried out in a similar manner to those employed for examination of the feed and tuyere cokes.

Subsequent to identifying the influencing parameters an attempt was made to determine the relative role each of the factors had in altering the structure of the coke material. Undoubtedly major changes in the coke's microstructure would have considerable effects on the strength of the material, which would be observed by an increased production of fines and a reduction of the mean lump size.

Detailed knowledge of coke structure, induced structural changes and relative effects of the parameters involved would enable conclusions to be drawn as to the most suitable methods to increase coke strength by eliminating or reducing the effects of the influencing parameters.

Electron Microscopy

2.1 History and Development

In 1931 the first electron microscope was built by Knoll and Ruska (Knoll and Ruska, 1932) with the first high resolution instrument, capable of resolving $0.05\mu\text{m}$, built in 1933 by the same pioneers, thus greatly improving on the information obtainable from the light microscope.

In 1924 de Broglie discovered the wave nature associated with an electron, which in turn suggested that, as the wavelength of an electron was shorter than light, improvements could be offered on light microscopy. Since the advent of the first electron microscope the search has been to build instruments with constantly increasing resolution, with the hope of imaging molecules and even atoms.

Electron optical theories and development of the instrument have been extensively reviewed (Zworykin et al., 1945; Hillier and Vance, 1945; Coslett, 1951, 1970, 1981; Hall, 1953; Hirsch et al., 1965) with practical techniques used in modern microscopy described by Kay (1965). Modern day commercial electron microscopes can approach atomic resolution, for suitable specimens, with resolution of atoms and atom clusters having been achieved for various systems (Hall and Hines, 1970; Murata et al., 1976; Iijima, 1977; Fryer, 1983; Smith et al., 1983).

Figure 22 shows the basic structural design and transmission operational mode of a high resolution electron microscope. The illuminating source is a fine beam of electrons, generated from a hot cathode emitter. The emitter usually takes the form of an electrically heated tungsten hairpin filament, owing to its high melting point, low vapour pressure and high mechanical strength. An increase in source brightness can be obtained using special pointed tungsten filaments (Wolf and Joy, 1971) or from lanthanum hexaboride cathodes (Ahmed, 1971) and field emission cathodes (Crewe et al., 1968) can replace electrical heating, with similar benefits.

In the electron gun the beam of electrons is accelerated through a potential of thousands of volts and an electromagnetic condenser lens system focuses the beam onto the specimen. A double condenser system is normally employed for high resolution studies. The first condenser lens produces a highly demagnified image of the electron source. This beam of reduced cross-section is then projected onto the specimen surface by the second condenser lens. This gives a very small minimum spot size, with the advantage of enhanced brightness over a small area. A three lens system (objective, intermediate and projector) magnifies the electron image of the specimen (up to one million times) onto a fluorescent screen or an image intensifier screen (both used for viewing) or onto a photographic plate to record the image detail.

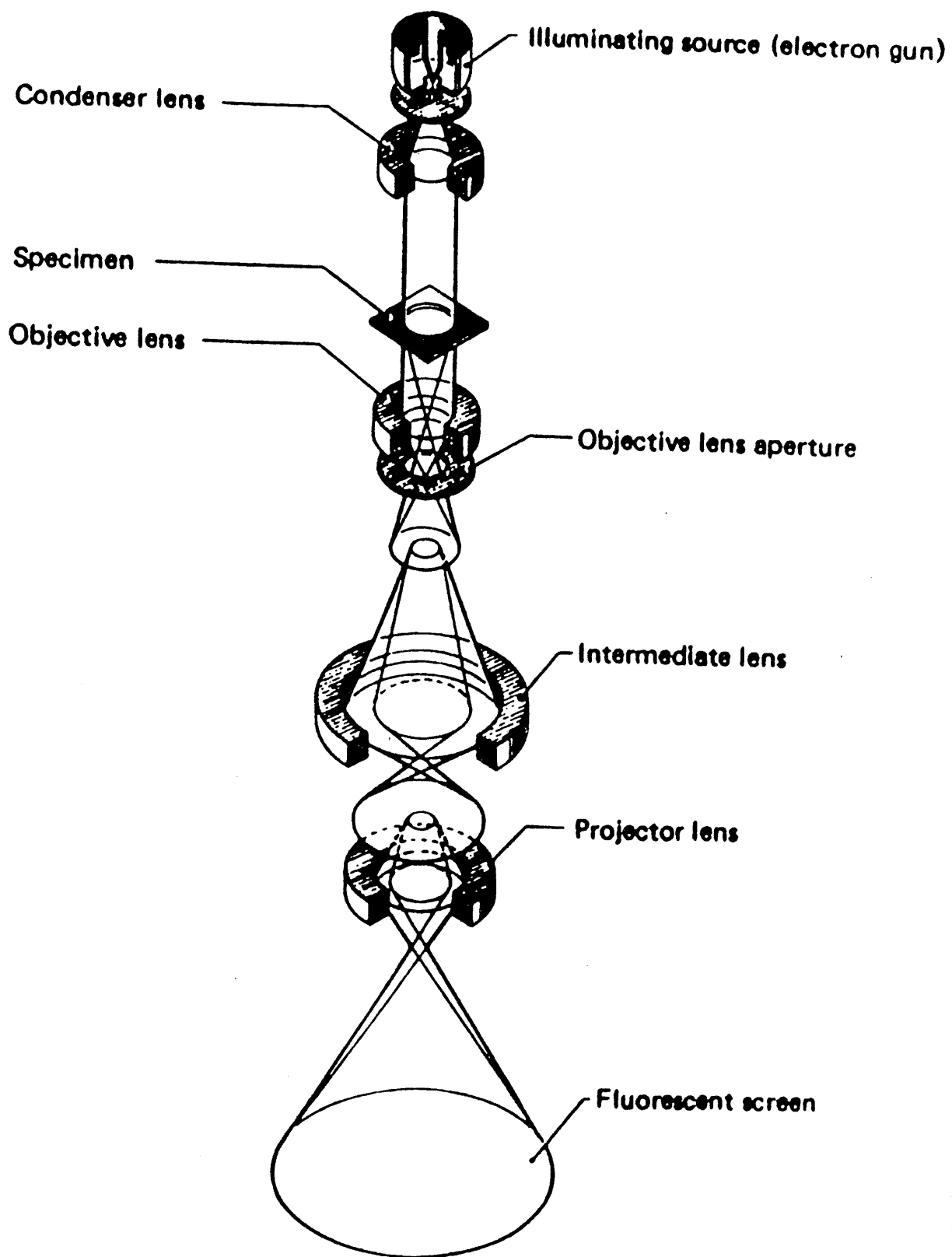


FIGURE 22

Basic Structural Design of a TEM

The objective lens detects, transmits and magnifies the modified electron beam and therefore its performance is critical to the overall microscope performance. Light microscopy employs a series of convergent and divergent lenses to compensate for individual lens defects. However, the nature of electrostatic lenses is always convergent and as such lens defects cannot be compensated for in the same manner as in light microscopy. High resolution TEM (transmission electron microscopy) thus requires an objective lens of extremely high quality. The intermediate and projector lenses, although less critical to overall microscope performance, transmit and further magnify the modified electrons from the objective lens.

The information which can be recovered from TEM is contained in the electrons scattered during passage through the specimen. The information desired is represented by perturbations in the electron waves. Electron optical defects can cause similar perturbations. However, if these are suppressed to a lower level than specimen perturbations then meaningful resolution may result, although interpretation can be complicated by lens aberrations.

2.2 Electron Scattering by the Specimen

The electron microscope is based on the principle of interaction between fast electrons and the electrostatic potential of the specimen (coulomb interactions). Almost all the incident electrons pass through (assuming that the specimen thickness is not too great), with only those

passing close to the atoms being deflected. This situation is described by Schrodinger's wave equation (Schrödinger, 1926) :-

$$\hbar^2 \nabla^2 \psi(r) - e \phi(r) = -i \hbar d\psi(r)/dt$$

In which $\psi(r)$ is a wave function such that $\psi(r)^2$ is the probability that an electron will be present in a unit volume. The electrostatic potential is described by $\phi(r)$; m is the mass of the electron and e is the charge on the electron. Solving this Schrodinger equation for electrons of a single energy describes the effect of the specimen on the incident electrons. The two dominant mechanisms of electron scattering are:-

- 1/ Elastic scattering occurs when the electrons of the probe interact with the nuclei in the specimen and are deflected without any loss of energy. The scattering angles are related, in crystalline specimens, to the geometry of the crystal lattice and to the electron wavelength by the Bragg law.
- 2/ Inelastic scattering is produced when the electrons of the probe interact with the orbital electrons of the specimen and are deflected with a loss of energy. Inelastic interactions with delocalised electrons in the specimen can give rise to collective oscillations of the whole system of conduction electrons, and is known as plasmon scattering (Pines, 1956, 1963).

Increasing atomic number, of the specimen nuclei, or increasing specimen thickness increases the elastic scattering of electrons. If elastic scattering occurs at very large angles to the optical axis of the incident electron beam, or if an aperture is inserted such that electrons scattered greater than the aperture angle are cut out, then image contrast arises and is referred to as "mass thickness" contrast or amplitude contrast, or for a specimen with a defined periodic structure "diffraction contrast". In such cases, areas of the specimen from which elastically scattered electrons have been removed are dark in contrast.

In inelastic scattering small deflections are imparted to the electrons along with alterations to their energies and hence their wavelengths. Recombination of these inelastically scattered electrons with similarly altered unscattered electrons results in increased or diminished intensities in the image contrast, depending on the relative phases of the interacting waves. This phenomenon is referred to as inelastic phase contrast. Elastic phase contrast correspondingly can be obtained if the aperture allows transmission of the phase altered elastically scattered electrons. Amplitude is again increased or diminished in the image contrast if focus conditions are selected to allow recombination of these with the undeviated electrons. If the elastically scattered electrons arise from a periodic structure in the specimen (for example a crystalline specimen with at least one lattice plane orientated parallel to the beam direction)

then a related periodicity in the image may be obtained. This information may only be obtained for periodicities normal to the electron beam. This is the basis for "lattice imaging" in high resolution TEM. Small periodicities normal to the electron beam produce widely elastically scattered electrons. These will be transmitted by a sufficiently large objective aperture, but will be focused at off-axis parts of the objective lens, as a consequence of lens aberrations which thus severely effects phase contrast image retrieval and interpretation.

Thin specimens ($< 10\text{nm}$) are the only ones for which elastic and inelastic phase contrast effects can be easily interpreted. Electrons entering thin specimens can be imagined to undergo only single scattering events and thus conform to kinematic approximations (Whelan, 1959; Hirsch et al., 1965). In reality, kinematical theory can be considered only a rough guide. Multiple scattering of electrons occurs and a more rigorous and accurate treatment has been developed to account for scattered amplitudes and phases in this case (Cowley and Moodie, 1957).

2.3 Contrast Transfer and Retrieval of High Resolution

Information

Scherzer (1949) considered the theoretical resolution limit of the transmission electron microscope and derived a wave mechanical formulation of image formation. This formulation took account of interactions of the incident electron wave with the specimen and subsequent effects of

the electron-optical system in transforming the propagated wave to the image plane. Thus the basis for the transfer theory of electron microscopy was formed- the idealised linear transfer theory, the limiting case of the more rigorous dynamical approach (Cowley and Moodie, 1957). The former can be qualitatively applied to meet most high resolution studies with the following salient features.

The specimen is regarded as a weak phase object (Grinton and Cowlie, 1971; Lynch and O'Keefe, 1972), single scattering conditions apply and scattered wave amplitudes are considered to be much smaller than those of the primary wave.

The image contrast, represented by the intensity transmitted to the image plane, can be explained quantitatively by consideration of the amplitude of the elastically scattered electrons forming the diffraction pattern in the back focal plane of the objective lens. Phase modulations, induced by the specimen and by defects in the electromagnetic objective lens are then accounted for and the resultant wave amplitudes are combined to form the amplitude distribution in the image plane. The intensity distribution can then be computed and corresponds to the contrast observed in the micrograph, if the stated approximations hold.

In mathematical terms, for a coherent, monoenergetic plane electron wave of unit amplitude, the effect of passage through a weak phase / amplitude object can be represented

by the equation:-

$$\psi_o(r) = \exp [i\delta \phi(r)] \quad (i)$$

In which : ψ_o is the transmitted amplitude of the object wave (ϕ).

r represents the real space coordinates.

i indicates the phase nature of the object.

δ is the interaction constant $\pi / \lambda w$, where λ and w are the relativistically corrected electron wavelength and accelerating potential, respectively.

If the approximation of the weak phase object holds, then the higher order terms in $\delta \phi(r)$ can be neglected and the equation becomes:-

$$\psi_o(r) = 1 + i\delta \phi(r) \quad (ii)$$

The Fourier transform (F) of this object wave gives the transmitted amplitude in the back focal plane (the diffraction plane) of the objective lens. Electromagnetic lenses are not perfect; the electrical and mechanical defects are accounted for by the inclusion of a phase modulator, $\chi(s)$, where (s) denotes reciprocal space coordinates. The objective aperture is also situated in the back focal plane of the objective lens and so therefore

an aperture function $A(s)$ is inserted, with value one inside the aperture, and zero elsewhere. The wave function in the diffraction plane is then:-

$$\psi_D(s) = F[\psi_o(r)] \exp[i\chi(s)] A(s) \quad (iii)$$

Under single scattering conditions, the resultant amplitude distribution is given by the difference between the primary undeviated wave amplitude, $\delta(s)$, and the elastically scattered amplitude distribution represented by (iii). Substituting for $\psi_o(r)$ from (ii), and performing the Fourier transform operation for all (s) inside the objective aperture gives:-

$$\psi_D(s) = \delta(s) - (\delta \phi(r) \sin\chi(s) - i \delta \phi(r) \cos\chi(s)) \quad (iv)$$

A second (inverse) transform of (iv) corresponds to the image plane and gives rise to the resultant amplitude distribution:-

$$\psi(r) = 1 - F(\delta \phi(r) \sin\chi(s) - i \delta \phi(r) \cos\chi(s)) \quad (v)$$

and the intensity distribution in the image plane (that observed on the micrograph) is given by:-

$$\begin{aligned} I(r) &= \psi \psi^* \\ &= 1 - 2 \delta \phi(r) * F \sin\chi(s) \end{aligned} \quad (vi)$$

where * indicates a convolution integral. Equation (vi) represents the intensity distribution in the image plane, within the limits of the weak phase approximation (Grinton and Cowlie, 1971; Lynch and O'Keefe, 1972) used in its derivation. The diffracted amplitudes were shown to be modified by an instrumental function. More correctly, the instrumental transfer function modulates the phases of the diffracted waves, as shown by equations (ii) and (iv). However, in the case of the weak phase object the imaginary terms are second order, so that the image intensity, calculated from the modulated diffraction amplitudes, holds good but only for these kinematic conditions. Despite these limitations equation (vi) demonstrates the importance of $\sin \chi(s)$, called the Phase Contrast Transfer Function (PCTF), which determines the transfer of object information to the image plane. For perfect lenses $\sin \chi(s) = 1$, and equation (vi) becomes:-

$$I(r) = 1 - 2\delta \phi(r) \quad (\text{vii})$$

and the object and the image are linearly related. The defects present in magnetic lenses preclude this possibility. However, an instrumental phase adjustment factor $\chi(s)$, first derived by Scherzer (1949) takes account of the main lens defects:-

$$\chi(s) = 2\pi / \lambda [\Delta f \alpha(s)^2 / 2 - C_s \alpha(s)^4 / 4] \quad (\text{viii})$$

where: $\alpha(s)$ is the scattering angle pertaining to reciprocal space coordinate (s).

C_s is the spherical aberration coefficient of the objective lens.

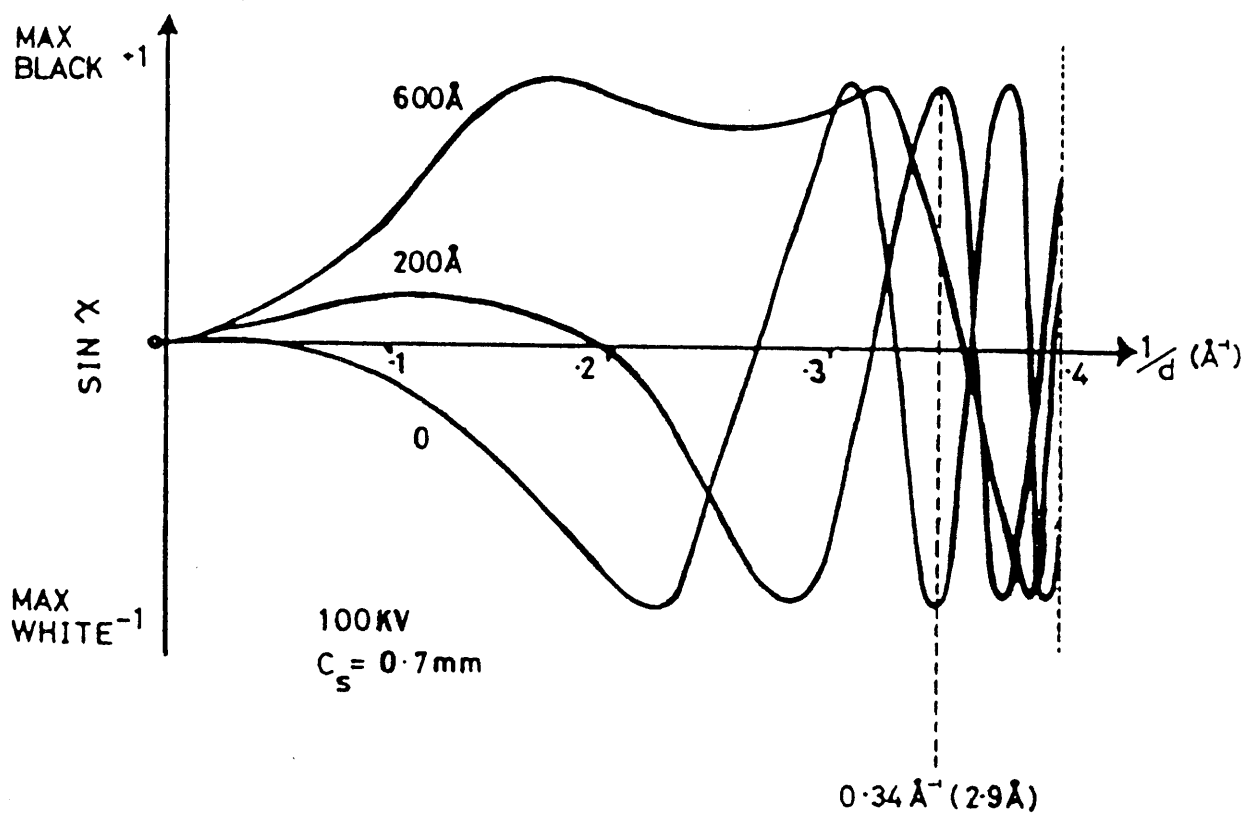
Δf is the lens defocus value.

The final image contrast is therefore dependent on the oscillatory function $\sin\chi$, having different values at different spatial frequencies, depending on the scattering angle for the particular frequency, the defocus value and the spherical aberration of the objective lens. Figure 23 shows $\sin\chi$ plotted against reciprocal periodicity $[1/d \text{ nm}^{-1} (= \lambda/\alpha)]$, assuming coherent illumination over a range of defocus values. The diagrams pertain to Jeol JEM 100 C microscope operated at 100 KeV. The polepiece spherical aberration coefficient for the microscope was $C_s = 0.67 \text{ mm}$ with an aperture of $50 \mu\text{m}$.

For most applications, it is desirable to operate the microscope at a defocus value where the appropriate transfer function value is identical and near unity over the maximum range of spatial frequencies, without contrast reversal. This "optimum defocus" value $\Delta f'$, first found by Scherzer (1949) is given by:-

$$\Delta f' = 1.2 \sqrt{C_s \lambda} \quad (\text{ix})$$

For the Jeol 100 C microscope $\Delta f'$ is equal to 60nm, as



Phase Contrast Transfer Functions for a range of defocus values, $\Delta f = 0, 200 \text{\AA}$ and 600\AA underfocus, with a $\sim 50 \mu\text{m}$ objective aperture cut-off.

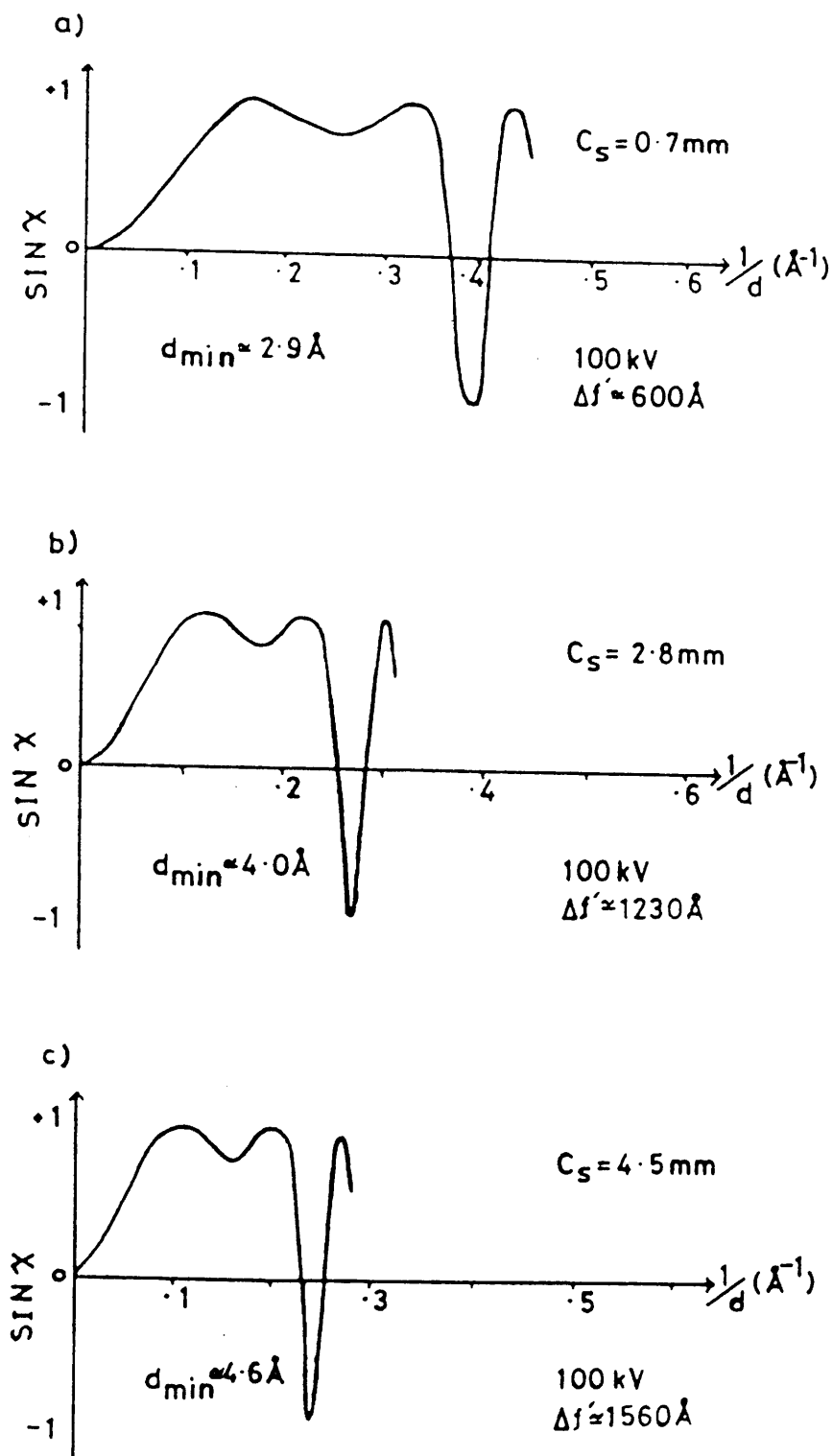
shown in figure 23. Figure 24 (a, b and c) shows the resolution loss with increasing Cs value for the optimum defocus value at 100 KeV.

The Scherzer cut-off, d_{min} , was calculated (Eisenhandler and Siegal, 1966) as :-

$$d_{min} = 0.65 C_s^{0.25} \lambda^{0.75} \quad (X)$$

The optimum defocus defines the limit of the most faithful reproduction over the maximum range of spatial frequencies. However, smaller structures can be resolved, in good contrast, if the appropriate defocus value is selected. For example, in the figure 24 a structural periodicity of 0.29 nm (0.34 nm^{-1}) would be imaged at high contrast at 20 nm defocus or in reverse contrast at zero defocus. However, greater care is required in image interpretation as the absence of detail from other periodicities can lead to spurious effects and thus erroneous observations.

The discussion so far has assumed (unrealistically) an electron source of perfect spatial and temporal coherence. In reality, the electron microscope has a finite source size and the electrons emitted are not completely monochromatic, so for a more complete treatment of the transfer theory these must be accounted for. This has been achieved by the inclusion of envelope functions (Hanzen, 1971; Hanzen and Trepte, 1971; Misell, 1973; Frank, 1973; Boerchia and Bonhomne, 1974).



Optimum defocus phase contrast transfer curves
for increasing spherical aberration coefficient

(a) $C_s = 0.7 \text{ mm}$ (c.f. JEOL 100 C UHR);

(b) $C_s = 2.8 \text{ mm}$ and (c) $C_s = 4.5 \text{ mm}$.

If the electron source approximates to a small disc-shape as determined by the final condenser lens aperture, and if chromatic aberration is assumed to arise from sinusoidal modulation of the finite energy electrons by the high voltage system and objective lens current, then the phase contrast transfer function can be further modified:-

$$\sin \chi_{\alpha, \epsilon} = \sin \chi(s) \cdot E_{\alpha}(s) \cdot E_{\epsilon}(s) \quad (\text{xi})$$

where: $E_{\alpha}(s)$ is the envelope function representing damping of the PCTF, due to partial coherence.

$E_{\epsilon}(s)$ represents the PCTF modification due to chromatic fluctuations.

However, this combined equation is an approximation as the partial coherence function is defocus dependant. A more correct description would be given by integration over an appropriate focal range. Frank (1973) showed that the coherence and chromatic envelopes have the form:-

$$E_{\alpha}(s) = \frac{2 J_1 [2 \pi \alpha (C_s \alpha^3 - \Delta f \alpha) / \lambda]}{2 \pi \alpha (C_s \alpha^3 - \Delta f \alpha) / \lambda} \quad (\text{xii})$$

$$\text{and } E_{\epsilon}(s) = J_0 (\pi \lambda \cdot \xi / d^2) \quad (\text{xiii})$$

where: J_0 and J_1 are the zero order and first order
bessel functions respectively.

α is the specimen illumination angle.

ξ is the focal variation due to high voltage
(v) and lens current (I) fluctuations,

given by:-

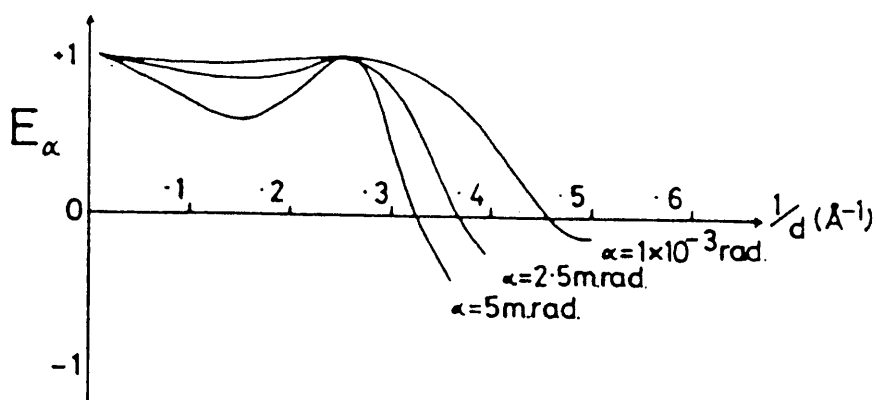
$$\xi = (\Delta V / V + 2 \Delta I / I) C_c \quad (\text{xiv})$$

C_c is the chromatic aberration coefficient
(1.1 mm for Jeol 100 C microscope fitted with a
UHR polepiece).

The coherence also depends on the illuminating angle α .
For a Jeol 100 C UHR, with conventional tungsten hairpin
filament, $\alpha \leq 1$ milliradian is possible at low beam
currents, and can be consistently obtained with pointed
filaments (Ohno, 1974).

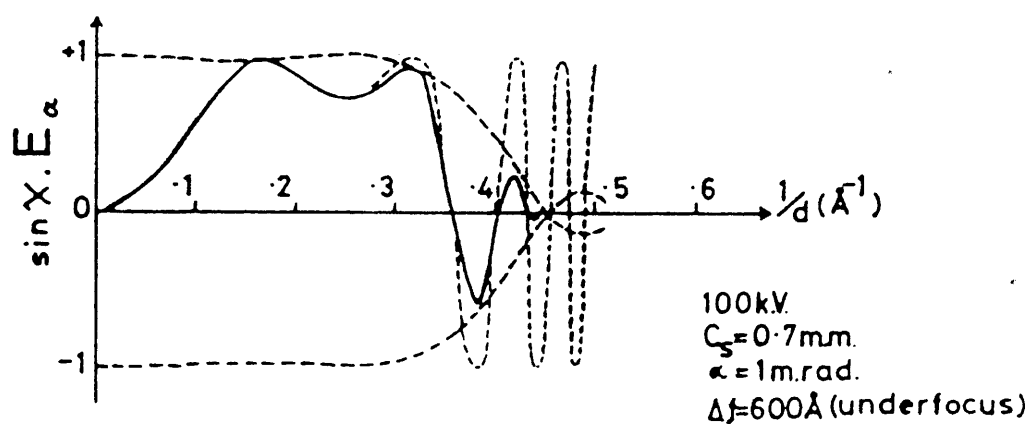
Figure 25 (a) shows respective envelope functions and
increased resolution loss for larger illumination angles.
Figure 25 (b) shows the optimum defocus PCTF modified for
illumination angle $\alpha = 1$ milliradian.

The effect of chromatic spread is shown in figure 26 (a)
for several focal variations (ξ). Calculations made for a
Jeol 100 C $\xi \leq 500$ nm, as calculated from (xiv), with



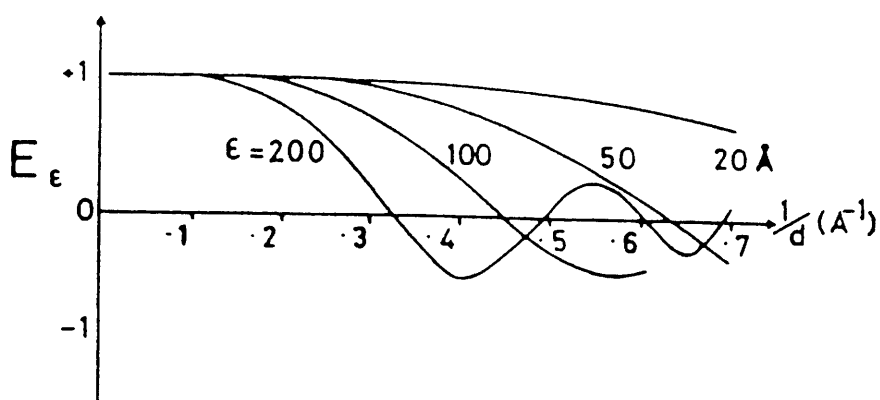
(a)

Partial coherence envelope functions for various specimen illumination angles (α).



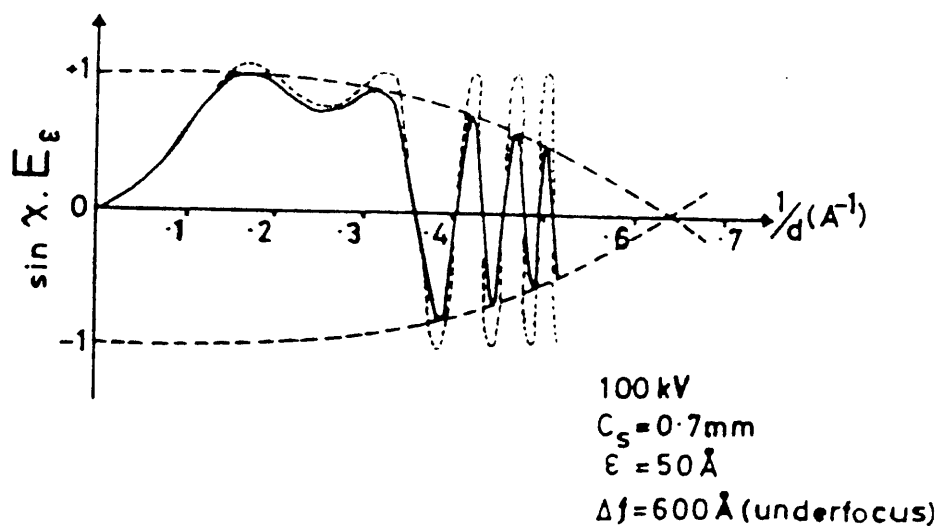
(b)

Optimum defocus Phase Contrast Transfer Function, modified for specimen illumination angle $\alpha = 1$ m.rad.



(a)

Chromatic aberration envelope functions for several focal variations (ϵ).



(b)

Optimum defocus Phase Contrast Transfer Function, modified for focal variation $\epsilon = 50$.

$\Delta V / V \leq 2 \times 10^{-6} \text{ min}^{-1}$, $\Delta I / I \leq 1 \times 10^{-6} \text{ min}^{-1}$ and $C_c = 1.1 \text{ mm}$. Figure 26 (b) shows the optimum defocus PCTF modified for chromatic focal variation $\mathcal{E} = 500 \text{ nm}$.

Phase contrast transfer theory thus provides a good guide, within the stated approximations, to the high resolution performance which can be expected.

Realistically, the kinematic approximations used in the derivation of the PCTF theory break down. Multiple scattering of electrons occurs as real specimens do not behave as ideal phase objects. To obtain the exact amplitudes and phases of the scattered waves the more rigorous dynamical treatment of Cowley and Moodie (1957) must be applied. In this approach, the object is assumed to be made up of thin slices, each an individual weak phase object scattering electrons only once. The Schrödinger equation is set up to describe an electron in the periodic potential of an infinite perfect crystal. Idealised boundary conditions are then applied and the model object becomes a series of planar potentials, projected normal to the electron beam, separated by vacuum gaps. Summation of successive phase and amplitude changes induced in the incident wave is then used to describe the resultant object wave.

Solutions can be obtained to varying degrees of approximation; the "two beam" condition assumes only the existence of the primary beam and singly diffracted beams. This condition, applied to a single slice, establishes the

analogy with the kinematic derivation.

More commonly, "n - beam" calculations are carried out using as many beams and slices as computer storage and time will allow.

Detailed mathematical treatment of dynamical theory have been outlined by various authors (Cowley and Moodie, 1957; Lynch and O'Keefe 1972; Allpress et al., 1972; Goodman and Moodie, 1974; Cowley, 1975).

2.4 Other Limitations to Retrieval of High Resolution

Information

2.4.1 Astigmatism

The effect of astigmatism, most critical in the objective lens, can limit the information available from TEM. Astigmatism arises from rotational variation in the focal length of the lens, and can be due to inaccuracies in manufacture, in homogeneities in the soft iron polepiece or can be induced by contamination within the microscope column, causing distorting fields due to charging. The latter can be minimised by maintaining extreme cleanliness on all surfaces, especially apertures, which are exposed to the electron beam. A compensating field is applied to correct residual astigmatism, this is established when the grain of a carbon support film appears symmetrical, or a symmetrical fresnel fringe is obtained around a hole in a "holey" carbon film (Haine and Mulvey 1954).

2.4.2 Specimen Contamination

The build up of amorphous, usually carbonaceous material on the specimen, enhanced by the electron beam, obscures fine structure in the specimen and causes a general loss of clarity. The residual atmosphere inside the column of an electron microscope will contain the normal atmospheric gases, oxygen, nitrogen, carbon dioxide and water vapours of hydrocarbon compounds. These may have originated from vacuum pumping fluids, vacuum sealing gaskets ('O'-rings) and any removable parts, e.g. specimen holders or stubs, plates or film holders, which are handled directly by the operator when they are removed from the microscope. Under normal conditions there will be a thin layer of hydrocarbon adsorbed on all surfaces within the column, including the specimen. Electron bombardment polymerises the surface film and permanently fixes it in place. The depleted surface layer of hydrocarbon is replenished by continued condensation of vapour and by diffusion of fresh condensed material inwards across the surface from outside the electron bombarded area. Thus, a permanent deposit grows on the specimen surface whenever it is under examination. The deposit is referred to as "contamination" and its rate of formation as the "contamination rate".

Modern electron microscopes reduce this problem by the attachment of anti-contaminators or by maintaining an extremely high and clean vacuum by the use of dry pumps such as a sputter ion and turbomolecular system. Anti-contaminators normally take the form of liquid -

nitrogen cooled jackets around the specimen area, to remove organic and other contaminant vapours by preferential condensation. Kumao et al. (1981) examined experimentally the effect of energy, temperature and electron current dependence on the contamination rate in a TEM. The conclusions were that when the density of the electric current illuminating the specimen is of the order of $10^{-3} \text{ A cm}^{-2}$, the contamination is proportional to $(V / C)^2$, where V and C are the velocities of the electrons and light respectively.

2.4.3 Specimen Stability

Specimen damage under electron beam irradiation is significant in most cases and is prohibitive to the study of many organics and polymers in which it can lead to total loss of specimen structure (Holland, Fryer and Baird, 1983), Fryer (1979) has tabulated critical doses for various organic and polymeric species and the topic has been surveyed by Jones (1975); Glaeser et al. (1975). Methods of extending the "lifetime", of the crystallographic structure of beam sensitive materials, have been investigated with encapsulation techniques (Fryer and Holland, 1984; Holland, 1984) proving extremely successful.

To aid focus adjustment, with these types of specimen, image intensifiers have been used at low beam doses (English and Venables, 1971; 1972) and minimal exposure techniques have been developed (Williams and Fisher, 1970) so that the specimen is subjected to exposure to the

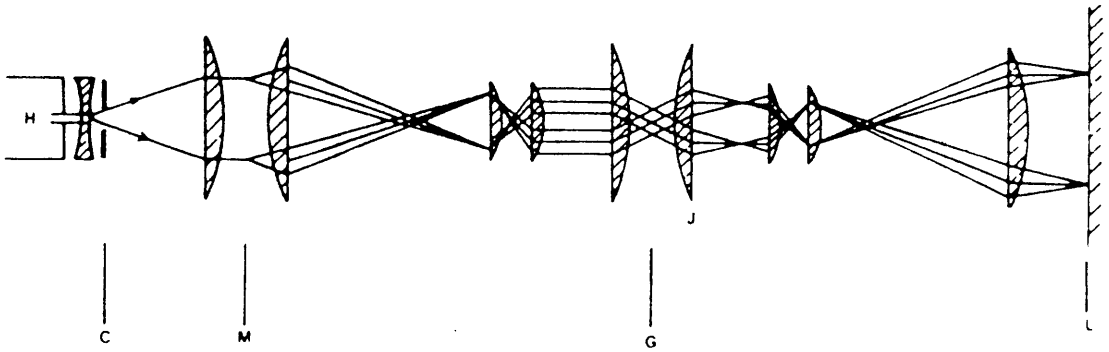
electron beam only for the duration of the photographic exposure.

2.4.4 Mechanical Stability

Mechanical stability, mainly residual drift in the specimen stage, can adversely affect microscope performance, especially during high resolution imaging. In the present study, equilibration under high resolution conditions was carried out and X-ray film was often used to reduce exposure times and thus minimise the effect of mechanical drift.

2.5 Optical Processing

To aid interpretation of high resolution micrographs, it is common practice to record a "focal series" of micrographs by successive stepwise variation of the objective lens defocus value. Such series reflect the difference in high resolution image content due to the variation in contrast transfer properties with defocus, as discussed previously. These differences can be quantitatively detected by producing optical diffraction patterns (optical transforms) from the micrographs using laser optics, on an "optical bench" as shown in figure 27. The optical transform provides an intensity map of spatial frequencies pertaining to the optical density distribution on the micrograph and therefore reflects the microscope transfer function at the time the micrograph was recorded. Spatial frequencies for which no information is contained in the micrograph



H - 1 mW Helium - Neon Laser; C - Collimator; M - Specimen;
 G - Optical Diffraction Pattern; J - Imaging Lens;
 L - Screen (image)

Ray diagram of Polaron optical diffractometer, showing position of object, diffraction pattern and reconstructed image.

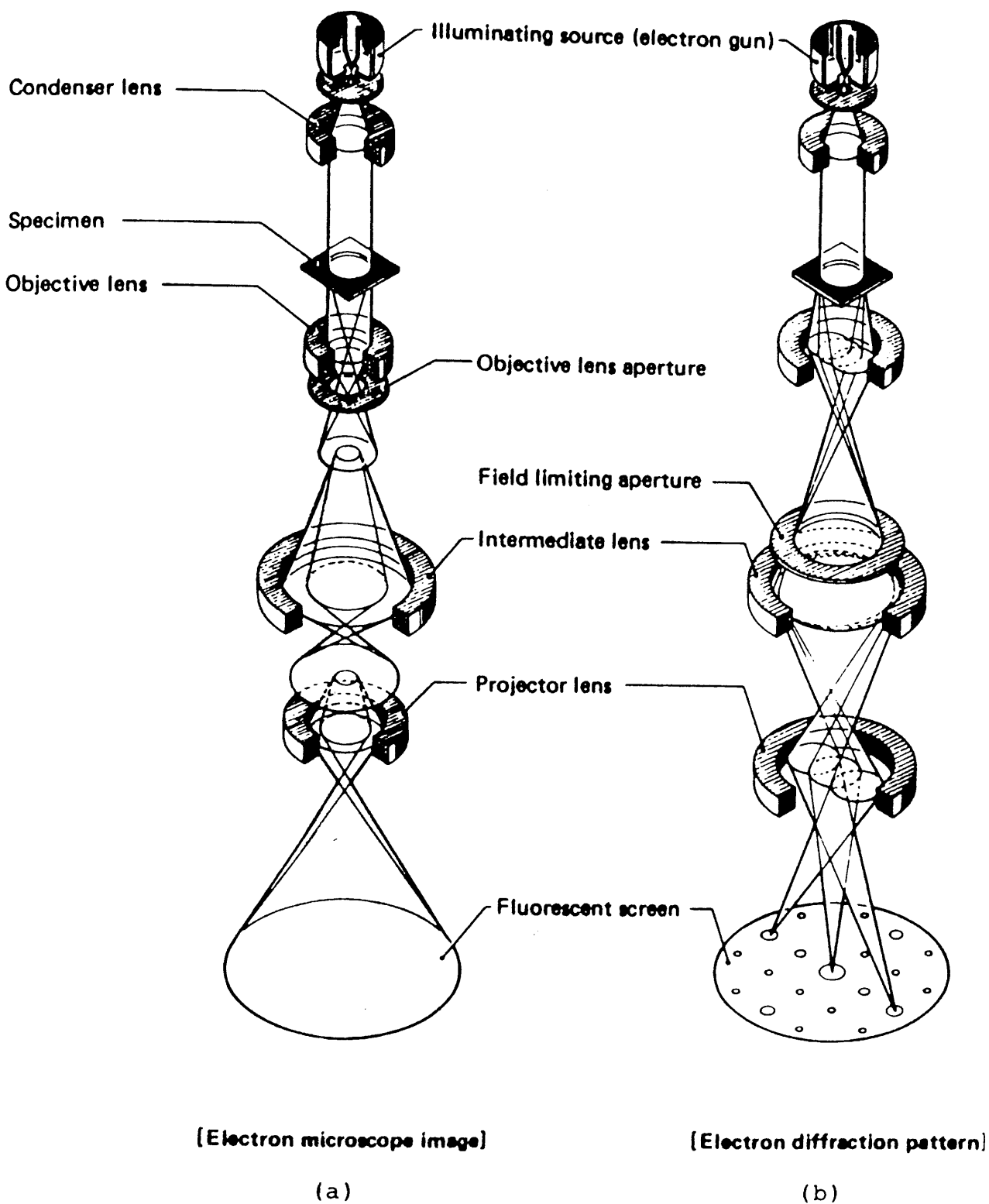
($\sin \chi(s) = 0$) appear dark in the optical transform and bright areas in the transform correspond to spatial frequencies for which contrast information was transferred to the original micrograph, this situation may be described by ($0 < \sin \chi(s) < +1$ or $0 > \sin \chi(s) > -1$). However, since the optical transform reflects an intensity distribution, the information content is related to the square of the transfer function, so the absolute value of the function, positive or negative is not revealed. Millward and Jefferson (1978) applied linear transfer theory to the optical diffraction technique, to demonstrate the information content of the optical transform. Instrumental defects, such as astigmatism and specimen drift can be diagnosed. Astigmatism leads to an elliptically shaped Fourier transform for the amorphous (carbon) support film as opposed to the circular pattern present for well corrected micrographs (Thon and Siegel, 1970). Specimen drift leads to loss of Fourier components in the direction of drift. Image filtering and reconstruction can also be carried out although care must be taken to avoid artefacts (Fryer, 1979).

2.6 Electron Diffraction

Specimen examination by electron diffraction provides a rapid visual assessment of the degree of structural ordering within the specimen and the extent of radiation damage before an image is recorded. Specimens with crystal planes parallel to the electron beam diffract electrons in accordance with the Bragg law. Undeviated incident

electron beams and diffracted beams are focussed at the back focal plane of the objective lens, and there form a diffraction pattern. The diffraction pattern and the intermediate image (figure 28), are always present in the microscope, and the intermediate lens setting determines which is projected on to the image plane. In transmission mode, the intermediate lens is focussed on the intermediate image (figure 28 (a)), whilst for electron diffraction, the intermediate lens is focussed on the diffraction pattern and corresponding adjustment of the projector system magnifies this on to the final image screen (figure 28 (b)).

The displayed diffraction pattern is formed from electrons incident on any part of the specimen (figure 28 (b)). Often, however, the diffraction pattern of a small area or crystallite is required, and this can be achieved using the selected area diffraction mode pioneered by Boerch (1936) and refined by Le Poole (1947). In the more detailed ray diagram (figure 29) a diffraction pattern of the whole of the illuminated area is seen to be produced in the plane at (C), and an image of the area produced at (D). An aperture is inserted in this plane to limit the rays which pass down the column. In the diagram it can be seen that any electrons which do not originate from an area on the specimen corresponding to the demagnified image of the selected area aperture are stopped. Thus the diffraction pattern formed at (E) by the intermediate lens is composed only from those electrons which originate within the selected area. The projector system then transfers this pattern to the viewing screen.



Comparison of Image Formation in the Electron Microscope.

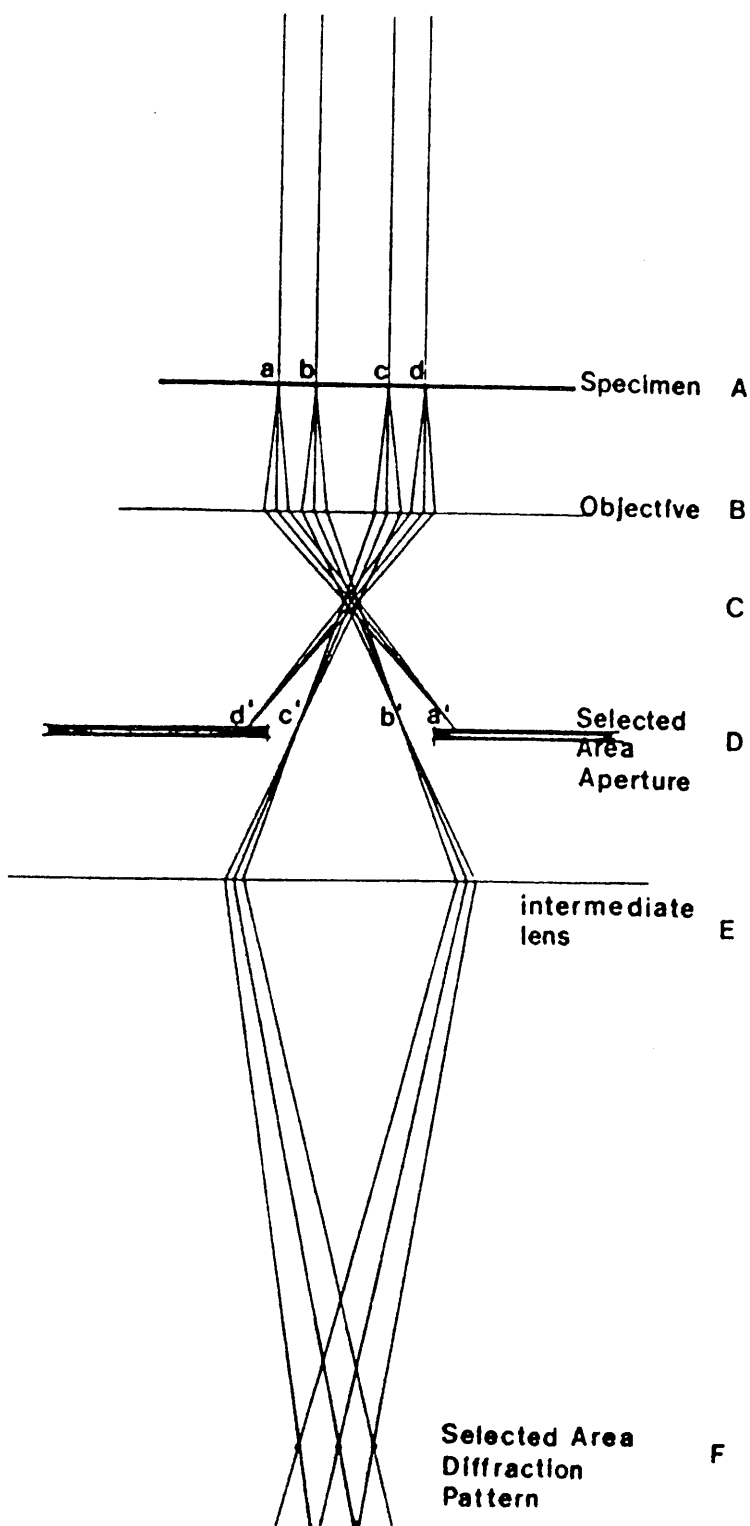


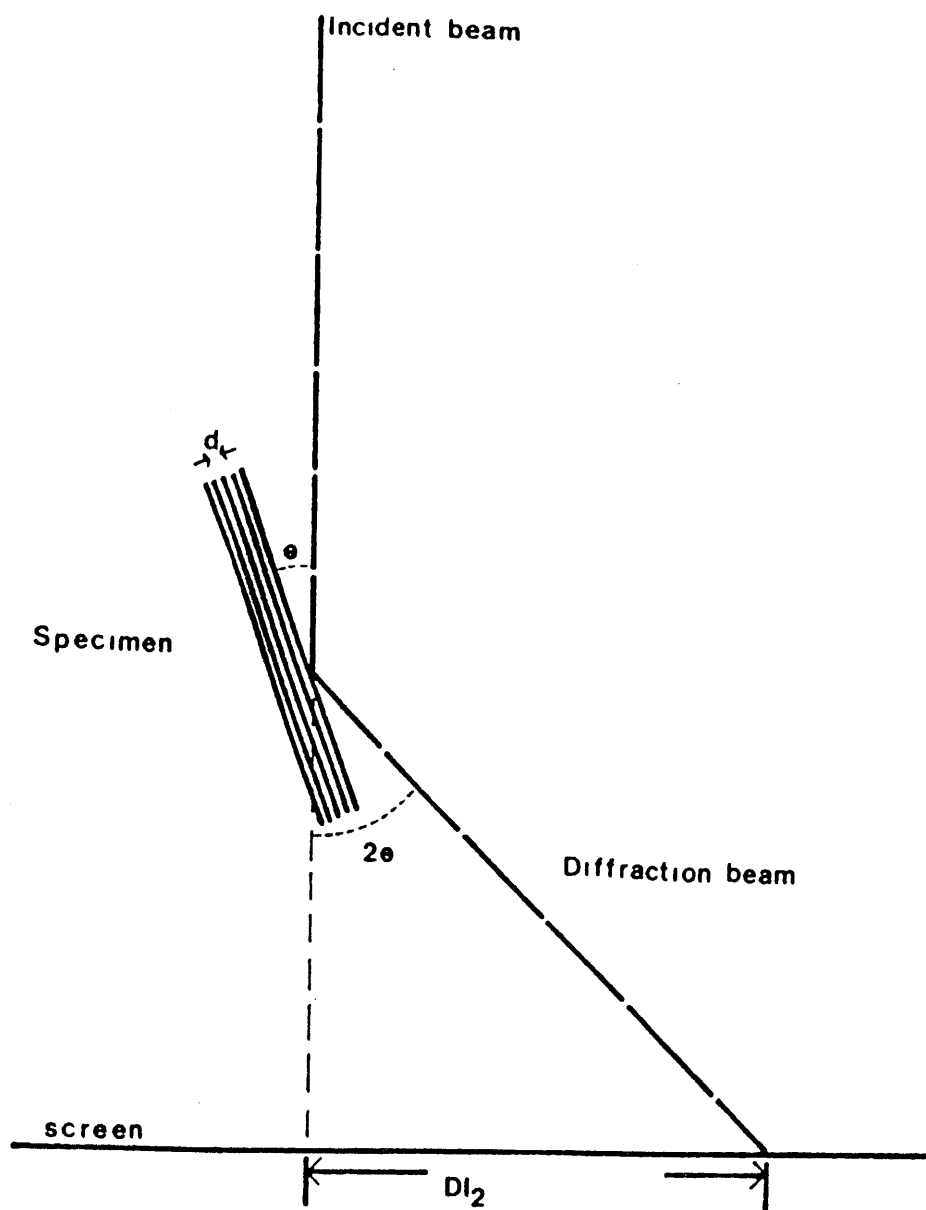
FIGURE 29

Electron Diffraction

The apertures inserted in the plane at (D) can typically be as small as $20\text{ }\mu\text{m}$ with an objective magnification of fifty times corresponds to a selected area of $0.4\text{ }\mu\text{m}$. However, these diagrams correspond to perfect thin lenses, whilst magnetic lenses are known to have large aberrations. Due to the effect of spherical aberrations, electrons scattered from areas other than the selected area can contribute to the diffraction pattern formed at (F). The significance of the contribution from these electrons depends on the angle at which the electrons pass through the objective lens (Agar, 1960). Thus the area of specimen contributing to the diffraction pattern varies for each spot and increases with increasing scattering angle. If this effect is to remain negligible for the scattering angles typically encountered, the selected area on the specimen should exceed for example $1\text{ }\mu\text{m}$ for a lens aberration of 3.33 mm and electrons with an energy of 100 KeV .

The diffraction pattern produced by this technique is recorded on a photographic emulsion placed close to the viewing screen. Due to the large depth of focus, the slightly differing positions of the viewing screen relative to the emulsion is unimportant. In this way a large number of diffracted beams are simultaneously recorded.

The electron microscope, used in the diffraction mode, can be considered as a simple electron diffraction camera. Figure 30 shows the construction for diffraction from a set of lattice planes, spacing (d), at an angle θ (theta) to



The electron microscope as a simple diffraction camera.

the electron beam. From the diagram:-

$$\tan 2 \theta = D / 2 L \quad (\text{xv})$$

and using Braggs law for first order diffraction ($n = 1$):-

$$\lambda = 2 d \sin \theta \quad (\text{xvi})$$

Since theta, exaggerated in the diagram, is normally less than three degrees, the approximation:-

$$\tan 2 \theta = 2 \sin \theta = 2 \theta \quad (\text{xvii})$$

can be used and combines with (xv) and (xvi) to give:-

$$D d = 2 \lambda L \text{ or } D d = K \quad (\text{xviii})$$

Since $2 \lambda L$, the camera constant, is fixed by the operating conditions. λ is the electron wavelength (0.0037 nm for 100 KeV electrons); L is the effective camera length, which is equivalent to the physical distance between the diffraction plane and the final image screen, given by:-

$$L = f_o M_1 M_2 M_3 \quad (\text{xix})$$

where f_o is the focal length of the objective lens and M_1 , M_2 and M_3 are the magnifications of the intermediate and projector lenses.

A standard is used to determine the camera constant and

unknown diffraction patterns are identified by comparison of spacings with tabulated X-ray data in the A.S.T.M. index (1965). To obtain accurate electron diffraction results, the diffraction mode must be precisely set up, in particular, the specimen height and post-specimen lens currents should be standardised for correlation of measurements. Even with these limitations, lattice spacings can be obtained to an optimum 1 % accuracy.

Andrews et al. (1967) noted a linear variation in the camera constant with diffraction ring diameter, due to the decreasing validity of expression (xvii) for greater theta values.

The diffraction pattern contains the structural data periodicities and orientations, for the plane projected normal to the electron beam. The restriction that only lattice planes near parallel to the electron beam will contribute to the diffraction pattern allows determination of specimen orientation, since the specimen lies normal to the plane giving rise to the recorded reflections. Formulae are available which allow calculation of interplanar spacings, angles between planes, zone axes (the direction normal to the diffraction planes) and angles between zone axes for the common crystal systems (Andrews et al., 1967; Beeston et al., 1972).

2.7 Special Operational Modes

2.7.1 Dark Field

The normal bright field image in the electron microscope is formed when scattered electrons, modified by the specimen and by instrumental characteristics, recombine with unscattered electrons of the partially coherent incident beam. If the unscattered electrons are removed by a physical aperture then a high contrast image of reduced intensity is produced by the scattered electrons. This is referred to as a "dark field" image. Displacement of the objective aperture, over a chosen reflection, to exclude the unscattered electron beam and allow passage of some of the scattered electrons (those corresponding to the chosen reflection) forms an off-axis dark field image. The illumination then comes from the chosen reflection only and those responsible for it appear as bright regions within the overall dark image. This image is of poor quality as the off-axis electrons, scattered through large angles, are subject to larger aberrations due to lens defects. Alternatively modern microscopes allow tilting of the incident beam at a chosen angle to transmit the scattered beams of interest, axially through the objective aperture to form an axial dark field image. This minimises aberrations and allows high resolution dark field imaging. Many aspects of dark field microscopy with respect to the structure of thin crystals have been fully discussed by Hirsch et al. (1965).

2.7.2 Tilted Bright Field

This is similar to the tilted dark field technique, except that the image is formed from the undeviated electron beam and a selected Bragg reflected beam. The theory of image formation, using tilted illumination has been presented by Howie et al. (1973); Ast et al. (1974) and Krivanek and Howie (1975). The technique has been used for lattice imaging (Komoda, 1966) and to study short range order in amorphous materials (Rudee and Howie, 1972; Krakow et al., 1976). To resolve lattice fringes by the tilted beam method, the incident illumination is tilted such that the undeviated electron beam and the appropriate Bragg reflected beam travel at equal angles to the electron optical axis. An objective aperture is inserted in the back focal plane of the objective lens, so that the image formation is dominated by interference between these two beams. The two beams suffer equal effects of objective lens spherical aberration and the symmetric beam configuration also minimises the defects of chromatic aberration. However, in this mode, contrast effects from inelastically scattered electrons can be significant (Parsons and Hoelke, 1974) and these complicate image interpretation.

2.7.3 High Voltage Microscopy

The two most obvious routes to improve resolution in the electron microscope are to decrease the spherical aberration coefficient by improving the objective lens, or

to increase the accelerating voltage, thereby reducing the electron wavelength. For example the electron wavelength at 100 KeV is 0.0037 nm whilst at 1000 KeV it is reduced to 0.00087 nm. The advantages of high voltage operation have been outlined in several publications, for example Dupouy and Perrier (1962); Cosslett (1969). As the energy of the incident electrons increases, the specimen becomes more transparent to the electron beam. Consequently useful information can be obtained from specimens too thick for 100 KeV microscopy by operation at higher voltage. Cosslett (1969) has calculated the increased penetration at higher KeV for carbon and gold. The reduced scattering cross section at higher voltages also results in less interaction of the electron beam with the specimen, reducing radiation damage to the specimen, although the improvement is not linear (Kobayashi and Sakaoku, 1965; Kobayashi and O'Hara, 1966) and the probability of nuclear displacement increases. Scattering angles decrease at higher KeV, the electron diffraction pattern contains more diffraction orders and there is a general improvement in electron diffraction information. Beeston et al. (1972) have discussed the potential of high voltage diffraction.

The Cambridge University 600 KeV high resolution electron microscope (Nixon et al., 1977; Cosslett, 1980; Smith et al., 1983) has been employed in parts of the present study to give an increase in accelerating voltage to aid in the examination of specimens too thick for examination at lower KeV.

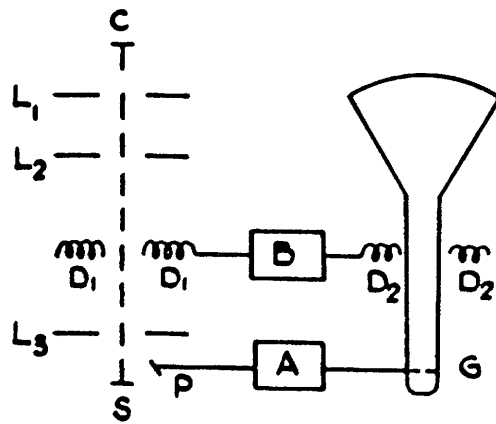
2.8 Scanning Electron Microscopy

2.8.1 Electron Emission from Solids

When an accelerated beam of electrons impinges on the surface of a solid, a reflection process occurs and electrons are emitted from the target. Rudberg (1936) demonstrated that emitted electrons have a range of energies from zero to that of the incident beam, this energy distribution being the basis for classifying such electrons. Electrons having emission energies from zero to fifty electron volts are termed true secondary electrons, while those above this energy are referred to as backscattered or inelastically scattered primaries. Scanning electron microscopy functions upon the electron emission ability of solids, particularly that of secondary electrons.

2.8.2 Principle of Scanning Electron Microscopy

The principle of scanning electron microscopy (SEM) is illustrated in figure 31 (Oatley et al., 1965). A beam of electrons accelerated by potentials up to fifty KeV, from a cathode (C), passes through electron lenses L1, L2 and L3, and is brought to a focus on the surface of a specimen (S). A portion of the electron current, mainly secondary emitted electrons, is collected by the detector at (P), and conveyed to the amplifier (A), the output of which controls the potential of the modulating electrode (G), of the cathode ray tube (CRT) and thus the brightness of the spot on the face of the tube.



Principle of the Scanning Electron Microscope

C, Cathode; L L L , Electron Lenses; D D , Scanning Coils;
 S, Specimen; P, Collector; A, Amplifier; B, Scan Generator;
 G, Control Grid in the Display Cathode Ray Tube

FIGURE 31

Deflections of the initial electron beam and the spot on the cathode ray tube are caused by the passage of current from a saw tooth generator (B), through pairs of coils D1D1 and D2D2 respectively. Two systems of this kind are used to produce deflections in two directions, at right angles, so that the initial beam and the CRT spot transverse zig-zag rasters in synchronism. Furthermore, since the current reaching P varies as the electron beam scans the specimen surface, the brightness of the CRT spot varies in sympathy and an image of the specimen is built up on the face of this tube. This variation in imaging current, usually of secondary electrons that reach the positively biased scintillator detection device, reflects varying details about the object. For any given specimen setting with respect to the primary beam, raised portions of the object experience greater irradiation and will act as enhanced sources of secondary electrons. Thus elevations and depressions will appear brighter and darker respectively in the final image. By changing the specimen orientation, the primary beam will impinge on other object areas, thereby revealing their details in the image. Thus the variation in image contrast reflects corresponding features about the object, especially those of its surface topography (Everhart et al., 1959).

Reflected electrons have high emission velocities and as such their path to the detector is essentially a straight line, while those of the secondary electrons can be affected by applied magnetic fields and are generally sharply curved. Consequently reflected electrons will only

yield information on parts of the specimen for which there is a straight line path between them and the detector. Secondary electrons are not subject to this limitation and will provide far more detail about a rough surface. Normally, the collector is set up for detection of secondary electrons and the reflected ones are ignored as far as possible. Everhart et al. (1959) demonstrated the superiority of secondary electrons, in comparison to reflected electrons for revealing specimen detail.

The disadvantage of scanning electron microscopy is the poor resolution compared to the transmission method. Pease and Nixon (1965) reported a best resolution of $15 \text{ nm} \pm 3 \text{ nm}$ and an average resolution value of $20 - 30 \text{ nm}$. Modern day scanning microscopes have an average resolution of around 5 nm with 2 nm attainable. However, the large depth of focus offered by the SEM eliminates the problems associated with replication associated with transmission microscope investigations of highly contoured surfaces. In scanning electron microscopy, object "illumination" is from a very narrow incident beam. This produces a large number of secondaries which travel to a wide angle detector by a variety of paths. This probe beam is fine enough to penetrate fissures and holes of the object and secondary electron production from them can reveal details of the internal structure of these features. Many of the emitted secondaries become trapped, but, if low magnifications are employed, a satisfactory signal may be obtained. Indeed some of the most striking results produced have been those where there was no interest in high resolution images.

Several authors have published reviews of SEM including Cosslett (1970); Fisher et al., (1970) and Kammlott (1971).

Experimental

3.1 Materials

3.1.1 Coke

The morphologies of several feed cokes were investigated. Initially cokes manufactured from single coals with a wide range of rank were examined with subsequent analysis of pairs of blast furnace feed and ex-tuyere cokes, along with cokes reacted using various treatments.

The analysis of the coals used to form cokes from single coals are shown in table 3 with the reactivity to CO_2 of the cokes produced shown in table 4.

The blast furnace feed cokes used were those sampled from the furnace skips, that is just prior to charging to the furnace. The ex-tuyere cokes were removed from the tuyere zone after a time period roughly corresponding to that for passage of the coke through the furnace. The ex-tuyere cokes were removed by raking inwards and upwards (to a height of around one metre) through the tuyeres. Analyses of feed and ex-tuyere coke pairs is given in table 5.

All coke samples, both in bulk and in powdered form, were supplied by the National Coal Board (renamed British Coal, 1986).

3.1.2 Gases

Industrial grade gases supplied by B.O.C. were used as the carrier gases. The purities of the gases are shown in table 6.

3.1.3 Reagents

BDH anhydrous potassium (analar grade) carbonate was used as the source of potassium when reacted in the furnace, in an intimate mixture with the coke.

3.2 Sample Preparation

In all cases samples taken for analysis were of the size fractions present in the area of interest.

Normally, five kilogramme representative samples were taken for crushing (in the case of feed, ex-tuyere and heat treated cokes). Initial crushing was carried out in a jaw crusher to reduce the coke size to around 25 mm, subsequent crushing by a swing-hammer mill produced coke of approximately 5 mm in size and this was reduced to a fine powder by crushing using a Raymond mill. The crushed coke was then sized by a series of sieves to give a coke of British Standard 72 mesh (approximately 212000 nm).

Coal Reference		1	2	3	4
Rank (CRC No.)		204	301b	501	502
<u>Charge Properties</u>					
V.M. Content (daf)	%	18.1	29.6	36.2	37.0
Ash Content (d.b)	%	5.6	5.3	5.6	8.7
Total Dilution	%	52	148	174	127
Bulk Density (d.b)					
Kg / m ³		730	710	680	710
<u>Carbonisation Conditions</u>					
Average Rate to 900 °C at					
Charge Centre mm / h		29	32	31	31
Carbonising Time to 900 °C					
at Charge Centre (Hours)		15.6	13.9	14.4	14.6
Total Carbonisation Time					
(Hours)		19.3	15.4	15.7	16.5
Arithmetic Mean Size of					
Skip Coke		59.2	53.2	49.0	51.4
Micum Test M40 Index.		67	70	57	59
M10 Index.		7.5	7.8	9.6	9.2
<u>Ultimate Analysis</u>					
Carbon (dmmf)	%	91.5	88.0	86.0	85.7
Hydrogen		4.6	4.7	5.4	5.3
Oxygen		2.2	4.3	6.0	5.9
Nitrogen		1.5	1.7	1.9	1.8
Sulphur		0.72	0.89	1.21	0.87
Chlorine		0.02	0.05	0.15	0.03
<u>Maceral Analysis</u> % Vol.					
Vitrinite		68	79	76	71
Exinite		0	1	9	4
Inertinite		32	18	15	23
Mineral Matter + Coal Shale		0	2	0	3
Mean Random Reflectance		1.47	1.06	0.85	0.84
<u>Ash Composition</u> %					
Na ₂ O		0.7	0.9	1.0	0.3
K ₂ O		2.3	1.8	2.0	1.4
Ca O		2.3	1.4	3.0	1.1
Mg O		1.0	0.7	1.8	0.7
Fe ₂ O ₃		5.1	8.5	11.6	7.7
Si O ₂		47.4	51.4	45.1	50.7
Al ₂ O ₃		35.7	33.7	29.8	32.6

Analysis of Coals used to form Single Coal Cokes

TABLE 3

Coke Reference	1	2	3	4
Bulk Reactivity (1000 °C 0-20% wt. loss)* % / h	1.4	1.9	3.8	2.7
Measured wt. losses in partial gasifications:- +20mm coke, target wt.loss				
20 %	20.3	20.7	21.0	21.3
30 %	30.7	30.5	29.2	30.4
60 - 80 mm fraction 20 %	20.1	20.2	20.5	20.5
Lump Reactivity ** (975 °C, 0 -3 hrs) % / h	2.3	2.5	5.6	3.5
Lump Abrasion Rate ** before reaction % / min	0.9	1.5	3.8	1.9
after reaction % / min	1.4	2.5	8.9	3.5
Lump Density ** before reaction g / cm ³	0.90	0.83	0.65	0.72

* plus 20 mm sample, 25 kg weight

** cores, 38 mm radius by 38 mm, from plus 60 mm lumps

Reactivity of Single Coal Cokes to CO₂

TABLE 4

Coke Reference	A	A'	B	B'	C	C'
Feed or Ex-tuyere Coke.	Feed	Tuyere	Feed	Tuyere	Feed	Tuyere
Coke Mean size. mm.	49.9	38.0	59.8	47.0	58.4	47.9
Micum Test* M40 Index.	85.2	-	91.8	-	90.3	-
M10 Index.	6.6	-	4.9	-	4.6	-
Apparent Density g/cm ³ .	0.93	0.89	0.95	0.95	0.95	0.95
Ash Content** %.	7.6	14.1	9.5	16.0	9.1	12.5
Volatile Matter*** %.	0.3	1.1	0.8	1.2	1.0	0.9
Content						
Ash Composition %.						
Na ₂ O	1.9	4.1	0.8	2.7	0.8	1.4
K ₂ O	2.7	12.4	1.8	6.0	2.1	6.1
Ca O	2.1	6.3	2.3	7.5	2.1	7.5
Mg O	1.1	1.8	1.1	3.3	1.1	1.7
Fe ₂ O ₃	15.3	16.0	8.2	9.3	7.3	15.8
Si O ₂	44.7	30.7	52.2	37.4	52.4	36.0
Al ₂ O ₃	29.2	18.9	30.2	26.3	30.3	23.6

* Micum test on plus 60mm coke.

** Carried out on a dry basis.

*** Carried out on a dry ash free basis.

Analysis of Feed and Ex-tuyere Coke Pairs.

TABLE 5

<u>Gas Type</u>	<u>Supplier</u>	<u>% Purity</u>
Argon	B.O.C.	> 99.998
Helium	B.O.C.	> 99.995
Nitrogen	B.O.C.	> 99.998

Purities of Industrial Gases Used.

TABLE 6

3.2.1 Sample Preparation for Transmission Electron

Microscope

Samples were prepared for analysis by transmission electron microscopy (TEM) using two methods. Feed and ex-tuyere samples were prepared by first further crushing the powdered coke (B.S. 72 mesh), in an agate mortar and pestle and then between glass microscope slides. This finely powdered coke was then placed in a micro test tube with water and placed in an ultrasonic bath for a period of half an hour. A slurry of the coke / water mixture was then withdrawn from the test tube using a finely drawn Pasteur pipette and a drop placed on a copper electron microscope grid, which had previously been coated with a holey carbon film (Philips bulletin, 1963). The microscope grids were then allowed to dry at around 30 °C, in a laboratory oven, before transfer to the microscope.

The feed cokes reacted with potassium could not be prepared in the above manner, due to the possibility of formation of intercalated material and the reactive nature of these species which readily degrade when in contact with air or water. These samples were prepared for TEM analysis by simply dusting the holey carbon coated copper grids with the reacted coke (crushed in an agate mortar and pestle and between glass microscope slides before reaction) in a glove box, in an inert atmosphere of argon.

A method involving coating nickel microscope grids with chrysotile asbestos, and then reacting the already mounted

coke sample with potassium was also tried but with less success.

Samples were run on Jeol JEM 100 C and 1200 EX microscopes operated at accelerating voltages of 100 KeV and 120 KeV respectively. The 1200 EX microscope was fitted with a lanthanum hexaboride (LaB_6) filament to increase the coherence of the electron beam. This microscope was also fitted with an image intensifier system to aid in viewing specimens. The images were recorded on photographic plate film (Ilford EM film and Kodak Industrex C X-ray film). Some samples were also run on the Cambridge University 600 KeV microscope (Nixon et al., 1977; Cosslett, 1980; Smith et al., 1983) in order to gain information from samples too thick for analysis at lower accelerating KeV.

3.2.2 Sample Preparation for Scanning Electron Microscopy

Coke lumps of around 50 mm diameter were sectioned using a diamond bladed rotating saw. Sections of approximately one square centimetre were cut from the centre of the coke lump. The sections were cut as thin as possible.

In order to obtain representative Energy Dispersive X-ray Analysis data, the sections were cut as flat as possible with the surface further ground in order to give an even sample height for effective X-ray detection.

The samples were then mounted on aluminium stub spindles using silver dag or carbon paint. The samples were run as

far as possible uncoated but in some cases a layer of palladium / gold was evaporated on to the coke sample in order to reduce the effects of charging.

Preparation of samples by dusting the powdered coke on to aluminium stubs coated with silver dag paint was useful for observing bulk structure but was less useful for X-ray analysis due to the large variations in the surface topography. Similarly the mounting of small coke lumps was useful for examination of bulk structure and some gasification studies but due to variations in sample height, of the lump coke, could not be used for collection of X-ray data by EDXRA.

All samples examined by SEM were run on a Philips PSEM 500 B microscope operated at an accelerating voltage of 15 - 30 KeV, using a spot size of 1000 - 2000.

3.3 Energy Dispersive X-ray Analysis (EDXRA)

The scanning electron microscope was fitted with an EDXRA system in order to facilitate analysis of the relative proportions and distributions of the constituent elements in the samples.

The multichannel analyser could accurately detect elements of atomic number greater than eleven. The element sodium (atomic number eleven) however, is on the edge of the limit of detection and as such analysis of this element by EDXRA is somewhat uncertain. This detection limit arises due to

the energies of the emitted X-rays. Those X-rays with low emission energies find it difficult to pass through the beryllium window of the detector and this, along with other problems, gives rise to a poor counting efficiency of the detector for X-rays emitted by these "light" elements. However, it has been shown (Chapman et al., 1983, 1984; Craven et al., 1984) by cross sectional areas and generation of Bremsstrahlung spectra that the counting efficiency of the detector can be taken to be nearly unity for those elements in the range 5 - 15 KeV, with the higher limit of these values being governed by the saturation of the detector amplifier. All samples were analysed by EDXRA until one thousand counts had been recorded, irrespective of count rate.

3.4 Preparation of Holey Carbon Films

Holey carbon films were required to increase contrast between the specimen and the support film. These "holey carbon films" were prepared as follows.

Standard one inch microscope slides were cleaned, dried and placed in the freezer compartment of a refrigerator. On removal from the refrigerator the slides were coated with a 0.25 % volume solution of Formvar (polyvinyl formal, molecular weight 24000 - 40000). The coating was carried out in a humid atmosphere in order to create small holes in the plastic film, by condensation of small water droplets.

The "holey" plastic films were subsequently floated off the

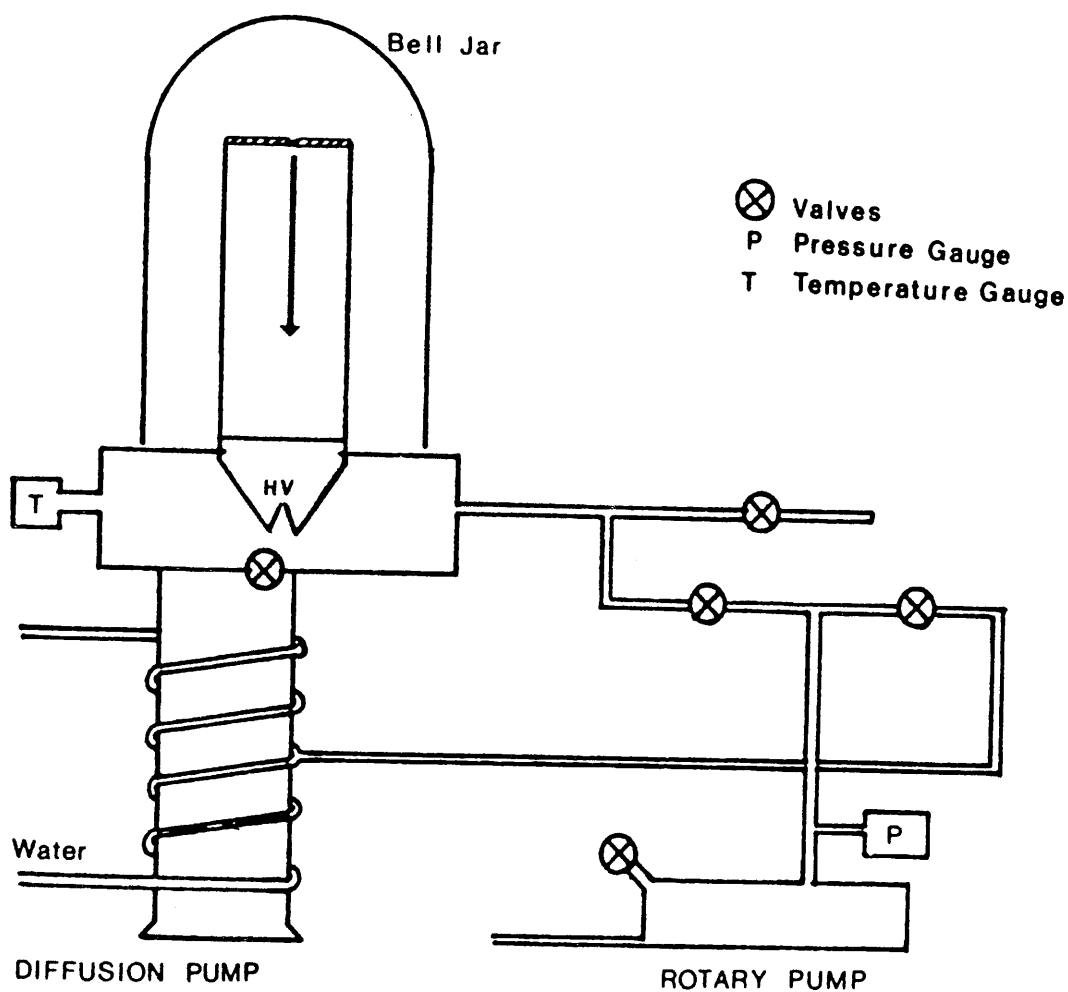
glass slides onto water and hence on to copper electron microscope grids (400 mesh) by draining off the water and letting the plastic film settle on to the grids which had been placed in the bottom of the floatation tank. The holes in the plastic film were then analysed for size in the microscope, using a low electron dose in order not to damage the radiation sensitive plastic film. The holes which proved too small for use could then be enlarged to a suitable size by irradiation with the electron beam, by focussing the condenser lens.

Those films which were found to be suitable for specimen mounting were subsequently carbon coated to stabilize them in the electron beam. This was carried out by passing an electric current (30 volts, 20 amperes) through two carbon rods in a vacuum of around 10^{-4} torr, as illustrated in figure 32.

3.5 Sample Preparation for X-ray Powder Diffraction (XRD)

Various coke samples were analysed by X-ray powder diffraction. Powdered samples were mounted on adhesive tape, rolled into a cylinder and placed in the XRD equipment. The XRD equipment used was a Philips diffractometer, which consisted of an X-ray generator and a diffractometer unit.

The sample was rotated through angles of $5 - 50^\circ$ (two theta values) whilst being exposed to Cu k_α radiation ($\lambda = 0.154178$ nm). The resulting X-ray diffraction



Edwards vacuum coating unit for preparation of "holey carbon films", by carbon evaporation, using spectroscopically pure graphite rods.

FIGURE 32

patterns were recorded on a chart recorder operating at one thousand counts per second. The lattice spacings for the samples were subsequently calculated using the Bragg equation:-

$$\lambda = 2 d \sin \theta$$

3.6 Sample Preparation for Thermogravimetric Analysis (TGA)

Various samples of powdered cokes were analysed by thermogravimetric methods.

The instrument employed for these studies was a Du Pont 990 analyser combined with a Du Pont 951 thermogravimetric unit. The powdered cokes were suspended in platinum boats. A stream of air (at a flow rate of 50 ml /min.) was passed over the material as it was heated. The samples were analysed in the temperature range of 0 - 1000°C, using a heating rate of 20 °C per minute. The temperature was measured using a Cr / Al thermocouple. The resulting weight loss was measured by the thermobalance and plotted as a percentage weight loss against temperature. The thermocouple was suspended about three millimetres above the sample, in order to obtain an accurate temperature measurement from the sample- as opposed to earlier TGA models in which the thermocouple was mounted in the furnace wall, and thus did not accurately measure the temperature of the sample.

As far as possible, samples were prepared for analysis by

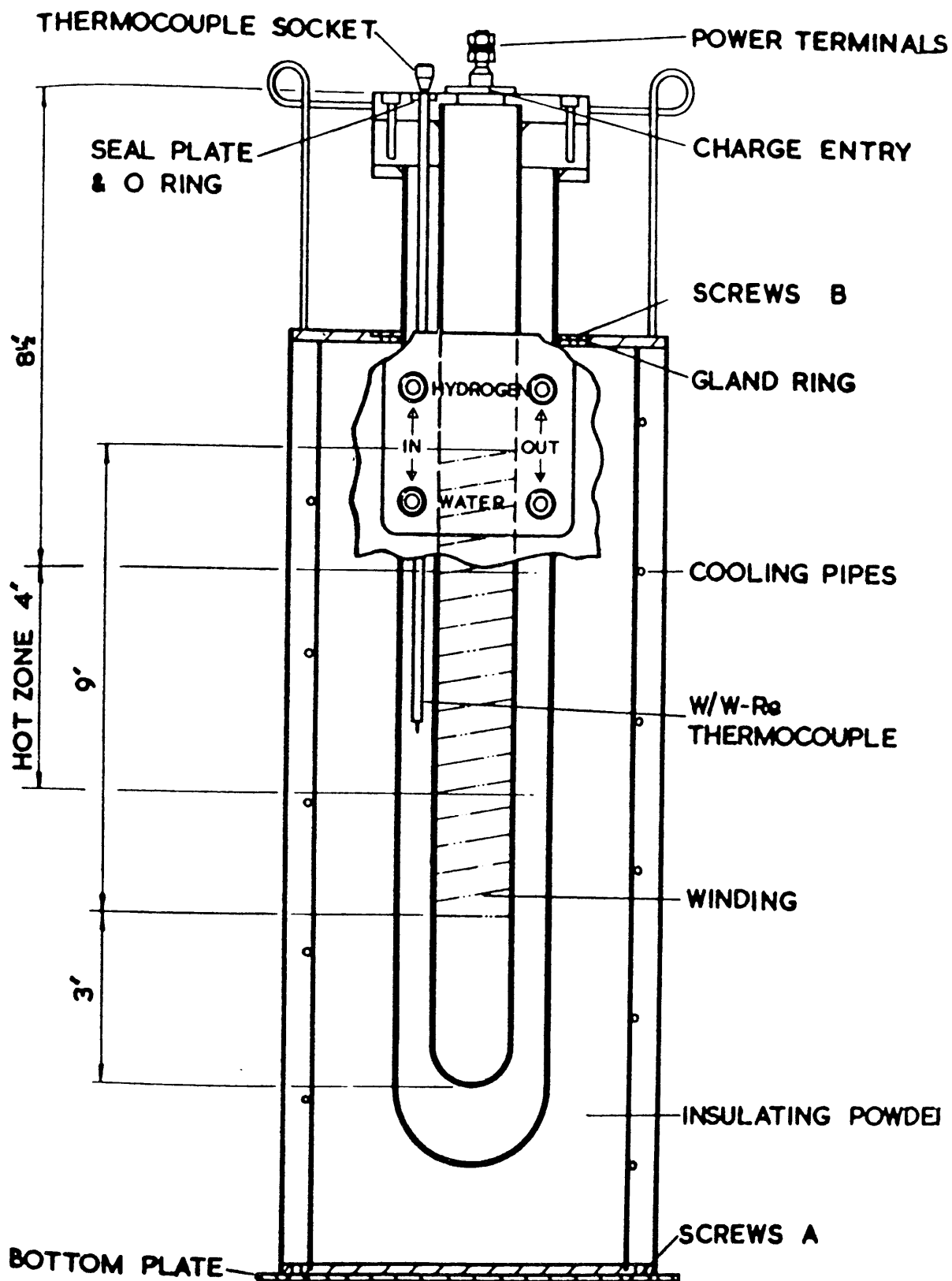
the same procedure. This was important in order to minimise problems arising from differences in sample weight, particle size and packing, which all combine to change the nature of the thermogravimetric curve. The equal treatment of each sample should also remove the effects of the production of gases when the sample is heated, which alter the heat transfer properties of the material and hence the thermogravimetric curve.

3.7 Furnace Construction

The furnace employed for the reaction of feed coke samples was a Metals Research PCA 10 laboratory furnace, as shown in figure 33.

The furnace was a small compact unit, suitable for heating small laboratory specimens at temperatures up to 1800°C, in closely controlled reducing, oxidising or neutral atmospheres. The furnace was sealable and within limits could also be used to carry out reactions in a vacuum.

The furnace comprised a fully sealed element assembly in a water cooled and insulated case. The element assembly consisted of an impervious alumina sheath which had a molybdenum element wound externally over the central portion of the sheath. The wound sheath was contained within an outer alumina sheath, the sheathes being joined by a water cooled metal header which sealed the annular space through which the hydrogen was passed (at around 60 ml /min.) to protect the molybdenum winding against oxidation.



PCA 10 Type Furnace

The furnace resistance increased by a factor of ten between room temperature and 1800 °C, thus necessitating a variable voltage supply. The furnace power supply consisted of a 2 kW variable transformer feeding a step down transformer, capable of providing an output of forty amperes at sixty volts. The furnace was constructed to prevent the flow of excessive currents, by an overload trip switch.

The furnace temperature was monitored by means of a tungsten / tungsten-rhenium thermocouple positioned in the annular space, between the two alumina sheaths, close to the centre of the windings.

3.8 Furnace Operation

The PCA 10 furnace was capable of being used in either the horizontal or vertical position. The majority of the reactions involved the coke samples being reacted with a stream of potassium vapour and thus required the furnace to be used in the horizontal position.

Charge handling in the furnace was performed using two designs. Figure 34 shows the first of these two handling methods. Small silica glass boats (O.D. 5 mm, 15 mm long) were inserted into a silica glass U-tube sleeve (I.D. 6 mm, O.D. 8 mm). The first boat contained the coke which was to be reacted, intimately mixed with anhydrous potassium carbonate. A stream of inert gas was introduced into the arm of the U-tube opposite to that which contained the boats. The gas cylinder was attached to the U-tube

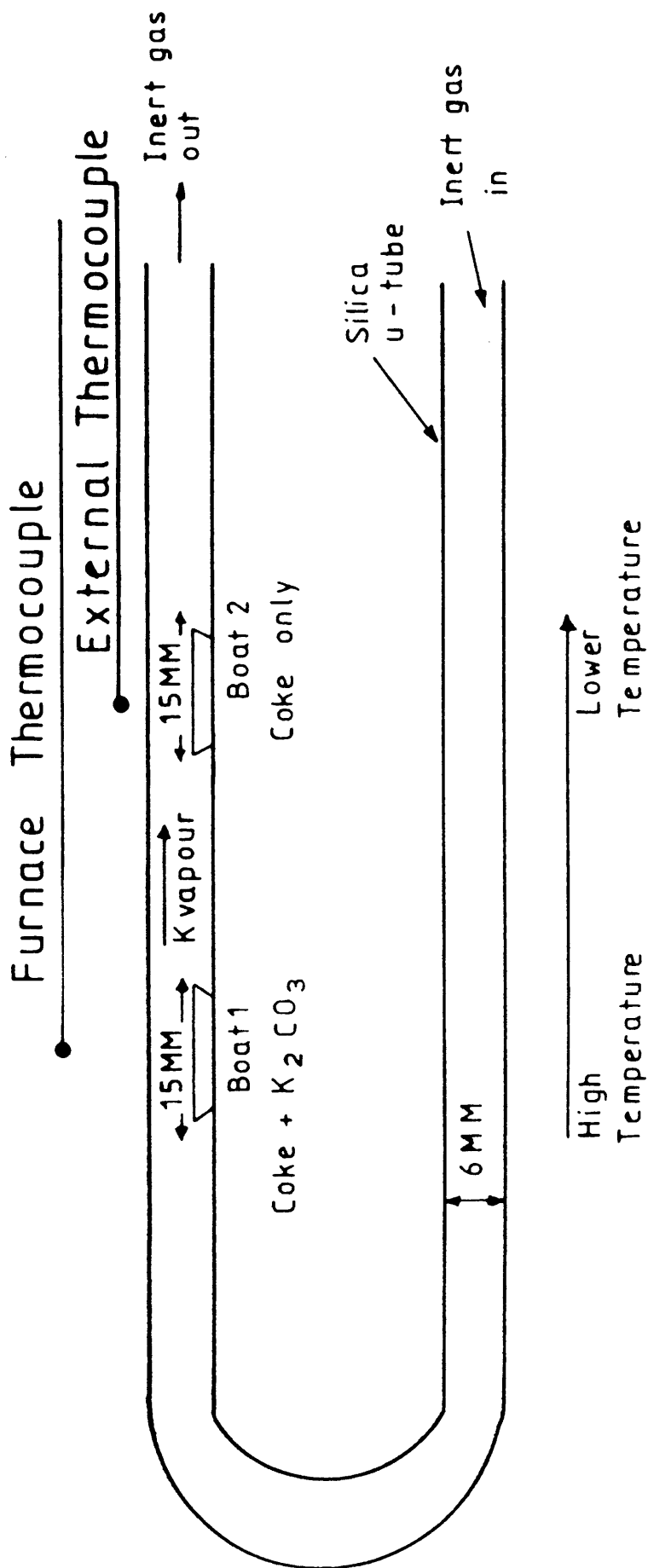


FIGURE 34

(opposite to the arm containing the boats) using tightly fitting polythene tubing. This carrier gas was used to carry the potassium vapour generated, from the coke / potassium carbonate reaction, over the second boat. The second boat contained a sample of the same powdered coke as used in the reaction with the potassium carbonate. The residual gases were vented to the atmosphere.

The reaction of the potassium vapour, with the feed coke material contained in the second boat, was continued until all the potassium vapour which was generated had passed over the second boat. During the reaction a purple vapour was observed in the arm of the U-tube containing the carbonate / coke mixture. This purple vapour was taken to be potassium vapour which flowed over the second boat during the reaction. The silica U-tubes were later analysed by EDXRA and showed only the presence of two large peaks corresponding to silicon and potassium. Thus, it is fairly certain that the observed purple vapour contained potassium. The amounts of carbonate and coke normally maintained a flow of potassium vapour for a period of around two hours. This was deemed to be sufficient time for any reaction between the potassium and the feed coke (boat 2) to have occurred. In all cases the furnace temperature was maintained at the peak temperature until no further generation of potassium vapour was observed. This ensured that any reaction occurring between the potassium and the coke had taken place at the maximum temperature attained by the second boat and did not occur during the furnace cooling period.

Furnace Thermocouple

External Thermocouple

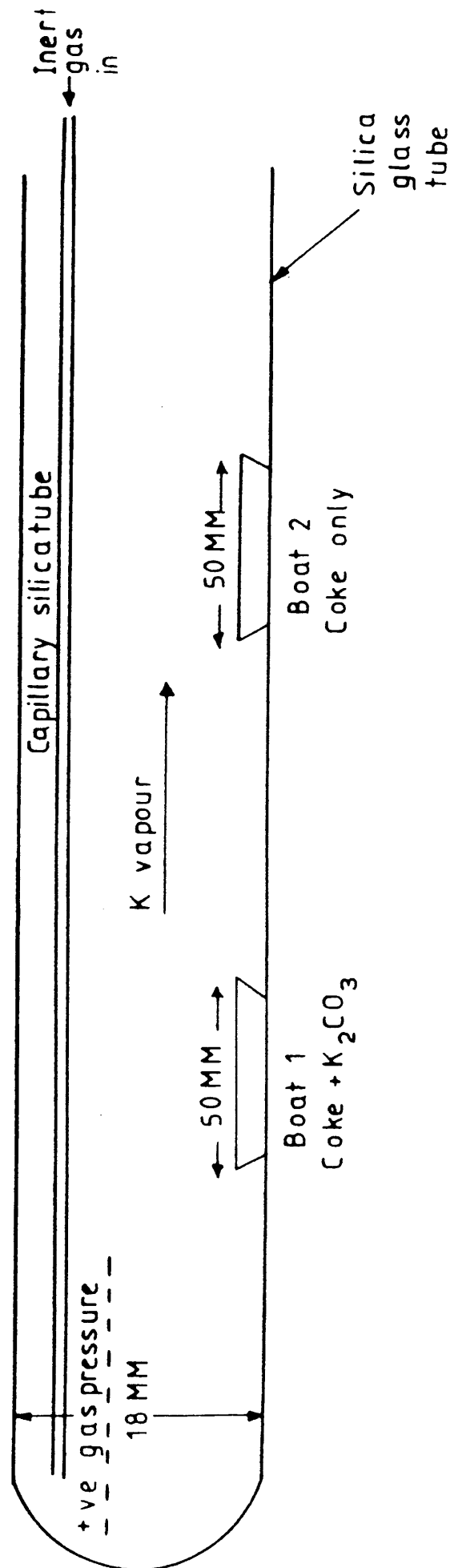


FIGURE 35

The second handling procedure used was employed for bulk sample production. A straight silica tube (20 mm O.D., 18 mm I.D.), which had been closed at one end was used as a sleeve for the reaction. Again two silica boats were employed in the reaction (10 mm O.D., 50 mm long). The first boat contained the coke / potassium carbonate mixture and the second a sample of the feed coke. A fine silica glass capillary tube was introduced to the bottom of the silica glass sleeve and the potassium vapour produced from the coke / carbonate reaction (observed as a purple vapour) was passed over the second boat using the positive gas pressure generated in the glass sleeve. This second reaction design is shown in figure 35, with the residual gases again being vented to the atmosphere.

As in the previous reaction set up (U-tube) portions of the silica tube were analysed by EDXRA. This revealed only significant portions of silicon and potassium to be present, thus confirming the nature of the purple vapour.

Again, the reaction between the coke and the generated potassium vapour was continued until no further purple vapour was observed, with the furnace maintained at its maximum temperature this ensured that any reaction between the coke and potassium had occurred at the observed temperature, and not during furnace cooling.

In both reaction set ups the carrier gases were passed from the cylinders to the furnace using stainless steel tubing,

Furnace Thermocouple

External Thermocouple

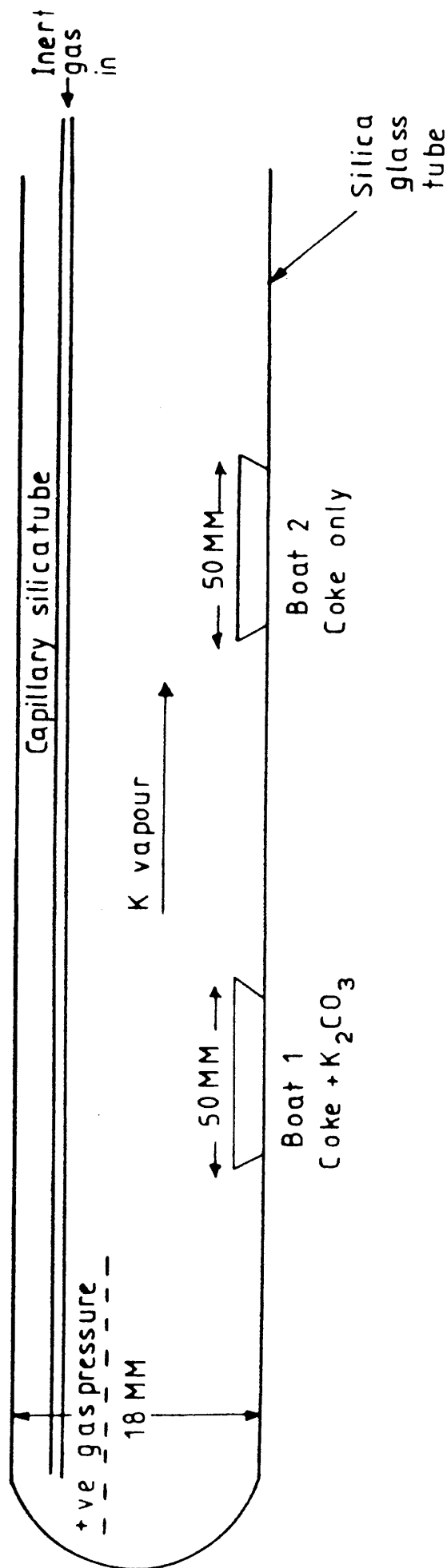


FIGURE 35

swagelock couplings and tight fitting polythene tubing. In both cases the furnace temperature was slowly raised until a maximum temperature of 1100°C was attained. This temperature was registered by the furnace thermocouple, corresponding to the centre of the furnace hot zone, at which point the boat containing the coke / carbonate mixture had been placed. The temperature of the second boat was monitored by means of an external thermocouple, which was introduced to the furnace to a position corresponding to that of the second boat. The temperature of the second boat, containing only feed coke, was normally found to be around 900°C .

3.9 Effects of Inert Carrier Gases

Experiments involving the reaction of feed cokes with potassium vapour were repeated many times. This was in order to obtain relevant data and reproducible results, as it has often been found that the nature of potassium reactions with carbons can be quite varied (Patrick, 1986). During the repetition of these experiments the reaction design was maintained although in some cases the inert carrier gas used was altered. This was in order to examine any possible effects due to the carrier gas, although in all cases the gases used were inert and it was thought unlikely that the gases would contribute to any obtained results. The samples were subsequently analysed by a variety of techniques.

3.10 Structural Changes Effected by Heating

3.10.1 High Temperature Treatment

In order to separate the effects of alkali attack from thermal effects, feed coke samples were heated in the absence of alkali. This was carried out in a small electric furnace (different from the PCA 10 furnace) in which around ten grammes of the relevant feed coke was heated to 1500°C in an atmosphere of nitrogen. The heating rate of the furnace was similar to that of blast furnaces. Once the temperature of 1500°C was attained this temperature was maintained for a period of around three hours. The samples were subsequently allowed to cool while maintaining the inert atmosphere of nitrogen. The samples were subsequently analysed by a variety of techniques. Samples were prepared for analysis in the same manner as described for the ex-tuyere samples.

3.10.2 Reaction of Feed Coke Samples at Below Carbonisation Temperature

Again, in order to separate thermal effects from chemical effects feed coke samples were reacted with potassium vapour at below their carbonisation temperatures. This ensured that any observed structural changes would be due only to chemical effects, as the cokes had previously been exposed to higher temperatures, for a considerable heat soak period, and would not be affected by reheating to a lower temperature.

The method employed for these experiments was identical to that used to react feed coke / carbonate samples at 1100°C. However, in this set of experiments the feed coke / carbonate mixtures were reacted at around 850°C, for a longer period. The reaction was continued until all the potassium vapour generated had passed over the second boat (hence the need for a longer reaction period- around four hours). Thus any reaction occurring between the coke and potassium vapour had occurred at the observed temperatures, and not during the furnace cooling period. The temperature of the second boat, which contained only feed coke, was found to be around 600 - 650°C in all cases. The samples were then allowed to cool, while maintaining the flow of inert gas. Samples were subsequently prepared for analysis by methods identical to those used for feed cokes reacted at higher temperatures with alkali vapour.

The performance of the furnace was limited by the ceramics available for the inner and outer sheathes. Very pure, recrystallised alumina was the most suitable material for the sheath, but it is susceptible to thermal shock, and thus excessive heating and cooling rates had to be avoided. The normal heating rate employed was 20°C / min., with the maximum temperature of 1100°C being attained in around nine hours.

3.11 Infrared Analysis (I.R.)

Attempts were made to characterise the coke's mineral matter by observing Si - O vibrational stretching modes by

infrared spectroscopy. The samples were analysed both by observation of reflection and transmission infrared data. A Perkin Elmer model 983 spectrometer was used for transmission analysis and a Beckman DK 28 spectrometer for reflectance analysis. Samples were mounted as both nujol mulls and KBr discs.

3.12 Density

Crude density measurements were made on some of the coke samples. This was done using a narrow bore, finely calibrated burette and carbon tetrachloride solution. The density measured was then calculated as the volume of carbon tetrachloride displaced by a specific mass of coke sample. Results were reported as g / cm³.

3.13 Temperature Programmed Reduction (TPR)

The TPR method of material analysis is a variation of the temperature programmed desorption (TPD) technique (Aben et al., 1972). A generalised diagram of the TPR system is shown in figure 36.

The TPR technique is suitable for studying systems whose characteristics are beyond the limits of detectability by other direct methods of structural analysis (eg. X-ray diffraction). The determination of the desorption characteristics of the material allows a fingerprint of the reduction to be obtained.

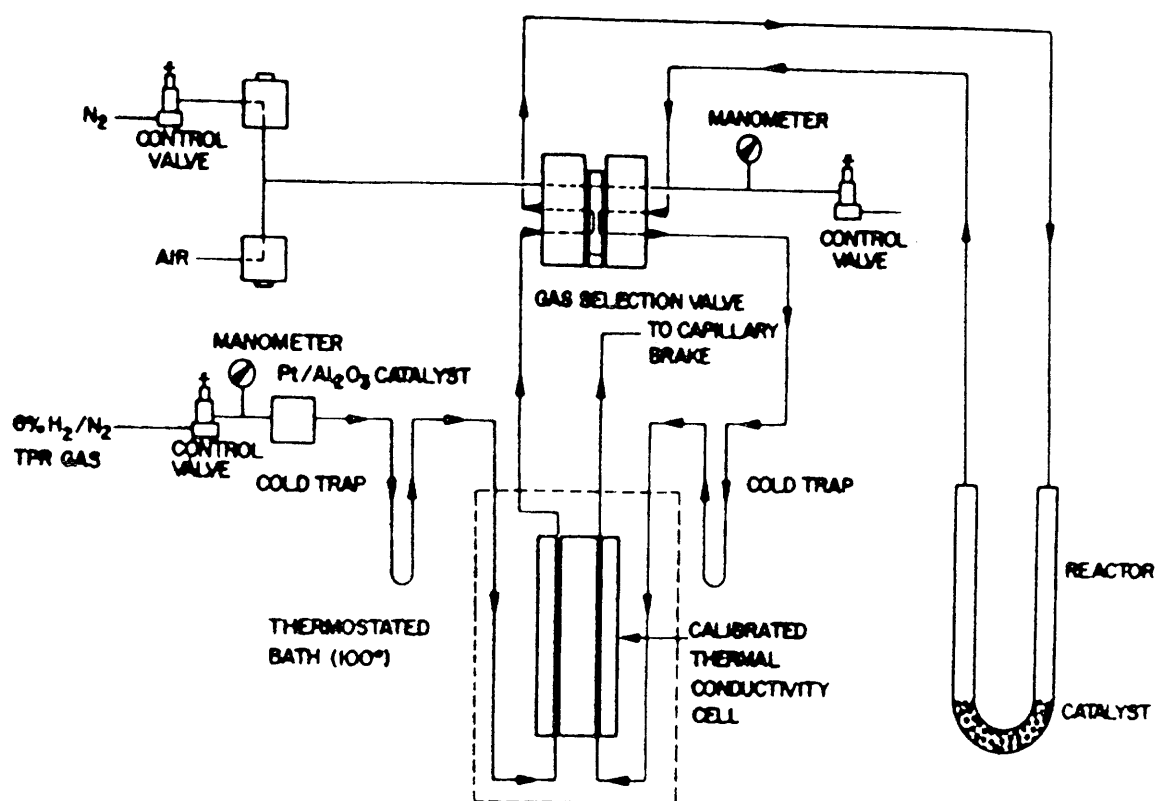


FIGURE 36

Generalised Diagram of TPR System

Temperature programmed reduction of the coke samples was carried out using a furnace coupled to a Stanton Redcroft linear temperature rate controller (model no. LVB/C840/R) and a Gow Mac hot wire detector.

A sample of around 250 mg was heated at a rate of $5^{\circ}\text{C} / \text{min.}$, in the range of 0°C to 800°C . A mixture of He / H_2 gases was passed over the sample and by analysis of the quantity of gas passed with that observed after passage over the sample the amount of gas adsorption was obtained. The quantity of gas adsorbed has been shown to be a function of the degree of intercalation occurring in the carbon (Watanabe et al., 1971; Terai and Takahasi, 1984) and as such was used in the present structural studies, in a comparison of the feed, ex-tuyere and reacted feed coke samples.

3.14 Detection of Potassium Penetration

An experiment was set up to try to detect the extent of potassium penetration in metallurgical coke. Samples of feed coke granules ($- 710$ to $+300$ microns) were refluxed for five hours in a 3% solution of potassium carbonate in water. Around five grammes of coke was refluxed in 250 ml of alkali solution. The coke samples were then removed, split into equal portions and allowed to dry in air on filter paper. Portions of the potassium carbonate solution were retained for analysis after refluxing with the coke.

The samples were subsequently washed with distilled

deionised water and the washings retained for analysis. The washings were taken as being representative of the surface potassium concentration (including the larger macropores), this being the most readily removable portion of the potassium which had been absorbed by the coke.

The coke samples remaining after washing were again allowed to dry in air and then leached with Aristar grade acetic acid. The coke samples were added to 10 ml of 2% acetic acid and shaken (end over end) overnight. The mixtures were filtered and the acetic portions retained for analysis. The potassium leached in this way was taken to indicate the portion of potassium of the original alkali solution residing in the smaller macropores and larger mesopores. The coke samples were once more allowed to air dry.

These dried samples were used in an acid-bomb test. The coke sample was placed in the teflon interior of the acid bomb along with 5 ml 18.3 M H_2SO_4 and 5 ml 15.6 M HNO_3 . The acid bomb was then sealed and placed on a sand tray. The sand tray was then heated to a temperature of 180°C for a period of three hours. After a period of cooling the acid bomb was opened and the contents filtered and retained for analysis. The potassium present in these samples was taken to have come from the smaller mesopores and micropores, as this portion would be the most difficult to remove from the coke. Release of this potassium would require the destruction of the carbon structure, which occurred during the acid bomb treatment.

The experiments were subsequently repeated with feed coke which had not been refluxed with alkali, but which had been treated in all other respects identically to those samples which had been refluxed with potassium carbonate. These "blank" samples were then used as a standard background count for potassium concentration.

All the collected samples were analysed for potassium content using a standard (Evans Electroselenium Ltd.) flame photometer. Standard curves for potassium concentration were plotted using atomic adsorption standard potassium nitrate solutions.

3.15 Graphite / Potassium Reactions

Two experiments were designed to investigate the formation of potassium / graphite intercalation compounds.

3.15.1 Graphite / Metal Reactions

The first of these investigations involved the reaction of graphite with potassium metal. Large flakes of Ticonderoga graphite (Leadhill mine, Ticonderoga, New York State, U.S.A.) were intimately mixed in a pyrex crucible with finely divided pieces of potassium metal, which had been dried and cleaned. The crucible was placed in a Speedivac 12 E6 / 1146 coating unit, a Pt / Rh thermocouple having been inserted into the crucible. The bell jar of the coating unit was then evacuated to a pressure of around 10^{-4} torr, and the mixture in the crucible heated by means

of the high tension electrodes of the coating unit. The temperature was raised slowly until the graphite / potassium mixture reached 300°C , and this temperature was maintained for a period of fifteen minutes. The sample was then allowed to cool before removal from the coating unit. The experiment was subsequently repeated using various powdered feed cokes (B.S. 72 mesh) in place of the graphite flakes.

3.15.2 Graphite / Potassium Carbonate Reactions

In order to test the possibility of creating potassium intercalates in coke by the reaction of the coke with potassium carbonate (cf. feed coke reactions with potassium vapour) it was decided to test this type of reaction by substituting graphite for coke. Graphitised carbons are known (Berger et al., 1975) to intercalate more readily than non-graphitised carbons. Thus a negative result for the graphite / potassium carbonate reaction would throw doubt on the possibility of obtaining potassium intercalates in the coke / potassium carbonate system.

Large flake, Ticonderoga graphite was placed in a reaction vessel, (figure 37). Anhydrous potassium carbonate (Analar grade) was added to the graphite and the reaction vessel evacuated by attachment to a vacuum line.

After evacuation the reaction vessel was sealed by separation of the vessel from the B14 cone by constriction of the capillary connection. The graphite / carbonate

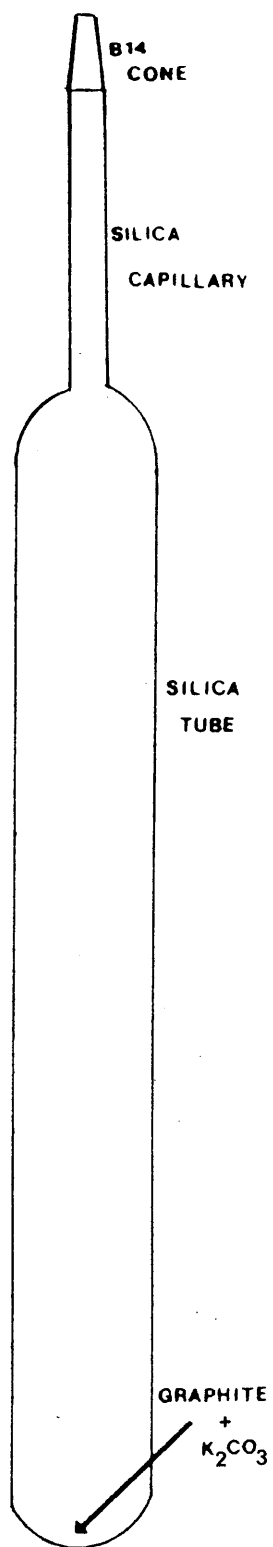


FIGURE 37

Reaction of Graphite with Potassium Vapour

sample was then evenly distributed along the length of the reaction vessel. The vessel was subsequently placed in a laboratory electric (barrel) furnace, with the centre of the reaction vessel coinciding with the centre of the furnace hot zone.

The furnace temperature was slowly raised until the decomposition temperature of potassium carbonate was reached. The furnace temperature was then maintained at this temperature for a period of fifteen minutes, then slowly decreased and the sample allowed to cool to room temperature. The reaction tube was removed from the furnace and the graphite sample examined. This experiment was subsequently repeated using various feed cokes in place of the large flake graphite.

3.16 Microporous Structure Determinations

Investigation of the microporous nature of a variety of coke samples, both feed and ex-tuyere samples, was carried out by application of Dubinin / Raduskevich type equations, at the University of Neuchâtel, Switzerland.

Results

The overall aim of this present work was first to characterise structural changes, and in particular microstructural changes, occurring in metallurgical coke during its passage through the blast furnace. Second, to determine the nature of the factors affecting these changes, in the hope that detrimental changes in structure could be avoided in the future by an understanding of the influencing conditions.

The results in this chapter are arranged in the order in which events occurred, during pursuit of these aims. The order of these results is hopefully a logical pattern in which industrial samples were analysed, followed by investigation of reactions involving these samples with subsequent analysis of the physical and chemical properties of the reaction products.

The initial set of results presented are in the form of a table of the chemical (including some physical) properties of all of the industrial coke materials examined. These results are fairly self explanatory and are referred to later, in a detailed discussion of the coke properties.

First, the coke material as supplied to industrial blast furnaces was examined to determine the nature of the basic material, in order that deviations from the original structure could be determined.

Second, analysis was made of the ex-tuyere coke material. This material had been removed from the base of industrial blast furnaces. As such this material had experienced the physical and chemical conditions within the furnace. Analysis of this coke material then revealed the nature of the structural changes which the feed coke had been subjected to during its interaction with the blast furnace environment.

With some knowledge of the blast furnace conditions, experiments were then designed to reproduce the effects induced by the blast furnace. In order to test the viability of the reaction design it was first tested using large flake graphite in place of the coke, as graphite often undergoes reactions more easily than cokes due to its greater three dimensional structure. Thus if the experimental design was successful using graphite then, with adjustment, it was hoped that the experiments could then be repeated using the metallurgical coke material.

The experimental design proved successful and the structural changes observed in the industrial tuyere cokes appeared to be fairly reproducible, in the laboratory, thus pinpointing some of the influencing parameters.

However, successful reproduction of tuyere coke microstructure raised a new set of questions, as to which of the factors involved in the laboratory experiments were responsible for reproduction of the tuyere coke morphology.

In order to observe the importance of thermal effects in determining tuyere coke microstructure, samples were heat treated, in the absence of a possibly influencing chemical environment.

Vice Versa, the chemical environment was reproduced at temperatures below the coke's carbonisation temperature, thus eliminating thermal effects.

Also of interest were the further reactions of the tuyere cokes with potassium vapour and examination of any further changes in the microstructure of the material.

Lastly, it was just possible that the inert carrier gas employed in the reaction design (to reproduce the tuyere coke morphology) contributed to determining some of the characteristics of the reaction products microstructure. Thus, different carrier gases were employed while other possible influencing factors were kept constant and the resulting reaction products examined.

Within each group of samples (feed cokes, tuyere cokes, reacted feed cokes etc.) various results from different methods of analysis are reported. The order in which these are presented, to some extent, reflects their importance to determination of the material's properties. The order of importance increases towards HREM and then decreases.

First, scanning electron microscopy gave an immediate indication as to any structural changes occurring in the

coke, on the macro scale. This method of analysis was quick and easy to perform and was complemented by an energy dispersive X-ray analysing probe (EDXRA), attached to the SEM. The EDXRA probe was used to observe any changes in elemental composition and distribution within the samples.

High resolution electron microscopy (HREM) was the most powerful tool employed for structure determination. The high resolution of the microscope made it possible to view changes in the lattice structure of the cokes, although it was time consuming and required analysis of many samples.

Powder X-ray diffraction studies were employed to complement the HREM analysis, although due to the averaging properties of this technique, many of the salient features observed by HREM were not revealed by powder X-ray diffraction studies of the cokes.

Further analytical techniques were also employed to complement the results obtained by HREM. These techniques included density measurements, analysis by infrared and Raman spectroscopy, and temperature programmed reduction studies.

Lastly, thermogravimetric analyses were made of several of the samples. The object of this being to enhance the information already available (by chemical analysis etc.) as to the nature of the coke material, as well as to observe, to some degree, the catalytic effects of the chemical treatments afforded some of the samples.

The results obtained from the main groups of samples (feed, ex-tuyere, and reacted feed cokes etc.) are given below. In general, samples examined within one particular group exhibited similar characteristics, as opposed to characteristics shown between different groups of samples. Specific differences, which may be of importance, between samples of a particular group will be discussed later.

The chemical analysis and strength determinations of all feed and ex-tuyere cokes, along with those cokes made with single coals are shown in tables 3,4 and 5 (page 134).

4.1 Analysis of Feed Cokes and Cokes Made from Single Coals

Industrial feed cokes and cokes made from single coals generally have the same type of morphology. Hence forth they will all be described as feed cokes except where their properties require that they be separated.

4.1.1 Scanning Electron Microscopy (SEM)

Examination of the feed cokes by scanning electron microscopy (SEM) demonstrated the high levels of porosity in metallurgical coke, as illustrated by plates 5 - 8. SEM did not reveal any obvious differences between any of the feed cokes. The observed pores were of various shapes and sizes, corresponding to the range from mesopores to macropores. Sectioning of the coke samples using a diamond saw produced some artefacts (plate 9) but these could be

clearly identified and thus not confused with the naturally occurring coke structures, or those induced by the coke's passage through the blast furnace.

4.1.2 Energy Dispersive X-ray Analysis (EDXRA)

Typical EDXRA readouts obtained from these types of cokes are illustrated in inserts in plates 5 to 8.

Quantitative analysis of the elements present was not possible using this system, however readouts did give some measure of the relative proportions present.

The cokes exhibited high levels of aluminium, silicon and in some cases chlorine. Calcium and sulphur were present to a lesser extent. There was also some iron present along with small traces of potassium.

When the detector was used to window individual frequencies elemental distributions could be observed. Plates 10 to 16 show typical distributions for sulphur, chlorine, potassium, iron, aluminium, silicon and calcium. The distribution of sulphur, chlorine and potassium appeared to be fairly random with no particularly densely concentrated areas. However, as can be seen from plates 13 to 16 there appeared to be areas where there were high concentrations of iron, aluminium, silicon and calcium in which the calcium, aluminium and silicon were intimately mixed with each other.

The presence of sodium had to be treated suspectly, as it lies on the limit of detection by the EDXRA system.

4.1.3 Transmission Electron Microscopy

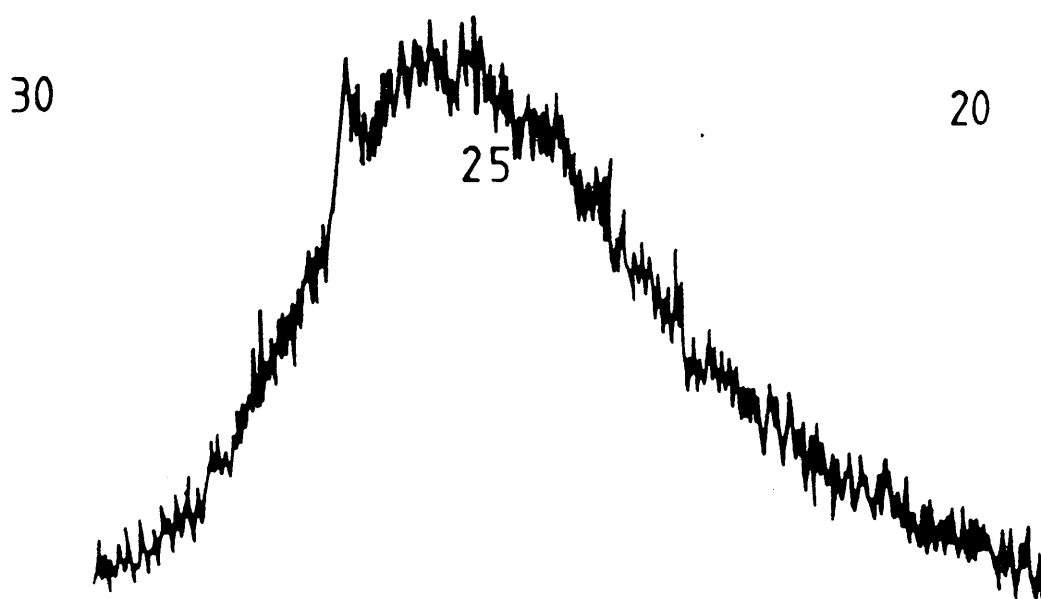
Low resolution micrographs of these feed and single coal cokes did not show any significant morphological differences between samples. The particles of the observed coke samples were of various shapes and sizes but were typically submicron in diameter. Examples of the coke's morphology are shown in plates 17 to 19.

High resolution electron micrographs of these cokes are shown in plates 20 to 24. All of these samples exhibited a typical non - graphitised carbon structure. The interplanar spacings were on average 0.34 nm, with very little 0.3358 nm lattice development and a large degree of turbostratic disorder.

Also present were areas of highly ordered crystalline material. This material is shown in plates 25 to 27 (arrowed) and had a wide range of lattice spacings, ranging from 0.32 - 1.8 nm.

4.1.4 Powder X-ray Diffraction Analysis (XRD)

Figures 38, 39 and 40 show typical powder X-ray diffraction patterns (2θ values) obtained from the feed cokes. The traces show a small broad peak, corresponding to a wide range of carbon lattice spacings, consistent with the

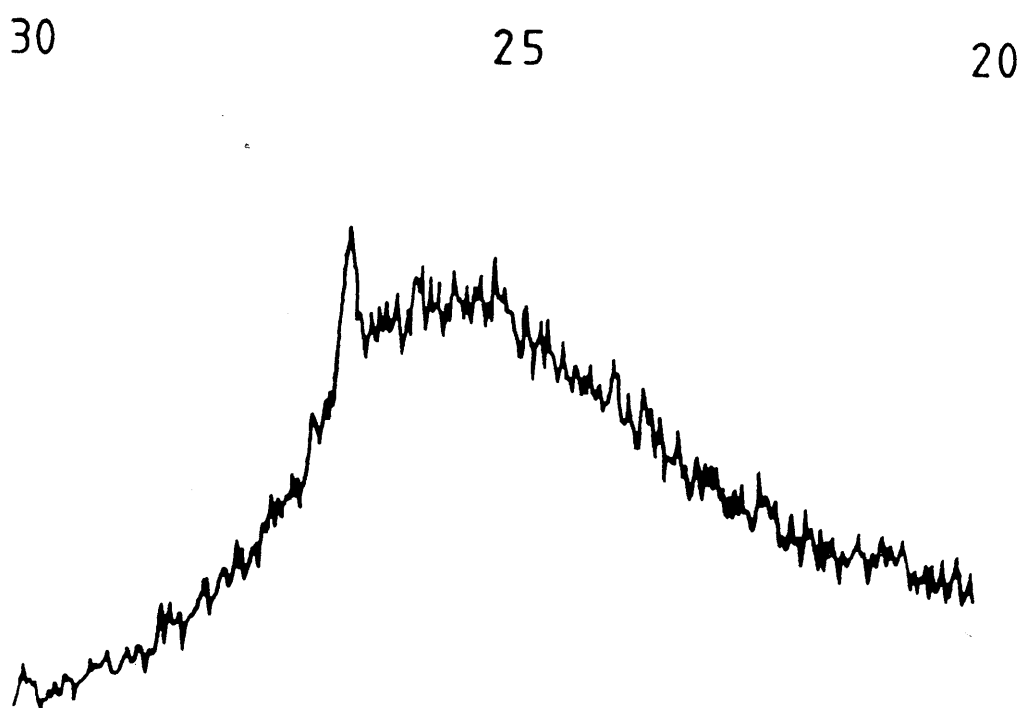


XRD Trace from Feed Coke



XRD Traces from Feed Coke

FIGURE 39



XRD Traces from Feed Coke

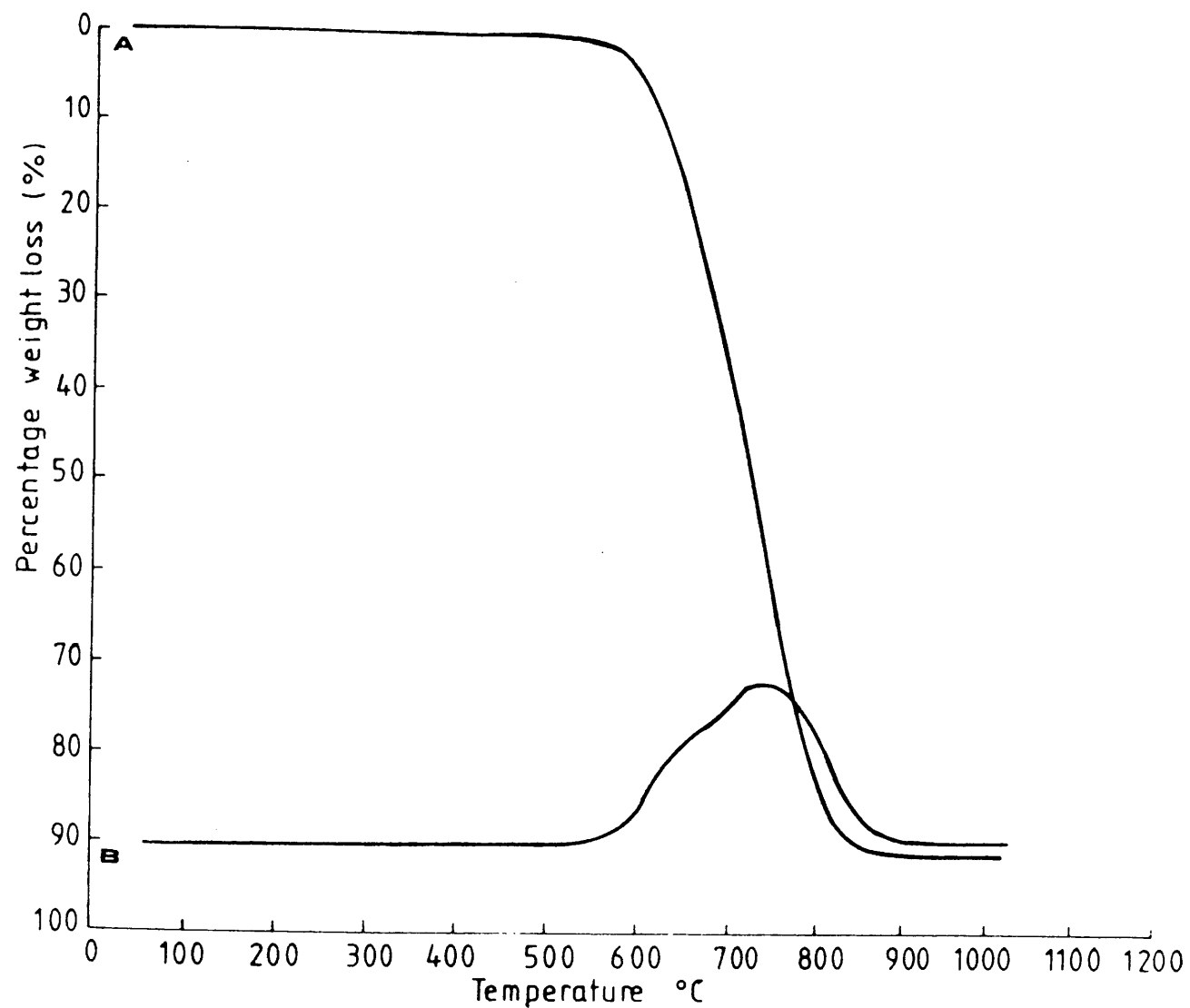
FIGURE 40

turbostratic nature of the feed cokes as observed by HREM.

The spacings range from 29.6° to 22.3° (0.30 to 0.39 nm). The feed coke traces have a typical distribution centred on (26.2 , 0.340 nm) indicating the relative proportions of the lattice spacings present. Little else can be seen from these XRD traces. There is no indication of mineral matter spacings and virtually no signal for the normal (h k l) spacings. Table 7 shows the standard graphite spacings (A.S.T.M.S. index 25 - 284, Holcombe, 1973).

4.1.5 Thermogravimetric Analysis (TGA)

Thermogravimetric analysis results for the feed cokes are shown in figures 41 to 43. Typically there appears to be a double peak present. This first peak (burn-off) starts normally around 550°C . This peak rises sharply and then is superceded by the second of these peaks which begins at around 650°C . The second and smaller peak, also rises sharply and then decreases until completion of the burn-off at around 900°C . This is total burn-off observed during TGA of the feed cokes and takes place over the range of 550°C to 900°C . The first of these peaks represents a 20 %. Weight loss with the second adding a further 68 % of the original sample weight. This remaining weight is then assumed to be largely composed of the inherent mineral matter in the coke which arises from the mineral matter present in the original coal, from which the coke is manufactured.



Trace A indicates % weight loss with temperature.

Trace B indicates rate of weight loss.

TGA Trace from Feed Coke

FIGURE 43

4.1.6 Temperature Programmed Reduction

General consideration of the TPR traces obtained from the feed cokes revealed very little hydrogen uptake to have occurred during the analysis runs.

4.1.7 Density Measurements

The densities of the feed cokes as found by carbon tetrachloride displacement were found to range between 1.65 g / cm^3 and 1.75 g / cm^3 , the average value being 1.70 g / cm^3 . This range illustrates some structural differences between the feed cokes, although this was not observed by any other technique. The crude densities of cokes, as determined by carbon tetrachloride displacement, may be misleading and should only be taken as approximate. Small differences observed between samples may be due to experimental error and not a true reflection of variations in mass / volume ratios.

4.1.8 Infrared Analysis

Due to the opaque nature of the dense black coke material no information was obtained either by transmission or reflectance infrared spectroscopy.

4.1.9 Raman Spectroscopy

It was found that the coke sample "burned" in the laser beam during analysis and hence no information on the coke

surface was obtained by Raman spectroscopy.

4.1.10 Penetration of Potassium

The results obtained from the experiments to analyse the degree of penetration of potassium were inconclusive but showed that the majority of the potassium to reside in the macro and mesopores of the coke. This however, is not unexpected due to the far larger surface area of these regions in comparison with any other region in the coke material. The potassium concentrations obtained from the various coke regions are shown in table 8; i.e. surface, easily leached macropores, not easily leached micropores and the coke lump centre.

4.2 Analysis of Ex-tuyere Cokes

4.2.1 Scanning Electron Microscopy (SEM)

Very few differences were found between the various ex-tuyere samples, when they were analysed by SEM. All samples showed high levels of porosity in the macro and meso pore size ranges (macropore range > 50 nm; mesopore range $2 - 50$ nm).

The ex-tuyere samples also showed some evidence of gasification (plates 28 to 30), which has occurred during the coke's passage through the blast furnace.

4.2.2 Energy Dispersive X-ray Analysis (EDXRA)

Typical EDXRA results obtained from the ex-tuyere cokes are shown in the inserts in plates 28 to 30.

The ex-tuyere samples showed similar concentrations of calcium, aluminium, silicon, sulphur, iron and chlorine as the feed cokes. However, the most outstanding feature of the ex-tuyere results was the high levels of potassium present in all of them. Thus, it can be seen that the passage of coke through the blast furnace greatly increases the ratio of potassium to the other elements present.

Using the detector to give distributions of the elements, gave almost identical results to those of the feed cokes. In other words the elements appeared to be distributed throughout the entire sample in a random manner, although there were regions high in silicon, aluminium and calcium concentration observed in the samples. The potassium observed appeared to be randomly distributed throughout the sample and was not localised in cracks or pores.

4.2.3 Transmission Electron Microscopy

No particular differences were observed between the various ex-tuyere samples when viewed using low resolution transmission electron microscopy (plates 31 to 33).

Three distinct carbon microstructures were observed in the ex-tuyere samples using high resolution electron microscopy.

Concentrations: VL = 0 - 9 ppm
 L = 10 - 39 ppm
 M = 40 - 59 ppm
 H = 60 - 79 ppm
 VH = 80 - 100 ppm

Sample	A	B	C
--------	---	---	---

Concentration of Potassium

Region:

Surface	H	H	M
Macropores	VH	VH	VH
Mesopores	L	M	L
Micropores	VL	VL	VL

VH - Very High; H - High; M - Medium;

L - Low; VL - Very Low

Potassium Penetration of Feed Cokes.

TABLE 8

First, in many regions there were areas similar to those observed in the feed coke material. That is, areas of turbostratic carbon (disordered) with lattice spacings of the order of 0.34 nm.

Second, there were areas of highly ordered carbon lattices; not present in the feed cokes (plates 34 to 36). These areas of extensively ordered (0002) carbon lattices had an average interplanar spacing of 0.34 nm, and had a long range order in the La direction of normally four times that of the disordered regions (0.34 nm) and occasionally up to a ten fold increase in order. There was however, not a great deal of difference between the Lc distances in the "crystallites" of the feed and ex-tuyere cokes.

Third, there were also areas of expanded, disordered carbon lattices. These areas maintained the randomly orientated "onion" type structure observed in the carbon regions of the feed cokes. However, these regions of turbostratic disorder were different in that the interplanar spacings had been greatly enlarged. This expansion of the carbon lattices was typically found to be around 0.45 to 0.47 nm (plates 37 to 39).

Also observed in the ex-tuyere samples were areas of highly ordered crystalline material similar to that observed in the feed coke material. This crystalline material had a wide range of interplanar spacings (0.32 - 1.8 nm) and is shown in plate 36 (arrowed).

4.2.4 Powder X-ray Diffraction (XRD)

Examination of the ex-tuyere samples by X-ray powder diffraction revealed a much sharper, more intense peak for the carbon - carbon interplanar distance than those obtained from the feed cokes (figures 44 to 46). This sharpening of the peak (centred on 0.34 nm) is indicative of a greater number of lattices within a smaller range of spacings. The range of this peak is 28.5° to 23.8° corresponding to a range of 0.31 nm to 0.37 nm. However, the XRD traces obtained from the ex-tuyere samples also showed a small number of slightly larger lattice spacings to be present at around 0.40 nm to 0.49 nm.

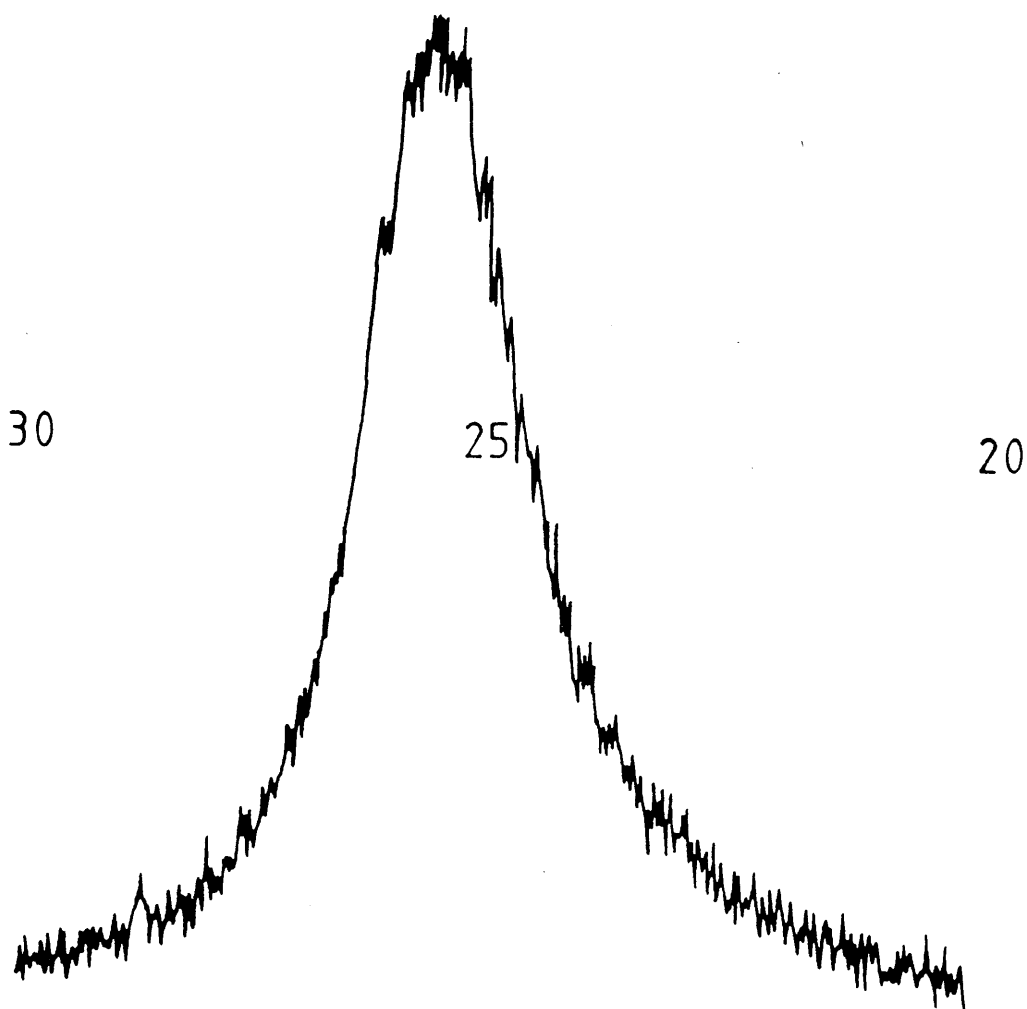
As observed in the feed cokes there was no indication of the presence of the crystalline material and it must be concluded that the signals from these regions are not sufficiently intense to be picked up by the detector.

4.2.5 Temperature Programmed Reduction (TPR)

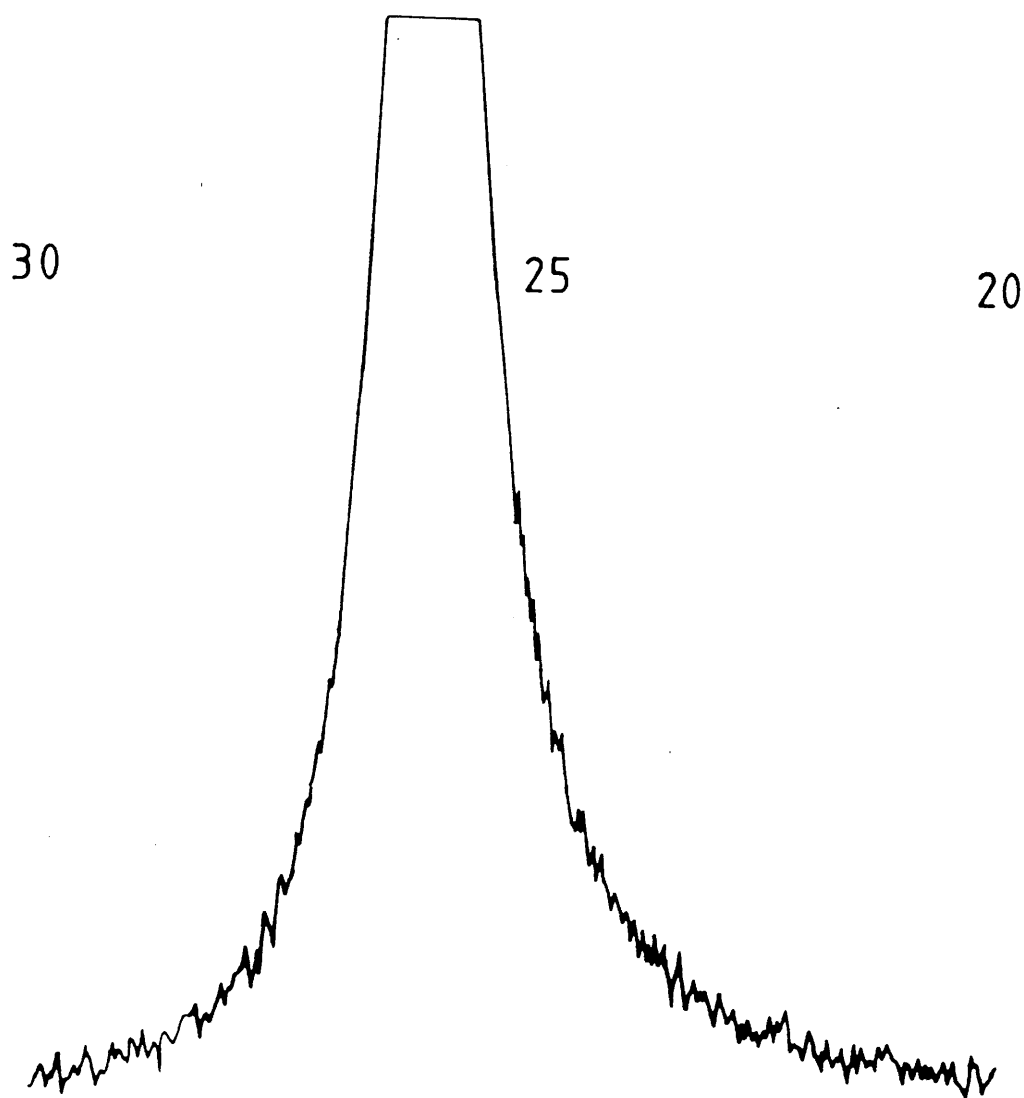
Although it appeared that very little hydrogen has been taken up by the ex-tuyere coke measurements the results had to be considered with respect to the feed coke samples, which shows a small but significant larger hydrogen uptake in the ex-tuyere samples compared with the feed coke.

4.2.6 Density Measurements

Carbon tetrachloride displacement measurements of the



XRD Trace from Ex-tuyere Coke



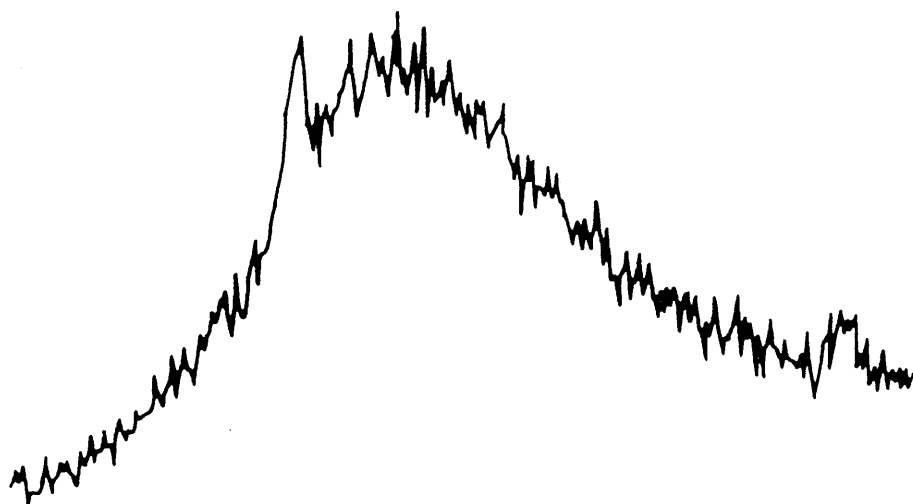
XRD Trace: from Ex-tuyere Coke

FIGURE 45

30

25

20



XRD Trace from Ex-tuyere Coke

FIGURE 46

ex-tuyere cokes has shown them to have densities in the range 1.88 g / cm^3 and 1.98 g / cm^3 , with an average value of 1.94 g / cm^3 . Again variances observed between tuyere cokes are small and may be accounted for by experimental error, as opposed to structural differences, due to the crude method employed to determine them.

4.2.7 Infrared Analysis

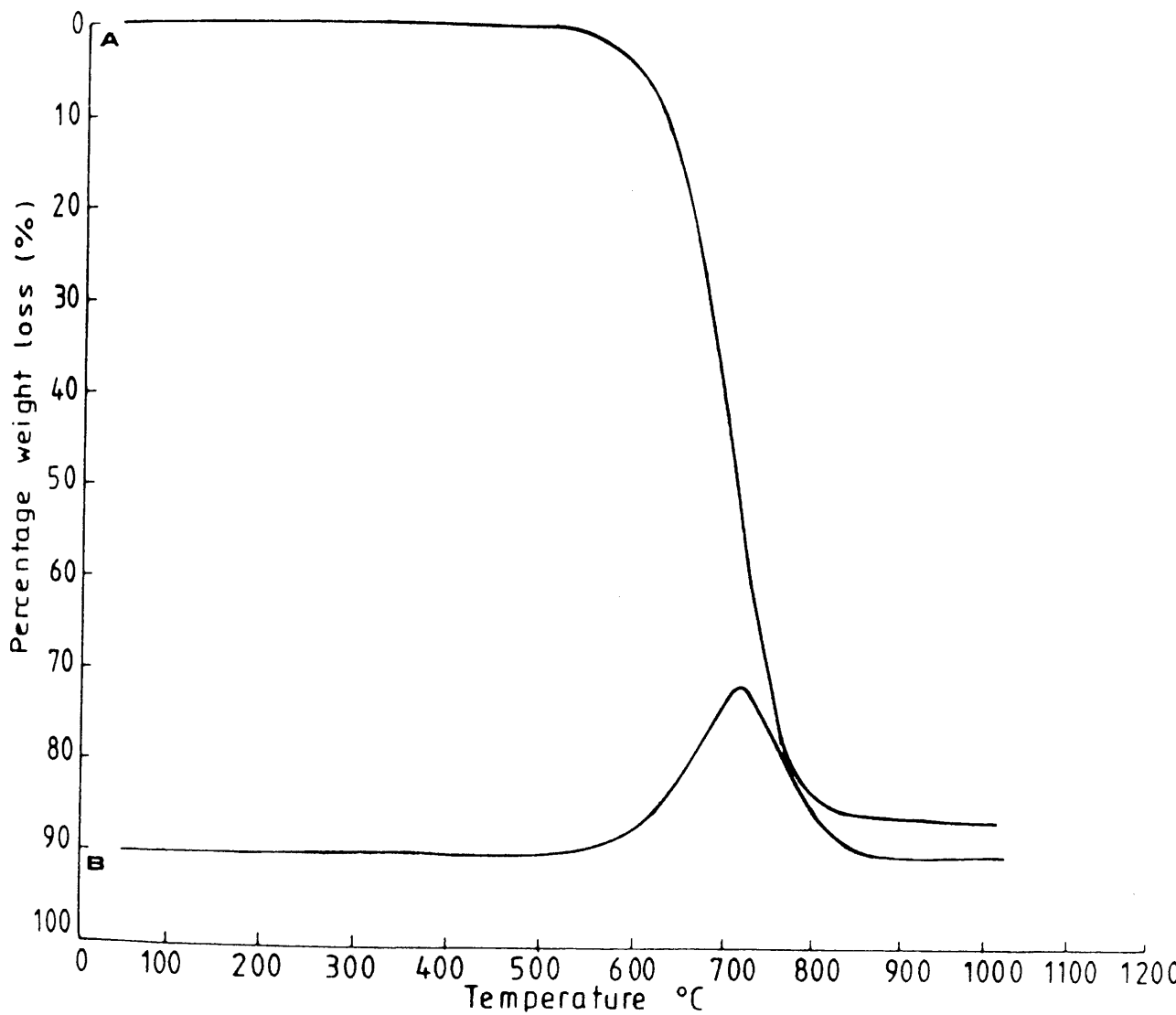
As found with the feed coke samples it was impossible to obtain any information on the ex-tuyere cokes by either reflectance or transmission infrared spectroscopy. This was due to the opaque nature of the coke material.

4.2.8 Raman Spectroscopy

Again as in the feed coke samples the ex-tuyere cokes "burned" when exposed to the laser beam. Thus no information was obtained on the surface of these samples by the technique of Raman spectroscopy.

4.2.9 Thermogravimetric Analysis (TGA)

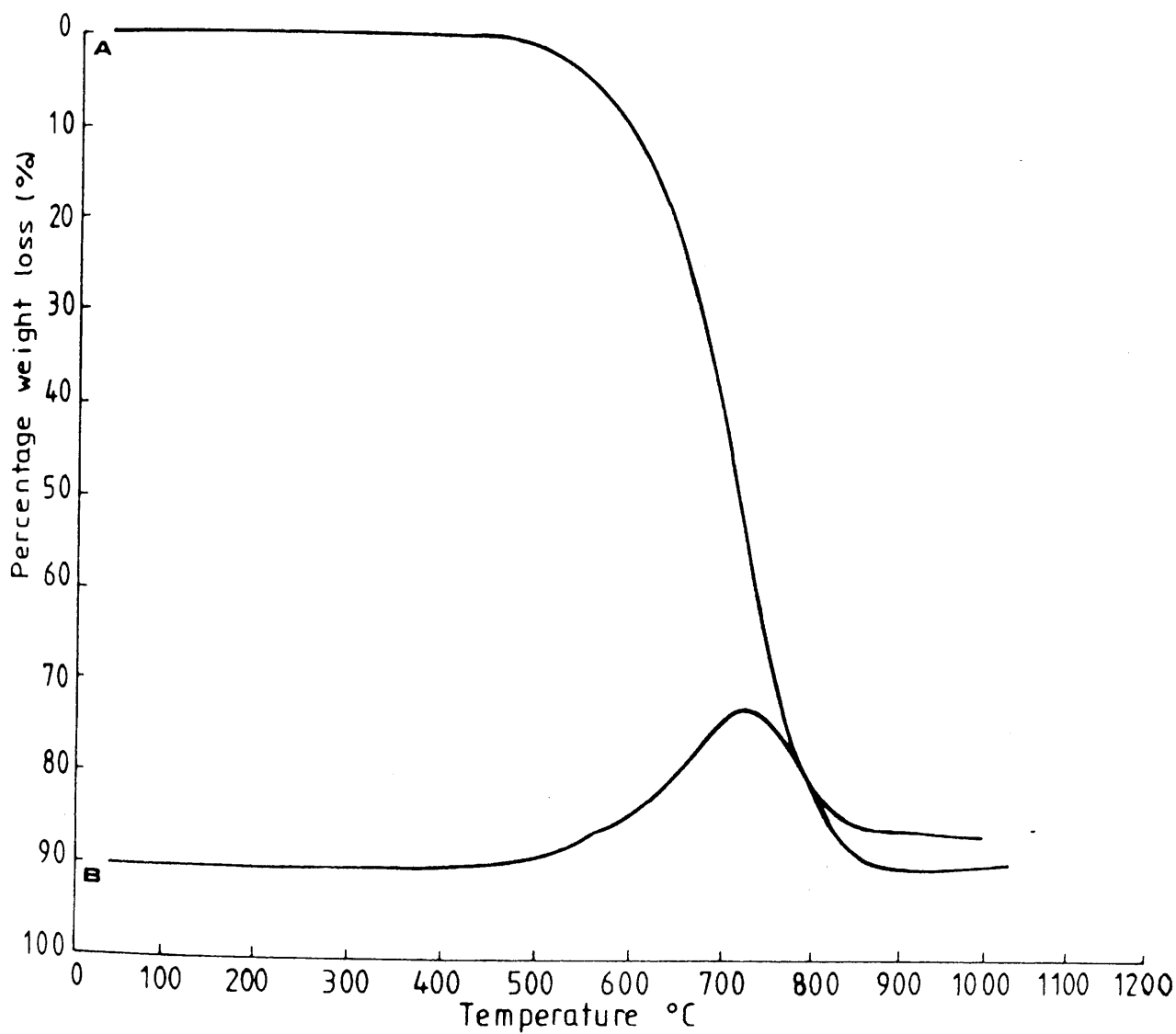
Figures 47 to 49 show traces typically obtained by thermogravimetric analysis of the ex-tuyere cokes studied. The traces show only one peak corresponding to an extensive weight loss in the sample over the range 510°C to 850°C . The total weight loss observed during the analysis can almost be attributed solely to this peak and accounts for a 88 % decrease in the original sample weight. The remaining



Trace A indicates % weight loss with temperature.

Trace B indicates rate of weight loss.

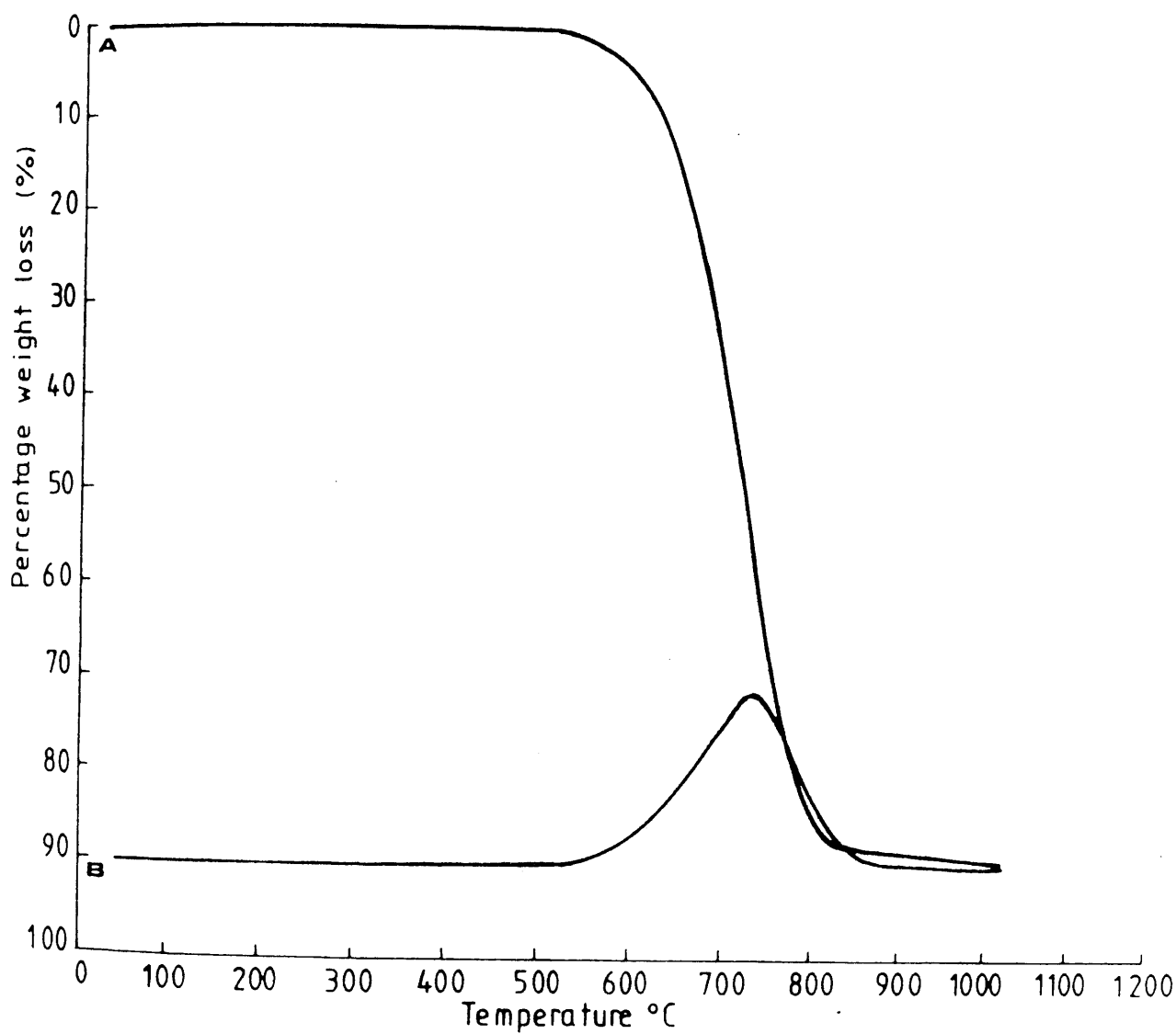
TGA Trace. from Ex-tuyere Coke



Trace A indicates % weight loss with temperature.

Trace B indicates rate of weight loss.

TGA Trace, from Ex-tuyere Coke



Trace A indicates % weight loss with temperature.

Trace B indicates rate of weight loss.

TGA Trace: from Ex-tuyere Coke

weight after analysis was assumed to be composed of ash and mineral matter, both of which were incorporated into the coke during its manufacture from the mined coal.

4.2.10 Penetration of Potassium

The results obtained from these experiments on the ex-tuyere cokes were similar to those of the feed cokes. Although the figures obtained for potassium penetration were not conclusive they showed the vast proportion of the potassium taken up by the coke samples to reside in the macropores and mesopores. The vast surface area covered by pores in this size range would indicate this result to have been expected.

The concentrations obtained from the various coke regions i.e. surface, macropores, less accessible macro / mesopores and from centre of the sample are shown in table 9.

4.3 Graphite / Potassium Reactions

The reaction of ticonderoga graphite with potassium metal under vacuum gave rise to the graphite exhibiting a bluish colour. This is indicative of the formation of a stage II type graphite potassium intercalate. The formation of potassium / graphite intercalates has been previously reported (Carr 1965, Saunders, 1978). The reaction of the ticonderoga graphite with potassium carbonate gave rise to an golden / yellow colour in the graphite. Graphite / potassium compounds of this colour have previously been

Concentrations: VL = 0 - 9 ppm
L = 10 - 39 ppm
M = 40 - 59 ppm
H = 60 - 79 ppm
VH = 80 - 100 ppm

Sample	A'	B'	C'
--------	----	----	----

Concentration of Potassium

Region:

Surface	H	M	H
Macropores	VH	VH	VH
Mesopores	M	M	L
Micropores	VL	VL	VL

VH - Very High; H - High; M - Medium;

L - Low; VL - Very Low

Potassium Penetration of Ex-tuyere Cokes.

shown to be stage I type (C_8K) intercalated potassium species. Thus the experimental design for reaction of feed coke material could give rise to intercalated material.

However, no colour change in the coke material was apparent when it was reacted with potassium metal in the same manner as the graphite. Neither was any colour change observed when the coke material was reacted with potassium carbonate under the same conditions as the graphite.

These results led to the conclusions that either the coke material did not form intercalates with potassium in the same manner as graphite or that any colour change which had occurred in the coke was not apparent due to its lack lustre character in comparison with the large flake ticonderoga graphite which had an extremely lustrous appearance.

The object of these experiments was to determine, by colour change, whether or not the reaction set up designed for the reaction of feed coke material with potassium vapour could give rise to the formation of carbon / potassium intercalates. This having been proved in the graphite case (though not proved or disproved for the feed coke material), no further examination of reaction specimens was carried out by HREM, XRD or any other technique.

4.4 Analysis of Reacted Feed Coke Samples

These experiments were repeated several times using the

feed cokes A, B and C. As in other studies of these three feed cokes and their reactions, all three behaved in a similar manner. Experiments were repeated several times in order to obtain reproducible results. Often the samples would react completely out of character from the general view of these results. These out of character results did not, in any way, occur in a reproducible manner. The reasons for their occurrence are likely to be highly complex and are outwith the scope of this study. However, the three cokes observed demonstrated a general trend and it is this trend which is described here.

4.4.1 Scanning Electron Microscopy

Scanning electron microscopy of the reacted feed cokes reacted with potassium carbonate at 1100°C showed very little difference in pore structures, sizes or general coke morphology from either the feed coke samples or the ex-tuyere samples. The reacted cokes did, however, have some gasification features common to the ex-tuyere samples. Plates 40 to 42 illustrate typical examples of the structures observed in all three of the reacted feed cokes.

4.4.2 Energy Dispersive X-ray Analysis (EDXRA)

Energy dispersive X-ray analysis of the reacted feed cokes were typically similar readouts to those observed during examination of the corresponding ex-tuyere coke samples. EDXRA determinations were carried out on samples which had been prepared by bulk reaction (lumps around 60 mm) of feed

cokes with potassium vapour by British Coal. These samples were subsequently sectioned using a diamond saw for EDXRA purposes. EDXRA measurements were also made on the samples of powdered feed coke reacted with potassium vapour and on sectioned samples which had been reacted (at Glasgow University) with potassium vapour, using the bulk method of sample reaction described in the experimental chapter.

These results were useful for general comparison with non-reacted feed cokes but were less reliable than results obtained from sectioned samples, as accurate EDXRA measurements require a flat surface to be exposed to the electron beam and the detector. Both powdered and sectioned samples did however give broadly similar results. The readouts for the reacted samples show (inserts plates 40 to 42) the presence of aluminium, silicon, calcium, sulphur, chlorine and iron to be present in roughly the same proportions as in the ex-tuyere coke samples. Also (c.f. ex-tuyere samples) the most marked difference between the reacted feed cokes and non - reacted feed cokes is the massive increase in potassium. In some areas of reacted feed cokes, potassium levels are higher than those of any other element examined in the area. Elemental maps of the samples constituent elements (those which lie in the analytical range of EDXRA) showed most of the elements to be randomly distributed throughout the sample. However, as in the non - reacted feed cokes and ex-tuyere cokes there appeared to be areas of high concentration of aluminium, calcium and silicon, where these elements were intimately associated with each other. The high levels of potassium

exhibited by the reacted feed cokes did not appear to be localised but randomly dispersed throughout the sample.

4.4.3 Transmission Electron Microscopy

Reacted feed cokes did not markedly differ in morphology from those of non-reacted samples or the ex-tuyere cokes when examined using low resolution transmission electron microscopy. The particle size did not appear to have been significantly altered and maintained the random shapes exhibited by the tuyere and feed cokes. Plates 43 and 44 show examples of low resolution micrographs obtained from the reacted feed cokes.

High resolution electron microscopy of the reacted feed cokes revealed the presence of three structural carbon forms.

First, there was the occurrence of turbostratically disordered carbon lattices with an interplanar spacing of 0.34 nm on average (plates 45 to 47). This type of morphology was also observed in the unreacted feed and the ex-tuyere samples.

Second, areas of expanded randomly ordered carbon lattice, 0.45 nm average spacing, were observed (plates 48 to 50). These expanded lattices were similar in nature to those observed in some regions of the ex-tuyere samples.

Third, as in the ex-tuyere samples, areas of highly ordered

carbon lattices were seen to be present in the reacted feed cokes. These ordered lattices had average interplanar spacings of 0.34 nm (plates 51 to 53).

Also, as in the tuyere cokes and feed cokes there was the presence of highly ordered crystalline material. This material was randomly distributed throughout the reacted feed coke samples and had interplanar spacings from 0.32 nm to 1.8 nm.

4.4.4 Powder X-ray Diffraction (XRD)

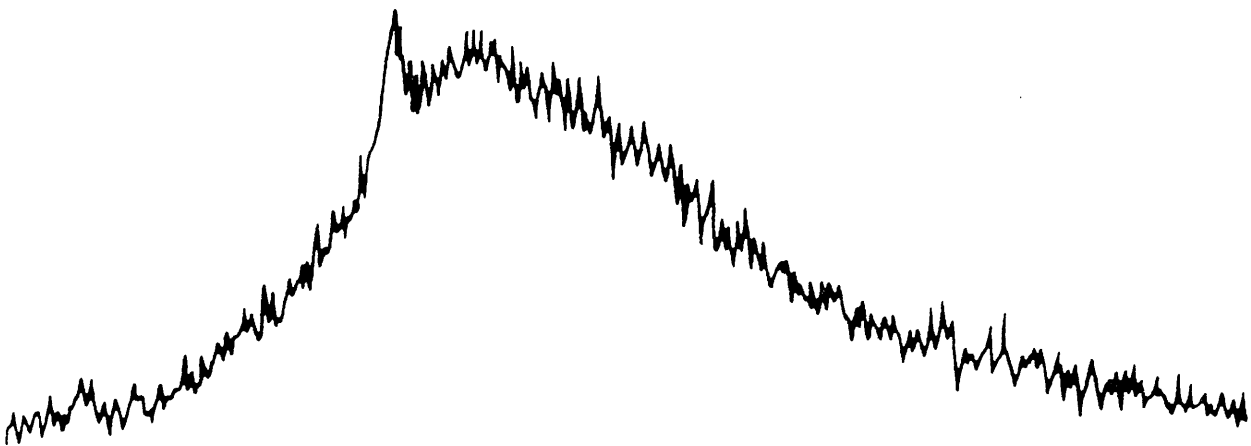
Typical results obtained by powder X-ray diffraction of the reacted feed cokes are shown in figures 50 to 52. These traces are similar to those observed for the ex-tuyere coke samples.

The reacted feed cokes show a sharper, more intense peak for the carbon - carbon interplanar spacing when compared with their respective non-reacted feed cokes. This again is indicative of a smaller range of d-spacings or a degree of reduction of the turbostratic nature of the material. The range of spaces for the reacted feed cokes is around 0.32 nm - 0.43 nm. This observed ordering of the carbon structure of the cokes (both by HREM and XRD) is not as extensive as the ordering observed in the ex-tuyere cokes. It is estimated that the increase in L_a distance is increased by a factor of six in comparison with the non-reacted feed cokes (L_c distances are not greatly enhanced). This is compared with an increase of between

30

25

20



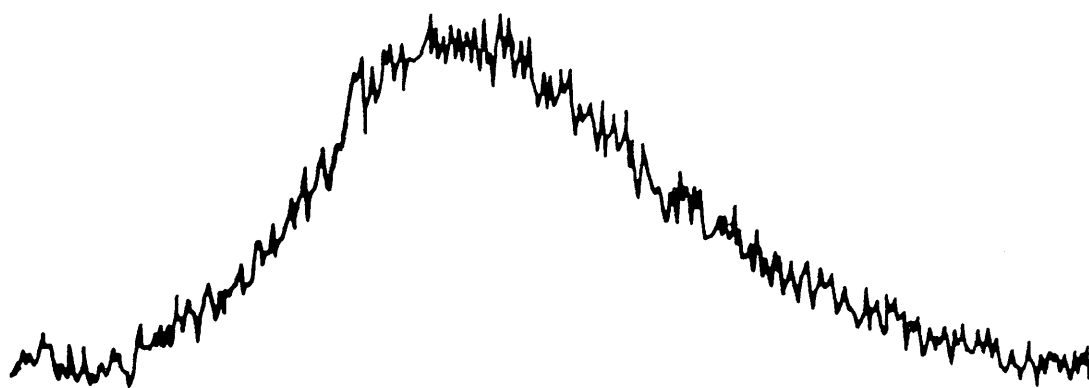
XRD Trace from Reacted feed Coke

FIGURE 50

30

25

20



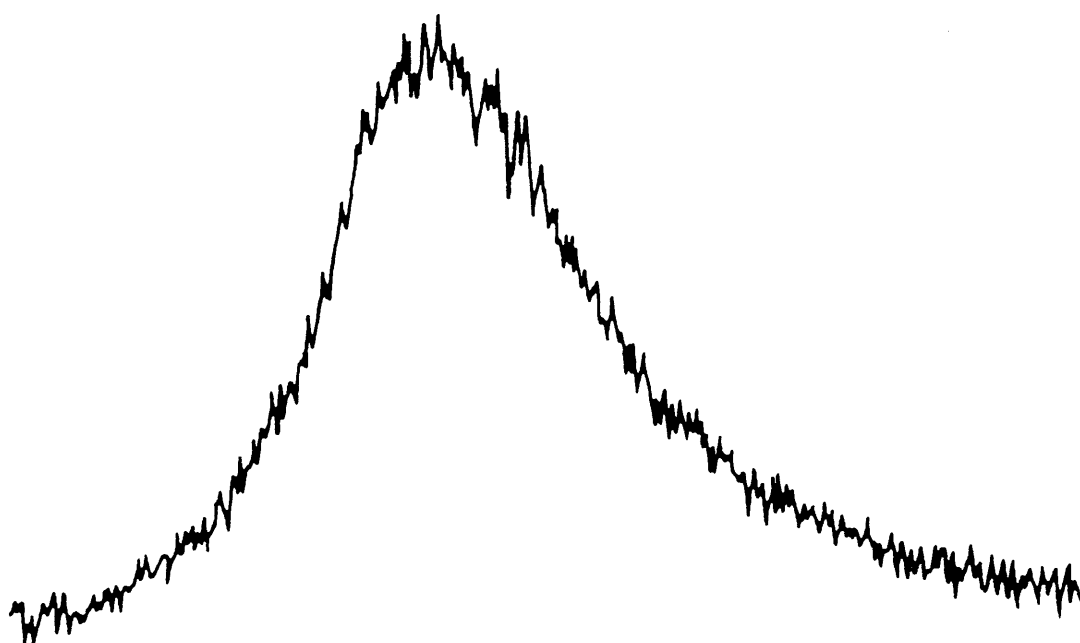
XRD Trace from Reacted feed Coke

FIGURE 51

30

25

20



XRD Trace from Reacted feed Coke

FIGURE 52

four and ten fold observed in the tuyere coke. Thus, perhaps the temperatures experienced by true blast furnace coke are significant in determining the structural changes or perhaps laboratory conditions have not entirely mimicked those (excluding temperature factors) of industrial coke. However, as observed in the ex-tuyere coke traces there is an indication of the presence of some intercalated material. The major peak does not completely "tail-off" until around 0.43 nm. Although the intensities of the spacings in the range 0.36 nm - 0.43 nm is very low, it is likely to be significant and although the spacing between 0.36 nm and 0.43 nm does not correspond to one of the normal carbon / potassium intercalates it is probably indicative of a residue compound formed from the collapse of the intercalated species.

4.4.5 Temperature Programmed Reduction (TPR)

TPR traces obtained from reacted feed cokes did not show a considerable degree of hydrogen uptake. However, as in the case of the ex-tuyere cokes these results have to be considered with respect to the non-reacted feed coke material. In this light there appeared to be a slight increase in hydrogen uptake in the reacted feed cokes in comparison with non-reacted and this may be due to the presence of some intercalated material or residue compound formed from such a species, such that an increase in surface area of the material is presented to the hydrogen due to the expanded structure.

4.4.6 Density Measurements

Displacement of carbon tetrachloride by finely ground reacted feed coke particles gave values of between 1.85 g / cm^3 and 1.95 g / cm^3 for the density of this material, the average value being 1.90 g / cm^3 . As with all measurements made using this technique small variances observed between the reacted feed cokes may be due to experimental error in determining the densities as opposed to structural changes between various reacted feed cokes.

4.4.7 Infrared Analysis

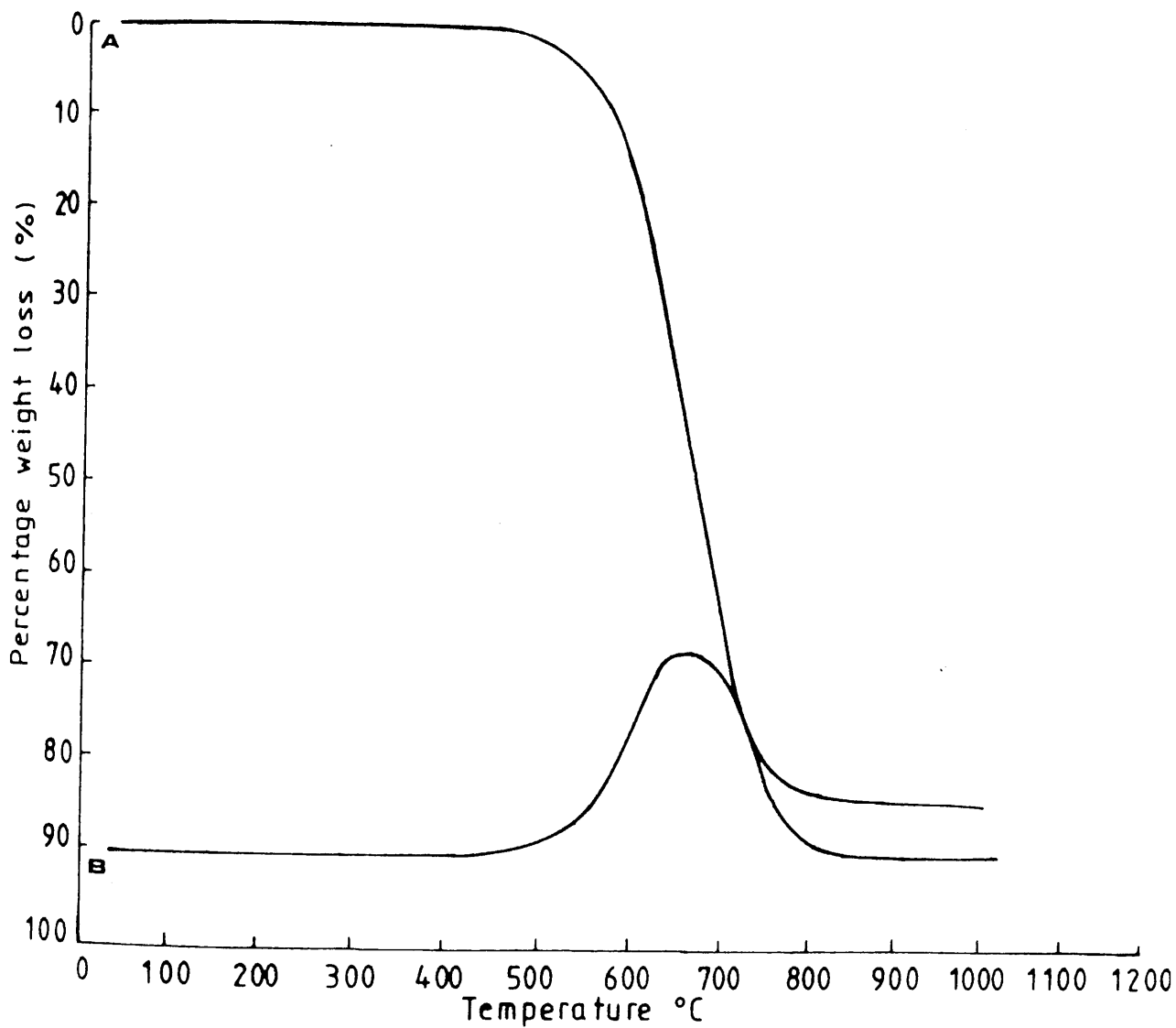
Again, as in the cases of feed cokes and ex-tuyere cokes infrared spectroscopic analysis did not yield any information on the reacted feed cokes due to the opaqueness of the material.

4.4.8 Raman Spectroscopy

As with the other two "classes" of coke material examined, laser Raman spectroscopy simply "burned" the coke rather than yielding any information as to the surface species present.

4.4.9 Thermogravimetric Analysis(TGA)

Typical traces obtained by thermogravimetric (TGA) analysis of the reacted feed cokes are shown in figures 53 to 55.

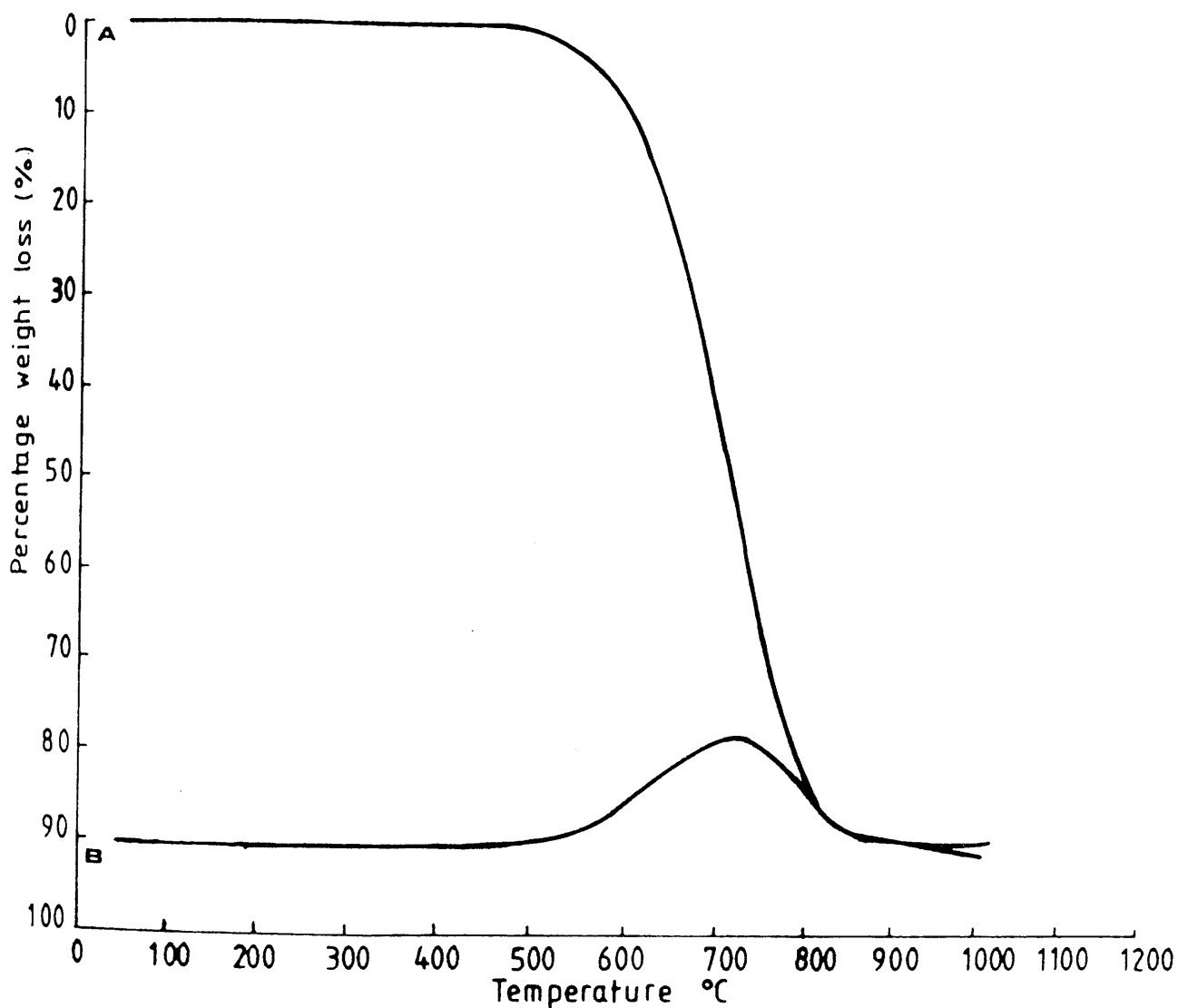


Trace A indicates % weight loss with temperature.

Trace B indicates rate of weight loss.

TGA Trace from Reacted Feed Coke

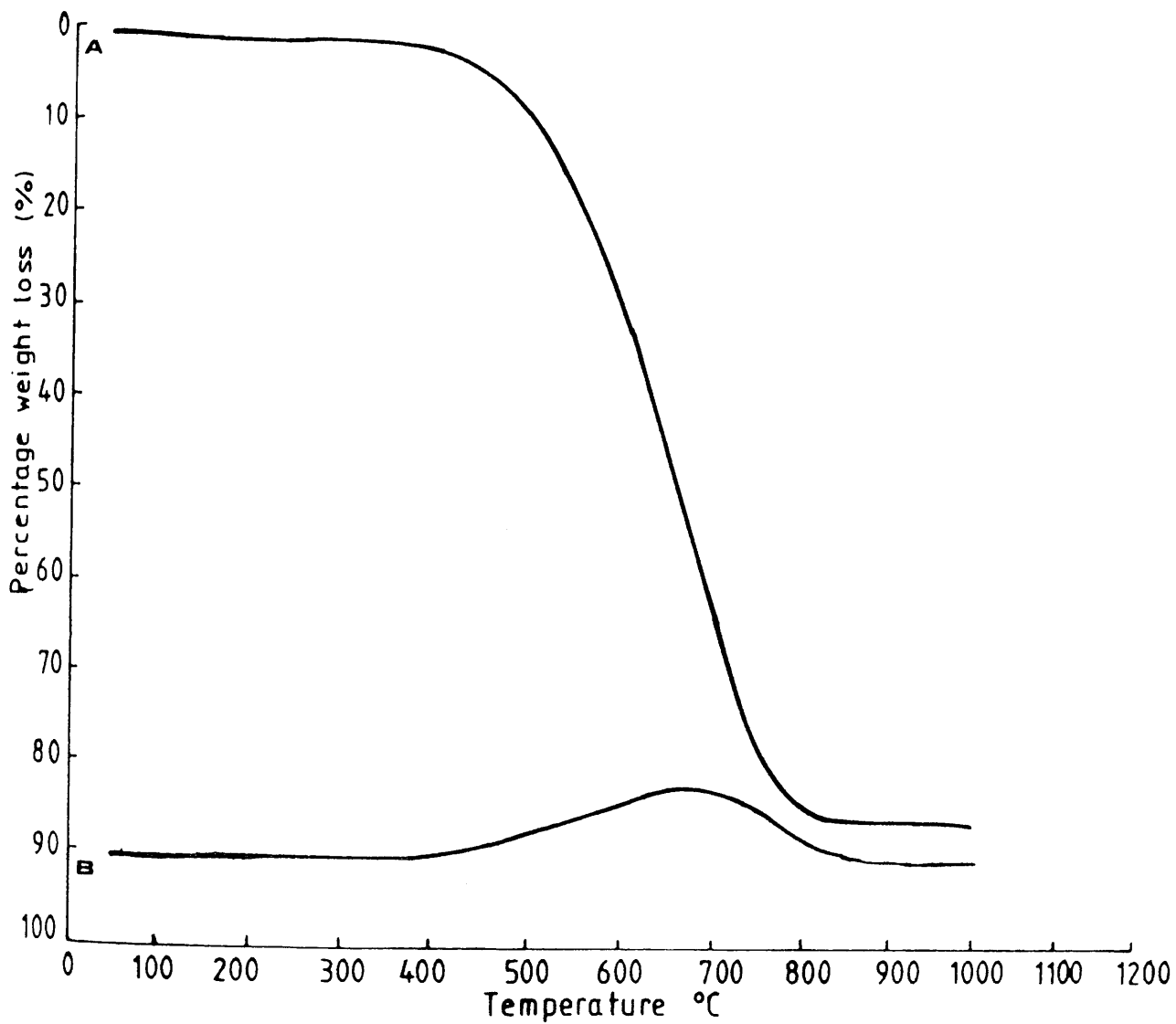
FIGURE 53



Trace A indicates % weight loss with temperature.

Trace B indicates rate of weight loss.

TGA Trace from Reacted Feed Coke



Trace A indicates % weight loss with temperature.

Trace B indicates rate of weight loss.

TGA Trace from Reacted Feed Coke

The single peak, normally in the range 420 - 850°C corresponds to an extensive weight loss (87%) in the material. This is due to burning of the coke.

However, more important than the degree of weight loss observed, is the range in which the weight loss occurs, and the fact that there is only a single peak present. Ash and mineral matter are assumed to account for the remaining weight fraction after burning had taken place.

4.4.10 Potassium Penetration

Due to the inconclusive results obtained from potassium penetration studies of the feed and ex-tuyere cokes it was decided not to repeat this analysis on the reacted feed cokes.

4. (a) Microporous Structure of Cokes

Examination of the microporous structure, (kindly carried out by Professor F. Stoeckli at Neuchâtel, Switzerland) using the Dubinnin / Raduskevich model, revealed no significant differences between individual feed cokes, reacted feed cokes, and their corresponding tuyere samples, nor between any of these classes of sample.

4.5. Effect of Temperature on Coke Structure

In order to more fully understand the results obtained from the tuyere cokes and reacted feed cokes, feed cokes were

heated in the absence of alkali vapour to 1500°C. Thus it was hoped that any changes effected by thermal treatment of the coke material could be separated from those effected by chemical treatment.

Three feed cokes were heated to 1500°C, in nitrogen, at a rate similar to that which the coke would experience in the blast furnace.

The results obtained on the three cokes, the three feed cokes described previously (A, B and C), were analysed after thermal treatment. The three cokes did not behave significantly differently from each other with respect to changes observed after heat treatment. This apparent similar behaviour was observed between the non-treated feed cokes, their corresponding tuyere cokes and reacted feed cokes. Thus the results obtained from the three heat treated feed cokes can be dealt with as if they arose from only one sample.

4.5.1 Scanning Electron Microscopy / Low Resolution

Transmission Electron Microscopy

Neither SEM nor LREM showed any differences to have arisen between the feed cokes and their corresponding heat treated samples. Thus heat treatment alone did not appear to have induced any structural effects on the macro scale (plates 54 to 57). There does not appear to have been any alteration of the porous structure (macro / meso) or of the three observed carbon types (by SEM) by the thermal

treatment of the feed cokes.

4.5.2 Energy Dispersive X-ray Analysis / Temperature

Programmed Reduction

Neither EDXRA nor TPR studies were made on the heat treated samples. These methods of analysis are orientated towards chemical changes having been induced in the samples. As no chemical treatment was made to the coke during heat treatment EDXRA and TPR studies were deemed impractical. There would be no potassium uptake to form intercalates, which could have been observed by TPR. The failure to observe chemical changes in the mineral matter composition of the coke from feed to ex-tuyere suggested that analysis of heat treated samples by EDXRA would prove fruitless.

4.5.3 Infrared / Raman / Penetration of Potassium

As virtually no information was obtained on previous coke samples by infrared and Raman spectroscopy these techniques were not employed to analyse the thermally treated feed cokes. Neither were any studies done to determine the possible penetration of potassium after heat treatment of the feed cokes, as previous such experiments on non-treated cokes and tuyere cokes had proved inconclusive.

4.5.4 Density Measurements

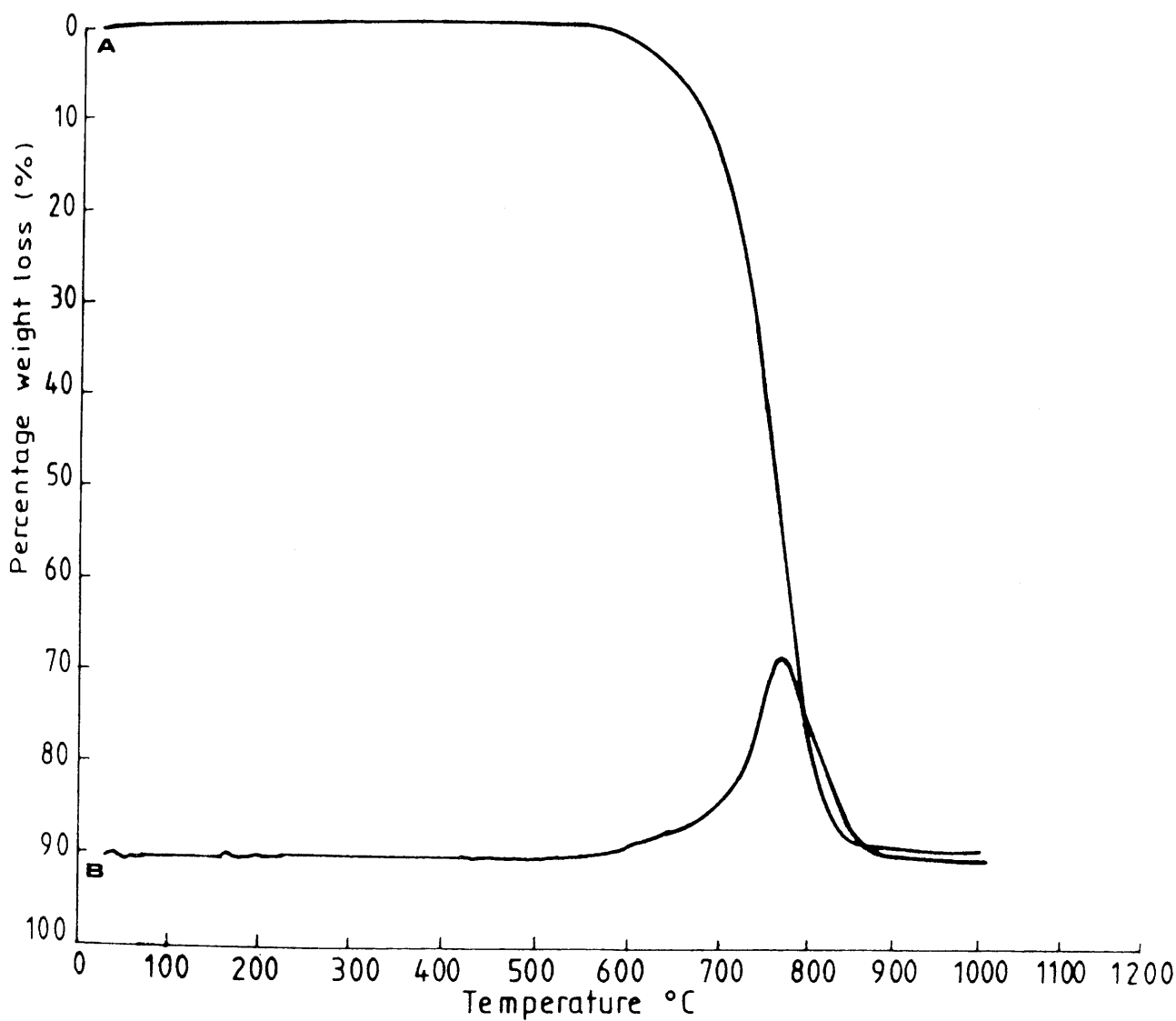
Density measurements as determined using carbon

CCl_4 gave an average value for heat treated feed cokes of 1.86 g / cm^3 , with a range of between 1.80 g / cm^3 and 1.92 g / cm^3 . The apparent structural variances between different heat treated samples may possibly be explained by experimental error in using this crude method for determining densities or may be actual differences.

4.5.5 Thermogravimetric Analysis (TGA)

Traces obtained from thermogravimetric analysis of the thermally treated feed cokes are shown in figures 56 to 58.

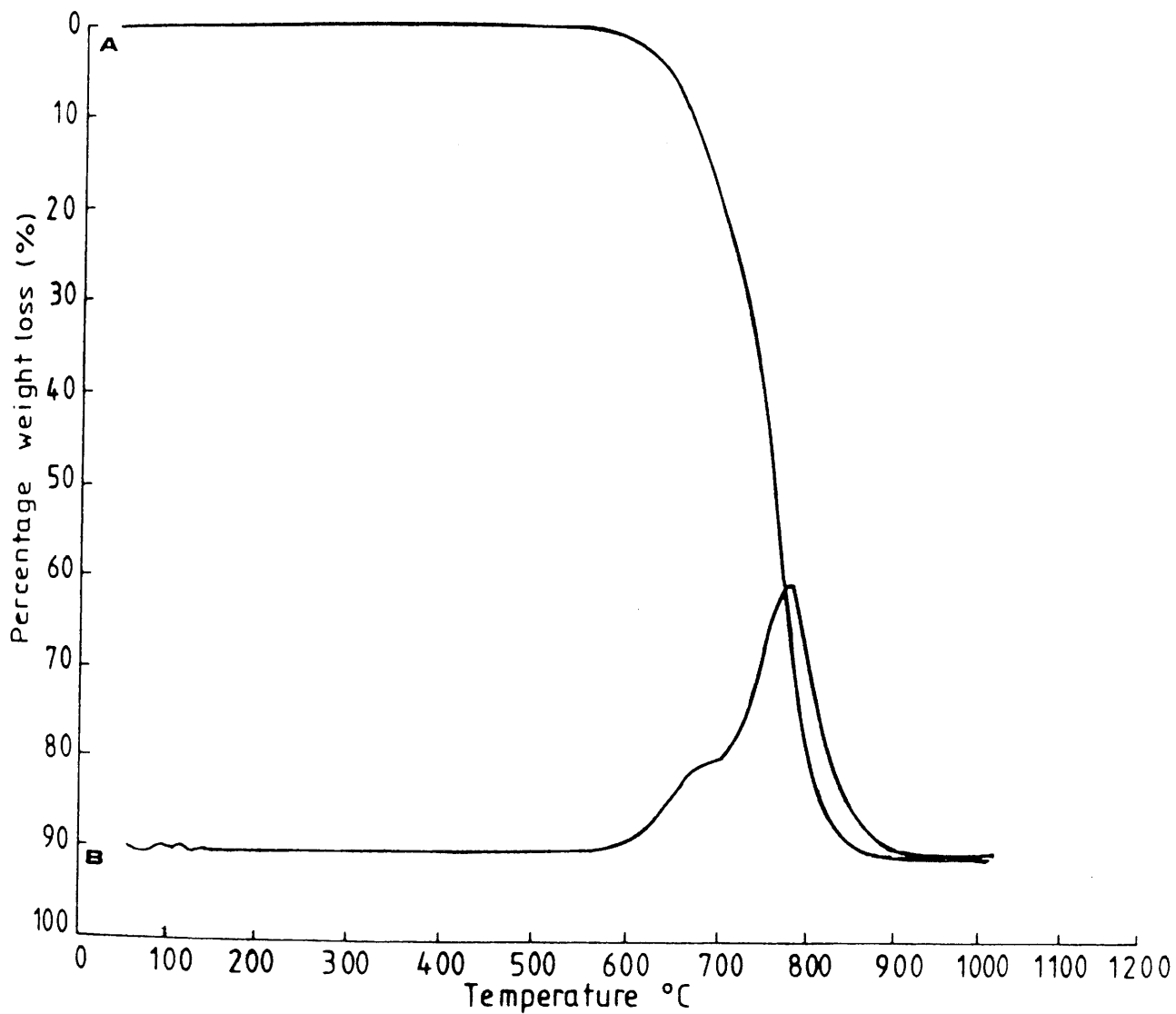
All three cokes degrade in the temperature range of $600 - 880^\circ\text{C}$. All commence at around 600°C and all attained their maximum weight loss at 880°C , thus showing the similar nature of their composition. All three cokes attain a ninety per cent weight loss over the temperature range thus indicating similar carbon contents after heating to 1500°C . Cokes A* and C* (corresponding to feed cokes A and C) exhibit only a single peak during the degradation. Coke B* however, shows a definite double peak similar to its feed coke. The commencement of the second peak is at 710°C (higher than the corresponding feed coke) and this second peak, from 710 to 880°C is the most rapid period of degradation. This however is similar to the other two heat treated cokes in that, although they do not exhibit a double peak, the period of most rapid degradation is between 710 and 880°C . The presence of the double peak in coke B* and the slow start of degradation for cokes A* and C* may be indicative of the presence of two types



Trace A indicates % weight loss with temperature.

Trace B indicates rate of weight loss.

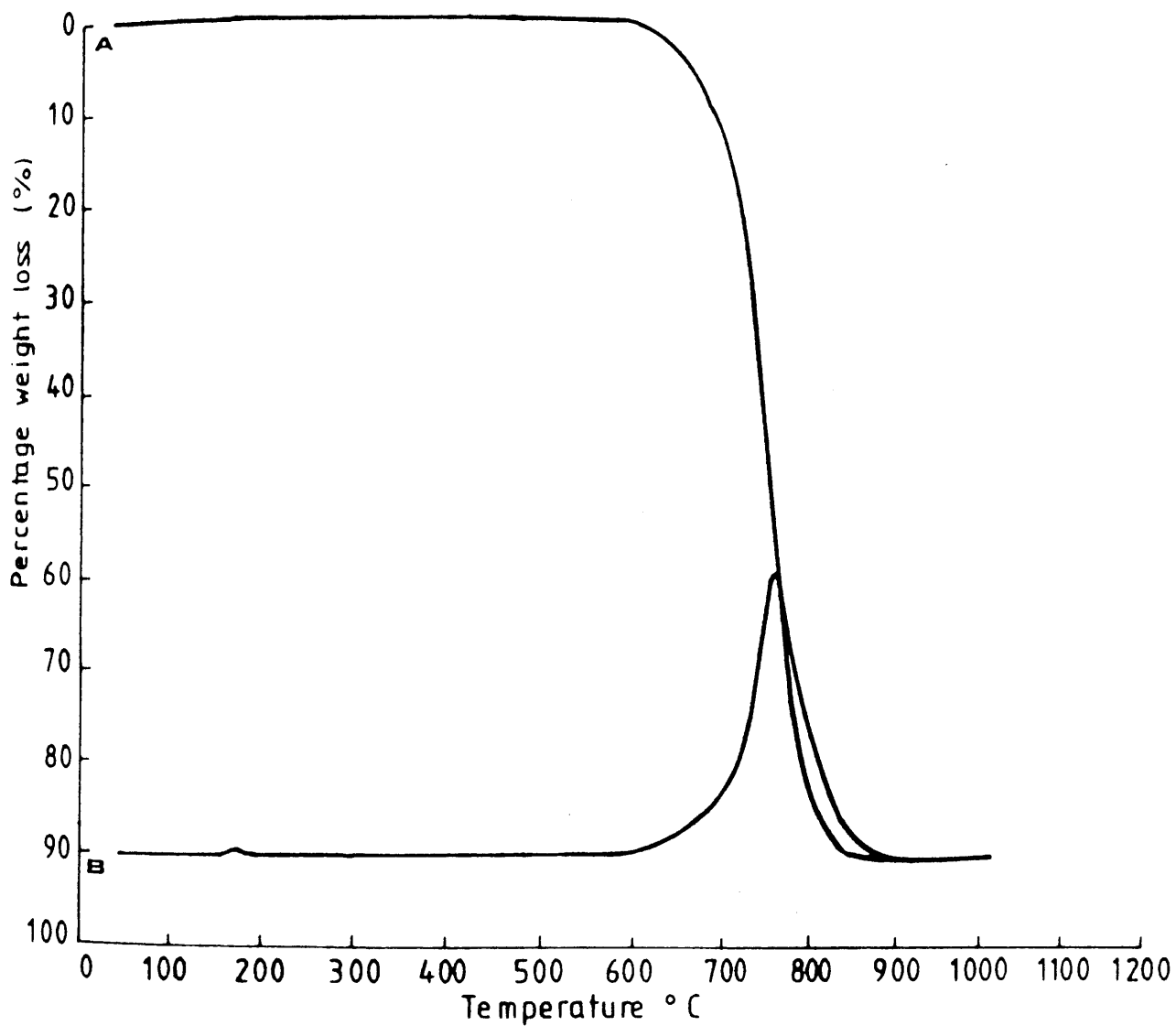
TGA Trace from Heat Treated Feed Coke



Trace A indicates % weight loss with temperature.

Trace B indicates rate of weight loss.

TGA Trace from Heat Treated Feed Coke



Trace A indicates % weight loss with temperature.

Trace B indicates rate of weight loss.

TGA Trace from Heat Treated Feed Coke

of carbon which burn at different rates and at of carbon which burn at different rates and at different temperatures.

4.5.6 High Resolution Electron Microscopy

High resolution studies of the thermally treated feed cokes revealed some structural changes to have occurred (plates 58 to 60).

Still apparent in the cokes were areas of disordered carbon lattices, as in the non-thermally treated feed cokes. These disordered carbon lattices had an average interplanar spacing of around 0.34 nm.

However, also present in the thermally treated material were areas of highly ordered carbon lattices. These areas were similar to the ordered regions observed in the reacted feed cokes and tuyere cokes. The average interplanar spacing of around 0.34 nm for these regions was also identical to that found in similar regions of the other samples. The observed structural ordering was found to be fairly randomly distributed throughout the sample, as had been found previously in other samples.

There was no evidence in the heated feed cokes of areas of expanded, disordered carbon structure, as observed in the tuyere and laboratory reacted cokes. This was expected as it was assumed that these areas of expanded carbon material were formed during a reaction between the coke and alkali vapour.

There was no evidence by HREM of any changes having occurred in the microporous structure of the thermally treated feed cokes. Still apparent in the thermally treated feed cokes were areas of crystalline material, with interplanar distances ranging from 0.4 nm to 1.86 nm. This was presumed to be the inherent mineral matter present in the metallurgical coke.

4.5.7 X-ray Powder Diffraction

The main feature of the powder diffraction patterns obtained for the three thermally treated feed cokes was a large peak corresponding to carbon and centred on 0.34 nm (figures 59 to 61). This type of spectra was typical for all types of metallurgical cokes analysed.

The thermally treated feed cokes had a narrower, more intense peak (smaller range of lattice spacings, more lattices with the same spacing) than the corresponding feed cokes which had not been heat treated to 1500°C. The width of the peak for the thermally treated cokes corresponded to a range of lattices from 29.1° (0.31 nm) to 23.4° (0.38 nm). These peaks were not as sharp or strong as those obtained from the ex-tuyere cokes but were sharper than those obtained from the feed cokes reacted with potassium vapour in the laboratory at around 900°C.

The obtained traces from the thermally treated feed cokes do not show any evidence of mineral matter. This is a trend exhibited by all types of metallurgical coke studied

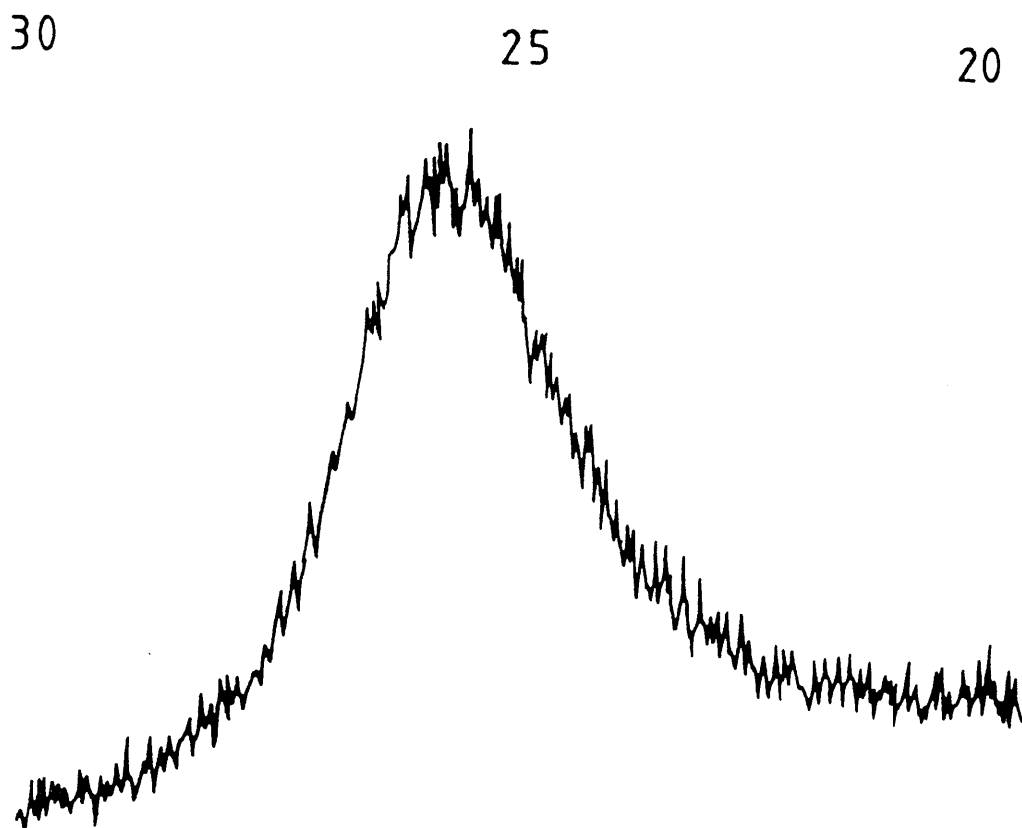


FIGURE 59

XRD Trace from Heat Treated Feed Coke

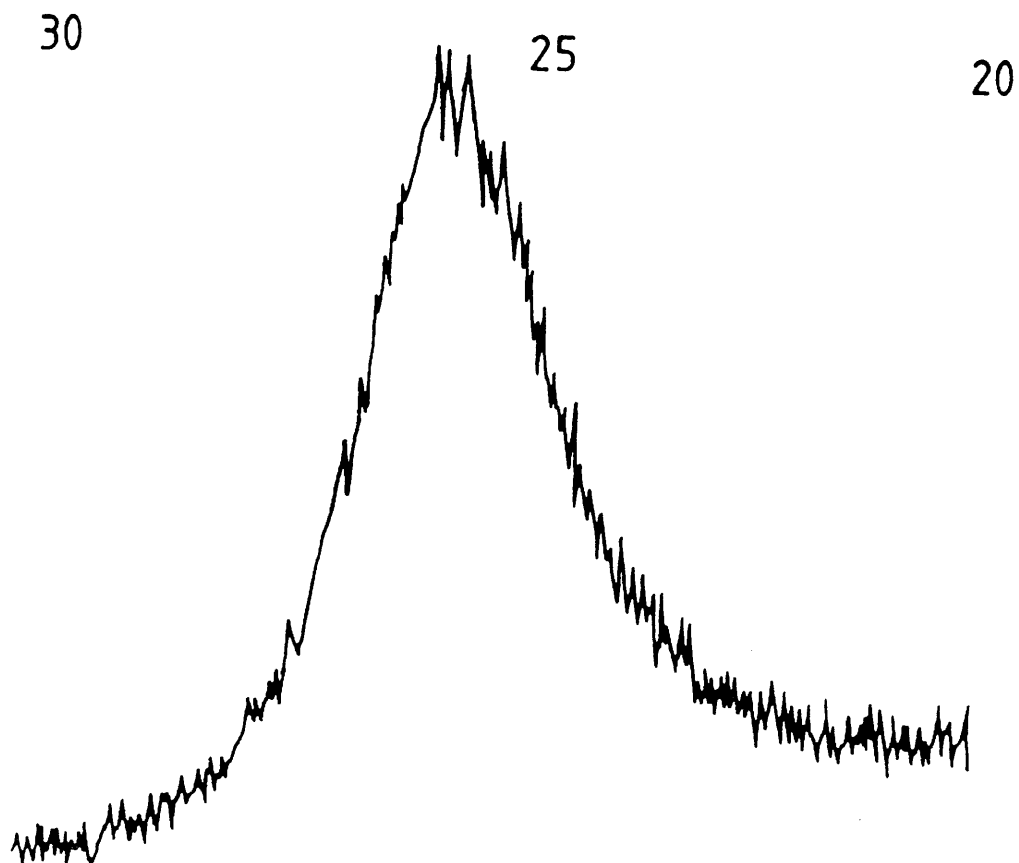


FIGURE 60

XRD Trace from Heat Treated Feed Coke

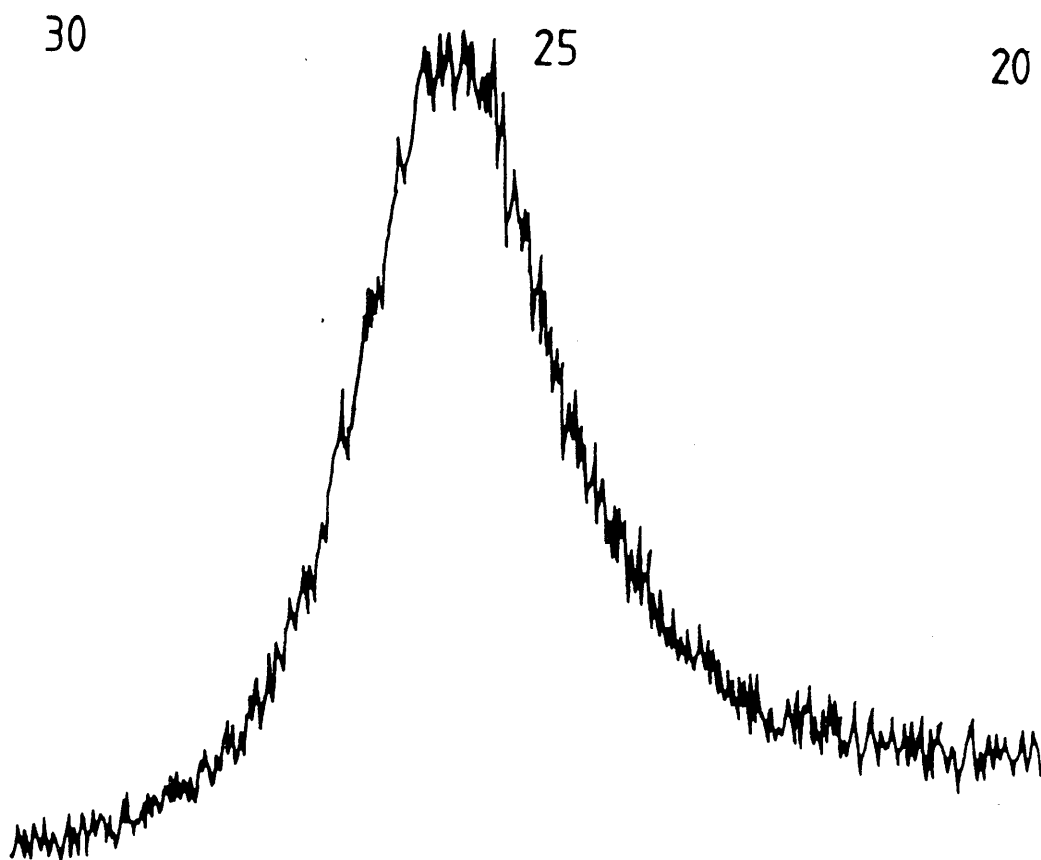


FIGURE 61

XRD Traces from Heat Treated Feed Coke

during the present work. The lack of X-ray evidence for this crystalline material is most likely due to its low concentration within the carbon matrix.

The structural ordering observed by HREM and XRD in the thermally treated feed cokes must be due to thermal effects, as no external chemical influence was exerted on the material during these experiments. As such, thermal effects would be expected to be significant in explaining structural ordering occurring in tuyere cokes and feed cokes which had been reacted with potassium vapour.

The extent of structural ordering in the thermally treated feed cokes was on average four times greater than the corresponding feed cokes. It was however, significantly less than that observed in the ex-tuyere cokes and as such may not be the only factor involved in structural alteration of the coke carbon matrix.

4.6 Reaction of Feed Coke Samples at Below Carbonisation Temperature

In order to further understand the microstructural changes observed to have occurred between the feed coke and both the ex-tuyere cokes and reacted feed cokes, experiments were carried out at below the coke's carbonisation temperature.

As the cokes, during their formation by the carbonisation of coal, had already been exposed to temperatures of

between 850°C and 900°C then if the coke was reacted at 650°C thermal effects would have a negligible effect on the microstructure. Thus, the resulting microstructure after a reaction of the feed coke with potassium vapour at a temperature of 650°C could be attributed only to chemical effects.

4.6.1 Scanning Electron Microscopy

Analysis of the feed cokes reacted at around 600°C, by SEM, did not reveal much structural change to have occurred during the reaction (plates 61 to 63). The porous structure did not appear to have been altered and there seemed to be no etching of the lamellar carbon structure often seen in the tuyere cokes etc., by SEM.

4.6.2 Low Resolution Transmission Electron Microscopy

LREM did not show any significant structural changes to have occurred, as a result of the feed cokes with potassium vapour, at below their carbonisation temperature.

4.6.3 Energy Dispersive X-ray Analysis

Traces obtained from these reacted feed cokes (inserts plates 61 to 63) were similar to those obtained from the tuyere cokes and the feed cokes reacted at around 900°C. As in the tuyere and 900°C reacted feed cokes the traces revealed the presence of high levels of aluminium and silicon. The occurrence of calcium was also noted

and this was often found to be associated with the aluminium and silicon when elemental dot maps of the samples were obtained. Also present were sulphur, chlorine and iron. The major factor observed in these samples was the increase in the potassium concentration compared with the very small concentration of this element found in the unreacted feed cokes. The potassium appeared to be evenly distributed throughout the samples and not associated with fissures or any of the other elements present. The increased levels of potassium must have arisen from the reaction of the feed coke, at 650°C , with the vapour produced from the coke / carbonate mixture.

Samples of the reaction tubes employed in these experiments were examined by EDXRA and revealed the presence of silicon and potassium, thus establishing the nature of the purple vapour, which was generated by the coke / carbonate mixture.

4.6.4 Temperature Programmed Reduction (TPR)

Studies of the samples by TPR showed very little difference from the corresponding feed cokes. It was hoped that TPR would reveal the coke / potassium vapour reaction to have formed some type of carbon / potassium intercalate. However, only a very small increase in hydrogen uptake was noticed in these samples, after reaction (increased hydrogen uptake being indicative of the presence of carbon / potassium intercalates). The small peaks observed

may have been indicative of small amounts of intercalate, but on the whole were inconclusive.

4.6.5 Infrared / Raman / Penetration of Potassium

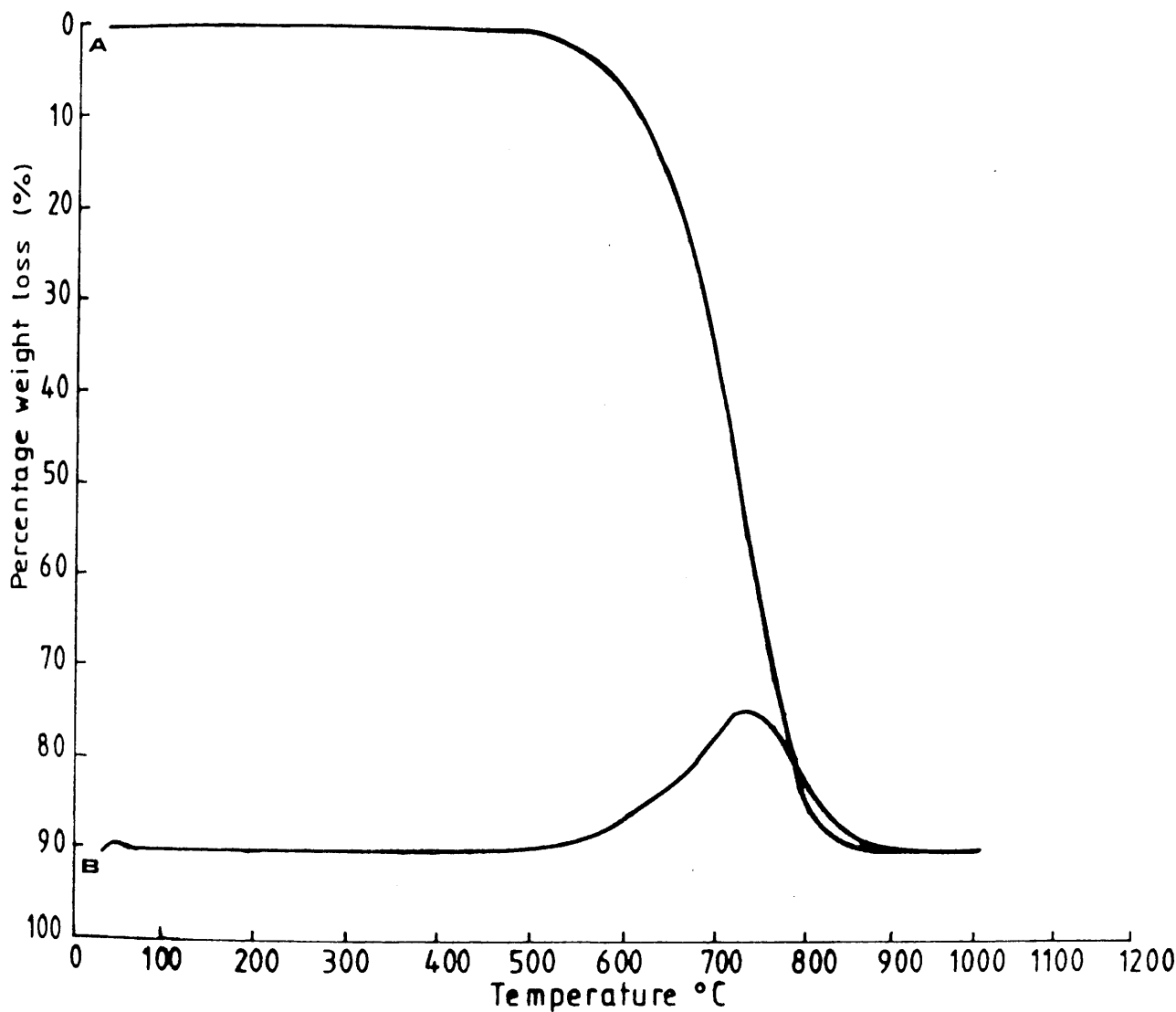
Infrared and Raman spectroscopy had proved fruitless in providing information, about previous metallurgical coke samples, and thus were not applied to the coke samples reacted at 650°C. Penetration of potassium, after reaction, studies were not carried out on these samples either as previous work, on other coke samples, using this technique had proved inconclusive.

4.6.6 Density

Density measurements, as measured by displacement of carbon tetrachloride, indicated a slight increase in the density of the cokes after reaction at 650°C, compared with the non-reacted cokes. The cokes after reaction appeared to have densities in the range 1.78 g / cm³ to 1.88 g / cm³, with an average value of 1.83 g / cm³. Differences observed between the three cokes were slight and although they may be significant, in relation to a change in structure, they may also arise from experimental error due to the crude methods employed to measure them.

4.6.7 Thermogravimetric Analysis (TGA)

Traces obtained from thermogravimetric analysis of the coke samples reacted at 650°C are shown in figures 62 to 64.

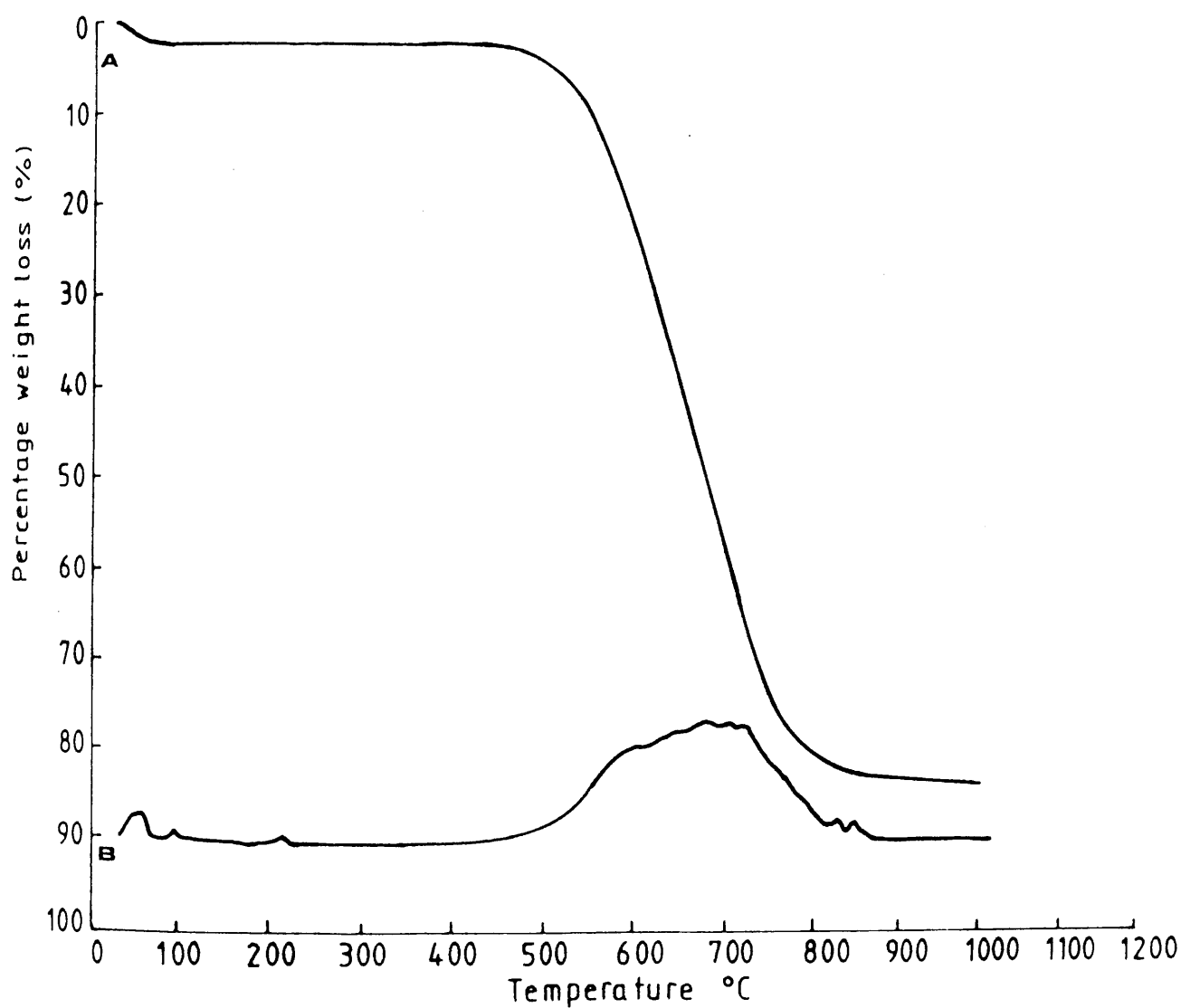


Trace A indicates % weight loss with temperature.

Trace B indicates rate of weight loss.

TGA Trace from Feed Coke Reacted Below

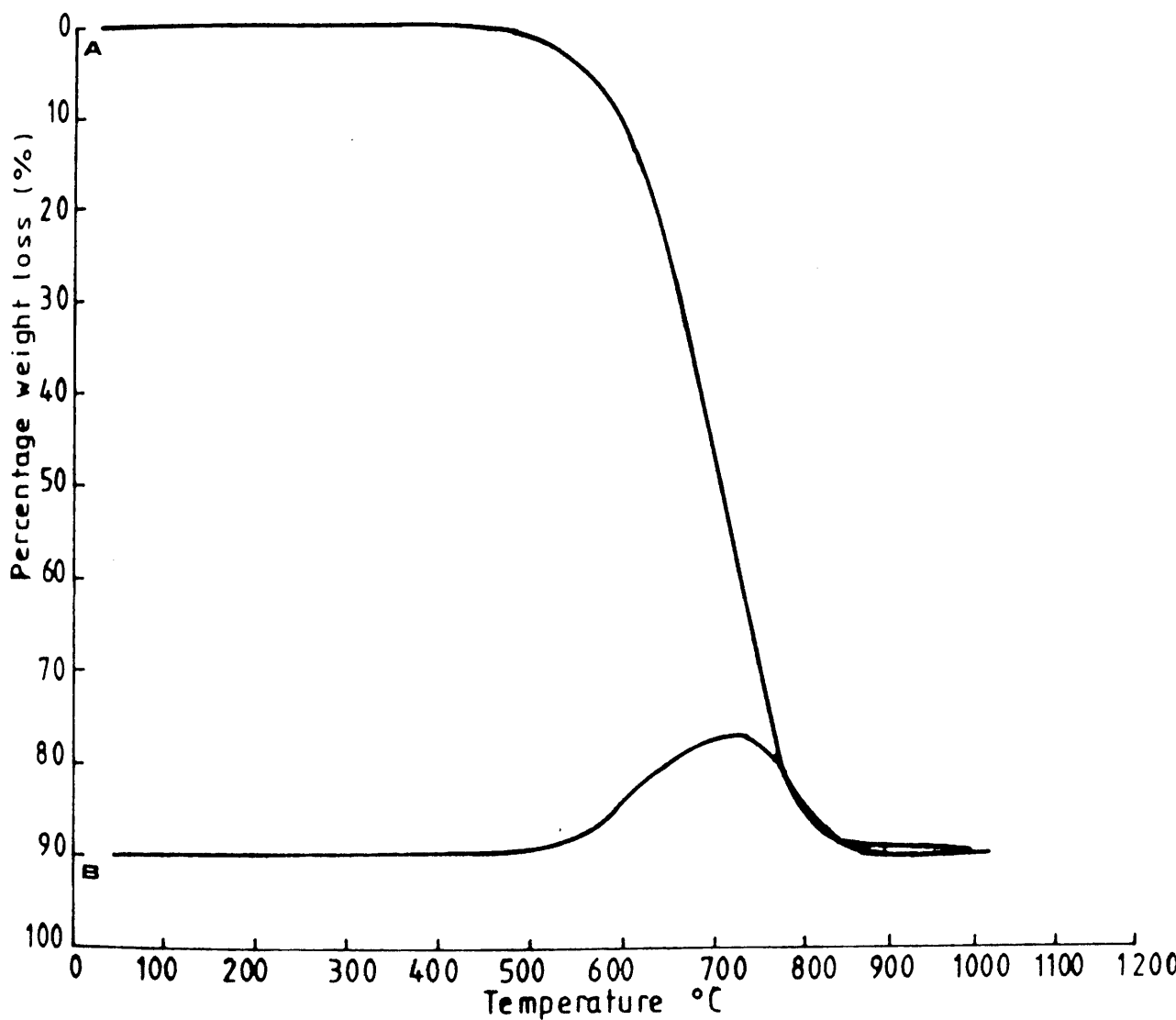
Carbonisation temperature



Trace A indicates % weight loss with temperature.

Trace B indicates rate of weight loss.

TGA Trace from Feed Coke Reacted Below
Carbonisation temperature



Trace A indicates % weight loss with temperature.

Trace B indicates rate of weight loss.

TGA Trace from Feed Coke Reacted Below
Carbonisation temperature

The vast proportion of sample weight loss (88 %) occurs over the temperature range 510 C to 860°C, for all of the feed cokes reacted at this temperature and is indicative of them all having reacted in a similar manner to this treatment.

4.6.8 Powder X-ray Diffraction (XRD)

Powder X-ray diffractograms obtained, from the 650°C reacted feed cokes, are shown in figures 65 to 67. These results show a slight sharpening of the main carbon peak, although not as pronounced as in the tuyere cokes or the 1500°C heat treated cokes. However, it is difficult to determine from the traces whether or not the sharpening of the main carbon peak is as great as for those feed cokes reacted with potassium vapour at 650°C as for those similarly reacted at 900°C.

This sharpening of the carbon peak is indicative of a smaller range of interplanar spacings. On average the samples gave carbon - carbon interplanar spacings in the range 0.31 nm to 0.39 nm, centered on 0.34 nm.

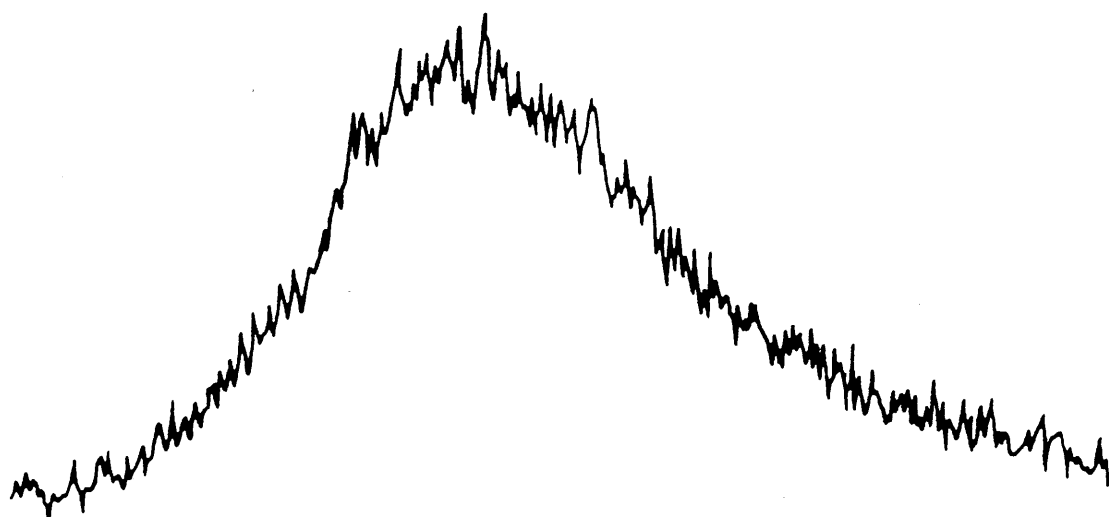
There does not appear to be any evidence for intercalated material from the diffractograms. Thus, any intercalates which may have been formed during the reaction are either present in very small concentrations or else have totally degraded by the time that the sample was analysed by XRD.

Again there is no evidence of any mineral material present

30

25

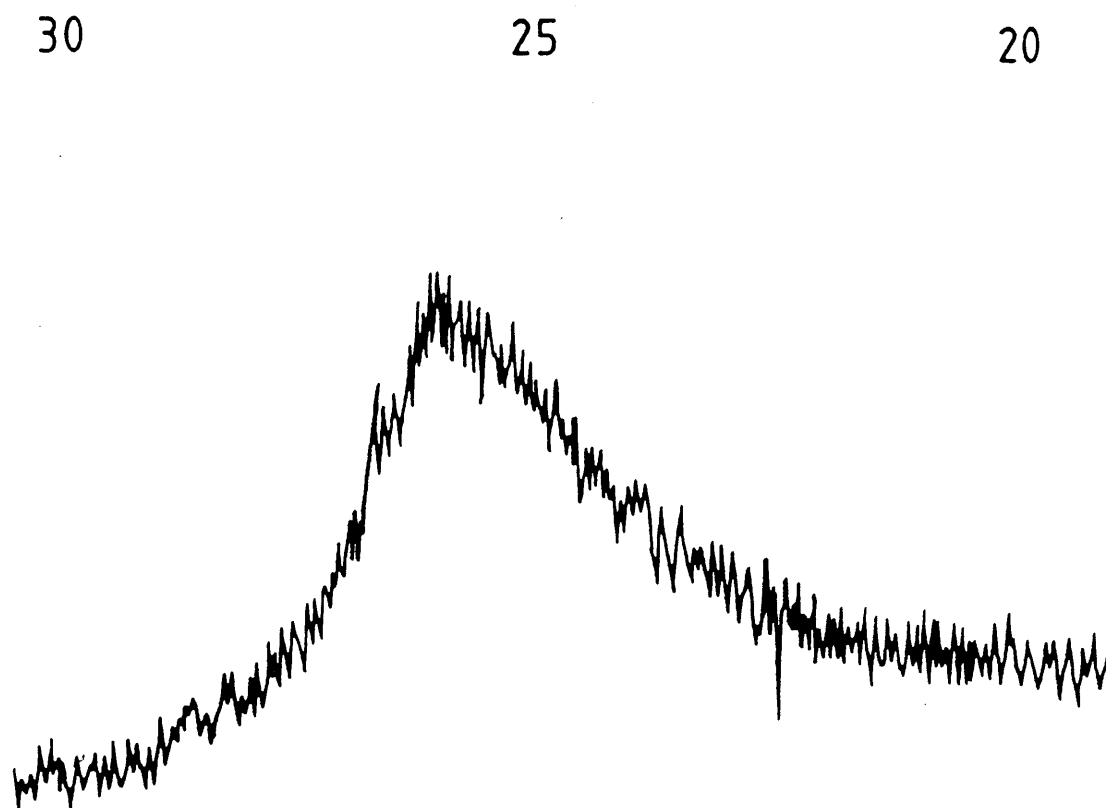
20



XRD Trace from Feed Coke Reacted Below

Carbonisation Temperature

FIGURE 65



XRD Trace from Feed Coke Reacted Below
Carbonisation Temperature

FIGURE 66



XRD Trace from Feed Coke Reacted Below
Carbonisation Temperature

FIGURE 67

in the cokes and thus it must be assumed that the concentration of this material in the carbon matrix is very low.

4.6.9 High Resolution Electron Microscopy

High resolution electron microscope examinations of the feed cokes reacted at 650°C with potassium vapour, show structural changes similar to those observed in the feed cokes reacted at 900°C.

Similar to the feed coke material there are many areas of disordered carbon lattices. These disordered areas have carbon - carbon interplanar spacings of around 0.34 nm.

Also apparent are areas of ordered carbon lattices. These are similar to those areas observed in the tuyere cokes and cokes reacted with potassium vapour at 900°C. The interplanar spacing in these regions is also on average 0.34 nm, with these ordered regions randomly dispersed throughout the sample (plates 64 to 66).

Increases in the La and Lc distances compared with the original feed material were measured by eye. The Lc distance was not found to be considerably altered but there appeared to be an average increase of between three and four fold in the La measured distance.

A third type of carbon structure was also observed. This type of structure was also found in the tuyere cokes and

coke laboratory reacted at 900°C . This structure was composed of expanded carbon lattices. These areas contained disordered carbon lattices with an interplanar spacing of around 0.45 nm. This structure was thought to have occurred during reaction between the coke and potassium vapour, to form an intercalated material. Although the structure does not conform to any of the common carbon / potassium intercalates it was thought that the observed expansion of some areas of the carbon matrix was a residue compound formed during degradation, occurring between the reaction furnace and the microscope (plates 67 to 69).

Although these regions of expansion were observed, randomly dispersed, in the cokes reacted at 650°C the number of such regions observed were not as numerous as in the tuyere cokes nor those reacted with potassium vapour at around 900°C .

Again, as in all the coke samples examined, there were areas of highly crystalline material. These regions had a wide range of interplanar spacings and could not be unambiguously identified. It is likely though that these are regions of mineral matter present in the coke originating from the parent coal material. It was found to be randomly distributed throughout the coke, as it was in all coke samples.

There appeared to be no obvious microporosity present in the cokes reacted at 650°C with potassium vapour.

The structural ordering observed by HREM and XRD to have occurred in the cokes reacted at 650°C with potassium vapour must be due to the chemical effects. The heat treatment afforded to these cokes (650°C) would not be sufficient to alter the coke structure, as during its formation the coke was heat soaked at a higher temperature.

This chemical structural ordering may be due in some part to the formation and collapse of the observed intercalated material (actually, probably a residue compound formed from the intercalate).

The extent of this structural ordering in the 650 C reacted feed cokes does not appear to be as extensive as that observed in the tuyere cokes or thermally treated cokes.

Comparison of structural ordering between those cokes reacted with potassium vapour at 650°C and those reacted in the same manner at 900°C would indicate slightly more ordering in the case of those reacted at 900°C. Thus it would appear that chemical effects alone do not account for all the observed structural changes in metallurgical coke.

4.7 Analysis of Reacted Ex-tuyere Cokes

4.7.1 Scanning Electron Microscopy

Scanning electron microscopy of ex-tuyere cokes reacted with potassium vapour at 900°C did not reveal any significant changes to have been induced, when compared

with non-reacted tuyere cokes. SEM analysis did not differentiate between the various reacted tuyere cokes (plates 70 to 72).

4.7.2 Energy Dispersive X-ray Analysis (EDXRA)

Analysis of the reacted tuyere cokes did not differentiate between the various reacted tuyere cokes nor between them and their corresponding non-reacted counterparts. Aluminium, silicon, calcium, sulphur, chlorine and iron were found to be in the same proportions as in the non-reacted tuyere cokes. The reacted tuyere cokes (inserts plates 70 to 72) exhibited an extremely strong potassium detection peak. However, corresponding non-reacted tuyere cokes also exhibited high concentrations of potassium and as in both cases the potassium readouts achieved a maximum scale deflection it proved impossible in the majority of cases to separate reacted from non-reacted tuyere cokes. Elemental dot maps of the reacted tuyere cokes gave similar results to those observed for the ex-tuyere cokes which had not been exposed to potassium vapour.

4.7.3 Transmission Electron Microscopy

Low resolution micrographs of the reacted tuyere cokes could not be distinguished from those of non-reacted tuyere cokes.

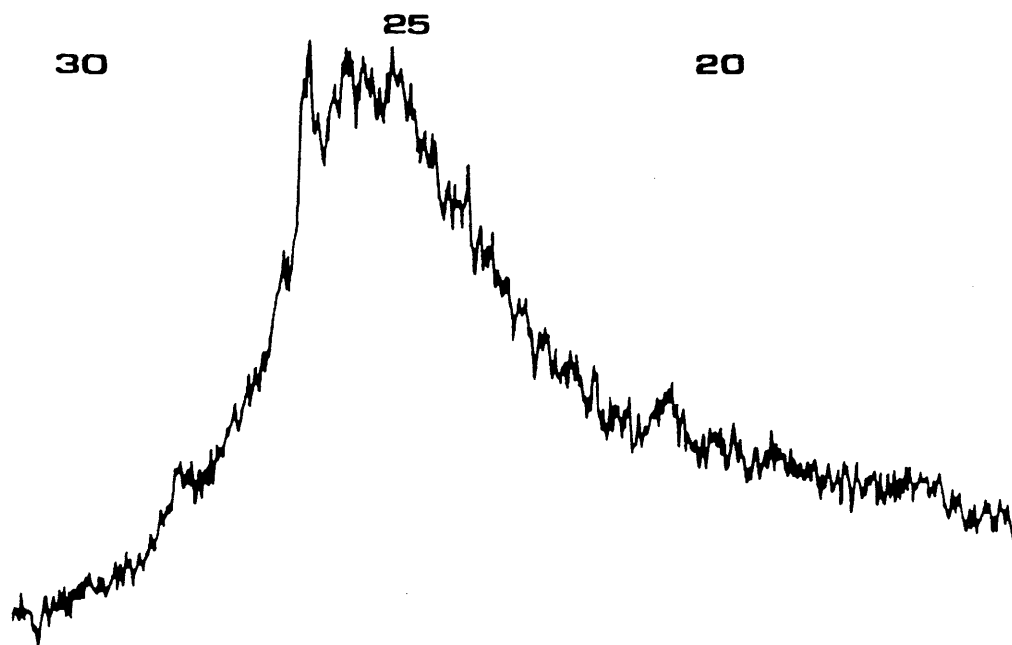
High resolution electron micrographs of the reacted tuyere

cokes revealed the same various types of microstructure that had been previously found in the non-reacted tuyere cokes. There was the presence of turbostratic feed coke type material ($d = 0.34$ nm), mineral material with interplanar spacings between 0.2 and 1.8 nm. Also present were areas of ordered carbon lattices ($d = 0.34$, plates 73 and 74) along with intercalated material. However, as the reacted tuyere cokes exhibited areas of staged intercalate as opposed to the non-reacted tuyere cokes which merely demonstrated, through the presence of a residue compound, that an intercalate had previously been present in the material. The staged intercalate in the reacted tuyere cokes had an interplanar spacing corresponding to a $C_{16}K$ type compound. These areas were composed of turbostratic carbon with an interplanar spacing of 0.43 nm (plate 75).

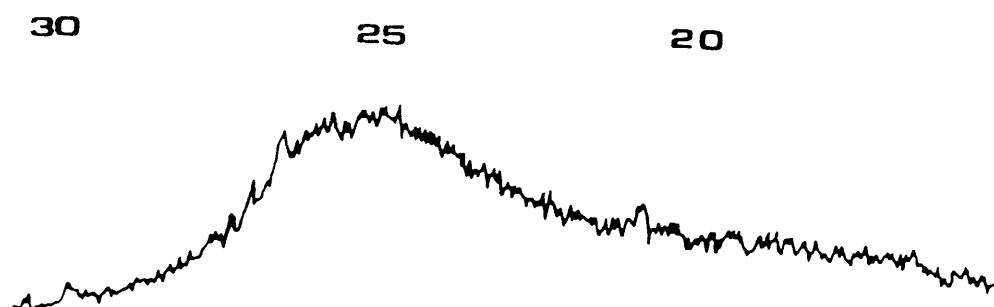
It proved impossible to draw any conclusions from the HREM evidence as to whether any increase in the ordering of the carbon lattices had taken place.

4.7.4 Powder X-ray Diffraction

Typical traces obtained from the reacted tuyere cokes are shown in figures 68 to 70. Immediately obvious was the sharp peak at a two theta angle of 20.8° . This peak corresponded to a $C_{16}K$ species (A.S.T.M.S. index 4 - 345, Schleede and Wellmann, 1932), with an interplanar spacing of 0.43 nm. This peak was not obtained from any of the other samples of metallurgical coke examined during this period of research. Subsequent refluxing of the staged

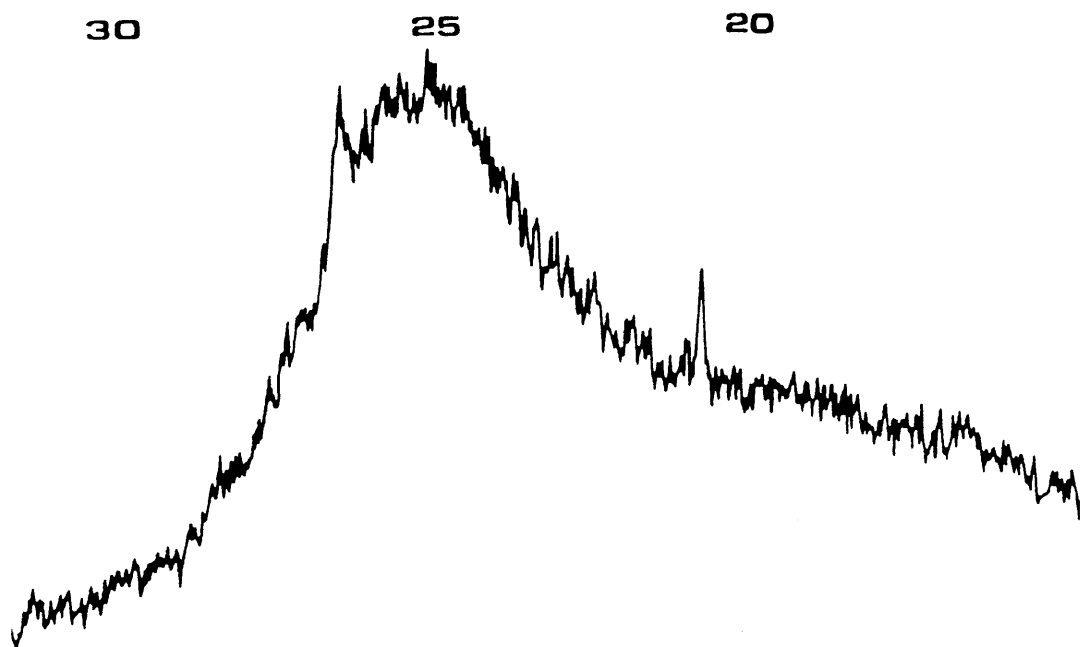


XRD Trace. from Reacted Ex-tuyere Coke



XRD Trace from Reacted Ex-tuyere Coke

FIGURE 69



XRD Traces from Reacted Ex-tuyere Coke

FIGURE 70

intercalated material, in iso-propanol for a period of three hours, destroyed the highly reactive intercalate.

The reacted tuyere cokes did not appear, using XRD, to have been markedly structurally ordered by their interaction with alkali. The main carbon peaks of the samples was not significantly sharpened, which would have indicated a reduction of the disorder present in the ex-tuyere cokes.

4.7.5 Temperature Programmed Reduction

TPR traces obtained from the reacted tuyere cokes did not show a considerable hydrogen uptake by the samples. However, a comparison of the traces obtained with those of the non-reacted tuyere cokes indicated that hydrogen uptake of the material may have been slightly increased, after laboratory reaction of the tuyere cokes with potassium vapour.

4.7.6 Density

Density measurements made on the reacted tuyere cokes, using carbon tetrachloride, did not reveal any changes to have been induced in the material during or after its interaction with potassium vapour. However, this crude method of measurement may not have been sensitive enough to have detected any changes which may have occurred.

4.7.7 Infrared / Raman Spectroscopy / Potassium Penetration

Analysis of the reacted tuyere cokes was not carried out, using these techniques, as they had previously proved unsuccessful in the analysis of other coke samples.

4.7.8 Thermogravimetric Analysis

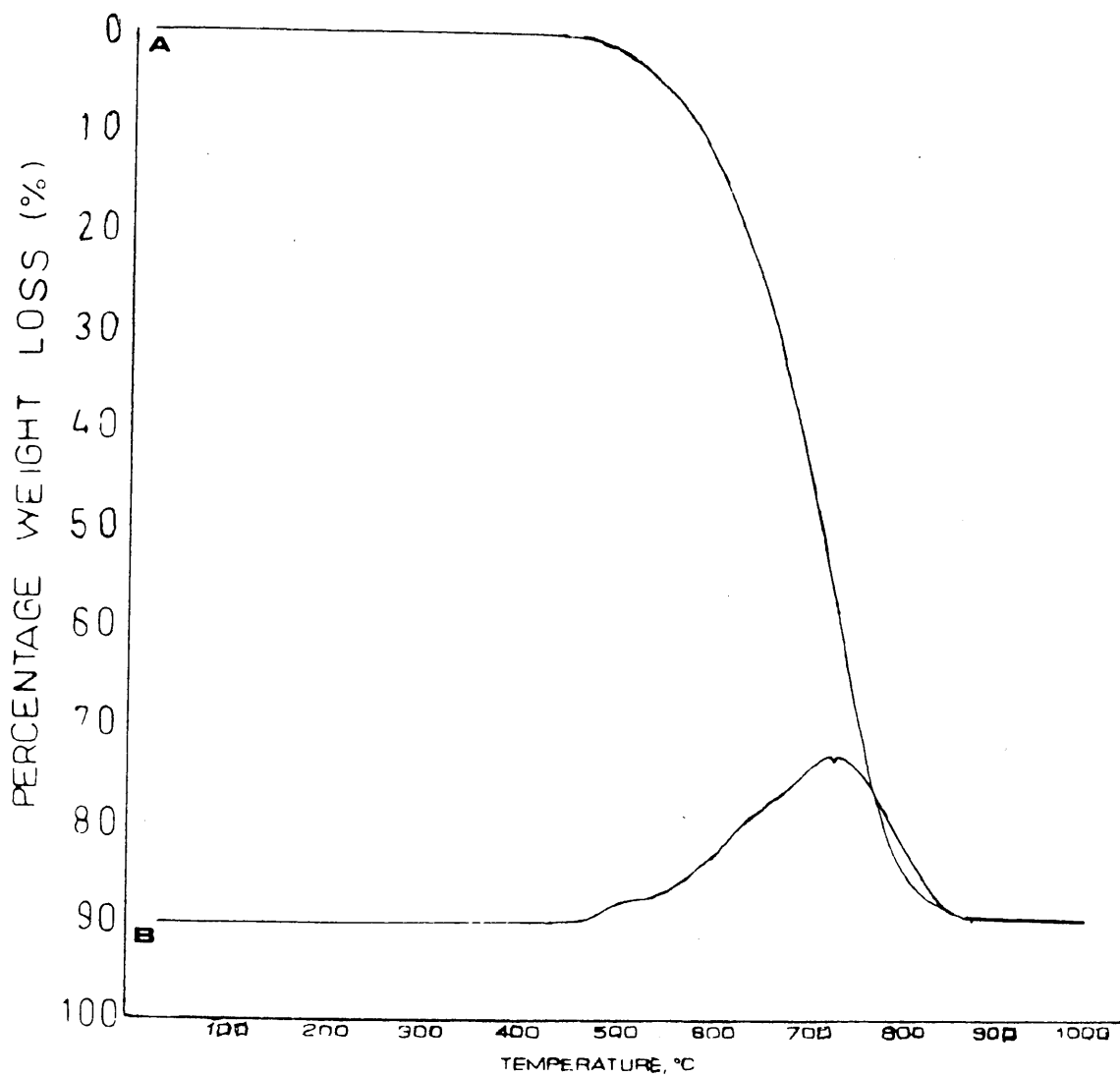
Typical TGA traces obtained from the reacted tuyere cokes are shown in figures 71 to 73.

The average weight loss observed for these samples was around 86 %. This weight loss occurred over the temperature range 440°C to 880°C. There was normally only one peak observed in the TGA traces, indicating the occurrence of a single mode of degradation. The fact that figure 72 does not exhibit a smooth curve was due to errors in the data collection system and did not appear to indicate more than one region of weight loss.

4.8. Effects of Inert Carrier Gases

Reaction of feed cokes with potassium vapour at 900°C were carried out using various inert carrier gases for the potassium vapour. This was done in order to observe whether the carrier gas had any significant effect on the microstructure during the potassium coke reaction.

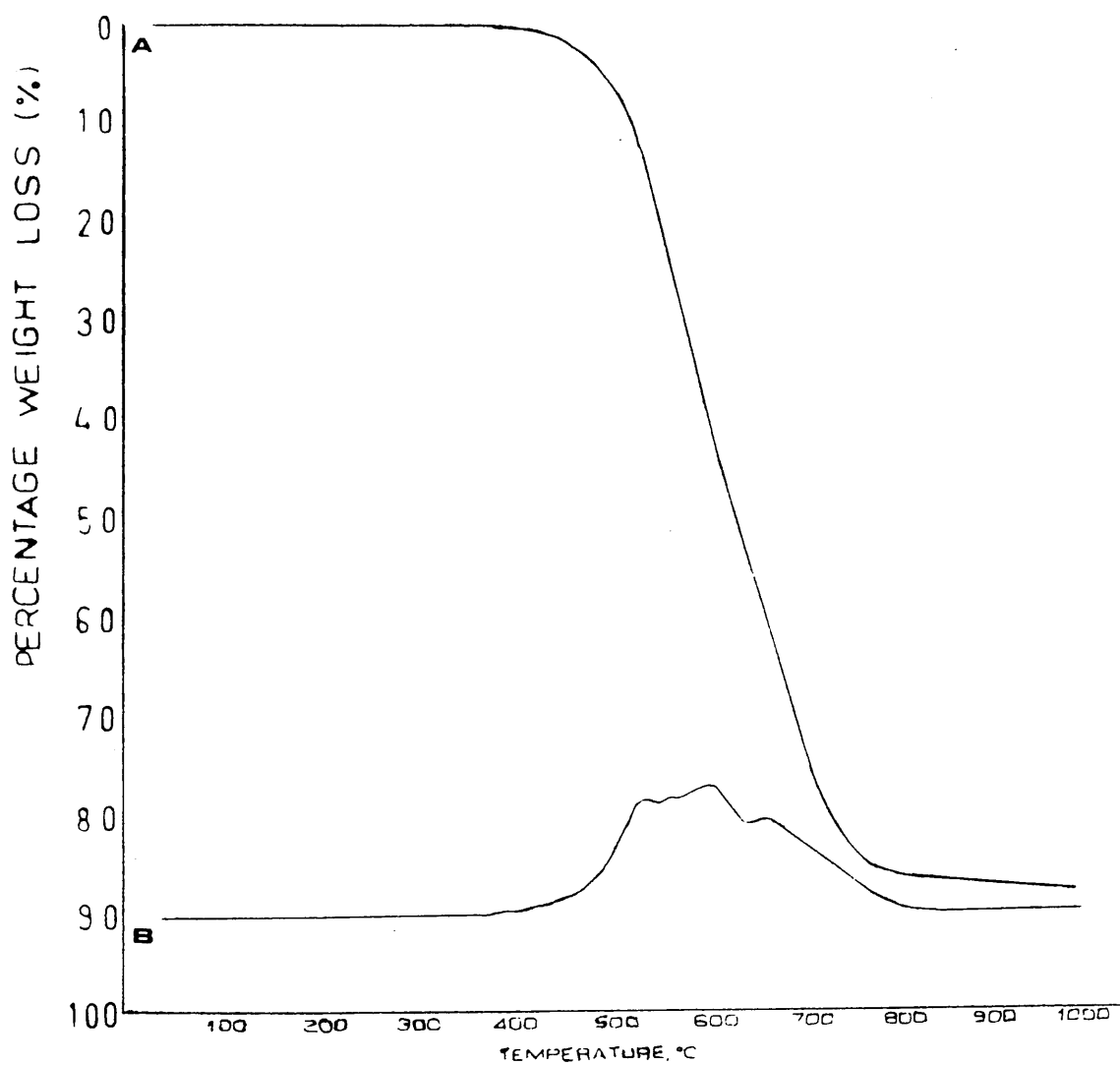
Examination of reacted feed cokes did not reveal any obvious structural dependence on the carrier gas. Neither



Trace A indicates % weight loss with temperature.

Trace B indicates rate of weight loss.

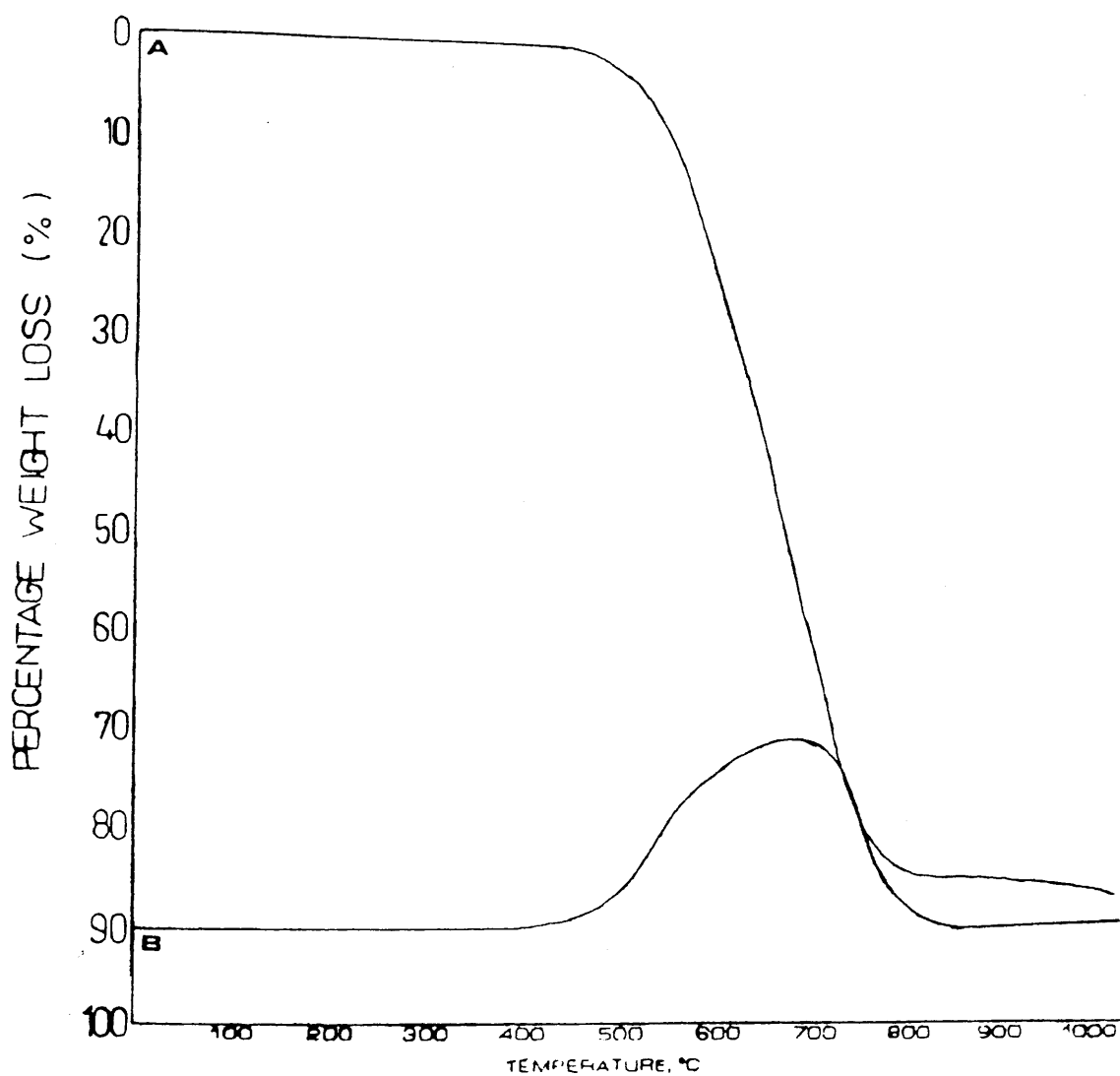
TGA Trace from Reacted Ex-tuyere Coke



Trace A indicates % weight loss with temperature.

Trace B indicates rate of weight loss.

TGA Trace from Reacted Ex-tuyere Coke



Trace A indicates % weight loss with temperature.

Trace B indicates rate of weight loss.

TGA Trace from Reacted Ex-tuyere Coke

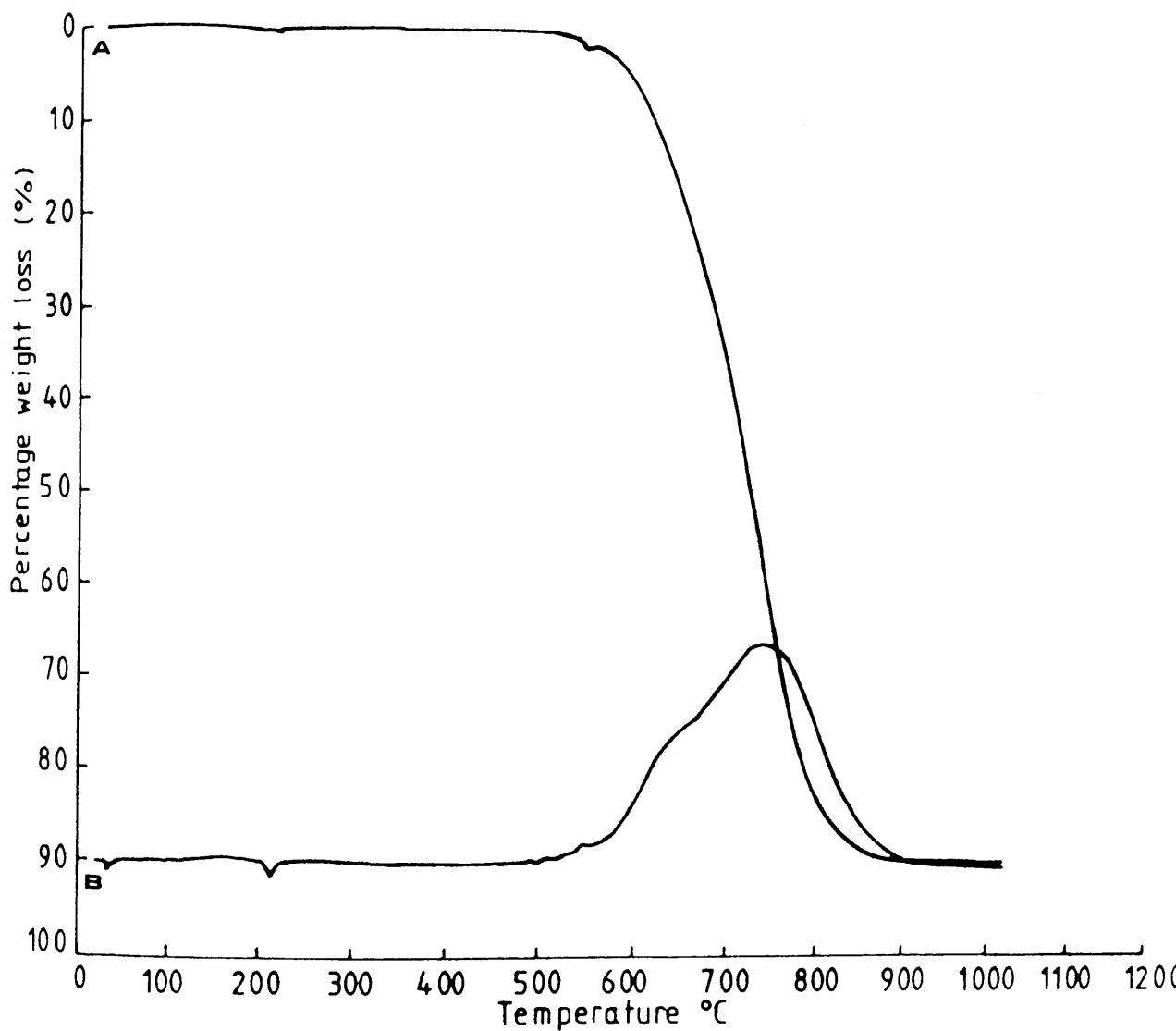
FIGURE 73

of the analysis techniques of HREM, TPR or XRD indicated that the observed microstructures after reaction had been influenced by choice of inert carrier gas. Analyses of the reacted cokes by EDXRA, SEM, density, infrared and Raman spectroscopy were not carried out as studies using HREM and XRD had indicated no structural dependence on the carrier gas. However, when the reacted samples were analysed by TGA there appeared to be a large dependence on carrier gas. Figures 74 to 76 show typical examples of the TGA traces obtained from reacted cokes when the carrier gas used was Ar, He and N₂ (oxygen free) respectively. A variety of features are apparent, indicating that the carrier gas used in the reaction may affect later gasification of the metallurgical coke.

The reaction carried out using argon gives the greatest weight loss of around ninety percent (argon was used in most of the experiments), similar to its corresponding feed coke. The reaction commences at around 520°C which is slightly lower than the feed coke (550°C) and may imply a catalytic effect by the alkali. The degradation ceases at around the same temperature as the feed material (880 °C).

With Helium as the carrier gas the sample loses just under ninety percent of its total weight. The reaction commences at around 520°C (same as for argon), increases slightly at around 680°C and finishes at around 880°C (similar to argon and feed coke reactions).

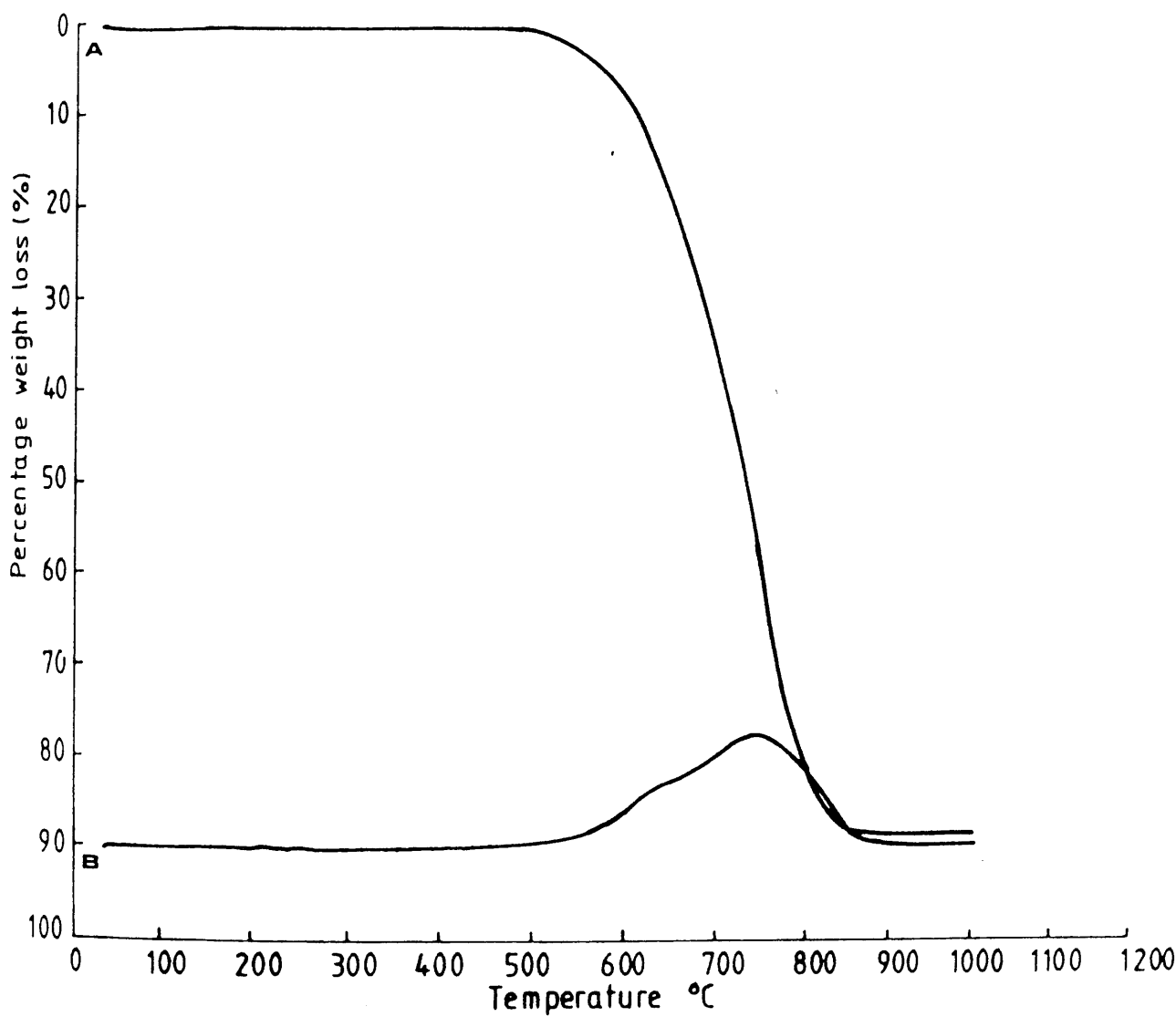
When nitrogen is used as the carrier gas there is an



Trace A indicates % weight loss with temperature.

Trace B indicates rate of weight loss.

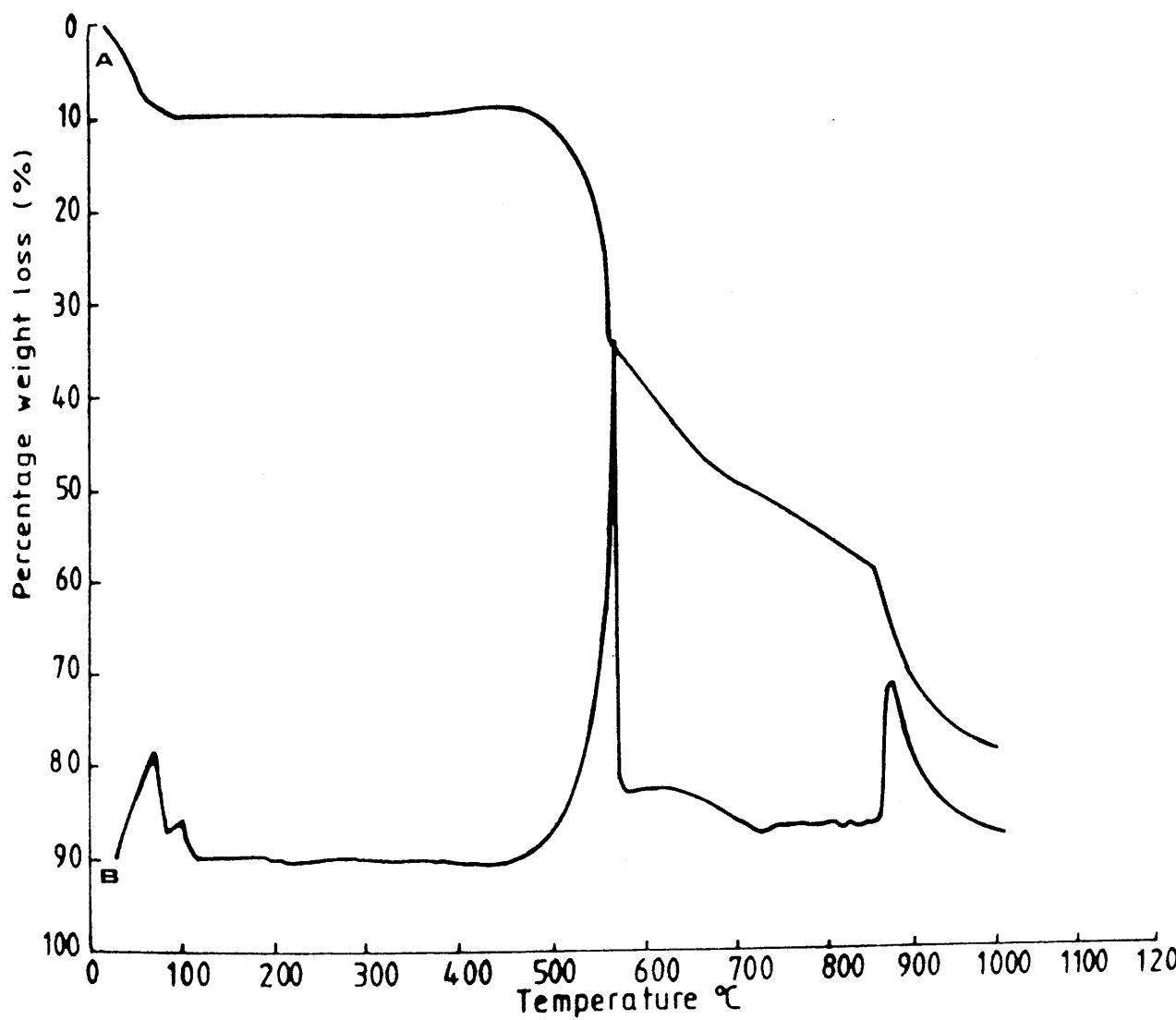
TGA Trace from Inert Carrier Gas Studies



Trace A indicates % weight loss with temperature.

Trace B indicates rate of weight loss.

TGA Trace from Inert Carrier Gas Studies



Trace A indicates % weight loss with temperature.

Trace B indicates rate of weight loss.

TGA Trace from Inert Carrier Gas Studies

immediate weight loss on commencement of the run. This weight loss is around ten percent and occurs over the temperature range from zero to slightly above 100°C . There is sharp loss of weight over the period of around 460°C to 580°C , accounting for a further twenty five percent weight loss. A slower weight loss of around twelve percent occurs between 580°C and 720°C . From 720°C to 880°C the weight loss is fairly constant and accounts for around ten percent of the total weight. Finally, there is a fairly rapid weight loss between 880°C and 1000°C , at which point the end of the run was reached. This last weight loss accounts for around twenty percent of the total weight loss, giving a total weight loss over the run ($0 - 1000^{\circ}\text{C}$) of only seventy eight percent (normally around ninety percent).

The possible reasons for these apparent variances in coke burning, when different inert carrier gases have been employed, during the reaction of coke with potassium vapour will be discussed later. However, it is clear that the nature of the "inert" gas may have profound effects on some coke properties and may be extremely important in gasification studies of the material.

Discussion

Analysis of the results presented for the feed cokes, ex-tuyere cokes and reacted cokes necessitated the need for not only an examination of each class of sample, but a comparison of each class with the others. Thus, for clarity, each set of results will be discussed in respect of each individual class, followed by a general discussion of their relevance, when taken in conjunction with the results obtained from the other two classes.

5.1 Macrostructure of Cokes

SEM investigations of the feed cokes showed the metallurgical cokes to have a macrostructure similar to many other carbonised materials. This macrostructure consisted of a vast interconnected pore network. The pores varied in size and shape and those observed by SEM fell into the macro and mesopore size ranges. These pores were evenly distributed throughout the samples from the external surface to the lump centre.

In all SEM studies described the images are secondary electron images (SEI) unless otherwise stated, for example backscattered electron images (BEI).

The feed cokes exhibited three distinct types of carbon structures. These can be described as smooth, lamellar and granular, and have been previously reported by Patrick (1986). The occurrence of these three macrostructural

forms was probably due to petrological forms created during the parent coal's formation. However, care must be taken not to confuse these structural forms with artefacts such as granular debris and lamellar type saw cuts created during sample preparation.

Thus, the heterogeneity of the material was established, with the occurrence of differing carbon forms and a wide range of pore shapes and sizes, and hence the necessity to analyse a number of samples of each coke type in order to get a characteristic representation of the material.

All of the feed cokes studied (by SEM) exhibited similar types of macrostructure, with the only variance being in the relative amounts of the carbon types and porosity. All samples had a vast interconnecting pore structure and all showed virtually no signs of gasification.

The ex-tuyere and reacted feed cokes had virtually identical macrostructures (as examined by SEM) and hence can be dealt with as one type of material.

Basically, these two classes of coke were similar to the feed coke samples. Still present were the three types of carbon structure (smooth, lamellar and granular) along with the extensive network of interconnected "open pores". The major difference from the feed coke material was some evidence of gasification of the carbon. This gasification preferentially took place around the rim of the pores, and in particular, the larger macropores.

This is shown in plates 28 to 30. There also appears to be some enhancement of the granular and lamellar structures. Patrick (1986) reported these feature enhancements with metallurgical coke oxidised in a plasma atmosphere of atomic oxygen. There also appeared to be an increase in size and number of macrofissures in the ex-tuyere samples in comparison with the feed coke samples, as shown in figure 77. These would indicate an increased stress present in the ex-tuyere cokes. This stress may arise from the weight of coke in the blast furnace shaft or may be related to the thermal and chemical conditions present in the furnace.

Although the reacted feed cokes had a larger number macrofissures than the original feed cokes they did not appear to have been as adversely affected as those removed from the tuyere zone of the blast furnace. The difference in fissuring characteristics of the ex-tuyere and reacted feed cokes is difficult to explain and it can only be surmised that it is due to the ex-tuyere samples being subjected to more extreme conditions.

There appeared to be little variance in macrostructure (by SEM) between different ex-tuyere samples or reacted feed coke samples. The reacted feed cokes also show gasification to have occurred around pore rims, but other than these features they showed little morphological differences from non - reacted feed cokes.

A comparison of sectioned ex-tuyere samples with lump

FIGURE 77

Coke Lump Before and After Alkali Attack.



FEED COKE



EX-TUYERE COKE

ex-tuyere samples showed that the gasification tends to be mainly on the external surface of the coke lumps. Analysis of the sectioned samples showed only a small degree of gasification, mainly restricted to around the entrances to the larger macropores. However, examination of the lump samples revealed a much greater degree of gasification. This gasification of the external surface of metallurgical coke agrees with the findings of Goleczka et al. (1983).

5.2 Energy Dispersive X-ray Analysis (EDXRA)

The results obtained from the EDXRA probe attached to the SEM must be regarded as qualitative and not quantitative. In obtaining sample spectra, the probe was allowed to collect data until sufficient counts were obtained, this value being the same for all samples. However, as maximum peak height for an element may be obtained before the data collection was terminated, the relative peak heights at the end of data collection are only approximate and some peak heights may indeed be much greater than indicated. The resolution obtained using the detector to map out elemental distributions was not particularly high and as such it was advisable to take these results merely as general indicators of distribution.

The EDXRA results from the feed cokes indicate (for elements heavier than sodium) that aluminium and silicon are the elements in greatest abundance. The elemental dot maps showed that in many cases these two elements were intimately associated with each other, as well as with a

large proportion of the calcium present. This then was indicative of a calcium - alumino - silicate species present in the metallurgical coke. This mineral material was inherent in the coke structure and presumably had arisen from the mineral matter present in the parent coal. Neither EDXRA nor standard chemical analysis gave any indication as to the precise nature of this alumino - silicate material. All that could be said of this mineral matter is that it was complex in nature and was probably a mixture of minerals, such as kalcilite, kaliophilite, leucite, etc.. However, the observance of this material, inherent in the feed cokes, does agree with the proposed alkali cycle which is presumed to occur in the blast furnace (Lu, 1980; Abraham and Staffanson, 1975). This material could also be observed as being distinct from the surrounding material when the scanning electron microscope was used to collect backscattered images (BEI) from the samples (plate 76).

The presence of sulphur and chlorine in the cokes was to be expected due to the nature of coal. These two elements however appeared to vary dramatically in concentration from feed coke to feed coke without giving rise to an obvious trend eg. variance on concentration with rank of parent coal. All feed coke X-ray spectra showed the presence of low concentrations of iron. Elemental dot maps of Fe, S and Cl showed the three elements to be randomly dispersed throughout the whole sample. They did not appear to be associated with other elements. As such the chlorine would fit in with the postulate of non easily leached

chlorine in coals being in the form of ions adsorbed on the coal (Saunders, 1979).

All feed cokes, examined in the present study, showed low levels of potassium. This potassium was randomly distributed throughout the coke samples (cf. dot maps) and as such could not be definitely associated with any of the other elements shown to be present, although the proposed alkali cycle associates the inherent potassium in coke with the complex alumino - silicate species present in the material.

EDXRA readouts from the ex-tuyere samples also showed high levels of aluminium and silicon and again these elements could be seen in many areas to be intimately associated with each other and also with some of the calcium present. Due to the qualitative nature of the EDXRA results it was not possible to observe whether any changes in composition of the alumino - silicate material had occurred during the coke's passage through the blast furnace. Again these regions of mineral matter could often be observed in the SEM, when the microscope was used to collect backscattered electron images (BEI), plate 77, instead of secondary electron images.

As in the feed coke samples there was a wide variance in concentration of chlorine and sulphur between different ex-tuyere samples and as such no firm conclusions could be drawn about these two elements, although as in the feed coke samples they both appeared to be randomly distributed

throughout the coke.

There appeared to be an increase in iron content in the ex-tuyere samples in comparison with the feed cokes. This would of course be expected for a material which is the solid matrix through which the molten iron percolates to hearth. The elemental dot maps showed localised areas of iron in the ex-tuyere samples in comparison with the feed cokes. This is consistent with liquid iron being deposited on the coke during reduction as opposed to the randomly dispersed inherent iron observed for the feed material.

The ex-tuyere samples all exhibited large increases in potassium concentration. In many cases the spectra obtained showed potassium to be the largest peak and when taken in consideration of the feed coke samples is indicative of between a four to ten fold increase in concentration and is consistent with previous findings (British Steel, 1983).

In contrast with iron however, the increased levels of potassium did not appear to be localised. The potassium distribution in the ex-tuyere samples appeared to be random, as in the feed cokes, when analysed by elemental dot mapping. There appeared to be evidence in some ex-tuyere samples of high levels of potassium associated with the observed macrofissures but lack of evidence for this from any other samples indicates no general association of fissures with the increased potassium levels.

Reacted feed cokes exhibited X-ray spectra very similar to ex-tuyere samples. Again, there are high localised levels of aluminium, silicon and calcium, corresponding to the inherent mineral matter in the coke. Again, there was the variance from sample to sample of chlorine and sulphur content. However, as would be expected the concentration of iron in these samples did not appear to have been altered from that present in the feed cokes. The reacted feed cokes had not been exposed to molten iron, as in a blast furnace, and the observed distribution of this element is random, as in the feed coke, with none of the localised regions observed in the ex-tuyere samples.

As observed in the ex-tuyere samples, the potassium content of the reacted feed cokes was dramatically increased. Again though, there did not appear to be any evidence for association of potassium with cracks produced and in general the potassium content was randomly dispersed throughout the coke samples.

Although data for sodium appear on many of the spectra observed (in all three classes of sample) this data will not be discussed. This is because sodium lies on the detection limits of the EDXRA probe and as such data collected is unreliable and often misleading. This situation may have been remedied by the use of electron energy loss spectra (EELS), which can detect the presence of elements with very low atomic numbers ("light element analysis") or by the use of a windowless EDXRA detector which, although not totally satisfactory, would have

increased the reliability of data collected at the detector limits. Thus during the coke's passage through the blast furnace there is a large increase in its potassium content. This is exactly what is expected from the blast furnace alkali cycle, recirculating potassium building up on the coke lumps. There also appears to be an increase in iron concentration between the coke as charged to the furnace and samples removed from the "bosh" region. Very little can be said about variations in concentrations of other elements present in coke by energy dispersive X-ray analysis, when comparing feed and ex-tuyere cokes.

All EDXRA results regarding relative concentrations of elements present in the coke samples were also checked by standard chemical analyses.

5.3 Chemical Analysis of Metallurgical Cokes

Looking at the mean sizes of the three sets of feed and ex-tuyere cokes in table 5 it is obvious that the coke lumps undergo a considerable size reduction during their residence time in the blast furnace. It is probable that this size reduction is a combination of gasification of the coke by the Boudouard and associated reactions and also by fracture of the coke lumps.

To calculate the degree of size reduction it is assumed that the coke lumps are spherical in nature. This is acceptable as the sieves, through which the lumps are sized, are repeatedly agitated to ensure that only coke

having a greater size than the sieve screen remains on the sieve. Thus for the three pairs of cokes, their volume (as spheres) would be:-

$$V = \frac{4}{3} \pi r^3$$

The volumes of the feed coke spheres would then be (mm³):-

A	B	C
<u>65057</u>	<u>111970</u>	<u>104288</u>

and for the ex-tuyere cokes would be (mm³):-

A'	B'	C'
<u>28730</u>	<u>54361</u>	<u>57544</u>

The radius of the coke sphere being half the mean size, as the sieve holes are circular.

Thus the percentage of the feed coke which remains after passage through the blast furnace ie. ex-tuyere coke is:-

A'	B'	C'
44.2	48.6	55.2

Therefore the percentage reduction in size is:-

A'	B'	C'
55.8	51.4	44.8

these percentage reduction factors are large and as such are unlikely to be accounted for by gasification alone, even catalysed gasification by alkali. Thus fracturing of the coke lumps must be involved in the process. As lump fracture more drastically affects size than gasification it can be taken to a first approximation as being the major factor involved in the degradation of metallurgical coke.

British Steel (1983) have described coke degradation as being a combination of effects. First, the coke size is reduced on route to the stockline. The coke size is lowered by around 5 mm during this period and the arithmetic mean size approaches that of the fissure free size (the limit at which no more breakage occurs by lump breakage, usually determined by extended micum drum tests).

Within the blast furnace alkalies are deposited on the coke at around $800 - 850^{\circ}\text{C}$. This increases the coke's reactivity but does not affect the coke size or strength.

Carbon solution loss reactions occur in the temperature region $900 - 950^{\circ}\text{C}$. The onset of the Boudouard reaction is determined by the coke reactivity and the level of solution loss (20 - 30%) is controlled by the operating conditions

prevalent to the furnace. This action accounts for between one and two millimetres in coke size.

At between 1100 and 1450°C the coke reacts with alkali metal vapour. This reaction lowers the coke's abrasion resistance and makes the coke highly susceptible to mechanical size reduction. This is likely to be the largest factor involved in coke degradation, accounting for between 15 and 20 mm of size reduction.

Thermal effects also reduce coke size. These effects occur between 1100 and 1500°C and directly reduce (by 1 - 2 mm) the coke size. Thermal effects also lower coke abrasion resistance making it more susceptible to mechanical degradation, accounting for a further size reduction of 3 - 5 mm.

The more unstable cokes, which are prone to volumetric breakage and have low abrasion resistance, tend to degrade more rapidly under raceway conditions, thus leading to unstable raceways.

The micum indices give an indication as to the abrasion and fracture resistance of the cokes. No information on the micum indices of the ex-tuyere cokes was available from the suppliers of the cokes. All micum results were obtained before shipment to Glasgow. Also there was no data regarding higher order micum tests on the samples eg. micum tests to determine fissure free size.

Feed cokes B and C exhibited similar M10 and M40 indices indicating similar characteristics towards fracture and abrasion of these cokes. Feed coke A had a lower resistance to fracture than B or C, shown by its lower M40 index production of fines. Thus all three cokes have broadly similar strength characteristics, as determined by basic micum tests, although feed coke A appeared to be marginally weaker than B or C, which have very similar strengths.

Apparent density results did not show significant changes to have occurred between the feed cokes and their corresponding tuyere cokes, or between individual feed cokes. Systems B / B' and C / C' had values of 0.95 gcm^{-3} for all feed and tuyere cokes. System A / A' varied slightly from the other two systems in that the feed coke had a lower value of 0.93 gcm^{-3} and the corresponding tuyere coke a value of 0.89 gcm^{-3} . These results did not reveal much as to the environment encountered by coke in the blast furnace.

Density measurements made using carbon tetrachloride did show substantial changes to have occurred between stockline coke (feed) and the tuyere level. These measurements indicated a considerable increase in density of the coke at tuyere level. The increases were normally around 0.24 g / cm^{-3} . The densities of individual feed cokes varied (using CCl_4) and this was usually reflected in the corresponding tuyere cokes. That is, a variation between two feed cokes was (reasonably accurately) often found to

be the same between the corresponding tuyere cokes.

Apparent densities were not measured for reacted feed cokes. However, densities as determined by carbon tetrachloride showed an average increase in density of around 0.20 gcm^{-3} for reacted feed cokes in comparison with non-reacted feed material. As in the ex-tuyere and feed comparisons, although variations in density between individual feed cokes occurred, this was usually reflected in the corresponding reacted feed cokes.

The increase in densities of the ex-tuyere and reacted feed cokes was an indication that the structure of the material had been significantly altered, presumably by the action of chemical and thermal effects.

The greater increase in density of the ex-tuyere cokes in comparison with the reacted feed cokes was perhaps an indication of more extreme conditions (eg. thermal, chemical and mechanical) present in the blast furnace compared with laboratory conditions.

The ash content, according to table 5, was much higher in the ex-tuyere cokes compared with the feed cokes. However, due to carbon burn-off, during the coke's passage through the blast furnace, the percentage weight is bound to appear considerably higher in the ex-tuyere cokes. That is, that although the sample weights from which the ash content is calculated are the same (for feed and ex-tuyere cokes), the ratio of carbon to ash is much higher in the feed material

than in the tuyere coke. Experimental results obtained for ash content from feed and tuyere cokes by plasma ashing (in dry H_2) to constant weight, agree with thermal ashing results.

Coke B had the highest ash content as a feed coke and as a tuyere coke. Feed coke C had a higher ash content than A but a lower ash content in the corresponding tuyere cokes. This fact may be accounted for by size reduction factors, coke A had the highest size reduction and C the lowest resulting from blast furnace conditions.

Feed coke C had the highest volatile matter content of the feed cokes, but had the lowest tuyere coke (C') volatile matter content. Coke B had the second highest volatile matter (VM) content of the feed cokes and the highest (B') VM content of the tuyere cokes.

Feed coke A had a much lower VM content than either B or C but the corresponding tuyere coke (A') has nearly as high a VM content as that of B'. Again these variations in VM content could be explained by looking at the degree of size reduction.

Figures in table 5 indicate an increase in ash content from feed to tuyere coke of around a factor of 1.5 on average. These results become more meaningful when corrected for size reduction.

Ash content	A	A'	B	B'	C	C'
corrected for size reduction of coke (%).	7.60	6.23	9.50	7.78	9.10	6.90

A comparison of these corrected figures indicated much less of a change between feed and corresponding tuyere cokes than was previously apparent. However the corrected values did appear to show a reduction of ash content in the tuyere cokes compared with the coke as charged. This reduction in ash content of the cokes would imply a loss of some of the elements comprising the coke's ash content.

Examination of the composition of the ash content of the cokes revealed, in some cases, large differences. However, it is probably more useful to examine these results when expressed a percentage of the total sample weight instead of as a percentage of the ash content, which is itself a percentage of the total sample weight. This gave ash composition percentage values of:-

	A	A'	B	B'	C	C'
Na ₂ O	0.14	0.59	0.08	0.43	0.07	0.18
K ₂ O	0.21	1.75	0.17	0.96	0.19	0.75
CaO	0.16	0.89	0.22	1.20	0.19	0.94
MgO	0.08	0.25	0.11	0.53	0.10	0.21
Fe ₂ O ₃	1.16	2.26	0.80	1.49	0.66	1.98
SiO	3.40	4.33	4.96	5.98	4.77	4.50
Al ₂ O ₃	2.22	2.67	2.87	4.21	2.76	2.95

Thus indicating less drastic changes occurring between feed and tuyere cokes.

Before a true comparison of the elemental composition of ash contents could be made it was necessary to correct for the amount of size reduction which the coke had undergone during the blast furnace process.

The figures for ash composition corrected for size reduction and expressed as a percentage of total sample weight (not ash content weight) are:-

	A	A'	B	B'	C	C'
Na ₂ O	0.14	0.26	0.08	0.21	0.07	0.10
K ₂ O	0.21	0.77	0.17	0.47	0.19	0.42
CaO	0.16	0.39	0.22	0.58	0.19	0.52
MgO	0.08	0.11	0.11	0.26	0.10	0.12
Fe ₂ O ₃	1.16	1.00	0.80	0.72	0.66	1.09
SiO	3.40	1.91	4.96	2.91	4.77	2.48
Al ₂ O ₃	2.22	1.18	2.87	2.10	2.76	1.63

Thus the ratio of ash composition could be calculated for each element. These values were corrected for burn-off and expressed as a percentage of total sample weight. Values are tabulated as the ratio of the element concentration in the feed coke to the element concentration in the ex-tuyere coke. However, as previously noted not all size reduction arises from solution loss. Thus the figures reported here can only be taken as a rough estimate, the true values for the ex-tuyere cokes being slightly lower than those estimated here.

	A' / A	B' / B	C' / C
Na ₂ O	1.86	2.63	1.43
K ₂ O	3.67	2.77	2.21
CaO	2.44	2.64	2.74
MgO	1.38	2.36	1.20
Fe ₂ O ₃	0.86	0.90	1.65
SiO ₂	0.56	0.59	0.52
Al ₂ O ₃	0.53	0.73	0.59

(values expressed as percentages)

The above table shows increases in sodium, potassium, calcium and magnesium in all three pairs of cokes. There also appeared to be a loss of aluminium and silicon from all three systems.

Calcium concentration appeared to be increased by approximately the same amount in all cases, by a factor of around two and a half.

Increases in sodium content varied in all three systems, the highest increase being B' / B followed by A' / A . These results being more accurate than EDXRA results for sodium.

Potassium exhibited the largest increase of any element. There was over a three and a half fold increase in system A' / A , with slightly lower increases both in B' / B and C' / C . These increases in potassium and sodium concentration have been previously reported (Tucker, 1985) with increases of up to ten fold, Hatano et al. (1980 (b)),

being common for potassium. Sodium concentrations are also often greatly increased but not to the same extent as those for potassium.

All three feed / tuyere pairs exhibited substantial increases in magnesium content, indicating that this element is "picked up" by the coke during its passage through the blast furnace.

Iron showed an overall loss in systems A' / A and B' / B . This conflicts with EDXRA results for this element, in which it was assumed that the observed localised regions of iron were due to percolating molten material passing through the coke bed matrix, with a slight increase in iron content shown in the sample spectra. However in the light of the chemical analysis it must be assumed that some of the iron present in the feed coke was removed during the smelting process. System C' / C appeared to have increased iron concentration in the tuyere coke and thus loss or addition of iron to metallurgical coke may be related to the structure and chemical composition of the coke material used and / or chemical conditions within the furnace. Thus the iron content of the ex-tuyere cokes may reflect both an uptake and a leaching of this element, during the passage of coke through the blast furnace.

All three pairs of coke exhibited substantial losses of aluminium and silicon. Studies of slag chemistry have previously reported aluminium - silicate minerals present in the slag material tapped off at the furnace hearth

(Abraham and Staffanson, 1975). It can, therefore, be postulated that at least some of these aluminium - silicate minerals are leached from the coke. It is impossible to state exactly how the concentration of aluminium and silicon has been altered, as the original composition of the minerals is not known. The leaching process however, is almost certainly highly complex.

Chemical analysis of the reacted feed cokes was not carried out. This was because the experiments with reacted feed cokes were designed purely to yield information as to the role of potassium in effecting structural changes in the coke. Due to the nature of these experiments detailed chemical data was not required and the elemental compositions (for those of atomic number greater than eleven) of the samples were determined using the EDXRA probe, which was sufficient for means of comparison without giving empirical values.

Neither micum indices, mean size data ash content, volatile matter content nor apparent densities of the reacted feed cokes were measured, as only structural changes were being investigated.

Thus it can be seen that modern blast furnace chemistry is extremely intricate and not as simple as the proposed alkali cycle implies. However, the main studies in this present work have been orientated towards the role that potassium plays in the degradation of metallurgical coke. This was because potassium appears to be most detrimental

to coke strengths (Goleczka et al., 1983; Goleczka and Tucker, 1985), more so than sodium, and is the element which exhibits the greatest increase in concentration in the coke from stockline to tuyere level.

5.4 Penetration of Potassium

Experiments were conducted to investigate potassium pick up, to determine the main areas of potassium deposition. The method of potassium impregnation was by reflux of coke samples with a solution of potassium carbonate.

The leaching / flame photometry results were inconclusive but showed the expected trend of potassium largely residing in the meso and macroporosity of the outer regions of the coke lumps as well as the coke surface, at the low reflux temperatures.

However, no attempt was made during these experiments to investigate further penetration, of deposited potassium, when the coke was heated to higher temperatures.

No evidence for potassium penetration to the inner coke lump was obtained from the leaching experiments at reflux temperatures. However, EDXRA results from sectioned tuyere cokes did show increased potassium concentrations, even at the lump centres. The tuyere cokes had been subjected to temperatures of around 1400°C to 1500°C in the furnace. This then may indicate further penetration of potassium into the coke lumps at elevated temperatures. It may also

reflect the method of potassium deposition, that is differences between reflux impregnation and deposition from metal vapour.

5.5 Transmission Electron Microscopy (TEM)

Little structural information was available from low resolution transmission electron microscopy.

There appeared to be virtually no differences structurally between individual feed cokes, tuyere cokes or reacted feed cokes, or between feed cokes and their corresponding tuyere and laboratory reacted material.

The porous structure of the coke was revealed by low resolution electron microscopy (LREM) to be a series of macro and mesopores, of varying shapes and sizes, evenly distributed throughout the material although no interconnection of pores was observed, due to the thinness of the samples prepared for transmission electron microscopy.

LREM showed very little evidence of sample gasification in the tuyere cokes. This could be due to sample preparation, where a significant proportion of the sample is composed of material from the centre of the coke lump as opposed to the peripheral lump regions. As stated previously, it has been shown (Goleczka et al., 1982) that coke gasification is, on the whole, restricted to the periphery of the coke lumps and thus evidence of gasification may be "lost" during TEM preparation.

LREM did not give any indication of the occurrence of different carbon types, as shown during SEM analysis. It is probable that the lamellar, smooth and granular types of carbon are surface topographical features which are not imaged when the microscope is set up in transmission mode as opposed to imaging using a secondary electron detector.

In contrast to LREM, high resolution electron microscopy studies of metallurgical coke gave the most detailed structural information of all the techniques applied.

5.6 Microstructural Analysis of Feed Cokes

High resolution electron microscope studies of the feed cokes have shown them all to be very similar in basic structure.

The carbon portions of the feed cokes all exhibited a highly disordered random structure. The carbon - carbon interplanar spacings had an average value of 0.34 nm, and a range of 0.30 - 0.39 nm.

There were slight variations between feed cokes in the degree of turbostratic disorder, either raising or lowering the average interplanar spacing, but it is extremely difficult to put figures as to the degree of disorder. The feed cokes have a very short range order (almost microcrystalline) with very little (0002) lattice development.

The nature of the microstructure of these metallurgical feed cokes i.e. turbostratic carbon with carbon - carbon interplanar spacing of around 0.34 nm is common to many other types of coke material (Oberlin, 1984). Problems of image contrast, in order to enhance the lattice structure, were overcome by the use of "holey carbon" support films. These support films allowed imaging of only the sample (areas above the holes) as opposed to images of the lattice structure of the sample superimposed upon a carbon background as would be the case with conventional support films.

Also observed in all feed coke samples were areas of highly ordered structures. This crystalline material has a long range order with a wide range of lattice spacings ranging from 0.2 - 1.8 nm.

The evidence from EDXRA and chemical analysis suggested the presence of regions of alumino - silicate material in the coke and that this is the crystalline material observed by HREM. This would be feasible, as many naturally occurring alumino - silicates have high interplanar spacings. The lack of any interface between regions of carbon and crystalline material illustrated the inherent nature of this material. Again, this was consistent with the elemental distributions observed by X-ray "dot maps" and with results obtained from coke material in work carried out by British Steel (1983). Clearly this postulate also fits the alkali cycle, with some of the recirculating alkali present in the blast furnace arising from the

inherent complex alumino - silicates in the charged coke.

However, the large range of lattice spacings observed for this mineral matter rendered its unambiguous identification impossible. The crystalline material was likely to be a complex mixture of two, three or more minerals. Further characterisation of this material by infrared spectroscopy (both transmittance and reflectance) to examine the vibrational frequencies of the Si-O bond proved unfruitful. The dense opaque nature of the coke material prevented the collection of any data of this kind. Powder X-ray diffraction of the samples did not reveal any definite spacings for the mineral matter. It is assumed that this was due to the low concentrations of these minerals within the sample; the X-ray trace being an average view of the sample.

It was difficult to put any figures as to the amount of mineral matter present in a specific sample by HREM, this would be more accurately done using standard chemical analysis means.

Thus all that can be said of this material, considering the data obtained from all the techniques used, is that the coke contained a highly complex mixture of alumino - silicate material (Abraham and Staffanson, 1975; Davies et al., 1978). This material was highly crystalline and randomly dispersed throughout the sample. The crystalline material was inherent in the coke structure, intimately mixed with the carbon host matrix and almost certainly

arose from the mineral material, present in the parent coal.

The feed cokes exhibited very little obvious "edge" microporosity, that is micropores around the edge of the coke samples. The amount of this type of microporosity was so small as to be insignificant. Due to the turbostratic nature of the coke material the samples were almost certainly microporous in regions of discontinuity between areas of layer planes. These pores would be extremely small, non-basal micropores. Due to the extremely small nature of these non-basal feed coke micropores it has proved almost impossible to characterise them. The edge micropores present are both micropores (less than 0.8 nm) and supermicropores ($> 0.8 < 2$ nm).

However, micropore analysis of a range of the feed cokes carried out at Neuchâtel revealed very little open microporosity. This type of result is fairly common in cokes (Stoeckli, 1986).

Thermogravimetric analysis (figures 41 to 43) of the feed cokes exhibited a broad peak (B) normally commencing at around 550 °C and ending at around 900 °C. This is the region of weight loss in the samples, accounting for a reduction of around 88 % of coke weight. The residual weight was normally consistent with the ash content of the material (within experimental error) as given by standard chemical analysis.

Often the TGA peak appeared as a double peak for the feed cokes. This was indicative of a two stage weight loss process. The first, and smaller, of the peaks accounted for around 20 % weight loss and had a much lower rate of weight loss compared with the second peak. The second peak accounted for the other 68 % weight loss. There were some variations in relative amounts of weight loss between samples, as can be seen in figures 41 to 43. These differences were thought to be due to volatile matter content, ash content etc..

X-ray powder diffractograms obtained for the feed cokes were complimentary to results obtained by HREM. The crystalline mineral material did not show up in the diffractograms, due to the averaging nature of the technique and the low concentration of the crystalline material. The major feature, of the diffractograms obtained from the feed cokes, was the main carbon peak which appeared as a small to medium height broad peak. This was indicative of a range of lattice spacings for the carbon material. The range of spacings found from XRD analysis agreed with those found for the feed cokes by HREM, to within acceptable errors, and were typical of a non-graphitised carbon.

5.7 Microstructural Analysis of Ex-Tuyere Cokes

Microstructural analysis of the tuyere cokes showed them to possess a variety of different microstructures, although in general it could be concluded that there was little

variance between individual tuyere cokes. Very little microporosity was observed and those pores which were imaged did not significantly vary from those of the feed cokes. There appeared to be no evidence of gasification of the micropores. Results obtained from Neuchâtel, on porosity studies of the cokes by application of the Dubinin Reduskevich equation, agreed with the HREM results. There appeared to be very little open microporosity. Thus blast furnace conditions had not markedly altered the microporosity of the cokes.

High resolution electron microscope studies of the ex-tuyere cokes revealed the presence of two additional distinct microstructural forms to those found in the feed cokes. All ex-tuyere cokes appeared to be composed of these microstructural types, with very little observable difference between various ex-tuyere cokes.

First, there was a random carbon structure, previously observed in the feed cokes. This turbostratic structure had a carbon - carbon interplanar spacing of between 0.31 nm and 0.37 nm with an average spacing of 0.34 nm. As in the feed cokes this structure had a very short range order of a very few nm.

Also present in all of the ex-tuyere samples were areas of highly ordered crystalline material. This material had d - spacings ranging from 0.2 nm - 1.8 nm and it was assumed that this was the same mineral matter observed in the feed cokes. Once again there was no observable

interface between the carbon portion of the sample and the crystalline material, indicative of the inherent nature of the crystalline material. Although infrared spectroscopy and XRD analyses were made of the ex-tuyere cokes, no further identification as to the precise nature and composition of this crystalline material was possible.

Consequently, it was once again deemed to be mineral matter, arising from the parent coal material, on consideration of chemical analysis and EDXRA data.

As it had previously proved impossible to unambiguously identify the mineral material in the feed cokes (or ex-tuyere cokes) it could not be identified whether or not the nature of the material had been altered during its passage through the blast furnace. However, the changes in aluminium and silicon concentrations (as identified by chemical analysis) between the feed and ex-tuyere cokes would suggest that some changes had occurred.

5.7.1 Intercalated Potassium

The first of the additional microstructures observed was similar to the carbon portion of the feed cokes. Although the random nature of the carbon lattices was still apparent, the interplanar spacing had been enlarged to around 0.47 nm.

Considering the chemical analyses and EDXRA readouts of the ex-tuyere coke, the major difference between them and the

feed coke samples was the greater amount of potassium present in the ex-tuyere cokes. This evidence along with the observed expansion of the carbon structure would indicate the formation of a potassium intercalated species. The assumption of a potassium intercalate as opposed to another intercalate has been made with reference to the relative ease of intercalation of potassium into graphite (Berger et al., 1975) with the other elements determined to be present in the ex-tuyere cokes. This postulate of a potassium intercalate is also consistent with the recirculation of alkali metal vapour (in particular potassium) as proposed in the alkali cycle, Davies et al. (1978). Lu (1980) has shown that potassium vapour alone can result in cracking of coke samples and states (1982) that although intercalation compounds are more stable at lower temperatures, high partial pressures of alkalies (available to form intercalates) prevail at high temperatures, in the blast furnace. Thus the potassium must have a direct effect on the coke structure (gasification not being involved) and Lu concluded that the effect of potassium manifests itself in the form of intercalates. Hawkins et al. (1974) also reported the occurrence of potassium intercalated in their examination of blast furnace refractory carbons.

Kondoh et al. (1981) reported that during potassium attack, the graphite crystal structure in coke became more amorphous, as observed by X-ray diffraction. These authors suggested that this result indicated that intercalation of potassium atoms into the aromatic carbon layers brings

about a disordering of the graphite crystal structure.

However, the expansion of the carbon matrix, in the present study, did not conform to one of the recognised staged intercalates, such as C_8K , $C_{24}K$, etc.. The observed expansion of the carbon structure has therefore been proposed as being due to a residue compound formed by degradation of the original intercalated material. The degradation of reactive alkali metal / carbon intercalates has been previously reported by a variety of authors, for example, Hennig (1952), Ubbelohde (1957) and Carr (1965). Hawkins et al. (1974) detected the presence of potassium hydroxide at cracked regions of their carbon samples which they found to be a decomposition product of a potassium intercalation compound. These authors also reported that if blast furnace intercalates were exposed to air, bicarbonates and carbonates were formed as part of the decomposition products.

The degradation of the highly reactive intercalated material, in the ex-tuyere samples would undoubtedly take place during the time between removal of the samples from the blast furnace and examination in the electron microscope. Further methods of analysis were then sought to analyse and characterise the intercalated material.

Powder X-ray diffraction analysis of the samples indicated the presence of some expansion of the carbon lattices. The tail-off of the carbon peak (at the lower theta values) for the tuyere cokes occurred at a higher point than for the

feed cokes. However, no characteristic staging was observed by XRD and the cut off of the carbon peak at slightly above 0.4 nm was indicative once again of the formation of some residue compound on degradation of a "true" intercalated compound.

Temperature programmed reduction studies were also carried out to identify the presence of intercalated material. The reactivity of potassium / carbon intercalates towards hydrogen, to form ternary compounds (Bartlett and McQuillan, 1982; Terai and Takahashi, 1984), may be used to test for intercalated compounds.

TPR studies of the tuyere cokes did not reveal any major uptake of hydrogen. However, slightly larger uptakes were recorded in the tuyere cokes than in the corresponding feed cokes. Thus some further evidence for the presence of a potassium intercalate was identified, with the small increase in uptake being attributed to the presence of residue compounds rather than intercalated lamellar compounds.

Formation of alkali metal intercalates, in the blast furnace, would be detrimental to coke strength due to a number of factors. When potassium penetrates the carbon structure, local stresses are set up due to the volume expansion experienced by the carbon matrix. These stresses enable cracks to propagate if they are not relieved. Local stress relief may occur if the intercalating material rapidly diffuses along the basal plane, (Hennig, 1959) or

by deformation of the crystallite itself, if suitable planes are glissile. The main glissile planes in graphite are the (0001) planes. However, these planes would not relieve stresses due to intercalation, as these stresses would be orientated along the c-axis. However, some stress relief may be obtained with deformation of grains of carbon units deforming to relieve neighbouring grains under stress, or through imperfections in the carbon crystal structure.

Hawkins et al. (1974) compared intercalation of petroleum and metallurgical cokes. They suggested that the non-alignment of crystallites in metallurgical cokes would relieve some stresses. However, cross-linkages in these cokes are strong and this would lead to stress build up, although these cross-linkages would make the metallurgical coke intrinsically stronger.

Lu et al. (1981) have reported that their findings indicated that the rate of penetration of potassium into the carbon structure decreased with decreasing temperature. Thus the potassium concentration gradient increased in the coke with decreasing temperature. This factor induced cracking in coke samples due to differential volume expansion of these carbons. Also reported by the same authors; if there are two different constituent carbons in the coke, differential volume expansion, after potassium attack, may lead to coke degradation.

Other possible reasons for degradation of coke by

intercalation may be:-

1. If the carbon contains mixed staged intercalates this may lead to cracking due to differential volume expansion.
2. Weakening of the coke structure by catalytic gasification. The catalysts for the gasification being alkali metal intercalates (Wen, 1980).
3. Initial expansion of the carbon matrix, by the intercalate, may make the structure more accessible for subsequent chemical reactions, either by further reactions of the intercalated material or by other chemical species.

Due to the wide range of interplanar spacings, observed for the mineral material, it was impossible to say whether or not the potassium had had any effect on the crystalline material. No significant changes were observed (by HREM or XRD) in the mineral matter of the tuyere cokes, which would have indicated insertion of potassium between the layer planes of this material. However, according to Kondoh et al. (1981) EPMA images reveal that potassium is observed to be absorbed in both the coke ash (mineral matter) and in the carbon matrix.

5.7.2 Structural Ordering

In addition to intercalated material, structural ordering of the carbon lattices was also observed in the tuyere cokes. Areas of extensively ordered carbon planes were

found in the tuyere cokes in comparison with the feed cokes, which exhibited only a random carbon structure. These tuyere coke areas contained extensively ordered (0002) carbon lattices, with interplanar spacings of an average of 0.34 nm and ranging between 0.34 nm and 0.35 nm. There was no significant expansion of the layer planes in which the ordering had occurred. This observed ordering manifested itself primarily in the L_a direction, with lesser increase in the measured L_c distance. The increase in order, revealed by HREM, was on average four times that of the feed cokes, with on occasion up to an ten fold increase being recorded.

XRD analysis of the tuyere coke samples confirmed the structural ordering to have occurred. The carbon peak of the tuyere coke had been sharpened and heightened compared with the feed cokes. This indicated a greater number of lattices in a smaller range of theta values, with the carbon - carbon spacings decreasing towards that of graphite.

Density measurements made on the ex-tuyere cokes using carbon tetrachloride also indicated structural changes to have occurred during the cokes passage through the blast furnace. The indicated increase in density in the tuyere cokes compared with the feed cokes was consistent with a "graphitisation" of the material (graphite has a density of around 2.25 gcm^{-3}). Thus an increase in the density of the turbostratic carbon would be consistent with an increased order of the structure.

It is postulated that the reason for the occurrence of structural ordering in the tuyere cokes was a collapse of the intercalated material (Carr, 1965). Crespin et al. (1977), found that a substantial reduction in the number of stacking faults in a coke, previously heated to 2600°C, occurred during intercalation desorption cycles with potassium. The structural imperfections in metallurgical coke are thus thought to be "smoothed out" by intercalation of potassium and subsequent departure of the intercalated metal.

Localised ordering of the carbon structure would be likely to reduce the coke's strength in several ways:-

1. The removal of areas of turbostratic carbon and replacement by an ordered structure would be likely to create voids in the carbon matrix.
2. Reduction of the strength of crystallographic shear after localised ordering had taken place.
3. Differences in thermal expansion between the ordered structure and the turbostratic carbon may lead to cracking of the carbon.
4. Shear between regions of ordered and disordered carbon would be possible.

Variations were noted in L_c , L_a and c - axis distances measured between different areas of the tuyere cokes and

between different tuyere cokes. However, these variances were random and difficult to put meaningful values to. Thus the values, of the parameters, reported here are the values averaged over all areas and samples of the ex-tuyere cokes examined.

Thermogravimetric analysis of the ex-tuyere cokes revealed only a single peak, in the majority of cases. The starting temperature of weight loss had been approximately reduced by 50°C and this probably reflected the catalytic gasification of the carbon, due to the potassium picked up by the coke during its passage through the blast furnace. This fact indicated a considerable increase in the reactivity of the carbon, by the time that it had reached the tuyere level. The occurrence of a single peak in the tuyere cokes, in contrast with the feed cokes, appears to indicate the loss of some type of material within the furnace. The material lost was observed to "burn" in the feed cokes at around $550 - 650^{\circ}\text{C}$. Considering this factor and the chemical analysis of the feed coke material the most likely thing to be lost within the blast furnace (by the time that the coke lumps reach the tuyere level) is carbon. If this is the case then the feed coke must have contained two different types of carbon, which burn at different temperatures. This would imply that the carbons may also react differently towards recirculating alkali and possess differing thermal expansion coefficients. The carbons may even be so different as to be "hard" and "soft" carbons.

5.8 Microstructural Analysis of Reacted Feed Cokes

Successful replication of all of the microstructural forms, observed in the tuyere cokes, was achieved in the laboratory. As this was accomplished by heating the cokes in a stream of potassium vapour this indicated that potassium was one of the major influences on coke structure changes, occurring in the blast furnace.

HREM images revealed the presence of intercalated material, localised ordering and areas of the original feed coke structure. The "original" feed coke areas had a completely random carbon structure and an average interplanar spacing of 0.34 nm. The intercalated areas were also randomly orientated, with an interplanar spacing of around 0.45 nm. Thus, as in the tuyere cokes, the intercalated areas were actually residue compounds formed from degradation of a true intercalate. No evidence was found of recognised staged intercalates, such as C_8K , $C_{24}K$ etc.. Degradation of the highly reactive intercalate must have taken place during transfer from the laboratory furnace and the microscope, although every care was taken to maintain the integrity of the intercalate.

The presence of areas of localised ordering were also identified in the reacted feed cokes. These areas were very similar to those observed in the ex-tuyere samples. The average interplanar spacing was 0.34 nm and the increase in structural ordering was again mainly directed along L_a , with some increase in L_c . The reacted feed cokes

exhibited on average a six fold increase in order, in the La direction. Also observed were areas of crystalline material, previously found in the feed and tuyere cokes. This material had a wide range of lattice spacings (0.32 - 1.80 nm) and was again presumed to be mineral matter in the coke, having come from the parent coals. No evidence was found for interaction of the potassium vapour with this crystalline material and no further attempts were made to characterise it, as this had proved fruitless in the cases of the feed and tuyere cokes.

XRD analysis of the reacted feed cokes agreed with the HREM findings. The main carbon peak was found to have sharpened, towards the 0.335 nm graphite spacing, thus indicating a reduction of the turbostratic nature of the carbon. XRD traces also gave some indication of the occurrence of intercalated material, the tail of the peak reaching above 0.4 nm, in contrast with the feed cokes.

Temperature programmed reduction studies indicated a slight increase in potassium uptake in the reacted feed cokes, compared with the original feed coke material. This was taken as further evidence of the formation of potassium intercalated material, in the reacted feed cokes.

Very little microporosity was observed in the reacted feed cokes by HREM. This again agreed with results obtained for the cokes by adsorption isotherms. The micropores that were observed by HREM were in the micropore and supermicropore ranges. There did not appear to be any

significant differences between the microporosity of the feed cokes and the reacted feed cokes, or between the reacted feed cokes and the tuyere cokes. This indicated very little effect of potassium vapour on the micropore system, at the temperature of reaction.

Thermogravimetric traces obtained from the reacted feed cokes were very similar to those obtained for the ex-tuyere cokes. The occurrence of a single peak, for the reacted feed cokes, contrasted with the double peak observed in the corresponding non-reacted feed cokes. As previously described for the tuyere cokes, the onset of weight loss for the reacted feed cokes had obviously been affected by the presence of potassium vapour. This reduction in combustion temperature was considerable (around 130 °C lower than non-reacted feed cokes) and greater than the reduction observed for the tuyere cokes. The loss of the double peak, found in the feed cokes, had similar connotations to those described for the tuyere cokes. There essentially must have been a loss of material, which corresponded to the first peak. The probability being that this material was carbon. This would then imply that the two different carbons might react in different ways to the chemical and thermal environment within the blast furnace.

Examination of the reacted feed cokes had shown that the structure of the cokes could be reproduced by the reaction of the feed cokes with potassium vapour, at the temperature described. The question subsequently arose as to whether the potassium vapour, the temperature or a combination of

these factors was the driving force behind the changes produced in the feed coke microstructure, during its passage through the blast furnace.

5.9 Effect of Temperature on the Feed Cokes

Analysis of feed cokes heat treated to 1500 °C revealed significant structural changes to have taken place. Examination of these cokes, by HREM and XRD, demonstrated that considerable ordering had been produced in the carbon matrix. However, this ordering of the carbon structure did not appear to be as extensive as that observed in the corresponding tuyere cokes, although both types of coke had experienced the same temperature. This reduction of the turbostratic nature of carbon material, by heat treatment, has been reported by a number of authors (Maire and Méring, 1970; Fischbach, 1971,; Pacault, 1971; Robert et al., 1973; Oberlin, 1984).

The lesser degree of ordering, found in the cokes which had purely been heat treated, implied the influence of another factor in the alteration of the coke's microstructure. The reacted feed cokes exhibited no interplanar expansion of the carbon lattices, as was expected, there being no external intercalating material present when the cokes were heated. However, there remained a sizeable proportion of the original feed coke material (randomly orientated carbon lattices) after heat treatment. This implied the possibility of the presence of two different types of carbon in the cokes, as they had

been heat soaked at 1500°C for a considerable time period. The interplanar spacings in the disordered and ordered carbon portions were both found to be on average 0.34 nm. The increase in order being between roughly four times greater than that found in the non-heat treated feed cokes. Once again the increase in order was in the La direction, the Lc distance only being slightly increased.

The morphology of the feed cokes reacted with potassium vapour, at below their carbonisation temperature, was found to be very similar to that of the tuyere cokes. Again there were three distinct microstructures. First, a turbostratic structure identical to that of the non-reacted feed cokes. That is areas of randomly ordered carbon lattices, with an average interplanar spacing of 0.34 nm. Second, an turbostratic structure, with an expanded interplanar spacing of around 0.45 nm. The expansion of this carbon structure was assumed to arise from potassium entering between the carbon layers, the guest species arising from the potassium vapour in which the cokes were heated. Third, areas of ordered carbon material. This ordering must have been effected by the presence of potassium vapour. The interplanar spacing of these areas was identical to the feed coke spacings (turbostratic carbon) of 0.34 nm and the increase in order observed in the La direction was around three to four times that observed in the non-reacted feed cokes. The cokes had been subjected to higher temperatures, than the reaction temperature, for a substantial time during the industrial carbonisation process, after which very little ordering was

seen to have occurred in the carbon matrix. The ordering induced in the feed cokes, by reaction with potassium vapour below the carbonisation temperature, was assumed to have been induced by intercalation / deintercalation cycles. The removal of inherent defects would then occur in a similar manner to that described by Carr (1965) and Crespin (1977). Although the ordering observed, by XRD and HREM, was substantial compared with the non-reacted feed cokes, it was not as extensive as that observed in the tuyere cokes. Thus it would appear that attack by alkali alone is insufficient to reproduce the effects observed in the tuyere cokes. The more considerable changes undergone in the tuyere cokes were therefore concluded to have been induced by a combination of thermal effects and alkali attack.

5.10 Analysis of Tuyere Cokes Reacted with Potassium Vapour

These cokes exhibited the presence of a definite staged potassium / carbon intercalate. This $C_{16}K$ peak (A.S.T.M.S. index 4 -345, Schleede and Wellmann, 1932) appeared as a very strong peak in the XRD analysis of these reacted cokes. As none of the other reacted cokes (feed cokes) exhibited such a staged intercalate it must be assumed that the more ordered structure of the tuyere cokes made it more susceptible to potassium intercalation. The ability of graphite to intercalate potassium has been reported (Berger et al., 1975) along with intercalation of this alkali metal into turbostratic carbons. It would appear that the ordered structure of graphite enables it to

intercalate readily and this is in agreement with the observations made on the ex-tuyere cokes reacted with potassium vapour. The staged ($C_{16}K$) intercalate was readily destroyed when the samples were refluxed in isopropanol.

The occurrence of this staged intercalate in the reacted tuyere cokes implied that intercalation takes place more readily after previous intercalation / deintercalation cycles, or into a more ordered structure (Berger et al., 1975).

5.11 Effects of Inert Carrier Gas

Studies of the effects of different carrier gases on the reacted feed cokes were made. However, no visible differences were observed in any of the microstructural forms, when a variety of carrier gases were employed, although it has been reported (Thakur and Brown, 1982; Britten et al., 1985) that the effects of non-reacting carrier gases can be profound on some coke properties. The present study suggests that these non-reacting carrier gases have no significant effect on the formation of the various microstructures, observed in the reacted feed and tuyere cokes. It is concluded therefore that the effects of non-reacting gases, on coke properties, are more important on the macro properties of the material. In particular the effects of inert carrier gases may influence gasification reactions, where the CO desorption step may be altered by the nature of the surrounding atmosphere.

5.12 GENERAL DISCUSSION

Coke degradation in the modern blast furnace is a highly complex process. It has been shown that alkali vapour recirculates within the furnace (Davies et al., 1978; Hatano et al., 1980 (b)). It has also been shown that alkali vapour catalyses the Boudouard reaction (McKee and Chatterji, 1975). However, the extent of coke degradation, found in the blast furnace, does not appear to be completely governed by gasification. The amount of size reduction found in blast furnace coke lumps is unlikely to, in theory, be caused by gasification alone. It has been shown that severe degradation of coke occurs in the presence of alkali vapour but in the absence of carbon dioxide (Lu et al., 1981). Tucker (1983) has demonstrated that coke lumps may be broken by hand, after being subjected to potassium vapour, at elevated temperatures, in an inert atmosphere of nitrogen. Thus it would appear that alkali metal vapour plays a greater role, in coke degradation, than merely catalysing carbon gasification.

The present study has proved that considerable structural changes are induced in the coke, during its passage through the blast furnace (Shevlin et al., 1984, 1985, 1986). Comparison of feed and ex-tuyere cokes has shown the formation of intercalated material and an ordering of the carbon structure to occur. Also present in the tuyere cokes were areas of feed coke carbon structure. This has suggested the possibility of there being two types of carbon in the coke, differing in their ability to be intercalated.

Reaction of feed cokes, with potassium vapour in the laboratory, successfully reproduced the microstructures observed in the tuyere cokes and thus established potassium as one of the major driving forces in producing these microstructures. The other possible driving force being temperature. From subsequent laboratory experiments it has been shown that both alkali attack and temperature affect the ordering found in the carbon matrix of the tuyere cokes. Both of the factors appeared to have roughly the same magnitude of effect on ordering but the greatest development of this microstructural form when both alkali attack and temperature were combined. Previous studies have demonstrated that intercalation / deintercalation cycles order carbon structure by lowering the number of defects in the original structure (Crespin et al., 1977). Also, it has been known for many years that the heat treatment temperature afforded a graphitising carbon can determine the degree of structural perfection of the resulting material. Thus it is not surprising that the combined effects of heat and alkali attack (as experienced by the tuyere cokes) produced the largest observed structural ordering of the material.

It has also been shown that the tuyere cokes intercalate potassium to a greater extent than any of the other cokes, on further exposure to potassium vapour. Thus it must be concluded that intercalation is influenced by the degree of structural perfection of the material. Consequently, repeated intercalation of potassium would be more detrimental to coke strength than a single intercalation of

the potassium between the carbon layers.

Taking account of all of these factors, it is assumed that the degradation of metallurgical coke (in addition to gasification) would generally be influenced as follows;

1. Formation of an intercalate would expand the carbon lattices. This expanded, disordered structure would be susceptible to degradation by chemical and mechanical attack. This attack may be by recirculating alkali or other species, as the intercalated material is highly reactive and expansion of the structure (including the microporous structure) makes it more accessible for reactions to take place.

2. Ordering of the structure would create voids thus weakening the material. Structural ordering would also be expected to reduce crystallographic shear in one direction within the coke. Interfaces between ordered and disordered carbon would develop which would also create a weakness of the carbon matrix.

The structural ordering is envisaged to occur by single or repeated intercalation of potassium into the carbon structure which on deintercalation orders the structure through the removal of crystallographic defects.

3. The occurrence of different microstructural forms would give rise to degradation through differential volume expansion. These differences in expansion coefficients may

be between ordered and disordered carbon, intercalated and non-intercalated material, mixed staged intercalations or any combination of these species, thus giving rise to localised stresses.

All of the above methods of degradation would be expected to be substantial in magnitude and are consistent with the observations of massive reduction of coke strength with reaction with alkali metal vapour, even in the absence of carbon dioxide gas. A comparison of degradation through catalytic gasification with the above mechanisms would suggest that a greater strength reduction and hence size reduction would occur with the above mechanisms as opposed to purely gasification of the coke.

Wen (1980) proposed that catalytic gasification of coke using alkali metals occurs through intercalated intermediates. The driving force for degradation of coke through the mechanisms described in the present work is the formation of alkali metal intercalates, either directly or indirectly as intermediates. Thus it can be concluded that although the degradation of metallurgical coke is a highly complex situation probably involving many varying reactions, the fundamental process involved in the weakening of the coke structure is the formation of alkali metal intercalates.

Future Work

The present study has demonstrated the necessity to negate, or at least to mitigate, the effect of potassium has in the blast furnace, thus improving coke strength.

The direct altering of the blast furnace chemistry to reduce the effect of potassium is unsatisfactory. Substantial changes in furnace chemistry would alter the slag chemistry and may reduce the iron output of the furnace and increase the sulphur content of the iron. The fractional removal of alkalis in the blast furnace is dependant on a number of operational parameters. The portion of alkali removed in the top gas depends on the overall temperature and distribution of the top gas, CO / CO_2 ratio. The fraction removed in the slag is dependent on slag volume, basicity, temperature, viscosity and the partial pressure of CO_2 in the bosh region of the furnace. In order to effect efficient removal of alkali in the slag it is necessary to regulate flame temperature, slag volume, basicity and hot metal temperature. However the optimum conditions for alkali removal in the slag are the opposite (except slag volume) to those required for low sulphur content in the metal.

Some operators employ a cleaner to reduce alkali build up in the furnace. This may involve the addition of a reagent or a reduction of the flux rate (limestone before dolomite) resulting in a lowering of the slag basicity, normally for two casts. However, it is possible that the effects of

alkali may be reduced indirectly. These methods are more directly related to the alkali effect on metallurgical coke, may take a variety of forms and have been suggested by the results obtained in the present work. These suggestions require further research but can be surmised as follows;

1. Determination as to whether thermal annealing of the coke at around (1000 - 1200°C) would maintain the integrity of the turbostratic carbon, thus making it more resistant to alkali attack.

2. Addition of certain mineral additives to the coal during manufacture to observe their effects on the level of potassium attack. Mineral additives such as mica and other silicates may sequester potassium by a cation exchange reaction. Should this prove fruitful then optimisation of potassium uptake could be made by careful choice of the most appropriate mineral blends.

3. Addition of non-graphitising carbon to the coke during carbonisation. It could prove to be the case that either graphitising or non-graphitising carbons may preferentially take up potassium at the expense of the other carbon species. These experiments would also further clarify the role of potassium in the observed structural ordering of the carbon matrix. Non-graphitising carbons may prevent localised alignment of the carbon planes and hence relieve some of the stress factors induced in the cokes during their passage through the blast furnace.

4. The wide variety of coals and cokes leads to a requirement for rationalisation. It is probable that there is a level below which potassium has little effect on coke strength at a given temperature. It is also likely that just above this value there is a dependence on potassium concentration until saturation is reached. It would be of value to both coke classification and to the significance of sequestration if this dependence could be determined.

5. Investigations of potassium attack on individually carbonised macerals would rationalise rank dependence on alkali attack. Should removal of potassium prove impossible then the effects of the alkali may be mitigated by improved coal blending.

Conclusions

The results obtained from the present work have led to a variety of conclusions regarding the nature of the effect of blast furnace conditions.

First, the nature of the inherent mineral matter is that it arises from the parent coal material and is randomly dispersed throughout the metallurgical coke. There is no apparent interface between the carbon matrix and the mineral matter, thus showing that the mineral matter is an integral part of the coke structure.

The reaction of the coke material with potassium vapour causes enhanced localised ordering. This ordering of the carbon structure can be extensive and is one of two additional microstructural forms found in the coke material after reaction with potassium vapour. Thermal treatment of the coke (to around 1500°C) has a similar effect, in producing enhanced localised ordering, as that of potassium vapour. However, the greatest degree of structural ordering has been observed when the coke material is exposed to alkali vapour at relatively high temperatures ($1100-1500^{\circ}\text{C}$). Thus it would appear that thermal and chemical treatments combine to significantly alter the microstructure of metallurgical coke.

Potassium intercalates are formed when metallurgical cokes are exposed to potassium vapour. These intercalates readily degrade when exposed to air, water, mechanical

treatment etc.. Intercalation also takes place more readily after the material has undergone a previous intercalation / deintercalation cycle. It is postulated that these intercalates are intermediates between the highly disordered feed coke structure and the areas of localised ordering observed in the cokes after passage through the blast furnace.

The observed changes in microstructure, after reaction of the feed cokes with potassium vapour, are independent of the type of inert carrier gas employed in the reaction.

All the changes in microstructure, described above, would almost certainly weaken the coke structure, either individually or in a combined manner. This weakening of the coke, by these effects, would be substantial and result in a greater structural weakening than would occur purely by gasification.

It is firmly believed that the mechanical degradation of metallurgical coke occurs primarily due to changes in structure at molecular level, as opposed to macrostructural changes, which arise as a direct consequence of the microstructural effects.

Thus, it may be assumed, at this time, that the effects described in the present work, combined with carbon gasification, constitute the major forces involved in the degradation of metallurgical coke.

REFERENCES

- ABEN P.C., van der EIJK H. and OELDERIK J.M., Paper # 48, 5th Int. Cong. Catal. (ed. J.W. Hightower), North Holland, Amsterdam, (1972).
-
- ABRAHAM K.P. and STAFFANSON L.I., Scand. J. Metallurgy, 4, 193, (1975).
- ABRAMSKI C. and MACKOWSKY M.T., In "Handbuch der Mikroskopie in der Technik" (ed. H. Freund), Vol II., pp. 311 - 410, Umschau - Verlag, Frankfurt, (1952).
- ADAIR R.R., BOULT E.H., FREEMAN E.M., JASIENKO S. and MARSH H., Carbon, 9, 763, (1971).
- AGAR A., British J. Appl. Phys., 11, 504, (1960).
- AHMED H., Proc. 25th Anniv. Meeting EMAG., 30, Institute of Physics, London, (1971).
-
- ALLPRESS J.G., HERVAT F.A., MOODIE A.F. and SANDERS J.V., Acta. Cryst., A28, 528, (1972).
- American Society Testing Materials Method, K18, (1939).
- American Society Testing Materials Method, pt. 3, pp. 24 - 27, (1939).
- American Society Testing Materials Method, D271 - 37. (1939).

- ANDREWS K.W., DYSON D.J. and KEOWN S.R., "Electron Diffraction Patterns", Hilger, London, (1967).
- ARMATORIO G.G., KEMNER W.F. and HEGEDUS G. S., "Blast Furnace Operating Problems With High Alkali Pellets", Presented at Chigago Regional Technical Meeting of AISI, (1971).
- AST D.G., KRAKOW W. and GOLDFARB W., Report No. 2328, Mats. Sci. Centre, Cornell Univ., (1974).
- A.S.T.M. INDEX, Publication P O 15 - 15i, (1965).
- BACON G.E., Acta Cryst., 3, 137, (1950).
- BACON G.E., Acta. Cryst., 4, 558, (1951).
- BACON G.E., Acta. Cryst., 5, 392, (1952(a)).
- BACON G.E., Acta. Cryst., 5, 492, (1952(b)).
- BACON G.E., Acta. Cryst., 7, 359, (1954).
- BACON G.E., AERE Report, M / R 2702, (1958).
- BACON G.E., Proc. 3rd Conf. Carbon, Buffalo, 1957, Pergamon Press, New York, p. 457, (1959).
- BAKER C., CHOU Y.T. and KELLY A., Phil. Mag., 6, 1305, (1961).

BAKER C., GILLIN L.M. and KELLY A., 2nd Ind. Carbon and Graphite Conf., Society of Chemical Industry, London, (1965).

BARRITT D.T. and ROBINSON V., "Coke Ovens: Retrospect, Prospect", Coke Oven Managers Yearbook, pp. 504 - 581, (1961).

BARTLETT N. and McQUILLAN B.W., In "Intercalation Chemistry", (ed. M.S. Whittingham and A.J. Jacobson), Chapt. 2, pp. 19 - 54, Academic Press, London, (1982).

BARTON S.S., HARRISON B.H. and DOLLIMORE J., J. Chem. Soc., Faraday Trans., I, 1039, (1973).

BEESTON B.E.P., HORNE R.W. and MARKHAM R., In "Practical Methods in Electron Microscopy", (ed. A.M. Glavert), North Holland, Amsterdam, (1972).

BEIMANN W., AUVIL H.S. and COLEMAN D.C., In "Chemistry of Coal Utilisation" (ed. H.H. Lowry), Supplementary Volume, chpt. 11, pp. 461 - 493, John Wiley and Sons, New York, (1963).

BENEDICT L.G. and THOMPSON R.R., International Journal of Coal Geology, 1, 19, (1980).

BENNIT H.L., Minerals Yearbook, U.S. Bur. Mines, Washington D.C., p. 869, (1939).

- BERGER D., CARTON B., MÉTROT A. and HÉROLD A., In Chemistry and Physics of Carbon (ed. P.L. Walker, Jr.), 12, 1, Marcel Dekker, New York, (1975).
- BERKOWITZ N., Proc. Blast - Furnace Coke Oven and Raw Materials Comm., AIME 19, 95, (1960).
- BERKOWITZ N., An Introduction to Coal Technology, Chapt. 2., Academic Press, N.Y., (1979).
- BERNAL J.D., Proc. Roy. Soc., A106, 709, (1924).
- BILLYEALD D. and PATRICK J.W., Extended Abst. 12th Bienn. Conf. Carbon, Pittsburgh, pp. 147 - 148, Pergamon Press, (1975).
-
- BISCOE J. and WARREN B.E., J. Appl. Phys., 13, 364, (1942).
- BLYHOLDER C. and NEFF L.D., J. Phys. Chem., 66, 1464, (1962).
- BOEHM H.P. and HOFFMAN U., Z. Anorg. Allg. Chem. 58, 278, (1955).
- BOERSCH H., Annalen der Physik., (5), 27, 75, (1936).
- BOERCHIA A. and BONHOMME P., Optik, 39, 437, (1974).
- BOLLMAN W., Phil. Mag., 5, 621, (1960).

BOLLMAN W., Proc. 5th Conf. Carbon, Phil. II, p. 303, Pergamon Press, London, (1961(a)).

BOLLMAN W., Proc. Eur. Reg. Conf. Electron Microscopy, Delft, p. 330, (1961(b)).

BOLLMAN W., Proc. 1st Int. Conf. Properties of Reactor Materials, p. 132, (1961 (c)).

BOTHAM J.C., LEEDER W.R. and REEVE D.A., Symposium on Coal Evaluation, Calgary, Alberta, (1974).

BOUDOUARD O., Bull. Soc. Chim., 21, pp. 465 - 7, 713 - 15, (1899).

BOUDOUARD O., Bull. Soc. Chim., 25, pp. 227 - 30, 833 - 40, (1901(a)).

BOUDOUARD O., Ann. Chim. Phys., 24, 1, (1901(b)).

BOURAOUI A. and MÉRING J., Carbon, 1, 465, (1964).

BRADSHAW K. and WILKINSON H.C., J. Inst. Fuel, 42, 112, (1969).

British Standard (Testing Methods), 1016, Part 12, (1980).

British Standard (Testing Methods), 1016, Part 13, (1980).

BRITISH STEEL CORPORATION, "Degradation of Coke in the Blast Furnace", ECSC Paper, Eur. 8703, (1983).

BRITTEN J.A., FALCONER J.L. and BROWN L.F., Carbon, 23, No. 6, 627, (1985).

BROOKS J.D. and TAYLOR G.H., In Chemistry and Physics of Carbon, (ed. P.L. Walker, Jr.), 4, 243, Marcel Dekker, New York, (1968).

BROWN R.L. and HIORNS F.J., In "Chemistry of Coal Utilisation" (ed. H.H. Lowry), Supplementary Vol., pp. 119 - 149, John Wiley and Sons, New York, (1963).

BRUNAUER S., EMMETT P.H. and TELLER E., J. Am. Chem. Soc., 60, 309, (1938).

CARR K.E., Ph.D. Thesis, University of Glasgow, (1965).

CHAPMAN J.N., GRAY C.C. and NICHOLSON W.A.P., X-ray Spectrometry, Vol. 12, No. 4, (1983).

CHAPMAN J.N., NICHOLSON W.A.P. and CROZIER P.A., Journal of Microscopy, Vol. 136, Part 2, pp. 179 - 181, (1984 (a)).

CHAPMAN J.N. and MORRISON G.R., J. Microsc. Spectrosc. Electron., Vol. 9., pp. 329 - 340, (1984 (b)).

COSSLETT V.E., In "Practical Electron Microscopy",
Oxford University Press, London, (1951).

COSSLETT V.E., Q. Rev. Biophysics, 2, 95, (1969).

COSSLETT V.E., Inst. Elect. Eng., 117, 1489, (1970).

COSSLETT V.E., Proc. R. Soc., London, A370, 1, (1980).

COSSLETT V.E., Contemp. Phys., no.2, 22, 3, (1981(a)).

COSSLETT V.E., Contemp. Phys., 22, no. 2, 147 - 182,
(1981(b)).

COULSON C. A., Nature, 159, 265, (1947).

COULSON C.A. and TAYLOR E., Proc. Phys. Soc., A, 65,
815, (1952).

COVER A.E., SCHREINER W.C. and SKAPERDAS G.T., Chem. Eng.
Prog., 69, (3), 31, (1973).

COWLEY J.M. and MOODIE A.F., Acta. Cryst., 10, 609,
(1957).

COWLEY J.M., In "Diffraction Physics", p. 221, North
Holland, Amsterdam, (1975).

CRACKNELL A.P., Adv. Phys., 18, (70), 681, (1969).

CRAVEN A.J. and ADAM P.F., 8th European Congress on Electron Microscopy, Vol.1, p. 371 (ed. A. Csanady, P. Rohlich and D. Szabo), (1984 (a)).

CRAVEN A.J. and BUGGY T.W., Journal of Microscopy, Vol. 136, Part 2, pp. 227 - 239, (1984 (b)).

CRAVEN A.J., ADAM P.F., NICHOLSON W.A.P., CHAPMAN J.N. and FERRIER R.P., Journal de Physique Colloque Cz, Supplement au No. 2, Tome 45, (1984 (c)).

CRESPIN M., TCHOUBAR D., GATINEAU L., BEGUIN F. and SETTON R., Carbon, 15, 303, (1977).

CREWE A., EGGENBERGER D.N., WALL J. and WALTER L.J., Rev. Sci. Inst., 39, 576, (1968).

CROFT R.C., Quarterly Reviews, 14, 1, (1960).

DAUMAS N. and HÉROLD A., Bull. Soc. Chim. France, 5, 1598, (1971).

DAVIES J., MOON J.T. and TRAICE F.B., Iron and Steelmaking, No. 4, 151, (1978).

DAWSON I.M. and FOLLETT M.A.C., Proc. Roy. Soc., A253, 390, (1959).

de BROGLIE L., Phil. Mag., 47, 446, (1924).

DEBYE P. and SCHERRER P., Phys. Z., 18, 291, (1917).

DENIG F., In "Chemistry of Coal Utilisation" (ed. H.H. Lowry), Vol. 1, Chapt. 21, pp. 774 - 833, Chapman and Hall Ltd., London, (1945).

DRYDEN I.G., J. Inst. Fuel, 30, 193, (1957).

DUBININ M.M., ZAVERINA E.D. and RADUSKEVICH L.V., Zh. Fiz. Khim., 21, 1351, (1947).

DUCKWORTH S.P., CRAVEN A.J. and BAKER T.N., Inst. Phys. Conf. Ser. No. 68, Chapt. 9, p. 339 (ed. T. Mulvey), (1983).

DUPOUY G. and PERRIER F., J. Microscopie, 1, 167, (1962).

DZURUS M.L and HENNIG G.R., J. Chem. Phys., 27, 275, (1957).

EBERT L.B., Annu. Rev. Mater. Sci., 6, 181, (1976).

ECHTEROFF H., Stahl Eisen, 81, 992, (1961).

EELES W.T. and TURNBULL J.A., Nature, 198, 877, (1963).

EELES W.T. and TURNBULL J.A., Proc. Roy. Soc., A283, 179, (1965).

EELES W.T. and WILSON A.J.C., Nature, 205, 66, (1965).

EISENHANDLER C.B. and SIEGEL B.M., J. Appl. Phys., 37, 1963, (1966).

EMMETT P.H. and BRUNAUER S., J. Am. Chem. Soc., 59, 1553, (1937).

ENGLISH C.A. and VENABLES J.A., Proc. 25th Anniv. Meeting EMAG., p. 40, Institute of Physics, London, (1971).

ENGLISH C.A. and VENABLES J.A., Proc. 5th European Conf. E.M., Manchester, p. 172, Institute of Physics Conference Series No. 14, (1972).

ERGUN S., Chem. Eng. Progress, 48, No. 2, 89, (1952).

ERGUN S., Carbon, 6, 141, (1968(a)).

ERGUN S., In Chemistry and Physics of Carbon (ed. P.L. Walker, Jr.), 3, 211, Marcel Dekker New York, (1968(b)).

ERGUN S. and GIFFORD T.J., J. Appl. Cryst., 1, 313, (1968).

ERGUN S. and GIFFORD T.J., Paper # 22, Paris Conf., J. Chim. Phys., p. 99, (1969).

EVANS E.L. and THOMAS J.M., J. Solid State Chem., 14, 99, (1975).

EVERHART T.E., OATLEY C.W. and WELLS O.C., J. Electronics and Control, 7, 97, (1959).

EWALD P.P., Sitzungsber Munch. Akad., 4, 7, (1914).

FIELDNER A.C., American Society Testing Materials; Sectional Committee on Classification of Coals, General Circ. 42, Sub - Comm II Rept., 7, (1933).

FINCH G.I and WILMAN H., Proc. Roy. Soc., A155, 345, (1936).

FINNEY C.S. and MITCHELL J., J. of Metals, 13, pp. 285 - 291, 373 - 378, 425 - 430, 501 - 503, 559 - 561, (1961).

FISCHBACH D.B., Chemistry and Physics of Carbon (ed. P.L. Walker, Jr.), 7, 1, Marcel Dekker, New York, (1971).

FISHER R.M., SZIRMAE A. and McALEAR J.H., Anal. Chem., 42, 362R, (1970).

FITZER E., MUELLER K. and SCHAEFER W., Chemistry and Physics of Carbon (ed. P.L.Walker), 7, 238, Marcel Dekker, New York, (1971).

FOX D.A. and WHITE A.H., Ind. Engng. Chem., 23, 259, (1931).

FRANCIS W., "Coal, Its Formulation and Composition", Edward Arnold Ltd., London, 2nd ed., (1961).

FRANK J., Optik, 38, 519, (1950).

FRANKE F.H. and MERAIB M., Carbon, 8, 423, (1970).

FRANKLIN R.E., Acta. Cryst., 3, 107, (1950).

FRANKLIN R.E., Acta. Cryst., 4, 253, (1951(a)).

FRANKLIN R.E., Proc. Roy. Soc., (London), A209, 196,
(1951(b)).

FREDENHAGEN K. and CADENBACH G., Z. Anorg. Chem., 158,
249, (1926).

FREDENHAGEN K. and SUCK H., Z. Anorg. Chem., 178, 353,
(1929).

FRIEDEL J., "Dislocations", Addison-Wesley, London, (1964).

FRYER J.R., Proc. 8th Int. Cong. Canberra, 1, p. 680,
(1974).

FRYER J.R., "Characterisation of Porous Solids", Proc.
Symp., Neuchatel, Switzerland, pp. 41 - 52 (ed. S.J.
Gregg, K.S.W. Sing and H.F. Stoeckli), Society of
Chemical Industry, London, (1978).

FRYER J.R., In "The Chemical Applications of Transmission
Electron Microscopy", Academic Press, London, (1979).

FRYER J.R., Mol. Cryst. Liq. Cryst., 96, 275, (1983).

FRYER J.R. and HOLLAND F., Proc. Roy. Soc., (London), A393,
353, (1984).

GEORGE D.W.R. and PEART J.A., Ironmaking Proc., 32, 40, (1973).

GIBSON J., "Commonsense of Carbonisation", 11th Carbonisation Science Lecture, (1979).

GLAESER R.M., In "Physical Aspects of Electron Microscopy and Microbeam Analysis" (ed. B.M. Siegel and D.R. Beaman), p.205, Wiley, New York, (1975).

GOLECZKA J., TUCKER J. and EVERITT G., Paper to ECSC Round Table Conference, Luxembourg, (1982).

GOLECZKA J., TUCKER J. and EVERITT G., Paper to ECSC Round Table Conference, Luxembourg, (1983).

GOLECZKA J. and TUCKER J., CEC Round Table, Coke Oven Techniques, Brussels, (1985).

GOODMAN P. and MOODIE A.F., Acta. Cryst., A30, 280, (1974).

GRABKE H.J., Carbon, 10, 587, (1972).

GRAINGER L. and GIBSON J., "Coal Utilisation Economics and Policy", Graham and Trotman Ltd., Great Britain, (1981).

GREEN S.J., "Industrial Catalysts", Macmillan, New York, (1928).

GRINTON G.R. and COWLIE J.M., Optik, 34, 221, (1971).

HAERING R.R. and MROZOWSKI S., Prog. Semicond., 5, 273, (1960).

HAIJITINK G.J., de BOER E., van der MEIJ P.J. and WEIJLAND W.P., Rec. Trav. Chim., 75, 487, (1956).

HAINE M.E. AND MULVEY T., Proc. 3rd Int. Conf. on Electron Microscopy, London, p. 698, (1954).

HALL C.E., In "Introduction to Electron Microscopy", London, (1953).

HALL C.E. and HINES R.L., Philos. Mag., 21, 1175, (1970).

HALL H.T., Proc. 3rd Carbon Conf., 74, Pergammon Press, (1957).

HALPIN M.K. AND JENKINS G.M., 3rd Conf. Ind. Carbons and Graphite, 53, Society of Chemical Industry, London (1971).

HANZEN K.J., Adv. Opt. Electron Microscopy, 4, 1, (1971).

HANZEN K.J. AND TREPTE L., Optik, 32, 519, (1971).

HARKER H., Proc. 4th Carbon Conf., Buffalo, (1959)., Pergamon Press, New York, pp. 125 - 139, (1960).

HARKER H., HORSLEY J.B. and ROBSON D., J. Nucl. Mater., 37, 331, (1970).

HARRIS P.S., Carbon, 10, 643, (1972).

HARRISON J.A., Proc. Illinois Mining Institute, 69th Year, pp. 17 - 43, (1961).

HASSEL O. and MARK H., Z. Physik., 25, 317, (1924).

HATANO M., MIYAZAKI T., SHIMODA T., KAJIWARA Y., IWANAGA Y. and KAMEI Y., McMaster Symposium, No. 8, 3.3 - 3.30, (1980 (a)).

HATANO M., MIYAZAKI T. and IWANAGA Y., Trans. ISIJ, 20, 744, (1980 (b)).

HATANO M., MIYAZAKI T. and IWANAGA Y., Ironmaking Proc., 41, 46, (1982).

HAWKINS R.J., MONTE L. and WATERS J.J., Iron and Steelmaking (Quarterly), No.3, 151, (1974).

HAYNES W.P., GASIOR S.J. and FORNEY A.J., Am. Chem. Soc., Div. Fuel Chem., Prepr., 18(2), 29, (1973).

HEDDEN K. and WICKE E., Proc. 3rd Carbon Conf., Buffalo, New York, pp. 249 - 256, Pergammon Press, New York, (1957).

HEDDEN K., KOPPER H.H. and SCHLUZE V., Z. Physik. Chem. (Frankfurt), 22, 23, (1959).

HEERSCHAP M., DELAVIGNETTE P. and AMELINCKX S., Carbon, 1, 235, (1964).

HEERSCHAP M. and DELAVIGNETTE P., Carbon, 5, 383, (1967).

HEINTZ E.A. and PARKER W.E., Carbon, 4, 473, (1966).

HENDRICKS T.A., In "Chemistry of Coal Utilisation", Vol. 1, p. 1-24, (ed. H.H. Lowry), Chapman and Hall Ltd., London, (1945).

HENNIG G.R., J. Chem. Phys., 20, 1438, (1952).

HENNIG G.R. and McClelland J.D., J. Chem. Phys., 23, 1431, (1955).

HENNIG G.R., Proc. 1st and 2nd Carbon Conf., Buffalo, USA., 103, Pergammon Press, New York, (1956).

HENNIG G.R., Progr. Inorg. Chem., 1, 125, (1959).

HENNIG G.R. Proc. 4th Carbon Conf., 221, Pergammon Press, New York, (1960).

HÉROLD A., C.R. Acad. Sci. Paris, 232, 1484, (1951).

HÉROLD A., Bull. Soc. Chim. France, 999, (1955).

HÉROLD A. and Carton B., Bull. Soc. Chim. France, 4, 1337, (1972).

HEUCHAMPS C., Thèse Ingénieur-Docteur, Université de Nancy, (1960).

HILLIER J. and Vance A.W., In "Electron Optics and the Electron Microscope", John Wiley and Sons New York, (1945).

HIRSCH P.B., HOWIE A., NICHOLSON R.B., PASHLEY D.W. and WHEELANS M.J., In "Electron Microscopy of Thin Crystals", Butterworths, London, (1965).

HOFFMAN E. and JENKNER A., Glückauf, 68, 81, (1932).

HOFMANN U. and WILM D., Z. Electrchem., 42, 504, (1936).

HOLCOMBE A., USAEC Oak Ridge Y-12 PLant, Report Y1887, (1973).

HOLLAND F., FRYER J.R. and BAIRD T., Inst. Phys. Conf. Ser., No. 68, Chpt. 1, 19 (ed. P. Doig), (1983).

HOLLAND F., Ph.D. Thesis, University of Glasgow, (1984).

HOLOWATY M.O. and SQUARCY C.M., J. Met., 45, 577, (1957).

HOOLEY J.G., In "Preparation and Crystal Growth of Materials with Layered Structures", (ed. R.M.A. Leith), pp.1 - 33, Reidel Publ., Dordrecht, Netherlands, (1977).

HOUSKA C.R. and WARREN B.E., J. Appl. Phys., 25, 1503, (1954).

HOWIE A., KRIVANEK O.C. and RUDEE M.L., Phil. Mag., 27, 235, (1973).

IIJIMA S., Optik, 48, (2), 193, (1977).

JALAN B.P. and RAO Y.K., Carbon, 16, 175, (1978).

JANSSEN R.E., "The Beginings of Coal", Scientific American, 179, 46, (1948).

JONES W., Surf. Defect Prop. Solids, 5, 65, (1975).

JÜNTGEN H. and SCHWUGER M., Chem - Ing - Tech, 38, 1271, (1966).

KAMMLOTT G.W., Surf. Sci., 25, 120, (1971).

KAY D.H., "Techniques for Electron Microscopy", Alden Press, Oxford, 2nd Edition, (1965).

KING C.D., Seventy-five Years of Progress in Iron and Steel, AIME, New York, pp. 1 - 48, 84 - 87, (1948).

KING J.G. and JONES J.H., J. Inst. Fuel., 5, 39, (1931).

KING J.G. and WILKENS E.T., Proc. Conf. Ultrafine Structure of Coals and Cokes (BCURA), pp. 44 - 56, (1944).

KISLYKH V.I. and SHISHAKOV N.V., "Catalytic Effect on Gasification in a Fluidised Bed", GASOV Promst., 5 (8), 15, (1960).

KNOLL M. and RUSKA E., Ann. d. Physik., 12, 607, (1932).

KOBAYASHI K., and SAKAOKU K., Lab. Inst., 14 (6), Pt. 2, 1097, (1965).

KOBAYASHI K. and O'HARA M., Proc. 6th Int. Cong. E.M., Kyoto, 1, 579, (1966).

KOHL A.L., HARTY R.B. and JOHANSON J.G., Chem. Eng. Prog., 74 (8), 73, (1978).

KOJIMA K., NISHI T., YAMAGUCHI T., NAKAMA H. and IDA S., Trans. ISIJ., 17, 401, (1977).

KOMODA T., Jap. J. Appl. Phys., 5, 179, (1966).

KONDOH M., KONISHI Y. and OKABE K., Iron and Steel Society of AIME, Iron Making Proc., 40, 454, (1981).

KOVALIK M.J., WOLFSON D.E. and FISCHLER F., "Studies on Thickness of Plastic Layer of Coals", U.S. Bur. Mines, RI 6568, (1964).

KRAKOW W., AST D.G., GOLDFARB W. and SIEGEL B.M., Phil. Mag., 33, 985, (1976).

KRIVANEK D.L. and HOWIE A., J. Appl. Cryst., 8, 213, (1975).

KROGER C. and ANGEW Z., Z. Angew Chem., 52, 129, (1939).

KUMAO A., HASHIMOTO M. and SHIRAISHI K., J. Electron Microscopy, 30, 161, (1981).

LAIDLER D. and TAYLOR A., Nature, 146, 130, (1940).

le POOLE J.B., Philips Tech. Rev., 9, 33, (1947).

LEONARD J.W. and CLENDININ J.D., Blast Furnace and Steel Plant, 49, 45, (1961).

LEWIS I.C., Carbon, 20, No. 6, 519, (1982).

LEWIS J.B., In "Modern Aspects of Graphite Technology", (ed. L.C.F. Blackman), Academic Press, New York, p. 129, (1970).

LIPSON H. and STOKES A.R., Nature, 149, 328, (1942 (a)).

LIPSON H. and STOKES A.R., Proc. Roy. Soc., A181, 101, (1942 (b)).

LOCH L.D and AUSTIN A.E., Proc. 1st and 2nd Carbon Conf., 65, Pergammon Press, New York, (1956).

LOISON R., PEYTAVY A., BOYER A.F. and GRILLOT R., In "Chemistry of Coal Utilisation" (ed. H.H. Lowry), Supplementary Vol., chpt. 4, pp. 150 - 201, John Wiley and Sons, New York, (1963).

LONG F.J. and SYKES K.W., J. Chim. Phys., 47, 361, (1950).

LONG F.J. and SYKES K.W., Proc. Roy. Soc. (London), A215, 100, (1952).

LOTHE J. and MELSOM S., Dragon Project Report, 372, A.E.E., Winfrith, England, (1965).

Lu W.K., McMaster Symposium, No. 8, 7b.1, Hamilton, Ontario, Canada, (1980).

LU W.K., SAMAAAN G. and URIBE M., Iron and Steel Society of AIME, Iron Making Proc., 40, 57, Toronto, Canada, (1981).

LU W.K. and HOLDITCH J.E., Iron Making Proc., 41, 194, (1982).

LUKESH J.S., Phys. Rev., 80, 226, (1950).

LUKESH J.S., J. Chem. Phys., 19, 384, (1951 (a)).

LUKESH J.S., J. Chem. Phys., 19, 1203, (1951 (b)).

LYNCH D.F. and O'KEEFE M.A., Acta. Cryst., A28, 536, (1972).

McCLURE J.W., Proc. 3rd Carbon Conf., Buffalo, 179, Pergammon Press, New York, (1959).

MCDONNELL F.R.M., PINK R.C. and UBBELOHDE A.R., J. Chem. Soc., 191, (1951).

McKEE D.W. and CHATTERJI D., Carbon, 13, 381, (1975).

McKEE D.W. and CHATTERJI D., Carbon, 16, 53, (1978).

McKEE D.W., In Chemistry and Physics of Carbon, (ed. P.L. Walker, Jr.), 16, 1, Marcel Dekker, New York, (1981).

MAIRE J. and MERING J., Proc. 3rd Carbon Conf., 337, Pergammon Press, New York, (1959).

MAIRE J., COLAS H. and MAILLARD P., Carbon, 6, 555, (1968).

MAIRE J. and MÉRING J., In Chemistry and Physics of Carbon, (ed. P.L. Walker, Jr.), 6, 125, Marcel and Dekker, New York, (1970).

MARQUARD W.B., U.S. Pat., 1,323,711, (1919).

MARSH H. and RAND B., Carbon, 9, 63, (1971).

MARSH H., J. ISI., 211, (5), 334, (1973 (a)).

MARSH H., DACHILLE F., ILEY M., WALKER P.L., Jr. and WHANG P.W., Fuel, 52, 253, (1973 (b)).

MARSH H. and WALKER P.L., JR., In Chemistry and Physics of Carbon, (ed. P.L. WALKER, Jr.), 15, 229, Marcel Dekker, New York, (1979).

MATUYAMA E., Nature, 193, 61, (1962).

MELMED A.J., J. Appl. Phys., 37, 275, (1966).

MÉRING J. and MAIRE J., J. Chim. Phys., 57, 803, (1960).

MILLWARD G.R. and JEFFERSON D.A., In Chemistry and Physics of Carbon, (ed. P.L. WALKER, Jr.), 14, 1, Marcel Dekker, New York, (1978).

MISELL D.L., Adv. Electronics and Electron Physics, 32, 63, (1973).

MOTT R.A. and WILKINSON H.C., Fuel, 36, 39, (1957).

MUKHERJEE M.M., "Review of the Evaluation of Blast Furnace Coke by Strength Indices, at Ambient and High Temperatures", Divisional Report, FMP 65 / 62 - CG, Fuels Division, Mines Branch, Dept. of Mines and Technical Surveys, Ottawa, Canada, (1965).

MURATA Y., BAIRD T. and FRYER J.R., Nature, 263, No. 5576, 401, (1976).

NANAVATI K.S. and COHEN G.M., Iron Making Proc. AIME, 31, 133, (1972).

NARITA K., ONOYE T., SATOH Y., MIYAMOTO M., TANIGUCHI K., KAMATANI S., SATO T. and FUKIHARA S., Trans. ISIJ, 21, 839, (1981).

NIXON W.C., AHMED H., CATTO C.J.D., CLEAVER J.R.A., SMITH K.C.A., TIMBS A.E., TURNER P.W. and ROSS P.M., EMAG, 13, (1977).

NOMINÉ N. and BONNETAIN L., C.R. Acad. Sci. Paris, Ser. C., 264c, 2086, (1967).

NOVIKOV Yu N., KAZAKOV M.E., ZVARYKINA A.V. ASTAKHOVA I.S. and VOL'PIN M.E., Zh. Strukt. Khimii., 12, (3), 486, (1971).

OATLEY C.W., NIXON W.C. and PEACE R.F.W., Adv. Electronics and Electron Physics, 21, 181, (1965).

OBERLIN A., TERRIÈRE G. and BOULMIER J.L., TANSO, No. 83, 29, (1975 (a)).

OBERLIN A., TERRIÈRE G. and BOULMIER J.L., TANSO, No. 83, 153, (1975 (b)).

OBERLIN A., Carbon, 22, No. 6, 521, (1984).

OHNO T., J. Electron Microscopy, Tokyo, 23, 1, (1974).

OKSTAD S. and HOY A., "New Method for Measurement of Reactivity, 2nd Conf. on Industrial Carbon and Graphite, Society of Chemical Industry, London, (1965).

PACAUT A., In Chemistry and Physics of Carbon, (ed. P.L. WALKER, Jr.), 7, 107, Marcel Dekker, New York, (1971).

PARKS B.C., In "Chemistry of Coal Utilisation" (ed. H.H. Lowry), Supplementary Volume, pp. 1 - 34, John Wiley and Sons, New York, (1963).

PARRY G.S. and NIXON D.E., Brit. J. Appl. Phys., 1, 291, (1968).

PARSONS J.R. and HOELKE C.W., Phil. Mag., 30, 135, (1974).

PARTICK J.W. and STACEY A.E., Fuel, 51, 81, (1972).

PATRICK J.W., STACEY A.E. and WILKINSON H.C., Fuel, 51, 174, (1972).

PATRICK J.W. and SHAW F.H., Fuel, 51, 69, (1972).

PATRICK J.W., STACEY A.E. and WILINSON H.C., Fuel, 52, 27, (1973).

PATRICK J.W., Proc. 4th Carbon Conf., Baden - Baden, p. 156, (1986).

PAUL D.E., LIPKIN D.E. and WEISSMAN S.E., J. Amer. Chem. Soc., 78, 116, (1956).

PAULING L., Proc. Natl. Acad. Sci., 56, 1646, (1966).

PEASE R.F.W. and NIXON W.C., J. Sci. Instr., 42, 81, (1965).

PERCH M. and RUSSELL C.C., Trans. AIME, 184, 205, (1949).

PERRET R. and RULAND W., Paper #21, Paris Conf., (1968 (a)).

PERRET R. and RULAND W., J. Appl. Cryst., 1, 308, (1968(b)).

PHILIPS BULLETIN, Philips Scientific and Analytical Bulletin, 79.177 / EM10, (1963).

PINES D., Rev. Mod. Phys., 28, 184, (1956).

PINES D., In "Elementary Excitations in Solids", New York, (1963).

POWELL A.R. and THOMPSON J.H., Carnegie Inst. Tech., Coop. Bull., 7, 3, (1923).

READ W.T., "Dislocations in Crystals", McGraw-Hill, New York, (1953).

RILEY H.L., Fuel, 24, 8, (1945 (a)).

RILEY H.L., Fuel, 24, 43, (1945 (b)).

ROBERT M.C., OBERLIN M. and MÉRING J., In Chemistry and Physics of Carbon, (ed. P.L. WALKER, Jr.), 10, 141, Marcel Dekker, New York, (1973).

ROSE H.J., In "Chemistry of Coal Utilisation" (ed. H.H. Lowry), Vol. 1, pp. 25 - 85, John Wiley and Sons, New York, (1945).

RUDBERG E., Phys. Rev., 50, 155, (1936).

- RUDEE M.L. and HOWIE A., Phil. Mag., 25, 1001, (1972).
- RUDORFF W. and HOFFMAN U., Z. Anorg. Allgem. Chem., 238, 1, (1938).
- RUDORFF W., Angew. Chem., 71, 487, (1959).
- RUDORFF W. and RUDORFF G., Z. Anorg. Allgem. Chem., 253, 281, (1947 (a)).
- RUDORFF W. and RUDORFF G., Chem. Ber., 80, 417, (1947 (b)).
- RUDORFF W. and SCHULZ E., Angew. Chem., 66, 305, (1954 (a)).
- RUDORFF W. and SCHULZ E., Z. Anorg. Chem., 277, 156, (1954 (b)).
- RUDORFF W., SCHULZ E. and RUBISCH D., Z. Anorg. Chem., 282, 232, (1955).
- RUFF O. and BRETTSEIDER O., Z. Anorg. Allgem. Chem., 217, 1, (1934).
- RULAND W., Paper #III - 12, Symp. Carbon, Tokyo, (1964).
- RULAND W., Acta. Cryst., 18, 992, (1965 (a)).
- RULAND W., Carbon, 2, 365, (1965 (b)).

RULAND W., Acta. Cryst., 22, 615, (1967 (a)).

RULAND W., Paper #5159, 8th Carbon Conf., Buffalo, (1967 (b)).

RULAND W., In Chemistry and Physics of Carbon, (ed P.L. Walker, Jr.), 4, 1, Marcel Dekker, New York, (1968).

RUSSELL C.C. and PERCH M., Trans. AIME, 154, 116, (1943).

SALZANO F.J. and ARONSON S., J. Chem. Phys., 47, (8), 2978, (1967).

SAUNDERS K.G., Ph.D. Thesis, University of Glasgow, (1978).

SAUNDERS K.G., Private Communication, (1979).

SCHAFHAEUTL P., J. Prakt. Chem., 21, 155, (1841).

SCHERZER D., J. Appl. Phys., 20, 20, (1949).

SCHILLER C., MÉRING J., CORNAULT P. and du CHAFFAUT F., Carbon, 5, 385, (1967 (a)).

SCHILLER C., MÉRING J., CORNAULT P. and du CHAFFAUT F., Carbon, 5, 507, (1967 (b)).

SCHILLER C. and MÉRING J., Paper # 5161, 8th Carbon Conf., Buffalo, New York, Pergammon Press, New York, (1967).

SCHLEEDE A. and WELLMAN M., Z. Phys. Chem., B18, 4, (1932).

SCHRÖDINGER E., Ann. Physik., 81, 109, (1926).

SCOTT H.D., WALKER J.F. and HANSLEY V.L., J. Amer. Chem. Soc., 58, 2442, (1934).

SELIG H. and EBERT L.B., Adv. Inorg. Chem. Radio Chem., 23, 281, (1980).

SEYLER C.A., "The Chemical Classification of Coal", Proc. South Wales I Engineers, 21, 483, (1899).

SCHAFHAEÜTL P., J. Prakt. Chem., 21, 155, (1841).

SHEVLIN M.J.F., FRYER J.R. and BAIRD T., EUREM'84, 1, 239, (1984).

SHEVLIN M.J.F., FRYER J.R. and BAIRD T., EUREM'84, 1, 239 (ed. A. Csanady, P. Rohlich and D. Szabo), (1984).

SHEVLIN M.J.F., FRYER J.R. and BAIRD T., Carbon, 24, No.5, 527, (1986).

SHORT M.A. and WALKER P.L., Jr., Carbon, 1, 3, (1963).

SIMEK B.G., LUDMILLA J. and STANCLOVA B., Mitt Kohlenforsch. Inst. Prag., 2, 48, (1935).

SIMMERBACH O. and SCHNEIDER G., Kokschemie, Julius Springer, Berlin, 3rd Edition, pp. 177 - 186, (1930).

SKOWRONSKI J.M., Fuel, 56, 585, (1977).

SLONCZEWSKI J.C. and WEISS P.R., Phys. Rev., 109, 272, (1958).

SMITH D.J., CAMPS R.A., FREEMAN L.A., HILL R., NIXON W.C. and SMITH K.C.A., J. Microsc., 130, 127, (1983).

SNOW R.B. and SHAPLAND J.J., AIME, Blast Furnace, Coke Oven and Raw Materials Proc., 9G, (1962).

SPENCER D.H.T., "Porous Carbon Solids", (ed. R.L. Bond), chpt. 3, Academic Press, London, (1967).

STARKOVICH J.A., PINKERTON J.D. and MOTLEY E., "Catalytic Conversion of Coal Energy to Hydrogen", (FE - 2206 -14), U.S. Dept. Energy, (1977).

STEIN C., POULENARD J., BONNETAIN L. and GOLÉ J., C.R. Acad. Sci. Paris, 260, 4503, (1965).

STEIN C., C.R., 264c, 16, (1967).

STOECKLI F., Private Communication, (1986).

STRONG S.L., Paper # SS - 12, 9th Carbon Conf., Boston, Pergammon Press, New York, (1969).

STUTZER O. and NOE A.C., Geology of Coal, University of Chicago Press, (1940).

SYSKOV K.I., OTN AN SSSR, 8, 68, (1943).

SYSKOV K.I., AS USSR Press, Moscow, (1949).

TATE M., SUZUKI K., CHANG T.S., KUWANO Y., GO H., HONDA K., MATSUZAKI M., TSUJI E. and NAKAMURA S., Trans. ISIJ, 19, 332, (1979).

TERAI T. and TAKAHASHI Y., Carbon, 22, No. 1, 91, (1984).

THAKUR S.C. and BROWN L.F., Carbon, 20, No. 1, 17, (1982).

THEISEN R. and SPRUNK G.C., U.S. Bur. Mines, Tech. Paper, 631, (1941).

THOMAS J.M. and WALKER P.L., Jr., Carbon, 2, 434, (1965).

THOMAS J.M., MILLWARD G.R., SCHLÖGL R.F. and BOEHM H.P., Mater. Res. Bull., 15, 671, (1980).

THON F. and SIEGEL B.M., B. Bunsen. Ges. phys. chem., 74, No.11, 1116, (1970).

TRZEBISTOWSKI W., Roczniki, Chem., 17, 73, (1937).

TSCHAMLER H. and de RUITER E., In "Chemistry of Coal Utilisation" (ed. H.H. Lowry), Supplementary Vol., pp. 35 - 118, John Wiley and Sons, New York, (1963).

TUCKER J., Private Communication, (1983).

TUCKER J., Private Communication, (1985).

TURNER H.G. AND ANDERSON H.V., Fuel, 11, 262, (1932).

UBBELOHDE A.R., Nature, 180, 380, (1957).

UBBELOHDE A.R. and LEWIS F.A., "Graphite and its Crystal Compounds", Oxford University Press, (1960).

UBBELOHDE A.R., J. Chem. Phys., 58, 107, (1961).

van KREVELEN D.W., Coal Elsevier, Amsterdam, (1961).

van NIEKERK W.H., DIPPENAAR R.J. and KOTZE D.A., J. South Afr. Min. Metall., Vol. 86, No. 1, 25, (1986).

VERRA M.J. and BELL A.T., LBL - 4498, Lawrence Berkley Laboratory, University of California, (1976).

VERRA M.J. and BELL A.T., Fuel, 57, 194, (1978).

VOL'PIN M.E., NOVIKOV Yu.N., KASAKOV M.E., ZVARYKINA A.V. and ASTAKOVA I.S., Zh. Strukt. Khimii, 12, (3), 486, (1971).

von BOGANDY L. and ENGEL H.J., "The reduction of Iron Ores", Springer - Verlag, Berlin, (1971).

WAGNER C., Unpublished, Quoted by JALAN B.P. and RAO Y.K., Carbon, 16, 175, (1978).

WALKER P.L., Jr., RUSINKO F., Jr. and AUSTIN L.G., In Advances in Catalysis, (ed. D.D. Eley, P.W. Selwood and P.B. Weisz), 11, 133, Academic Press, New York, (1959).

WALKER P.L., Jr., SHELEF M. and ANDERSON R.A., In Chemistry and Physics of Carbon, (ed. P.L. WALKER, Jr.), 4, 287, Marcel Dekker, New York, (1968).

WALLACE P.R., Phys. Rev., 71, 622, (1947).

WALLACE P.R., Solid State Commun., 4, 521, (1966).

WARREN B.E., Phys. Rev., 59, 693, (1941).

WARREN B.E., Proc. 1st and 2nd Carbon Conf., Buffalo, 1953, 1955, p. 49, Waverly Press, University of Buffalo, New York, (1956).

WARREN B.E. and BODENSTEIN P., Acta. Cryst., 18, 262, (1965).

WARREN B.E. and BODENSTEIN P., Acta Cryst., 20, 602, (1966).

WASA A., NAKAI T. and SASAKI S., Int. Organ. Stand.,
ISO TC27 / SC3, No. 12, (1974).

WATANABE K., SOMA M., ONISHI T. and TAMARU K., Nature Phys.
Sci., 233, 160, (1971).

WEN W.Y., Catal. Rev.-Sci. Eng., 22(1), 1, (1980).

WHELAN M.J., Inst. Metals, 87, 392, (1959).

WILKINSON H.C., Fuel, 44, 191, (1965).

WILLIAMS R.C. and FISHER H.W., J. Mol. Biol., 52, 121,
(1970).

WOLF R.J. and JOY D.C., Proc. 27th EMAG, 34, Institute of
Physics, (1971).

WOODRUFF E.M., J. Chim. Phys., Special Issue, p. 96,
(1969).

YANCEY H.F. and GEER M.R., In "Chemistry of Coal
Utilisation", (ed. H.H. Lowry), Vol. 1, pp. 145 - 159, John
Wiley and Sons, New York, (1945).

ZCHEMCHUZHNIKOV Y.A., Inst. Mekhanicheskoi Obrabotki
Poleznuikh Iskopaemuikh "Mekhanober", 15 yrs. Socialistic
Ind. Service, 1, 37, (1935).

ZORENA P.J., HOLOWATY M.O. and SQUARCY C.M., Blast Furnace
Steel Plant, 48, 443, (1960).

ZWORYKIN V.K., MORTON G.A., RAMBERG E.G., HILLIER J. and
VANCE A.W., In "Electron Optics and the Electron
Microscope", Wiley, New York, (1945).

TABLEPage

1 & 2	Macerals in Coal	16
3	Analysis of Coals used to form Single Coal Cokes	134
4	Reactivity of Single Coal Cokes to CO ₂	134
5	Analysis of Feed and Ex-tuyere Coke Pairs	134
6	Purities of Industrial Gases Used	135
7	ASTM Standard Carbon Spacings as Determined by X-ray Diffraction	<u>162</u>
8	Potassium Penetration of Feed Cokes	164
9	Potassium Penetration of Ex-tuyere Cokes	169

<u>FIGURE</u>		<u>Page</u>
1	Dilatometry Curve of Carbonisation	1
2	Vitrinite	2
3	Condensation Process in Carbonisation	3
4	Essential Units Comprising a Modern Coking Plant	5
5 & 6	Products of Coal Carbonisation	7
7	Coalification, Compaction and Composition	12
8	Gray-King Swelling Profiles	13
9 & 10	Coal Classification as used by British Coal	14
11	Hexagonal Form of Graphite	42
12	Graphite Unit Cell Basal Plane Projection	43
13	Rhombohedral and Hexagonal Forms of Graphite	43
14	Stages of Graphitisation	53
15	Alkali Cycle Within the Blast furnace	58
16	Band Structure of graphite	87
17	Band Structure of n-type Intercalation Compounds in Graphite	88
18	Band Structure in p-type Intercalation Compounds in Graphite	88
19	Simple Intercalation Model	94
20	Arrangement of Potassium in Graphite Intercalates	95
21	Herolds Bent Layer model	96
22	Basic Structural Design of a TEM	104
23	Phase contrast Transfer Function (PCTF)	113
24	Resolution Loss with Increasing Cs	114
25	Effect of Envelope Functions on PCTF	116
26	Effect of Chromatic Spread on PCTF	116

<u>FIGURE</u>		<u>Page</u>
27	Optical Processing on an Optical bench	121
28	Electron Diffraction and Imaging Modes	123
29	Electron Diffraction	123
30	The Electron Microscope as a Simple Diffraction Camera	124
31	Principle of SEM	130
32	Carbon Coating of Holey Films	140
33	PCA 10 Laboratory Furnace	142
34	Sample Handling Method 1	143
35	Sample Handling Method 2	145
36	Generalised Diagram of TPR System	149
37	Reaction of Graphite with Potassium Vapour	153
38 - 40	XRD Traces from Feed Cokes	161
41 - 43	TGA Traces from Feed Cokes	162
44 - 46	XRD Traces from Ex-tuyere Cokes	167
47 - 49	TGA Traces from Ex-tuyere Cokes	168
50 - 52	XRD Traces from Reacted feed Cokes	174
53 - 55	TGA Traces from Reacted Feed Cokes	176
56 - 58	TGA Traces from Heat Treated Feed Cokes	180
59 - 61	XRD Traces from Heat Treated Feed Cokes	182
62 - 64	TGA Traces from Feed Cokes Reacted Below Carbonisation temperature	186
65 - 67	XRD Traces from Feed Cokes Reacted Below Carbonisation Temperature	187
68 - 70	XRD Traces from Reacted Ex-tuyere Cokes	192
71 - 73	TGA Traces from Reacted Ex-tuyere Cokes	194
74 - 76	TGA Traces from Inert Carrier Gas Studies	195
77	Coke Lump Before and After Alkali Attack	199

PLATEPage

1	From Coal to Coke	2
2	Coke Ovens on a Modern Coke Plant	6
3	Coke Oven During Carbonisation	8
4	Pushing Hot Coke from the Coke Oven	9
5 - 8	SEM of Feed Cokes + EDXRA	159
9	Artefacts Produced when Cutting Coke	159
10 - 16	Elemental Distributions in Feed Cokes	160
17 - 19	LREM of Feed Cokes	161
20 - 24	HREM of Feed Cokes	161
25 - 27	Crystalline Mineral Matter	161
28 - 30	SEM of Ex-tuyere Cokes + EDXRA	164
31 - 33	LREM of Ex-tuyere Cokes	165
34 - 39	HREM of Ex-tuyere Cokes	166
40 - 42	SEM of Reacted Feed Cokes + EDXRA	171
43 & 44	LREM of Reacted Feed Cokes	173
45 - 53	HREM of Reacted Feed Cokes	173
54 - 57	SEM / LREM of Heat Treated Feed Cokes	178
58 - 60	HREM of Heat Treated Feed Cokes	181
61 - 63	SEM of Feed Cokes Reacted Below Carbonisation Temperature	184
64 - 69	HREM of Feed Cokes Reacted Below Carbonisation Temperature	189
70 - 72	SEM of Reacted Ex-tuyere Cokes	191
73 - 75	HREM of Reacted Ex-tuyere Cokes	192
76	BEI of Feed Cokes	201
77	BEI of Ex-tuyere Cokes	202



ELECTRON MICROSCOPY 1984

VOLUME 1

INSTRUMENTATION PHYSICS AND MATERIALS SCIENCE APPLICATIONS I

Proceedings of the
EIGHTH EUROPEAN CONGRESS
on
ELECTRON MICROSCOPY

Budapest, Hungary
August 13—18, 1984

Editors: Á. Csanády, P. Röhlich and D. Szabó

Published by the Programme Committee of the Eighth European
Congress on Electron Microscopy

Budapest, 1984

Microstructural Analysis of Cokes and Intercalated Species.

M.J.F. Shevlin, J.R. Fryer, T. Baird.

Chemistry Dept., University of Glasgow, Glasgow G12 8QQ, Scotland.

The structural weakening of metallurgical cokes is believed to be due partially to potassium intercalated species.⁽¹⁾ As potassium penetrates the carbon structure it sets up stresses due to differential volume expansion of the carbon lattice. These stresses may be relieved by crack formation which leads to a decrease in the coke's strength.

Samples of both blast furnace feed cokes and ex-tuyere cokes have been examined for the effects of intercalation, by HREM at 500kV (figs.1-4).⁽²⁾ The ex-tuyere cokes were obtained through a series of holes in the "bosh" or hot-zone of the furnace; this and the feed coke samples were prepared for HREM analysis by ballmilling them to a fine powder, further grinding with a mortar and pestle and then placing the powder in ultrasonics in an aqueous medium. A droplet of the suspended particles was then placed on a carbon coated holey film and transferred to the microscope.

Figures 1 and 2 show examples of two feed cokes of similar rank. Both of these samples exhibit the typical "onion" type carbon structure of cokes, with the lattice spacing of an average of 3.4Å. Also present in both samples are areas of highly ordered crystalline mineral matter (arrowed) with lattice spacings of 4.5-18Å. This mineral matter has been shown by elemental analysis to be rich in aluminium and silicon, and is inherent in and randomly distributed throughout the coke.

Figure 3 shows one area of the ex-tuyere coke. The random onion structure is still apparent although the lattice spacing has been enlarged to 4.7Å.

Elemental analysis shows negligible amounts of potassium in the feed cokes and in contrast high concentrations of potassium evenly distributed throughout the ex-tuyere sample. This result along with the well documented alkali cycle⁽¹⁾ which is present in the blast furnace would be consistent with the formation of an intercalated compound. Previous work⁽³⁾ on graphitizable carbons has shown that the average distance between potassium atoms in an intercalated species is slightly lower than 3.92Å, which is also consistent with the present work.

Figure 4 shows areas of extensive ordering of the carbon lattices in the ex-tuyere sample. Here the lattice spacing has collapsed to the original distance of 3.4Å. This phenomenon has been previously reported⁽⁴⁾ and is probably due to the highly reactive nature of intercalated species. Thus it appears that in the furnace the coke sample undergoes potassium attack to form a disordered intercalated species which subsequently forms a residue compound of greater order. The increased order probably results from single or repeated intercalation.

work is being carried out at present on simulating blast furnace chemical effects in an electric furnace, in the hope that HREM analysis of these samples will verify and increase an understanding of the weakening of metallurgical cokes due to the formation of intercalated species.

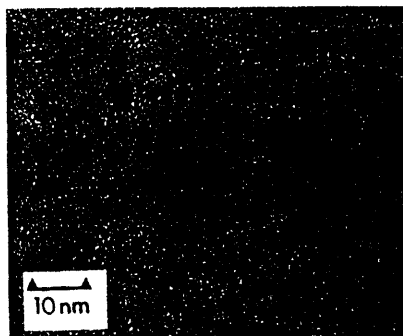
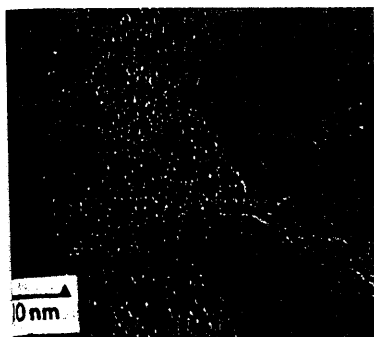


Fig. 2

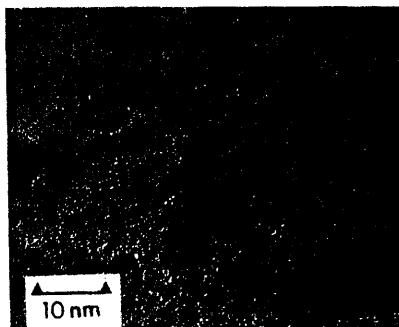


Fig. 4

References:

- Abraham K.P., Staffanson L.I., Scand. J. Metallurgy 4, 193, (1975)
 Smith D.J., Camps R.A., Freeman L.A., Hill R., Nixon W.C., Smith K.C.A., J. Microsc. 130 127, (1983)
 Berger C., Carton B., Metrot A., Herold A., in Chemistry and Physics of Carbon vol. 12, P.1, (1975), (Ed. P.L. Walker Jr. & P.A. Thrower), Marcel Dekker New York.
 Carr K.E., Carbon 8, 155, (1970).

Thank D.J. Smith and L.A. Freeman of the Cambridge HREM group for assistance with HREM of the samples.

ELECTRON MICROSCOPY 1984 (series ISBN 963 01 5620 2):

Volume 1 Instrumentation. Physics and Materials Science
Applications I.
ISBN 963 01 5621 0

Volume 2 Applications II. Film Session. Life Sciences I.
ISBN 963 01 5622 9

Volume 3 Life Sciences II.
ISBN 963 01 5623 7

Published by the Programme Committee of the Eighth European
Congress on Electron Microscopy
c/o Congress Bureau MOTESZ Budapest, P. O. Box 32, H-1361 Hungary

© Copyright rests with the author. No part of this book may be
reproduced without written permission from the author(s)
Responsible for publication: Sz. Virágh

Printed in Petőfi Nyomda, Kecskemét, Hungary

Microstructural analysis of metallurgical cokes and intercalated species

M J F Shevlin, J R Fryer, T Baird

Chemistry Dept., University of Glasgow, Glasgow G12 8QQ, Scotland

The presence of recirculating alkali within the blast furnace is believed to be a major factor in the degradation of metallurgical cokes (Hawkins et al, 1974; Abraham and Staffanson 1975; Goleczka et al 1983), leading to a decrease in output and fuel efficiency of the furnace. The presence of alkali gives the possibility of the formation of potassium intercalated species, causing expansion of the coke's semigraphitic layers, resulting in both mechanical and chemical weakening. Penetration of the structure by potassium sets up stresses, caused by differential volume expansion of the carbon lattices which is possibly relieved by crack formation (detrimental to the coke strength), and expansion of the microporous structure makes it more accessible to reactive species at the relatively high temperatures involved.

The microstructure of both blast furnace feed cokes and ex-tuyere cokes have been examined by HREM (figs 1-4). Particular emphasis has been placed on the use of lattice imaging and elemental analysis techniques in investigating the effect of alkali attack on the microstructure, and in assessing the distribution of mineral matter in the coke. The ex-tuyere samples were obtained from the furnace high temperature region in which coke strength is of vital importance and the samples have undergone alkali attack. The feed cokes used were the material as charged to the furnace.

Figures 1 and 2 show examples of two feed cokes of similar rank. Both of these samples exhibit a typical non-graphitised carbon structure, with the lattice spacing of an average of 0.34 nm, of short range order, and very little 0.35 nm (0002) lattice development. Also apparent in both samples are areas of highly ordered crystalline material (arrowed) with lattice spacings 0.32 - 1.8 nm. This material has been shown by EDXRA and elemental mapping techniques to be mineral matter (of an aluminosilicate nature) randomly distributed throughout the sample and inherent in the coke from its formation.

The ex-tuyere samples show two distinct types of microstructure. Figure 3 shows one area of the ex-tuyere coke. The random, "onion" type carbon structure of the feed coke is still apparent although the lattice spacing has been enlarged to around 0.47 nm.

Elemental analysis shows negligible amounts of potassium in the feed cokes, and in contrast very much higher concentrations of potassium in the ex-tuyere samples. The well documented alkali cycle as reported by Lu (1980), together with the observed expansion of the carbon lattices (0.47 nm)

and levels of potassium in the samples are consistent with the formation of an intercalated compound. The (0002) lattice expansion however is not as extensive as would be expected for a species such as C_8K , $C_{16}K$ or $C_{24}K$ and is probably a residue compound formed from the intercalated material during the period of removal from the furnace to transfer to the microscope (Carr 1970).

Figure 4 is an example of the other type of microstructure observed throughout the ex-tuyere sample. These areas contain extensively ordered (0002) carbon lattices with spacings of an average of 0.34 nm, no significant expansion of the layer planes is observed within the areas of ordering. The reasons for the occurrence of two microstructural forms are as yet not fully understood but is postulated as being due to one of two processes. Firstly, lattice spacing collapse, of the expanded layer planes, to the original feed coke spacing of 0.34 nm. This phenomenon has been previously reported in graphite (Carr 1970) and is probably due to the highly reactive nature of intercalated species. In this mechanism the coke sample would undergo potassium attack to form a disordered intercalated species which subsequently forms a residue compound of greater order. The increased order probably being the result of single or repeated intercalation. The second possibility for the occurrence of two microstructural types is the creation of two carbon species during the mesophase in coke production. These two carbon types can then be envisaged as having differing properties with respect to alkali attack and/or heat treatment.

Reproduction of the ex-tuyere microstructure has been successfully carried out in the laboratory. Reaction of feed coke samples with potassium carbonate in an electric furnace has given rise to areas of extensively ordered carbon lattices and substantiated the formation of intercalated species occurring in metallurgical coke.

The separation of the effects of alkali attack and the heat treatment causing ordering of the carbon lattices in the ex-tuyere samples is currently under investigation.

References

- Abraham K P and Staffanson L I 1975 *Scand. J. Metallurgy* 4 193
Carr K E 1970 *Carbon* 8 155
Goleczka, Tucker J and Everitt G 1983 ECSC Round Table, Coke, Luxemburg
Hawkins R J, Monte L and Waters J J 1974 *Iron and Steelmaking* (Quarterly)
3 151
Lu W K 1980 In McMaster Symposium 8

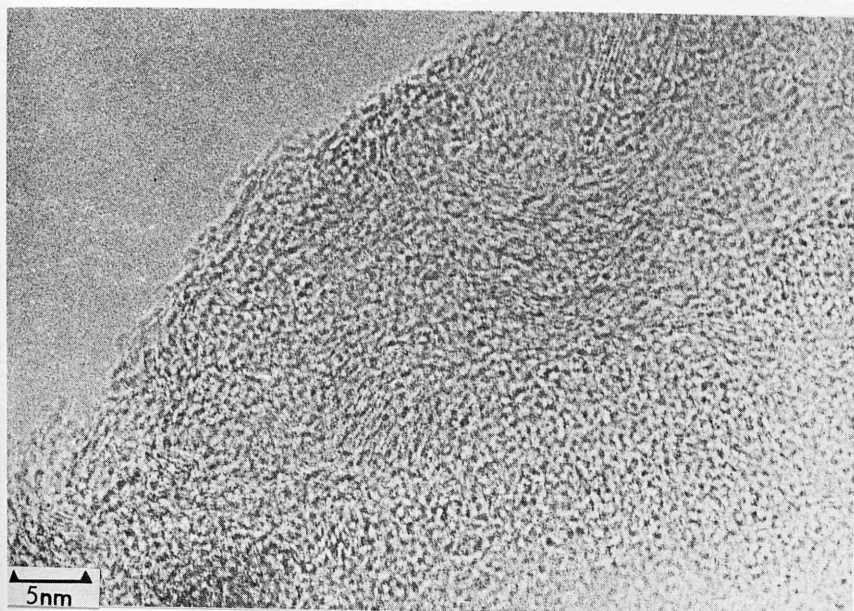


Figure 1.

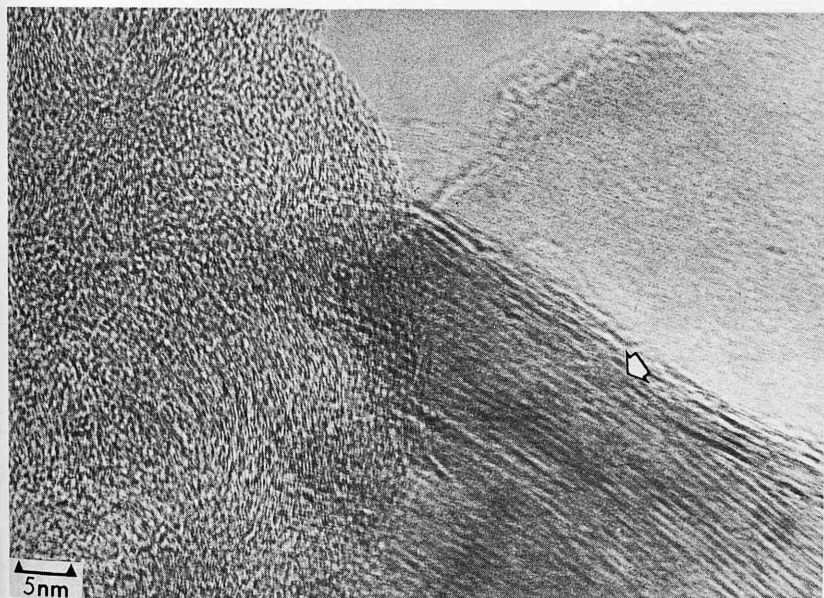


Figure 2.

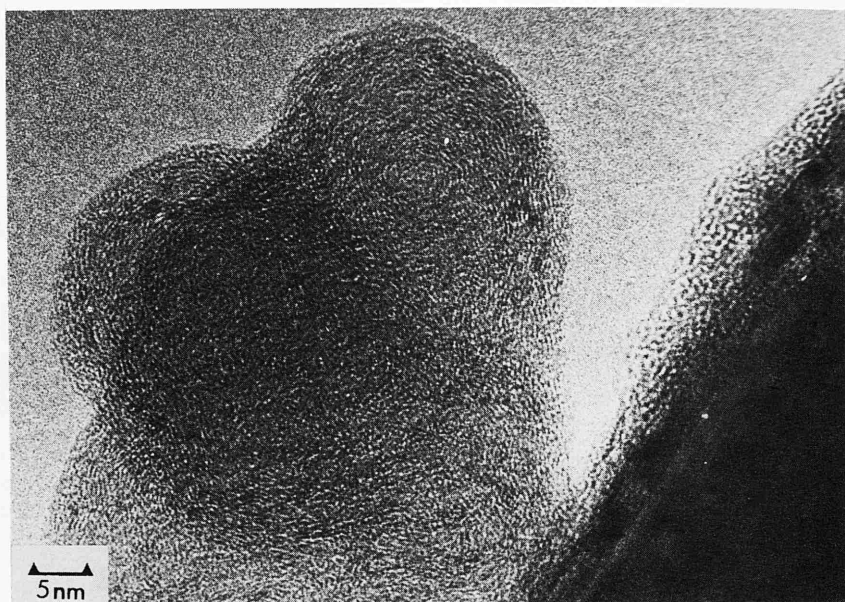


Figure 3.

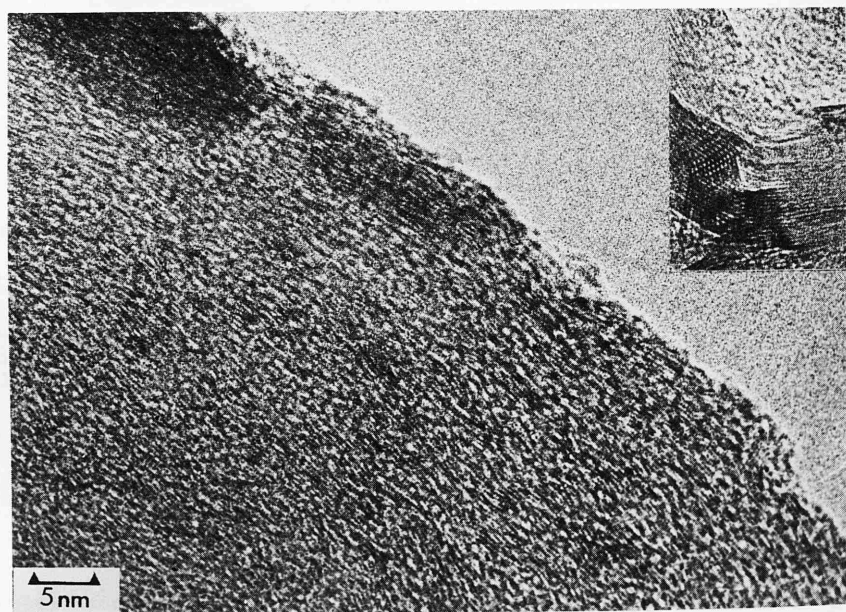


Figure 4.

Inset showing extreme case of ordering.

MICROSTRUCTURAL ANALYSIS OF METALLURGICAL COKES AND INTERCALATED SPECIES

M. J. F. SHEVLIN, J. R. FRYER and T. BAIRD
Chemistry Dept., University of Glasgow, Glasgow G12 8QQ, Scotland

(Received 18 September 1985)

Abstract—The microstructure of metallurgical cokes has been investigated using high resolution electron microscopy (HREM) and complementary techniques. The object of the study was to evaluate the role of recirculating alkali, present in blast furnaces, in the weakening and subsequent degradation of the coke. It is shown that the microstructure of cokes charged to the furnace markedly differs from samples removed from the high temperature regions of the furnace. The feed cokes show a turbostratic structure of short range order, whereas the ex-tuyere cokes show two distinct, additional microstructural species, viz. an intercalated material retaining the turbostratic disorder and an extensively ordered carbon structure. It has also been found that the nature and distribution of the mineral matter inherent in metallurgical cokes is that of randomly dispersed aluminosilicates. Successful replication of the ex-tuyere microstructural forms has been achieved by reaction of the feed coke with potassium carbonate in laboratory experiments. The major factors contributing to the degradation of metallurgical coke are discussed.

Key Words—Metallurgical coke, intercalation, microstructure.

1. INTRODUCTION

The presence of recirculating alkali within the blast furnace is detrimental to the strength of metallurgical coke. The alkali causes degradation of the coke lumps leading to a decrease in the permeability of the coke bed matrix and as a consequence decreases the output and fuel efficiency of the furnace.

The alkali is believed to recirculate according to the mechanism proposed in Fig. 1[1,2]. As well as promoting catalysed gasification of the coke, the alkali is also thought to give rise to potassium intercalated species[3], thus causing expansion of the coke's semi-graphitic layers and resulting in both mechanical and chemical weakening of the structure. Potassium penetration of the microstructure could lead to stresses, caused by differential volume expansion of the carbon lattices—possibly relieved by crack formation (detrimental to coke strength)—with the expansion of the microporous structure making it more accessible to reactive species at the relatively high temperatures involved.

The importance of catalysed gasification in the degradation of metallurgical coke, by the Boudouard and associated reactions, has been discussed by many authors[4-6]. However, although gasification is important in reducing lump size, resulting in the production of coke fines, volumetric breakage of the coke is by far the greatest size reduction factor. It has been shown[7] that volumetric breakage of lump coke remains high if the coke is reacted with alkali at elevated temperatures, even in the absence of carbon monoxide gas.

The purpose of the present study has been to elucidate the nature of the microstructure of both un-

reacted cokes (i.e. feed cokes) and those which have encountered the environment within the blast furnace (i.e. the ex-tuyere cokes). In addition laboratory experiments have been designed to reproduce the structural changes observed within blast furnace cokes. The majority of the work has been carried out using high resolution electron microscopy (HREM) to observe the carbon lattice structure and hence to investigate the possible mechanisms of alkali attack on the microstructure. Other techniques such as chemical analysis, x-ray powder diffraction and thermogravimetric analysis were used to enhance understanding of the degradation process.

2. EXPERIMENTAL

2.1 Materials

The properties of the metallurgical cokes employed in this investigation are described in Table 1. The feed cokes are those as sampled from the blast furnace skip and the ex-tuyere samples those removed from the tuyere zone (Fig. 2) by raking inwards and upwards to a height of around one metre. In all cases samples analysed were representative of the size fractions present on removal. The coke samples were subsequently crushed to a size corresponding to B.S. 72 mesh.

Finely divided potassium carbonate (Analar, anhydrous) was used in the laboratory experiments.

2.2 Apparatus

The apparatus consisted of a horizontal tube furnace. The reaction tube was a silica U-tube of internal diameter 8mm, and was attached to the carrier gas

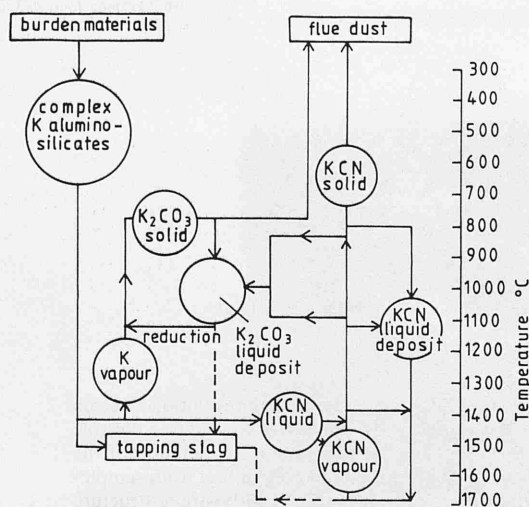


Fig. 1. Proposed mechanism for recirculating alkali within the blast furnace.

cylinder by a glass to metal seal. The furnace temperature was controlled by a Variac rheostat. The temperature was monitored by means of a W/W-26%Re thermocouple mounted in the middle of the furnace hot-zone. The temperature of the sample reacting with the generated potassium vapour was monitored by a second thermocouple attached to the outside of the reaction tube.

2.3 Procedure

Feed coke fines and potassium carbonate were mixed in proportions designed to give the maximum yield of potassium vapour on heating. Mixing was carried out in an agate mortar. The use of potassium carbonate is consistent with the proposed alkali cycle[1]. Coke and carbonate agglomerates were crushed and mixing continued until an even distribution of materials was achieved.

Two grammes of this mixture was weighed into a silica boat and the boat inserted into the reaction tube to a distance corresponding to the centre of the furnace hot-zone. Around 300 mg of feed coke fines were weighed and placed in a second silica boat which was inserted into the reaction tube to a region corresponding to a temperature of around 750–850°C. The reaction tube was subsequently attached to the cylinder of carrier gas, such that the potassium vapour generated from the coke/carbonate mixture at around 1100°C was carried over the second silica boat, containing only feed coke. The carrier gas used was dry Argon (>99.5 vol.% Ar) at a pressure of around 2.5 psi.

The reaction tube was flushed with the carrier gas for a period of two hours, after which the reaction was started. The furnace temperature was raised slowly until a temperature of 1100°C was achieved, and this was maintained until all of the generated potassium vapour from the coke/carbonate mixture had passed downstream over the sample of feed coke. The furnace was then switched off and allowed to cool slowly, while maintaining the gas flow. Once cool the sample of feed coke which had thus been exposed to alkali vapour was removed from the reaction tube, under an inert atmosphere, and transferred to the microscope for examination.

2.4 Microscopy

Samples analysed by HREM were examined on a Jeol 1200 EX microscope operated at an accelerating voltage of 120 KeV. Analysis by scanning electron microscopy (SEM) was carried out using a Philips PSEM 500 microscope fitted with an energy dispersive X-ray analyser (EDXRA), the resolution of the analyser being 10 eV/channel. HREM samples were mounted by dusting finely ground coke (unreacted or reacted) on to microscope grids coated with holey carbon film. Samples analysed by SEM and EDXRA were cut from coke lumps, to around 1 cm², using a

Table 1. Chemical analysis of feed and ex-tuyere cokes

Coke Reference	A	A'	B	B'	C	C'
Feed or Ex-tuyere Coke	Feed	Tuyere	Feed	Tuyere	Feed	Tuyere
Coke Mean Size	49.9	38.0	59.8	47.0	58.4	47.9
Micum Test* M40 Index	85.2	—	91.8	—	90.3	—
M10 Index	6.6	—	4.9	—	4.6	—
Apparent Density g/cm ³	0.93	0.89	0.95	0.95	0.95	0.95
Ash Content**	7.6	14.1	9.5	16.0	9.1	12.5
Volatile Matter***	0.3	1.1	0.8	1.2	1.0	0.9
Ash Composition %						
Na ₂ O	1.9	4.1	0.8	2.7	0.8	1.4
K ₂ O	2.7	12.4	1.8	6.0	2.1	6.1
Ca O	2.1	6.3	2.3	7.5	2.1	7.5
Mg O	1.1	1.8	1.1	3.3	1.1	1.7
Fe ₂ O ₃	15.3	16.0	8.2	9.3	7.3	15.8
Si O ₂	44.7	30.7	52.2	37.4	52.4	36.0
Al ₂ O ₃	29.2	18.9	30.2	26.3	30.3	23.6

*Micum test on plus 60 mm coke.

**Carried out on a dry basis.

***Carried out on a dry ash free basis.

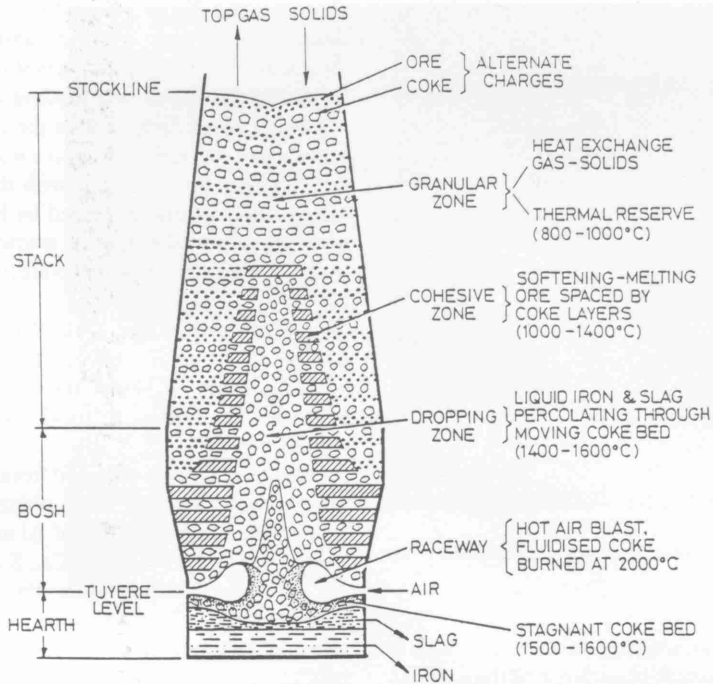


Fig. 2. Schematic diagram of a blast furnace.

diamond saw and mounted uncoated on aluminium stubs.

2.5 X-Ray powder diffraction (XRD)

Samples examined were mounted in the usual manner and scanned through a 2θ range of $5-50^\circ$.

2.6 Thermogravimetric analysis (TGA)

Samples of around 200 mg of coke fines were analysed. The samples were heated in a stream of air in the temperature range of $0-1000^\circ\text{C}$ and a plot of percentage weight loss with temperature recorded.

3. RESULTS

3.1 Comparison of feed and ex-tuyere microstructures

Figure 3 shows a typical SEM picture of the coke samples. Very little difference is observed between the feed and ex-tuyere cokes at this resolution, although on average the feed cokes have a greater degree of macroporosity than the ex-tuyere samples.

Figures 4 and 5 show examples of feed cokes of similar rank, as imaged by HREM. Both exhibit a typical non-graphitised carbon structure. The inter-

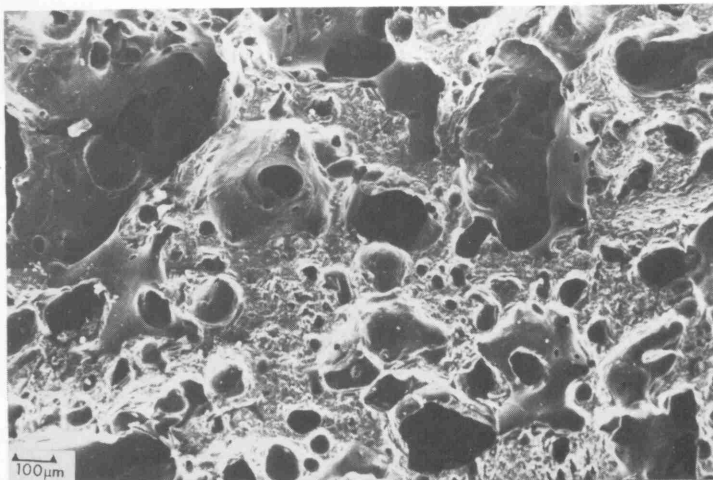


Fig. 3. Typical SEM of coke samples.

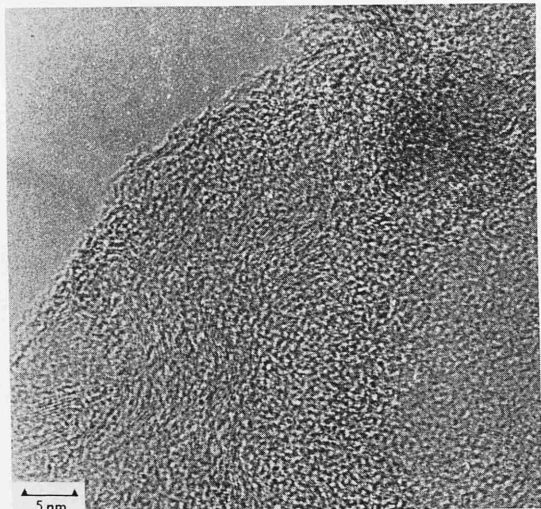


Fig. 4. HREM showing carbon lattice structure of feed coke.

planar spacing is of an average of 0.34 nm, with a large degree of turbostratic disorder, and the samples show very little 0.335 nm (0002) lattice development.

Also apparent in these samples are areas of highly ordered crystalline material (arrowed, Fig. 5), randomly dispersed throughout, with interplanar spacings ranging from 0.32–1.8 nm. Chemical analysis (Table 1) suggests that this crystalline material is mineral matter inherent in the coke from its' formation. EDXRA microprobe readouts from the feed coke show large amounts of Al and Si, with some Ca, S and Fe present. Very little potassium is found in the feed coke samples. When the probe is used to give

characteristic X-ray elemental maps of the sample, discrete areas high in Al, Si and Ca are revealed. Backscattered electron images show these regions to be distinct from the surrounding coke mass.

Powder X-ray diffraction of the coke reveals a small broad peak, corresponding to a wide range of carbon lattice spacings, consistent with the turbostratic nature of the material observed by HREM. Scattering of the X-rays by the mineral matter is not strong due to the concentration of this material in the coke sample.

Figure 6 shows one area of ex-tuyere coke. Although the random, "onion" type, carbon structure of the feed coke (0.34 nm) is still apparent, expansion of the carbon lattices to (0.47 nm) is now observed in some areas.

EDXRA readouts obtained from the ex-tuyere coke samples are similar to those obtained from the feed coke. High concentrations of Al and Si are observed along with the presence of Ca, S and Fe. However, the ex-tuyere samples show the presence of large concentrations of potassium in contrast to the feed cokes, a fact confirmed by standard chemical analysis.

Figure 7 is an example of another type of microstructure found in the ex-tuyere samples—but not present in the feed cokes. These areas contain extensively ordered (0002) carbon lattices, with spacings of an average of 0.34 nm. There is no significant expansion of the layer planes within the regions in which ordering has occurred. Also observed in the ex-tuyere samples are areas of highly ordered crystalline material corresponding to the inherent mineral matter.

Examination of the ex-tuyere samples by X-ray

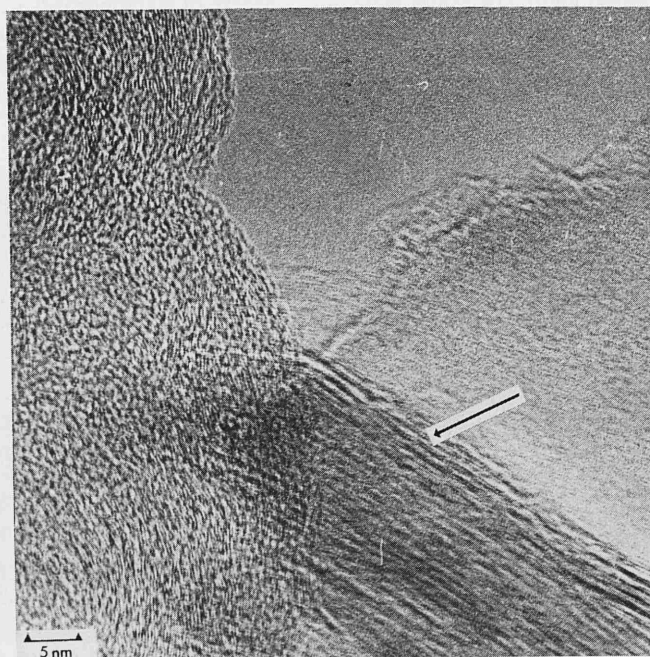


Fig. 5. HREM showing carbon lattice structure of feed coke and inherent mineral matter (arrowed).

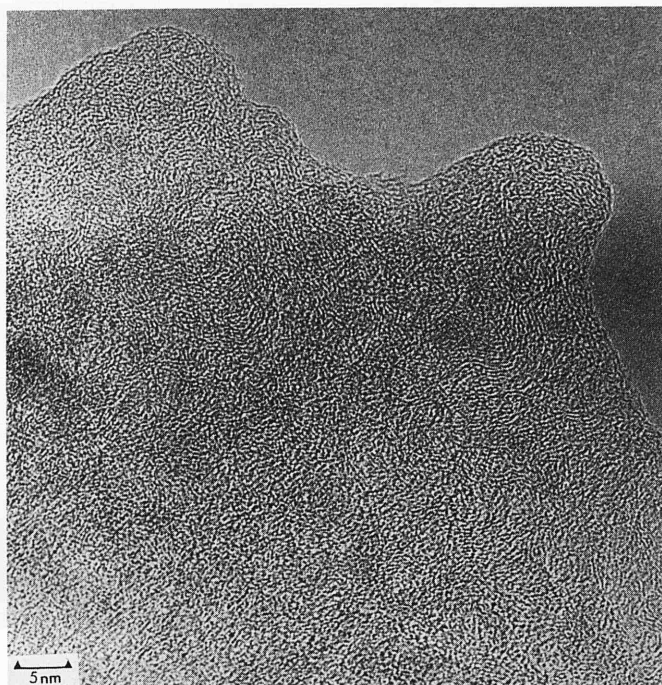


Fig. 6. HREM of ex-tuyere coke showing expanded carbon lattices (0.47 nm).

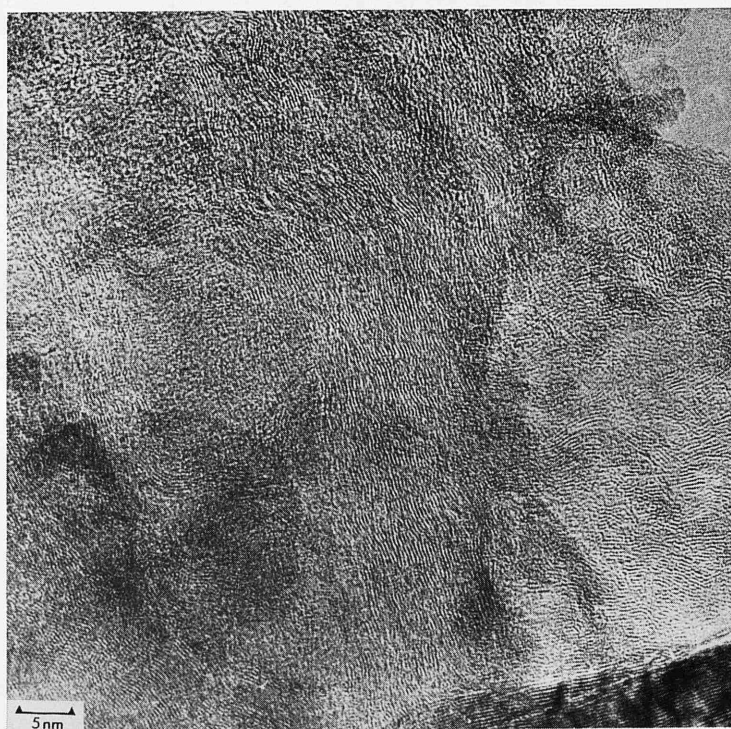


Fig. 7. HREM of ex-tuyere coke showing extensive ordering of the carbon microstructure.

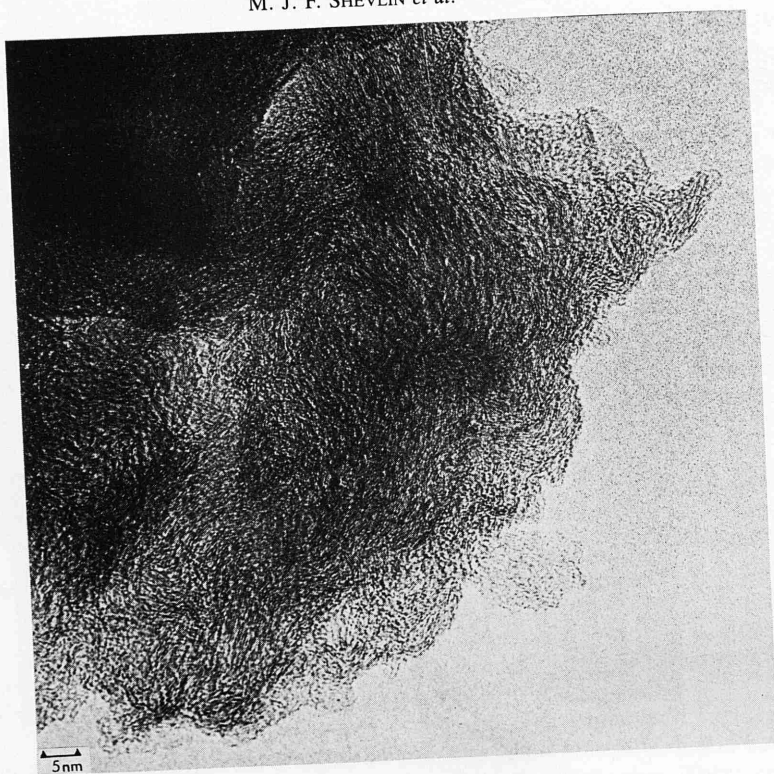


Fig. 8. HREM of feed coke reacted with potassium carbonate. Micrograph shows presence of intercalated material (expanded carbon lattices, 0.45 nm).

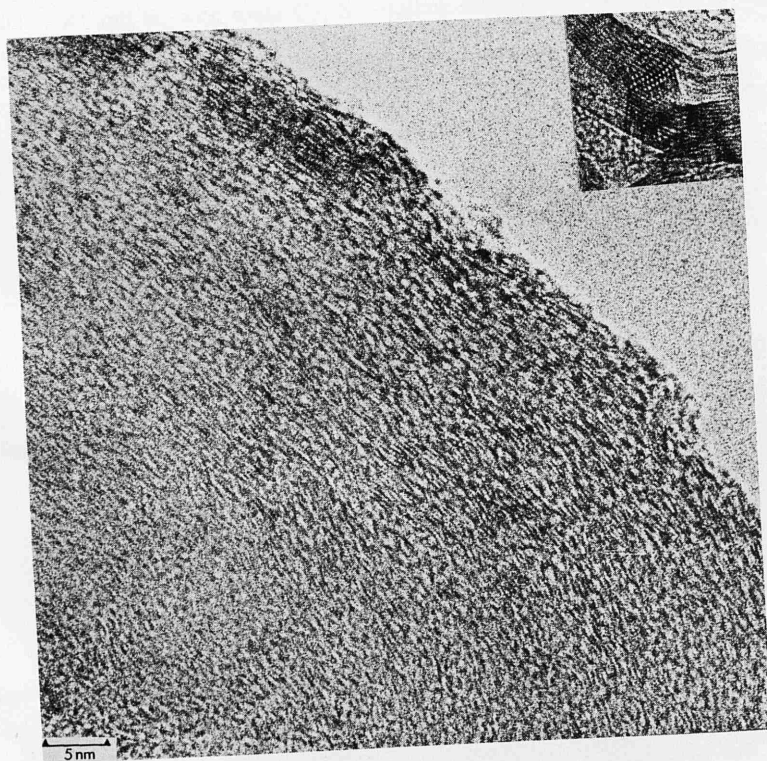


Fig. 9. HREM of reacted feed coke showing extensive ordering of microstructure. Inset shows an extreme case of ordering and a rotational Moiré pattern.

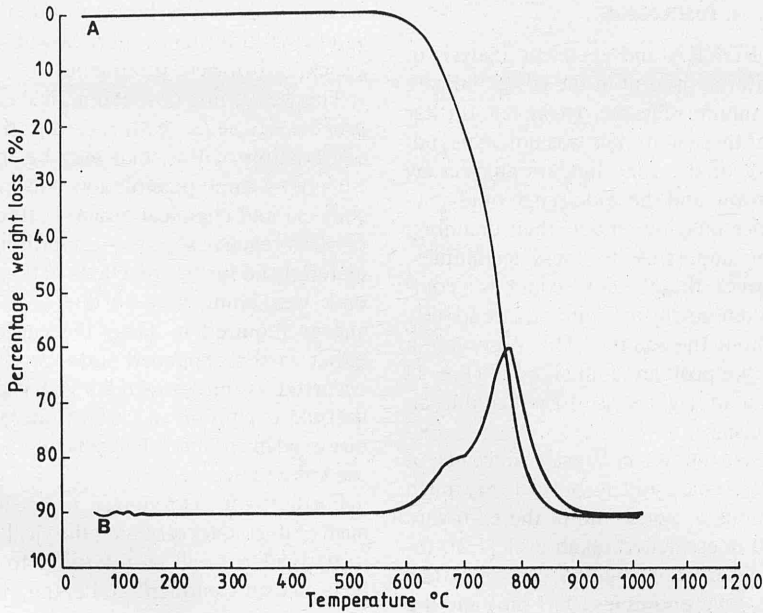


Fig. 10. Thermogravimetric trace from feed coke. Trace A indicates % weight loss with temperature. Trace B indicates rate of weight loss.

powder diffraction reveals a much sharper, more intense peak for the carbon-carbon interplanar spacings. This is indicative of a greater number of lattices within a smaller range of spacings.

3.2 Laboratory experiments

HREM examination of the feed coke samples reacted with potassium carbonate in the laboratory experiments shows the presence of all the microstructural forms found in the ex-tuyere coke samples. Areas of expanded (around 0.45 nm) disordered carbon lattices are observed Fig. 8 along with areas in which

the microstructure has been extensively ordered. An example of the latter structural form is illustrated in Fig. 9, with interplanar spacings of 0.34 nm. The reacted feed coke samples when analysed by XRD give traces similar to those of the ex-tuyere morphology.

Thermogravimetric analysis shows a double peak (Fig. 10) in the case of the feed cokes, indicative of the presence of two types of carbon. The ex-tuyere samples show catalytic gasification as manifested by a distinct reduction in the temperature at which combustion commences (Fig. 11).

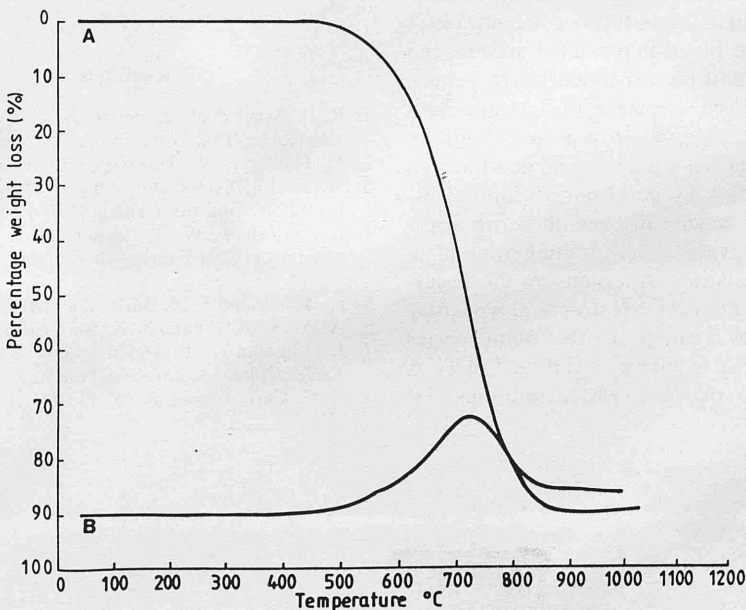


Fig. 11. Thermogravimetric trace from ex-tuyere coke. Trace A indicates % weight loss with temperature. Trace B indicates rate of weight loss.

4. DISCUSSION

The results of EDXRA and chemical analysis of the crystalline material present in the cokes indicate the presence of aluminosilicates. However, further characterisation of these materials was not achieved; the opaque nature of the coke hinders analysis by infrared spectroscopy, and the wide range of *d*-spacings found by lattice imaging renders their unambiguous identification impossible by these techniques. It is evident, however, that the coke contains a complex mixture of aluminosilicate minerals, randomly dispersed throughout the sample. This observation is consistent with the postulated alkali cycle (Fig. 1) in which mineral matter gives rise to potassium vapour within the furnace.

Elemental analysis shows negligible amounts of potassium in the feed cokes and in contrast very much higher concentrations of potassium in the ex-tuyere samples. The well documented alkali cycle [1,2], together with the observed expanded carbon lattice structure in the ex-tuyere samples (0.47 nm) and the higher levels of potassium in the samples are all consistent with the formation of an intercalated compound. Potassium intercalates have been extensively reported in the chemistry of graphite [8]. The (0002) lattice expansion observed in the cokes is not as extensive as would be expected for a species such as C_8K , $C_{16}K$ or $C_{24}K$ but may indicate a residue compound. The formation of these residue compounds is likely to occur during the period of removal from the furnace to insertion into the microscope. The degradation of such reactive intercalated materials has been previously reported [8]. XRD analysis does not reveal the presence of the intercalate due to the weak signal from the relatively low concentration of intercalated material.

The occurrence of the two additional microstructural forms observed in the ex-tuyere coke may result from the formation of an intercalated species and subsequent collapse of the expanded lattice planes, to the original feed coke spacing of 0.34 nm. This phenomenon has been previously reported for graphite [8]. In this mechanism it is envisaged that the feed coke undergoes attack by potassium to form a disordered intercalate which subsequently forms a residue compound of greater order resulting from single or repeated intercalation. Alternatively the occurrence of the two additional microstructural types may be explained by the creation of two carbon species during the mesophase in coke production. The TGA analysis of the feed cokes is consistent with this pos-

tulate. These two carbon types can then be envisaged as having differing properties with respect to alkali attack and/or heat treatment.

The weakening of metallurgical coke is a complex process. However, with regard to the present study, degradation of the coke may be thought of as occurring by three possible mechanisms. First, by mechanical and chemical attack—either by alkali and/or other reactive species—on forming an intercalated material and further reactions of this intercalate. Second, weakening may be due to a decrease in the energy required to shear the carbon layer planes, either in the expanded state or after ordering has occurred. A third possibility is that differences in the thermal expansion of carbon microstructural forms observed may establish localised stresses that weaken the coke structure.

Further work is required to elucidate the mechanism of degradation of metallurgical coke more fully. In particular it will be necessary to separate the effects of heat treatment and alkali attack.

5. CONCLUSIONS

Metallurgical coke, as formed, has a complicated microstructure containing turbostratically disordered carbon units and complex mixtures of aluminosilicate material. Passage through the blast furnace causes morphological changes in carbon structure creating both an ordering of carbon layer planes and the formation of intercalated species. The development of these two new, distinct morphologies is thought to be influenced by alkali recirculating within the blast furnace.

Acknowledgements—The authors wish to acknowledge the gratitude to the National Coal Board for their support this work.

REFERENCES

1. R. R. Adair *et al.*, ECSC Research Contact Committee and Round Table Conference, Luxembourg (1979).
2. M. Hatano *et al.*, *Trans. ISIJ* **20**, 593 (1980).
3. W. K. Lu, Symposium held at McMaster University, Hamilton, Ontario, Canada (1980).
4. J. C. Botham, W. R. Leeder and D. A. Reeve, Symposium on Coal Evaluation, Calgary, Alberta, Canada (1974).
5. H. Marsh and I. Mochida, *Fuel* **60**, 231 (1981).
6. A. A. Adjorlolo and Y. K. Rao, *Carbon* **22**, 173 (1984).
7. J. Goleczka, J. Tucker and G. Everitt, ECSC Round Table, Coke, Luxembourg (1983).
8. K. E. Carr, *Carbon* **8**, 155 (1970).



VOLUME II

MICROSTRUCTURE OF METALLURGICAL COKES

BY

MARTIN JOHN FRANCIS SHEVLIN

being a thesis submitted for the degree of Doctor of
Philosophy in the Chemistry Department of the University of
Glasgow.

MAY 1987

VOLUME I Text & Figures

VOLUME II Plates

© MARTIN J.F. SHEVLIN 28th MAY 1987

CONTENTS

<u>PLATE</u>		<u>Page Vol. I</u>
5 - 8	SEM of Feed Cokes + EDXRA	159
9	Artefacts Produced when Cutting Coke	159
10 - 16	Elemental Distributions in Feed Cokes	160
17 - 19	LREM of Feed Cokes	161
20 - 24	HREM of Feed Cokes	161
25 - 27	Crystalline Mineral Matter	161
28 - 30	SEM of Ex-tuyere Cokes + EDXRA	164
31 - 33	LREM of Ex-tuyere Cokes	165
34 - 39	HREM of Ex-tuyere Cokes	166
40 - 42	SEM of Reacted Feed Cokes + EDXRA	171
43 & 44	LREM of Reacted Feed Cokes	173
45 - 53	HREM of Reacted Feed Cokes	173
54 - 57	SEM / LREM of Heat Treated Feed Cokes	178
58 - 60	HREM of Heat Treated Feed Cokes	181
61 - 63	SEM of Feed Cokes Reacted Below Carbonisation Temperature	184
64 - 69	HREM of Feed Cokes Reacted Below Carbonisation Temperature	189
70 - 72	SEM of Reacted Ex-tuyere Cokes	191
73 - 75	HREM of Reacted Ex-tuyere Cokes	192
76	BEI of Feed Cokes	201
77	BEI of Ex-tuyere Cokes	202

PLATE 5

SEM of Feed Coke Material.

Magnification = X 380

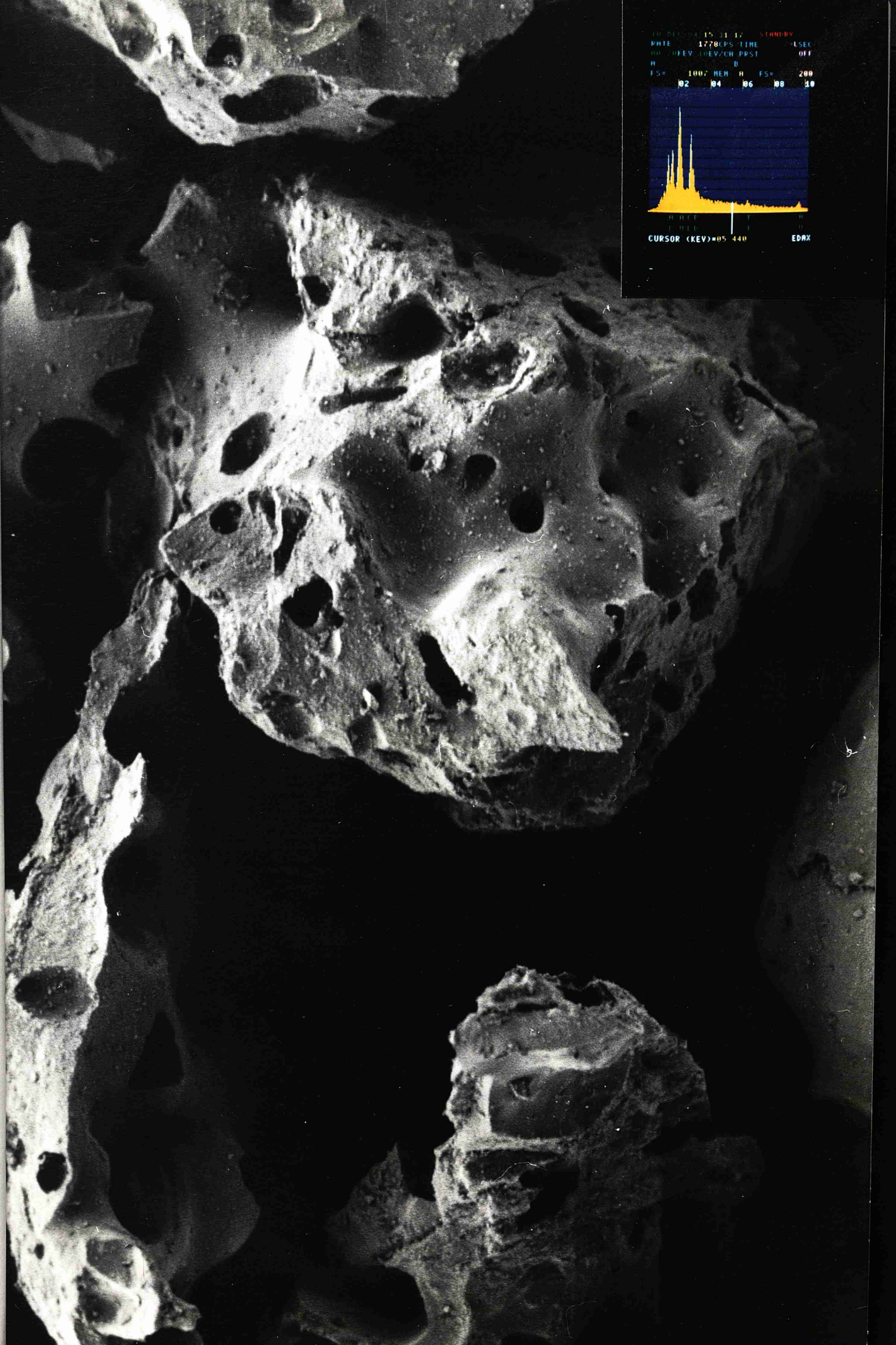


PLATE 6

SEM of Feed Coke Material.

Magnification = X 172

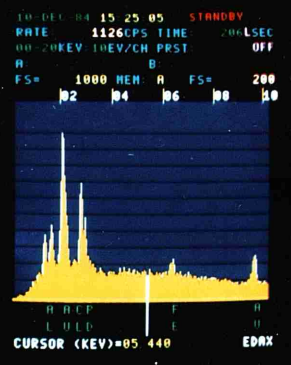
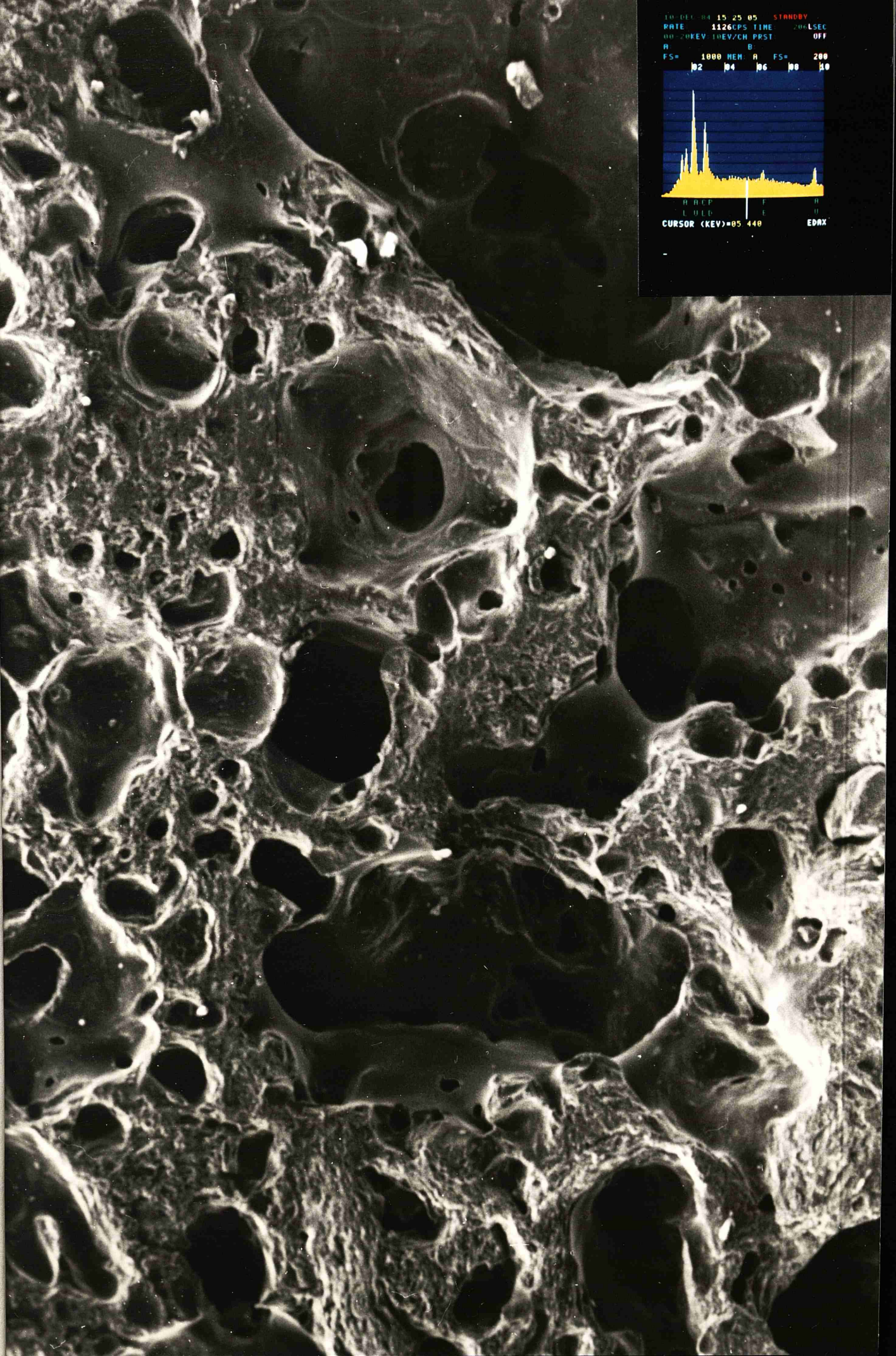
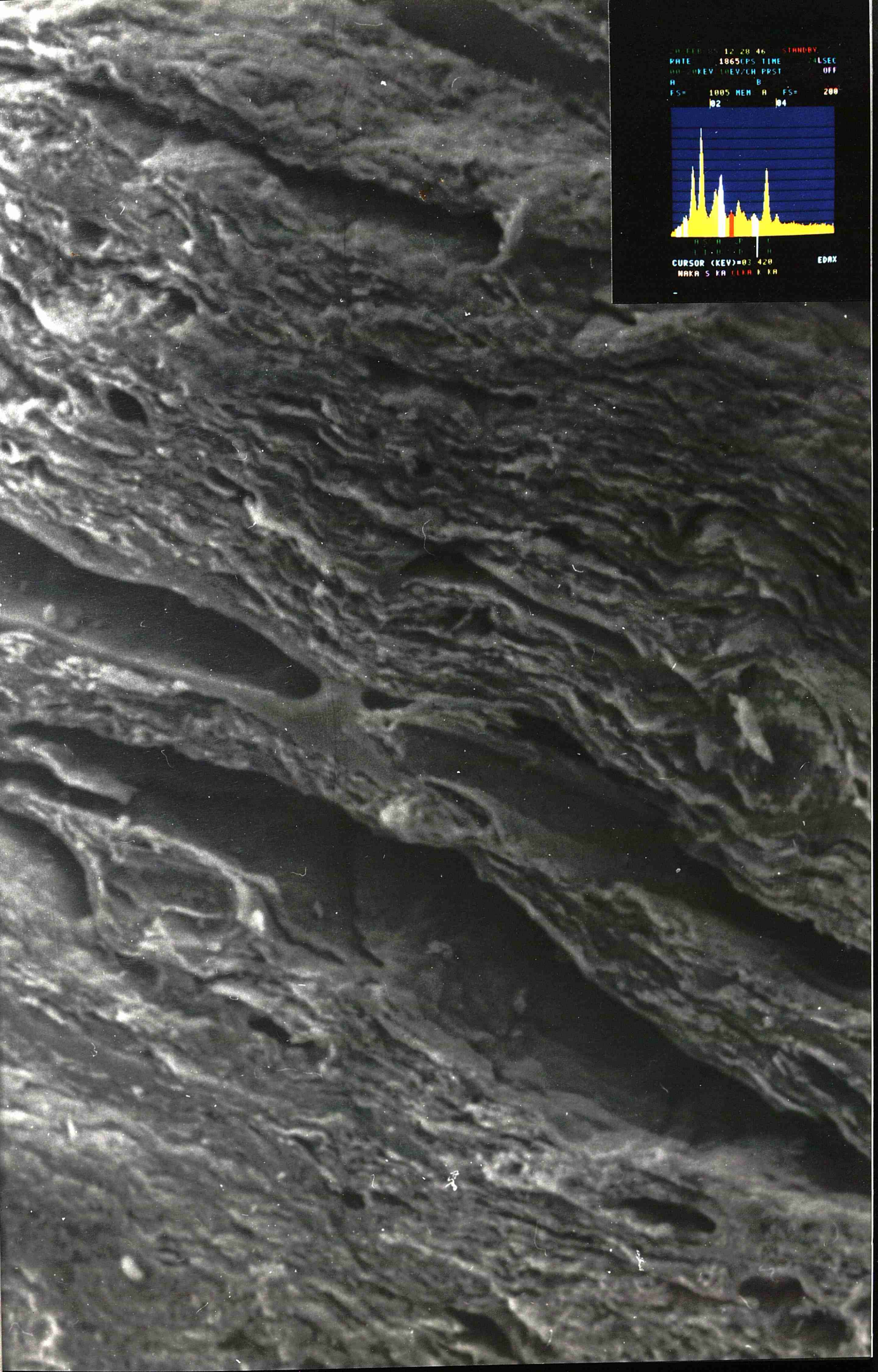


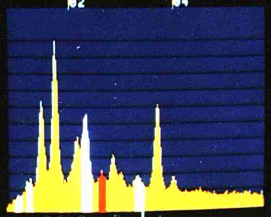
PLATE 7

SEM of Feed Coke Material.

Magnification = X 1568



DATE 12-20-46 STANLEY
PATE 1865 PPS TIME 04 SEC
H 0 KEV 1 KEV/CH PPST OFF
H B
FS 1005 MEM H FS 200
02 04



CURSOR (KEV)=03.420
MAKA S KA CLKA R KA
EDAX

PLATE 8

SEM of Feed Coke Material.

Magnification = X 1568

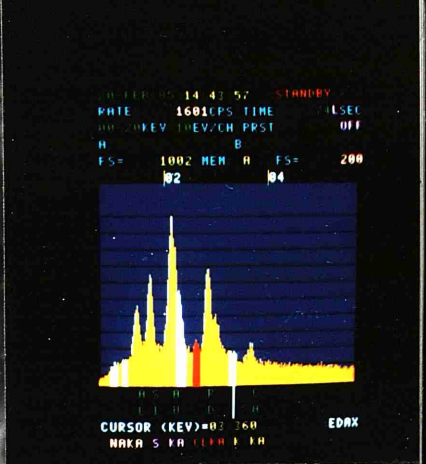


PLATE 9

SEM Showing Effect of Diamond Saw on Coke Structure.

Magnification = X 384



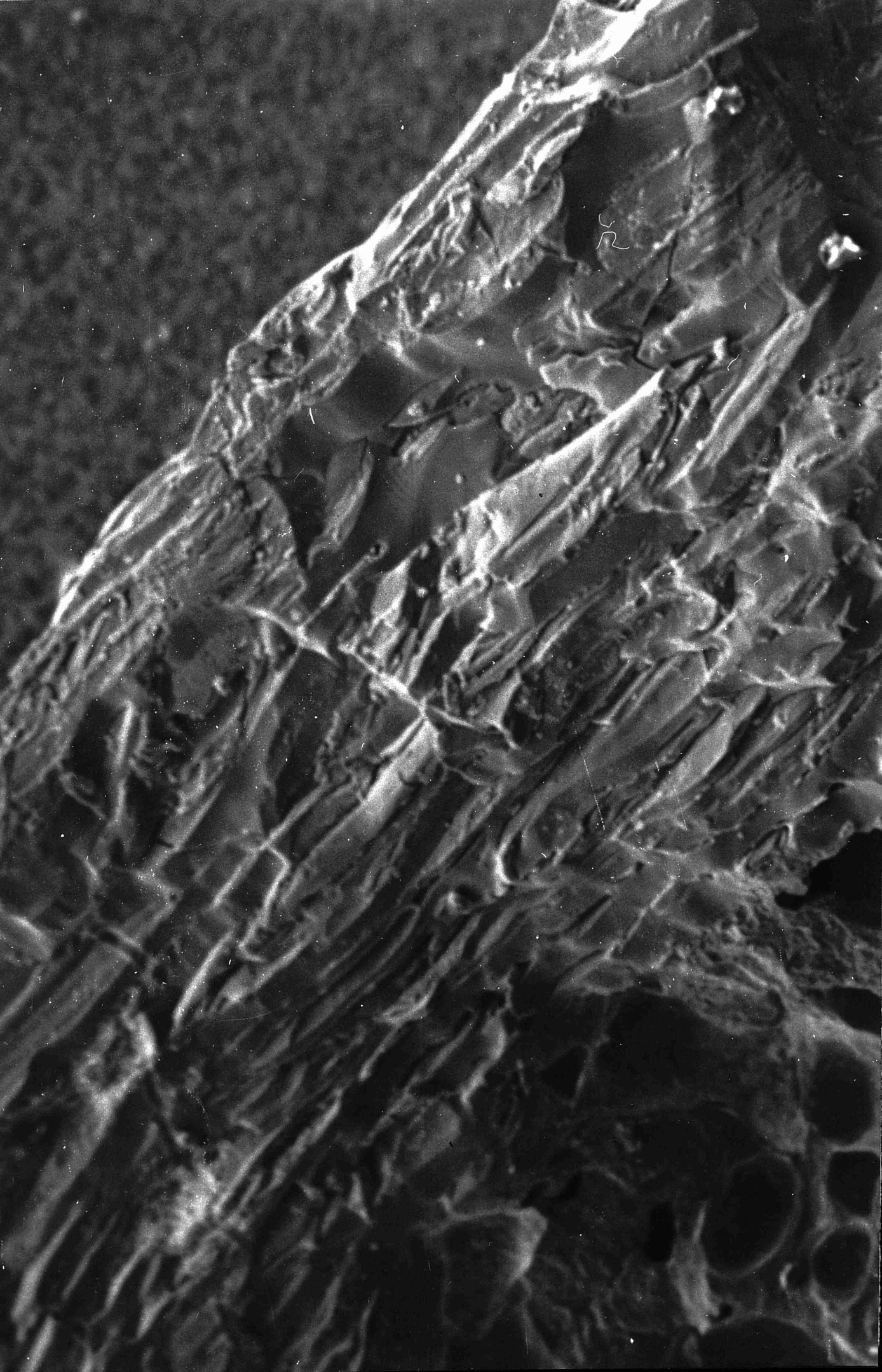




PLATE 10

Magnification = X 640

Distribution of Sulphur in Feed Coke.



PLATE 11

Magnification = X 640

Distribution of Chlorine in Feed Coke.



PLATE 12

Magnification = X 640

Distribution of Potassium in Feed Coke.

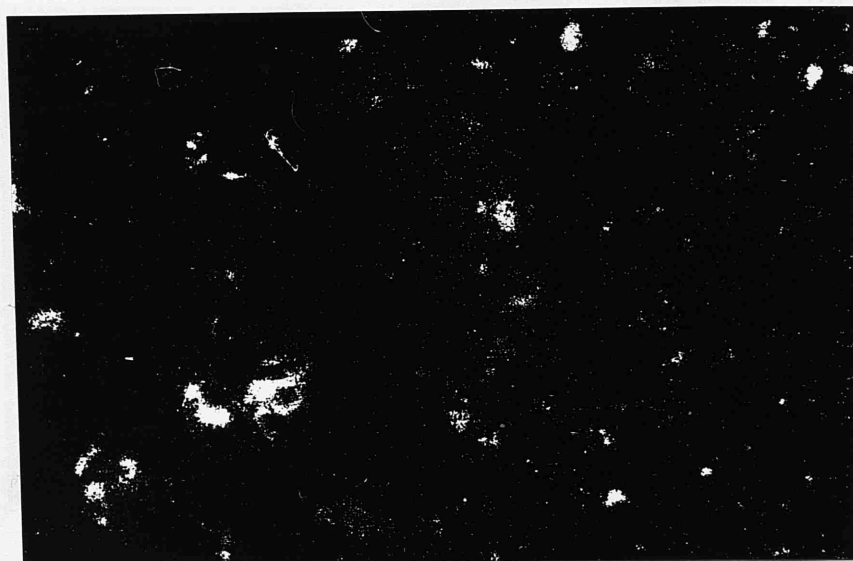


PLATE 13

Magnification = X 640

Distribution of Iron in Feed Coke.

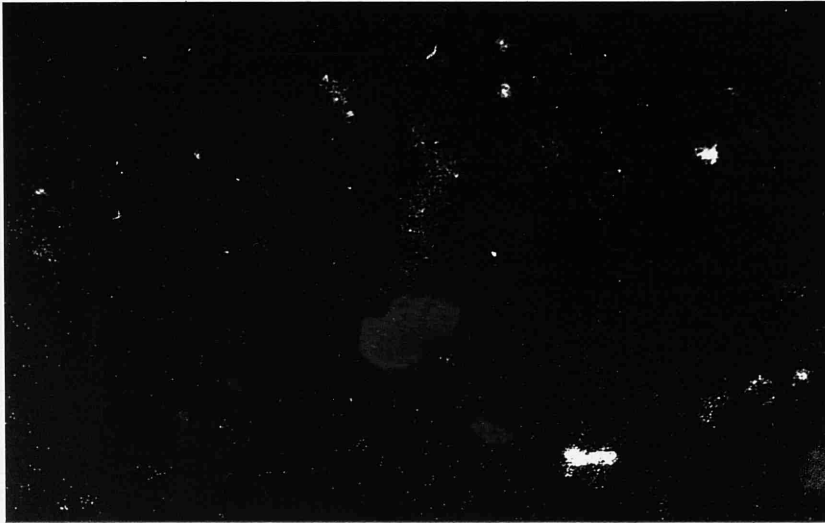


PLATE 14

Magnification = X 640

Distribution of Aluminium in Feed Coke.



PLATE 15

Magnification = X 640

Distribution of Silicon in Feed Coke.

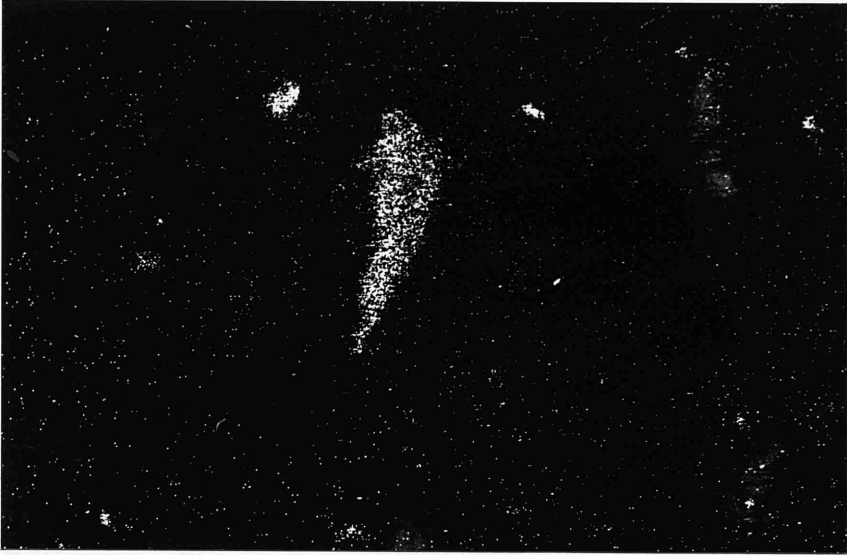


PLATE 16

Magnification = X 640

Distribution of Calcium in Feed Coke.

PLATE 17

Low Resolution Electron Micrograph of Feed Coke.

Magnification = X 735300

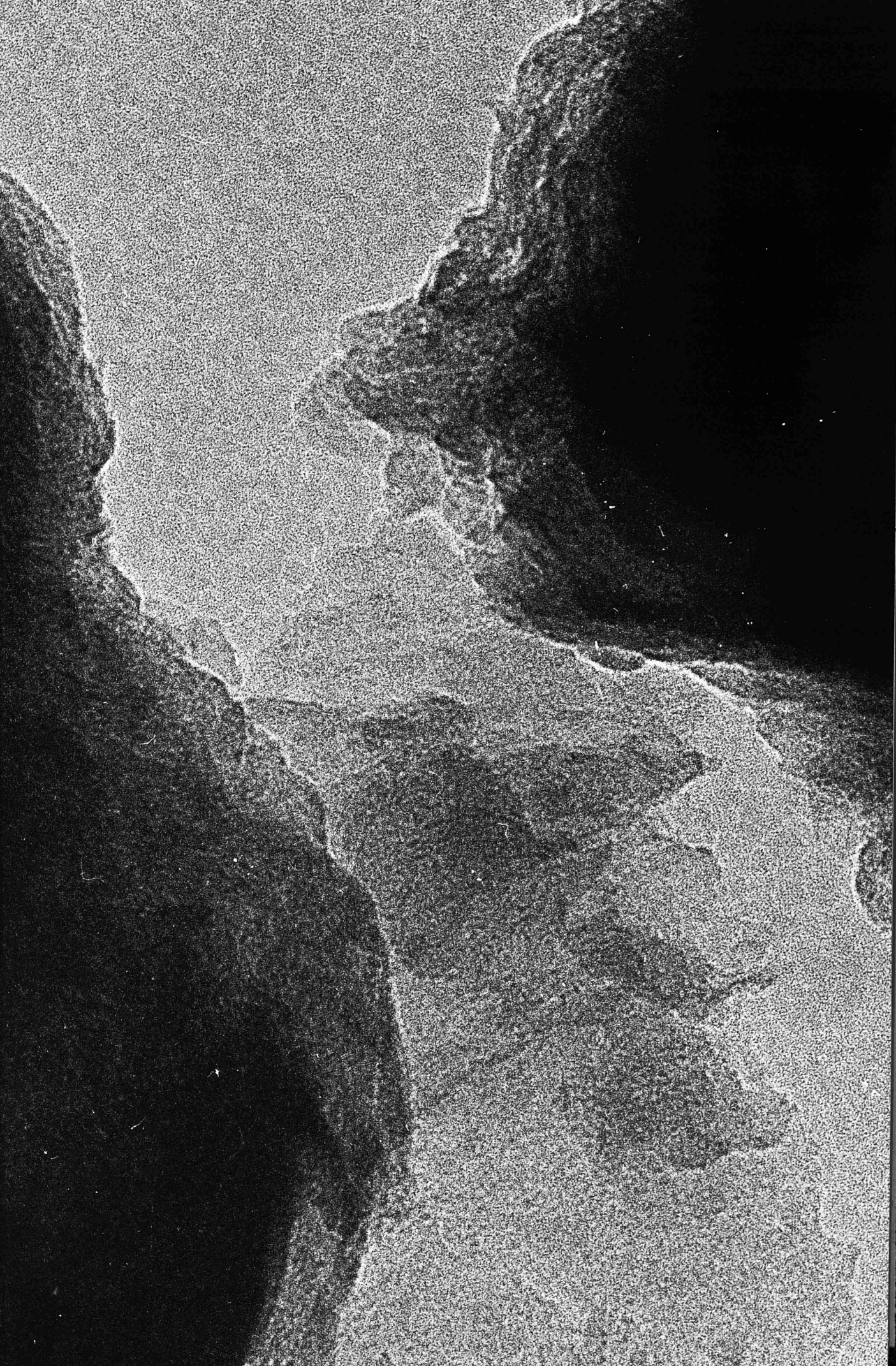


PLATE 18

Low Resolution Electron Micrograph of Feed Coke.

Magnification = X 86355



PLATE 19

Low Resolution Electron Micrograph of Feed Coke.

Magnification = X 353400

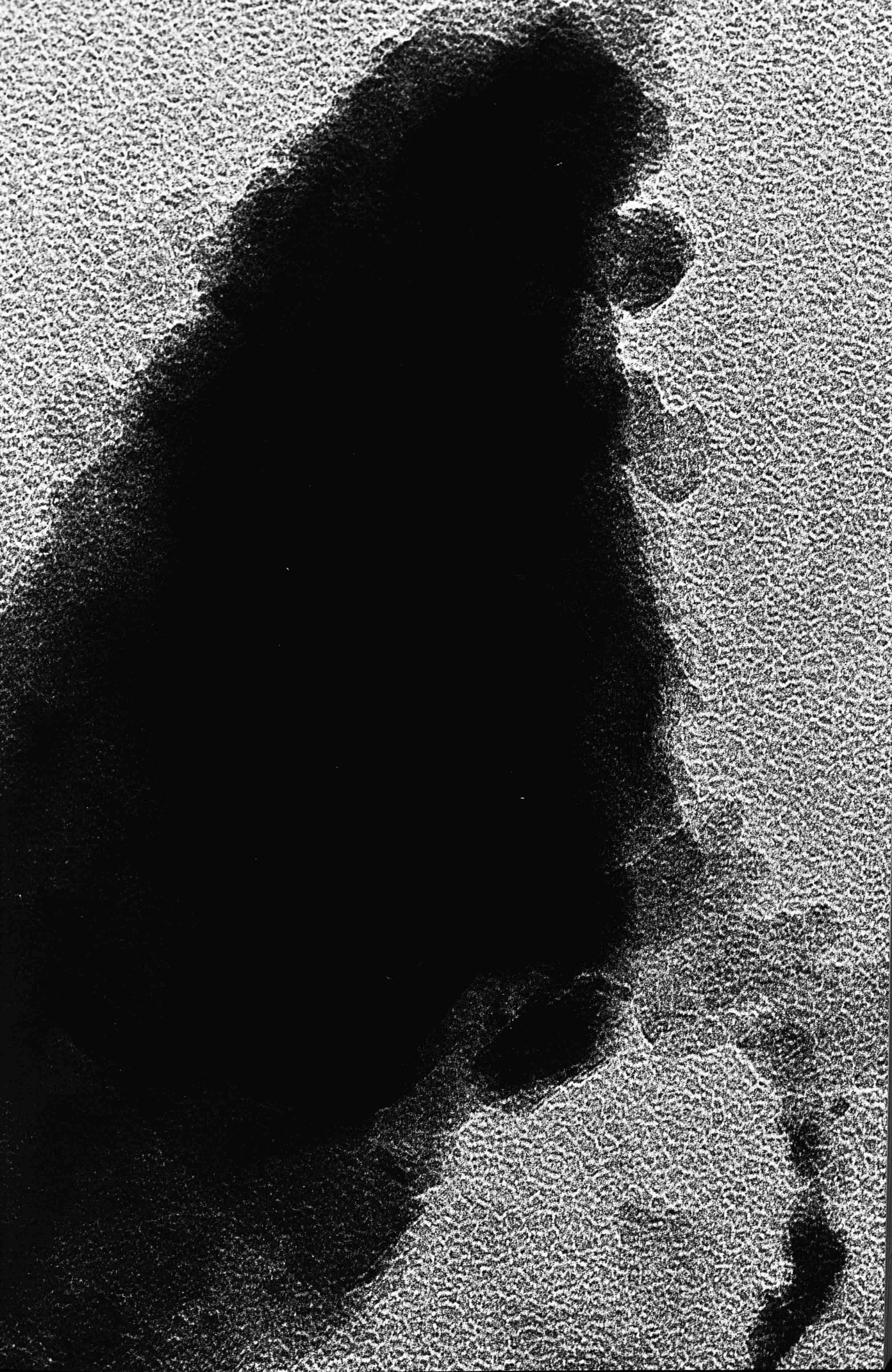


PLATE 20

High Resolution Electron Micrograph of Feed Coke.

Magnification = X 3778050

PLATE 21

High Resolution Electron Micrograph of Feed Coke.

Magnification = X 4298700

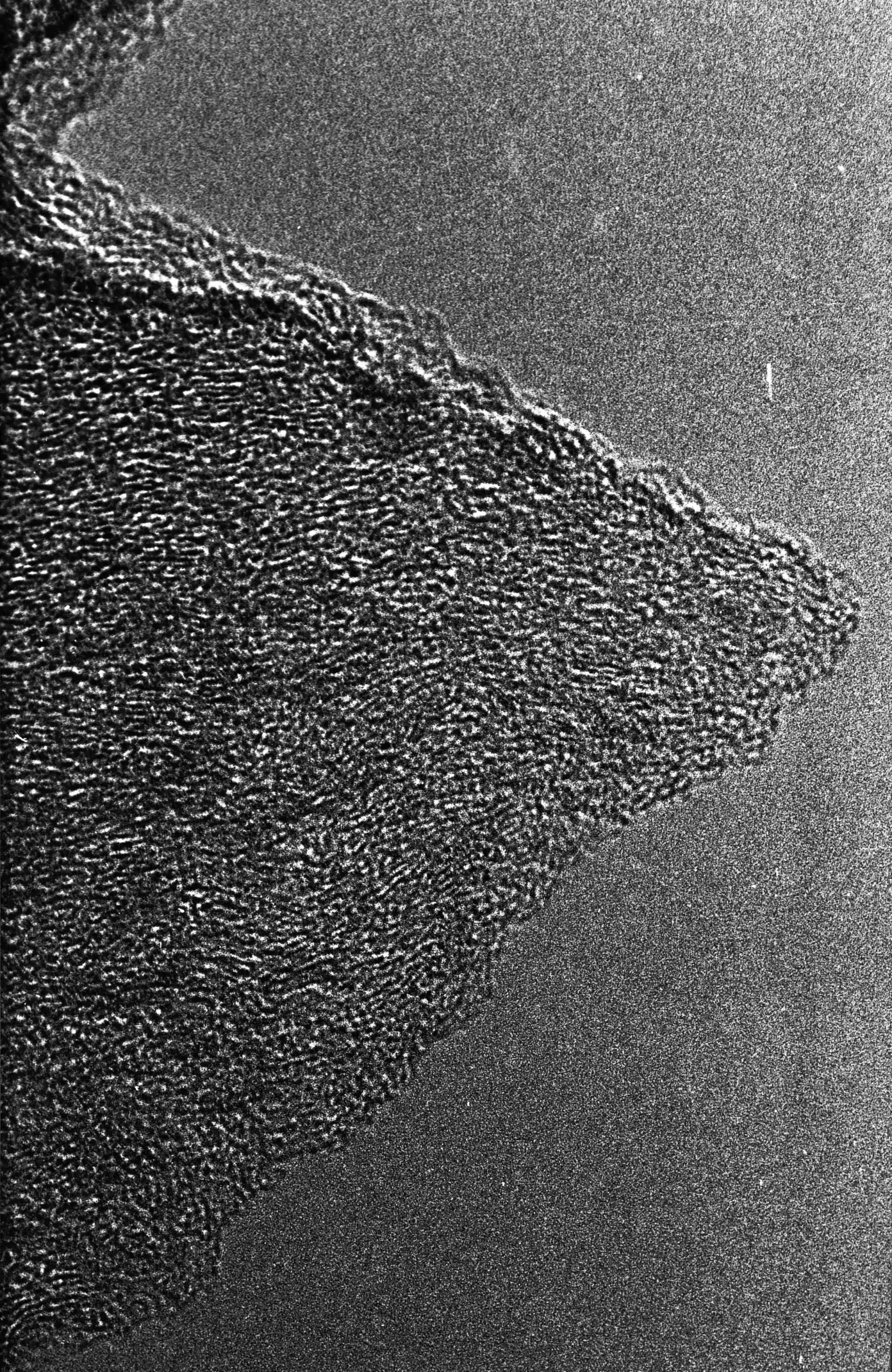


PLATE 22

High Resolution Electron Micrograph of Feed Coke, Showing
Random Nature of the Carbon Matrix.

Magnification = X 4298700

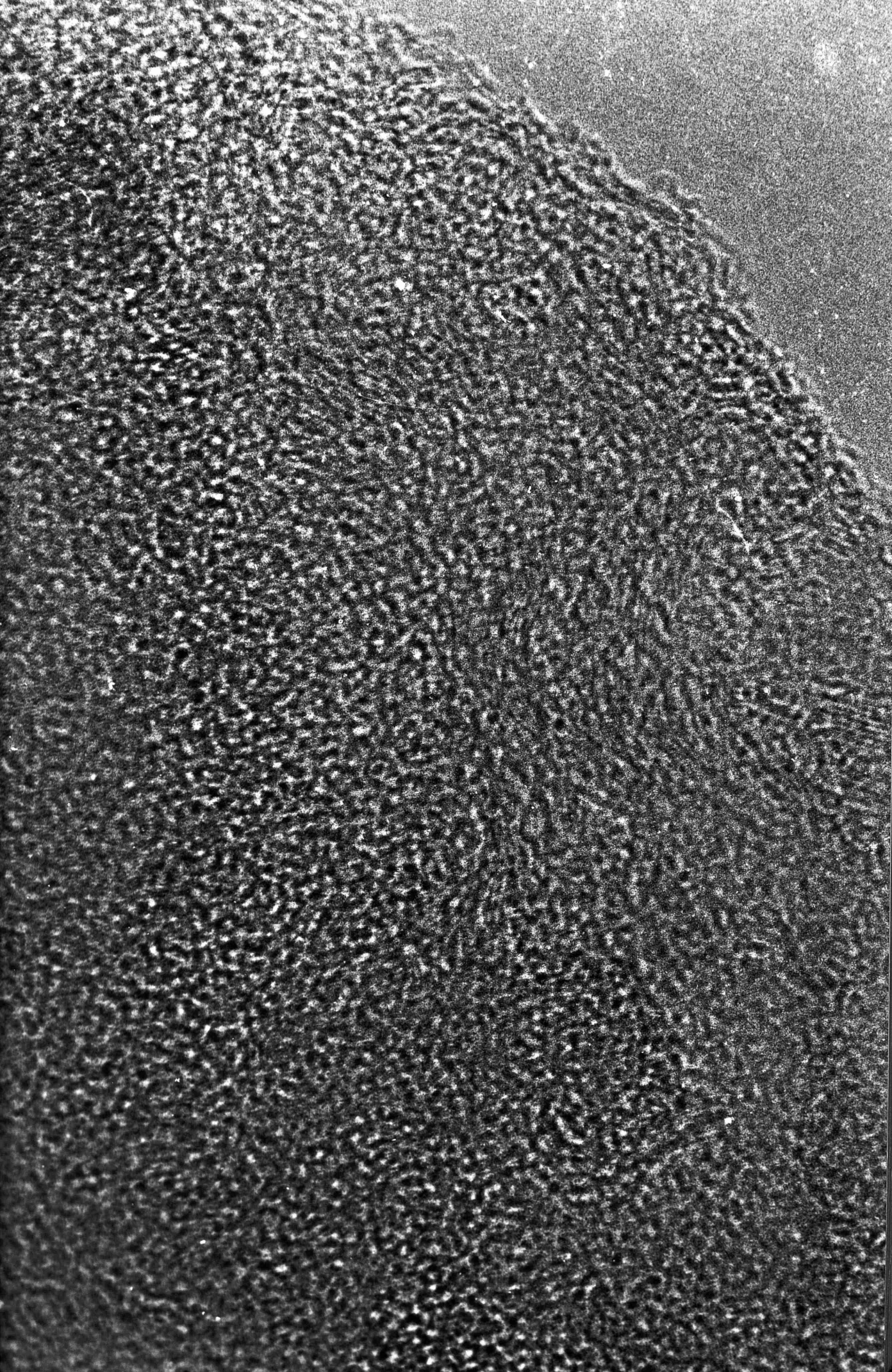


PLATE 23

High Resolution Electron Micrograph of Feed Coke, Showing
Random Carbon Structure.

Magnification = X 4298700

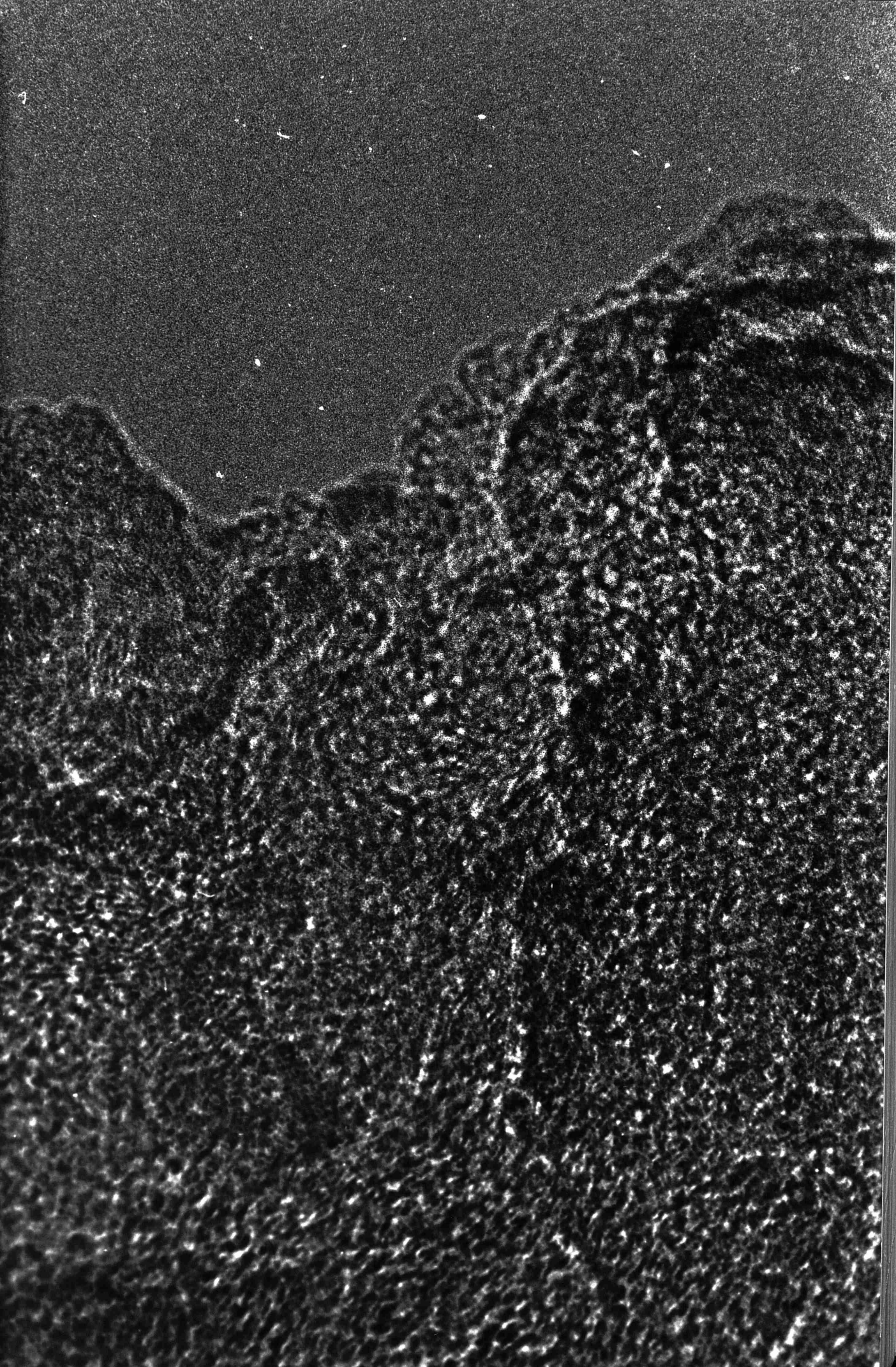


PLATE 24

High Resolution Electron Micrograph of Feed Coke.

Magnification = X 3404250

PLATE 25

HREM Showing Crystalline Mineral Matter.

Magnification = X 2856900



PLATE 26

HREM Showing Inherent Mineral Matter in Coke.

Magnification = X 4343400



PLATE 27

HREM of Feed Coke Showing Inherent Mineral Matter.

Magnification = X 4325400

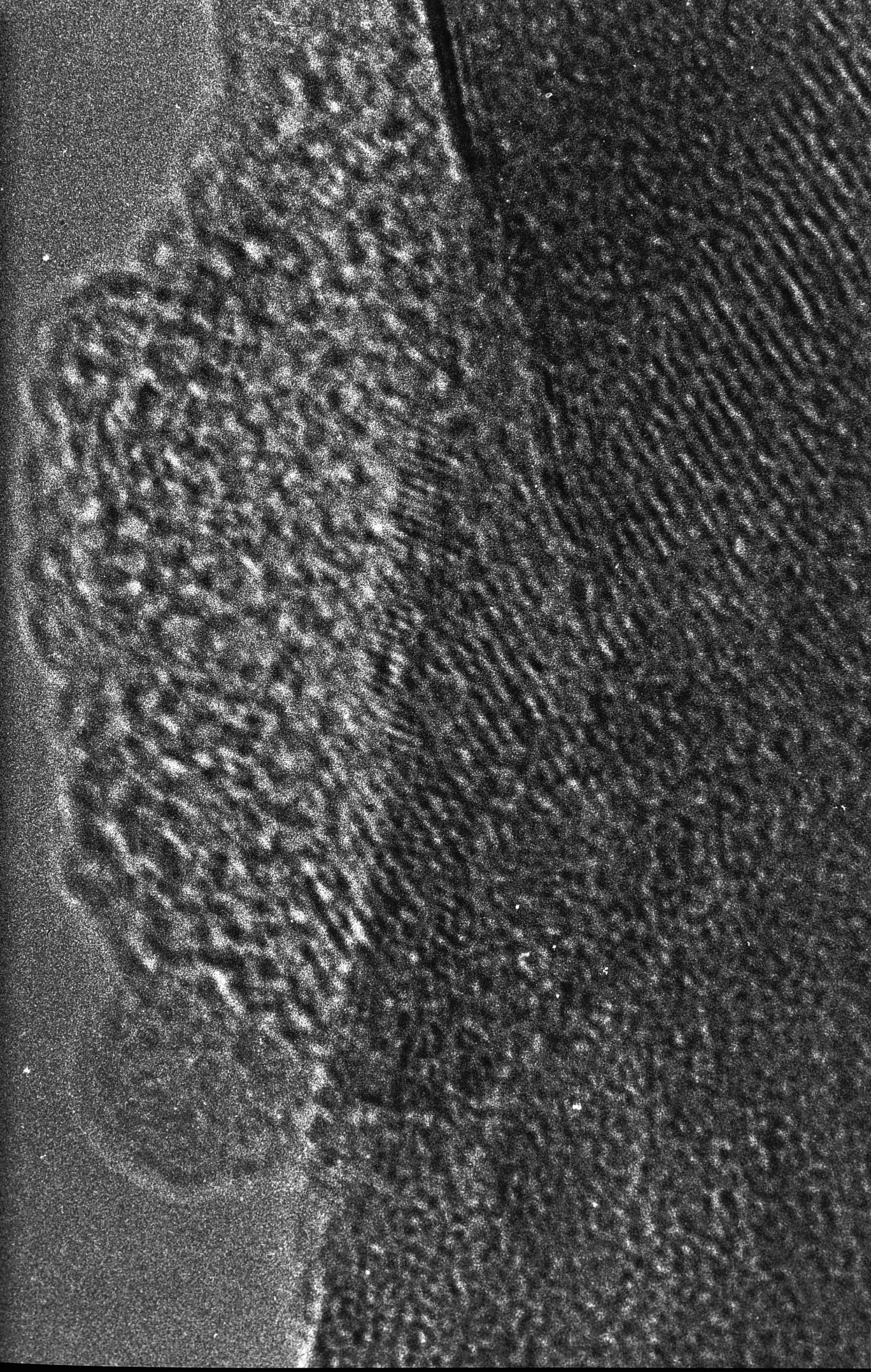


PLATE 28

SEM of Ex-Tuyere Coke.

Magnification = X 1984

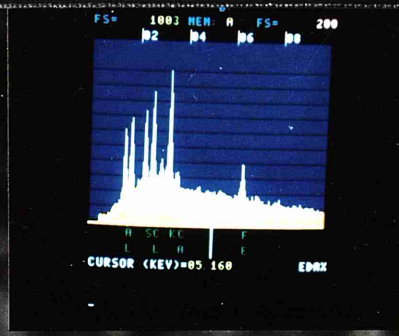
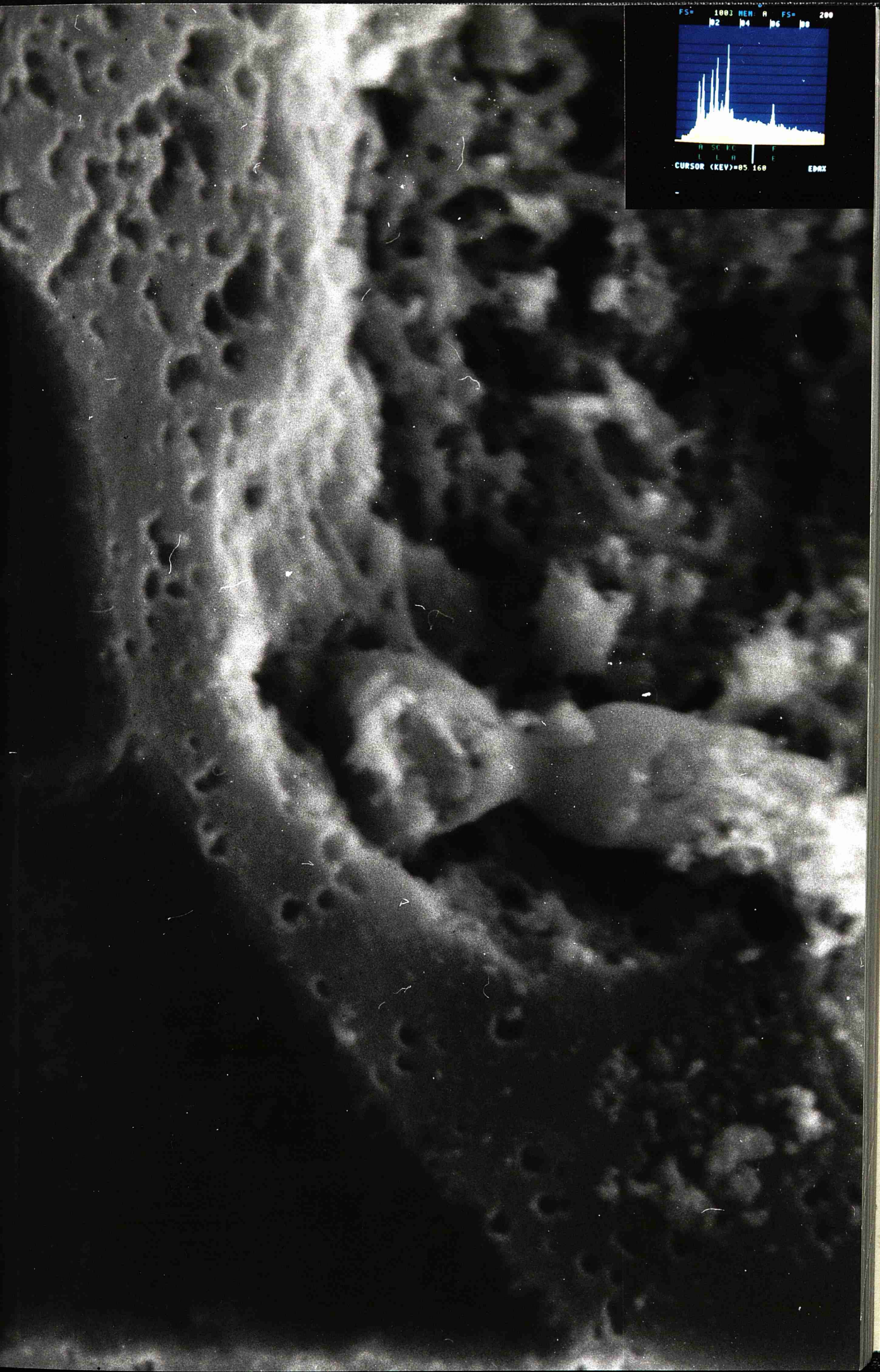


PLATE 29

SEM of Ex-Tuyere Coke Showing Carbon Gasification.

Magnification = X 808

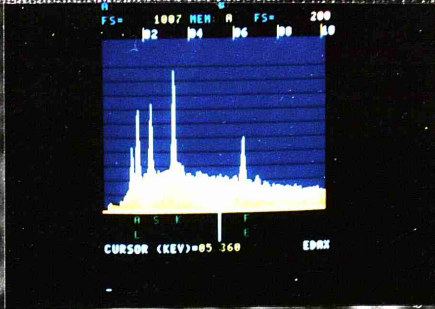
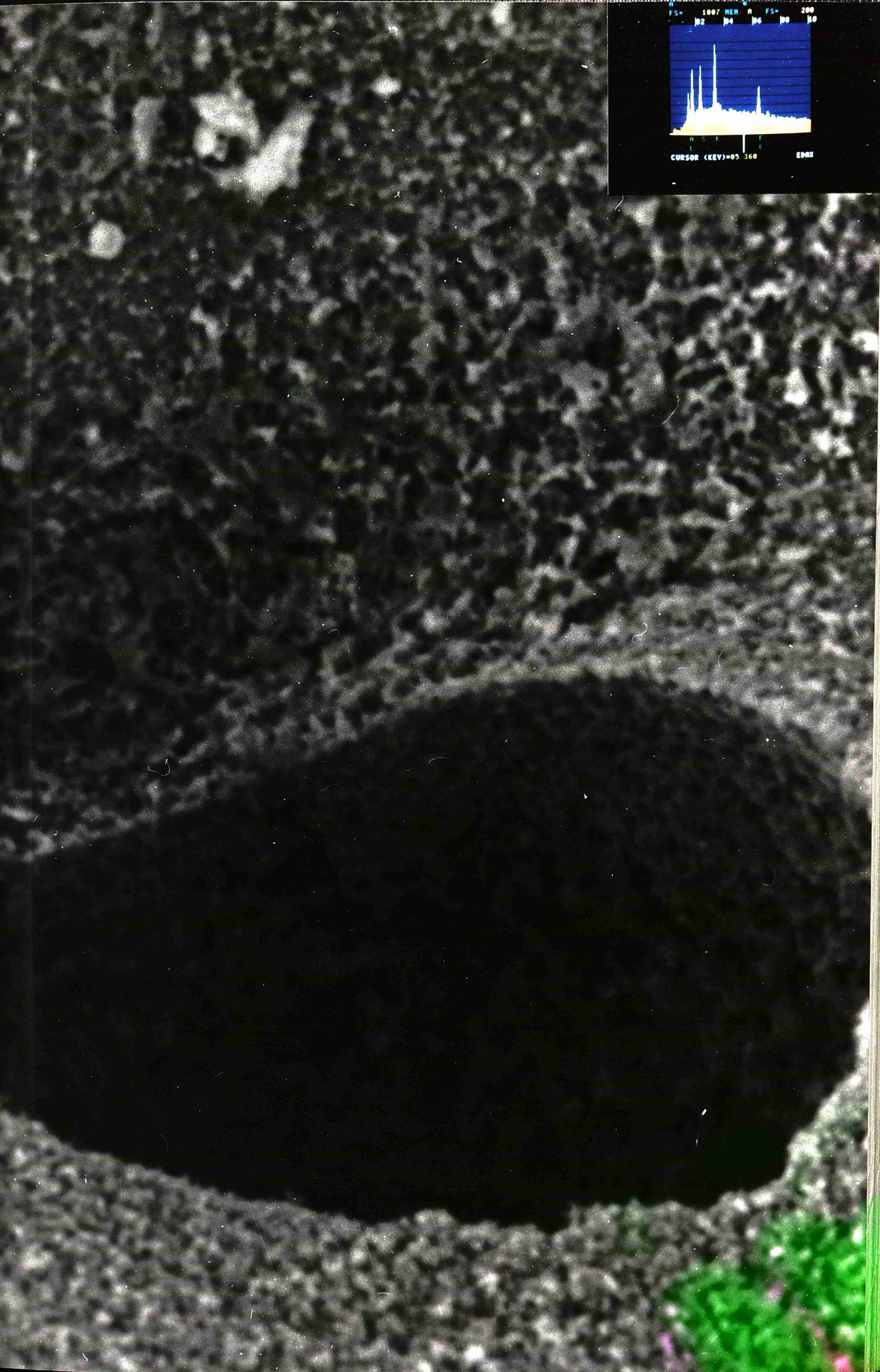


PLATE 30

SEM of Ex-Tuyere Coke Macrostructure.

Magnification = X 1600

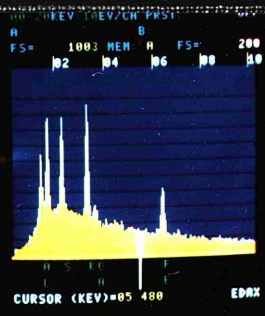
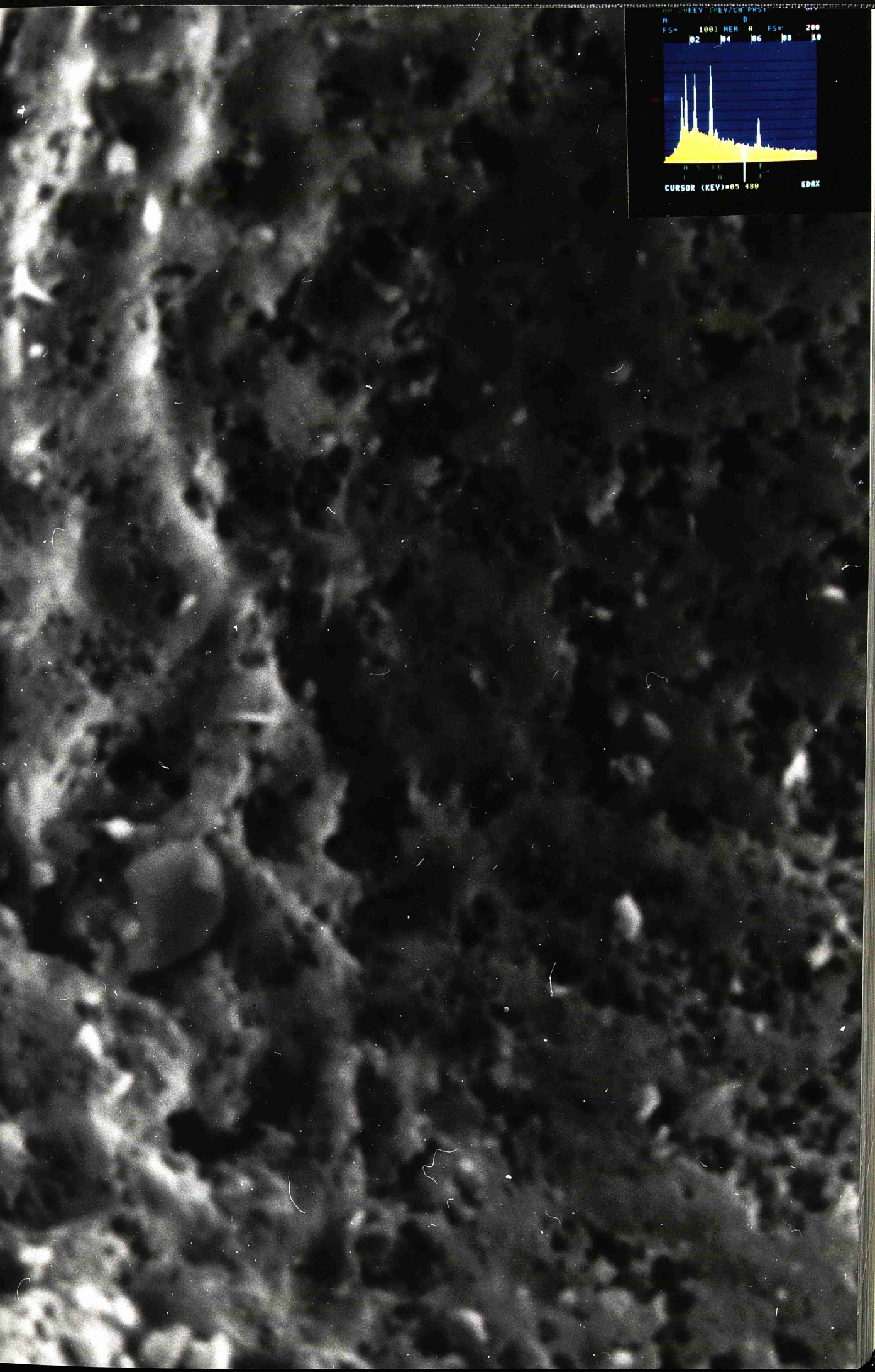


PLATE 31

LREM of Ex-Tuyere Coke Structure.

Magnification = X 287850



PLATE 32

LREM of Ex-Tuyere Coke.

Magnification = X 612000

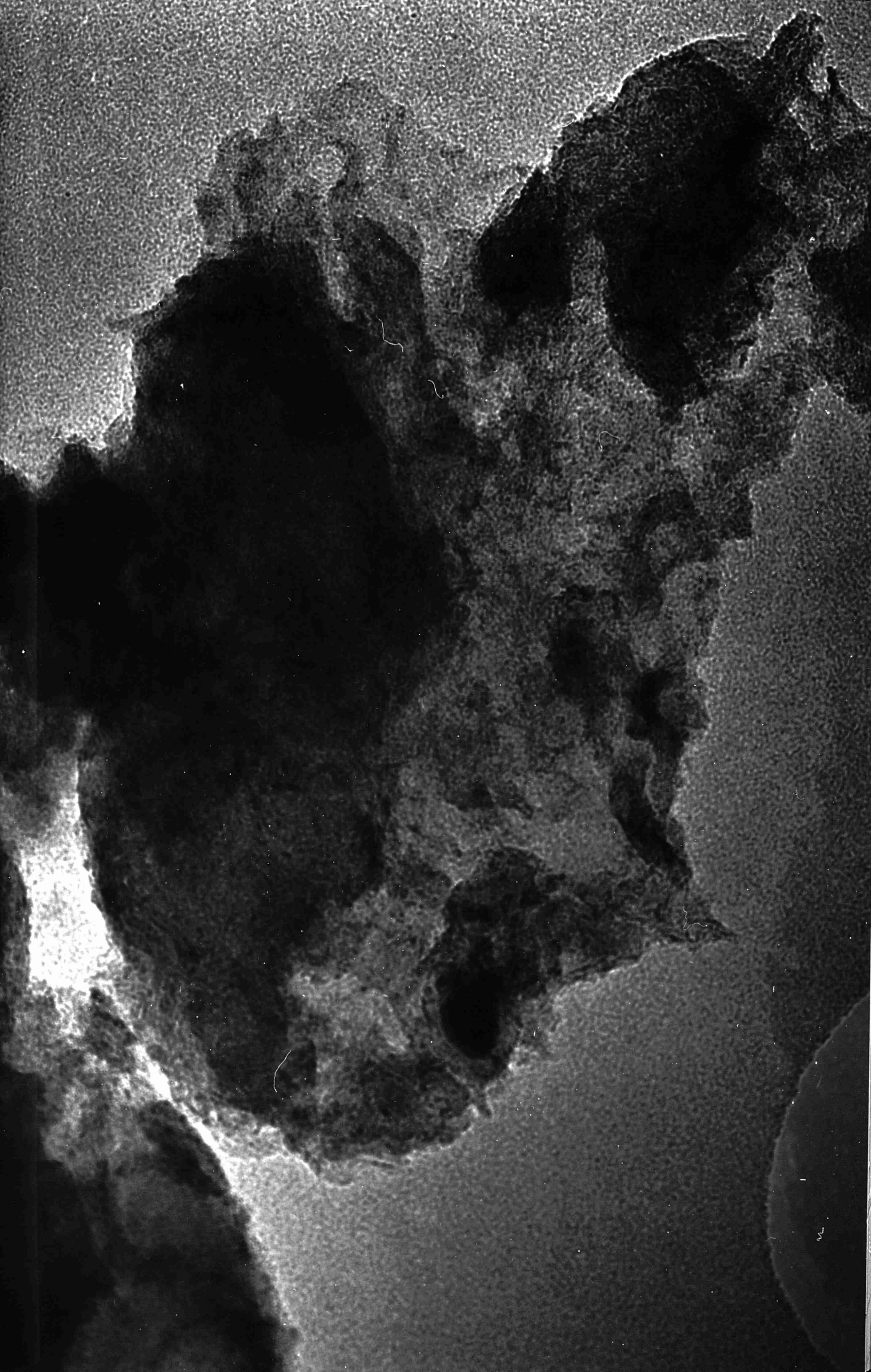


PLATE 33

LREM of Ex-Tuyere Coke Morphology.

Magnification = X 636000



PLATE 34

HREM Showing Ordering of Carbon Lattices in Ex-Tuyere
Cokes.

Magnification = X 4298700



PLATE 35

HREM of Ex-tuyere Coke Illustrating Structural Ordering of
the Carbon Matrix.

Magnification = X 2100000

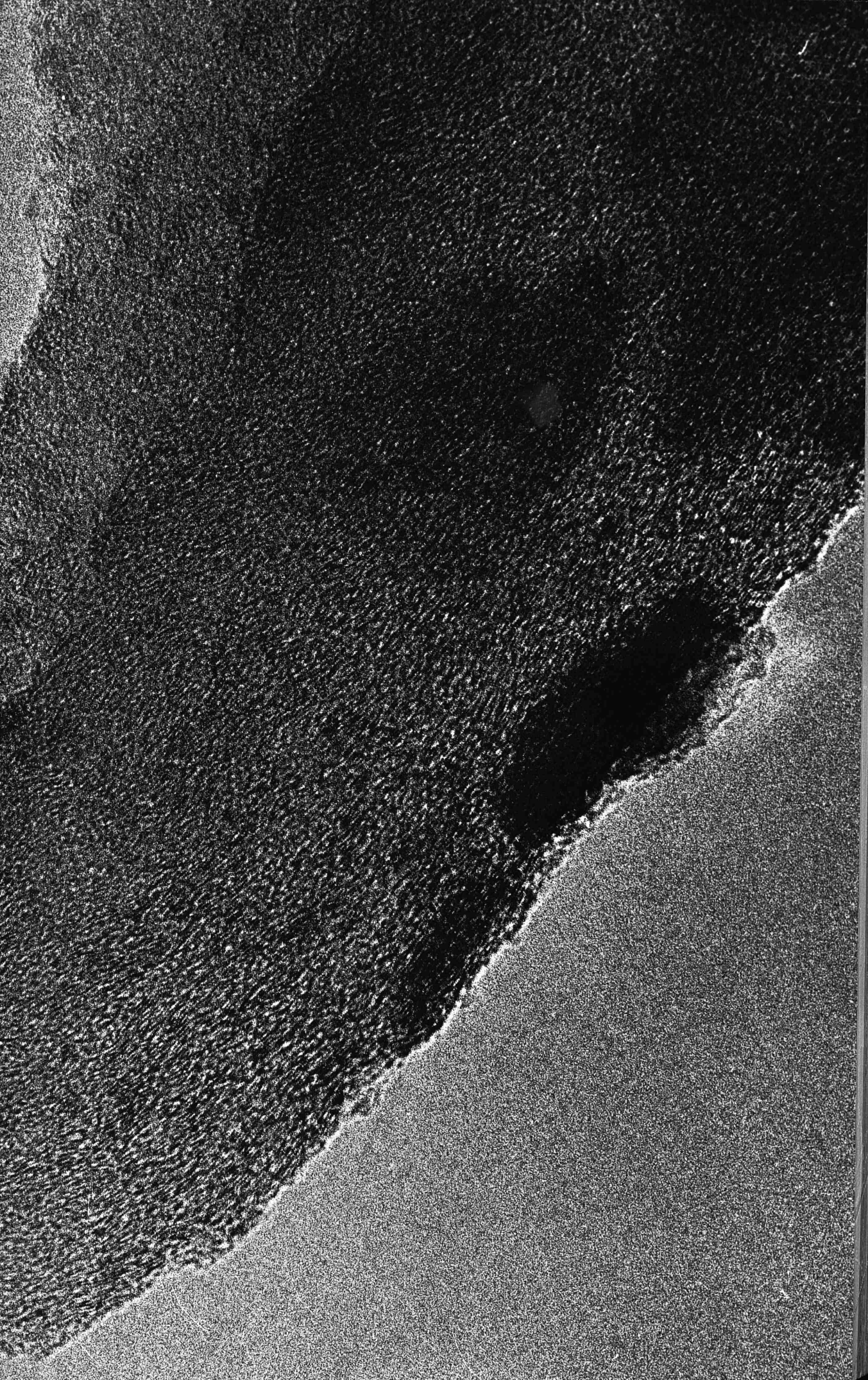


PLATE 36

HREM Illustrating Areas of Structural Ordering in Ex-tuyere
Cokes.

Magnification = X 1882350

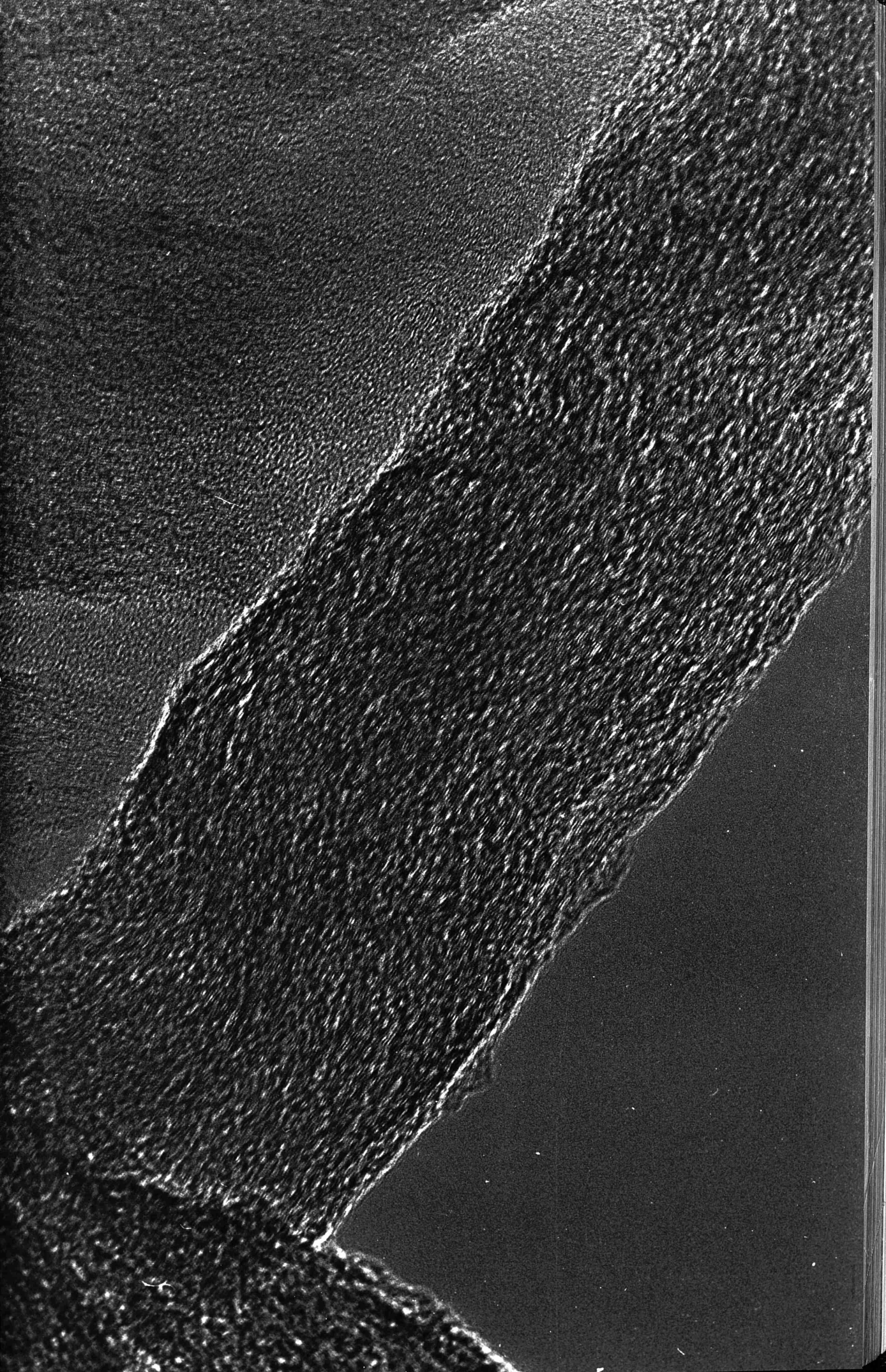


PLATE 37

HREM of Expanded Carbon Lattices Present in Ex-tuyere
Cokes.

Magnification = X 3936800

PLATE 38

HREM of Ex-tuyere Coke Morphology Showing Expansion of
Carbon Structure.

Magnification = X 4905000

PLATE 39

HREM of Ex-tuyere Coke Showing Expanded Disordered Carbon Structure.

Magnification = X 1643500

PLATE 40

SEM of Reacted Feed Coke.

Magnification = X 1536

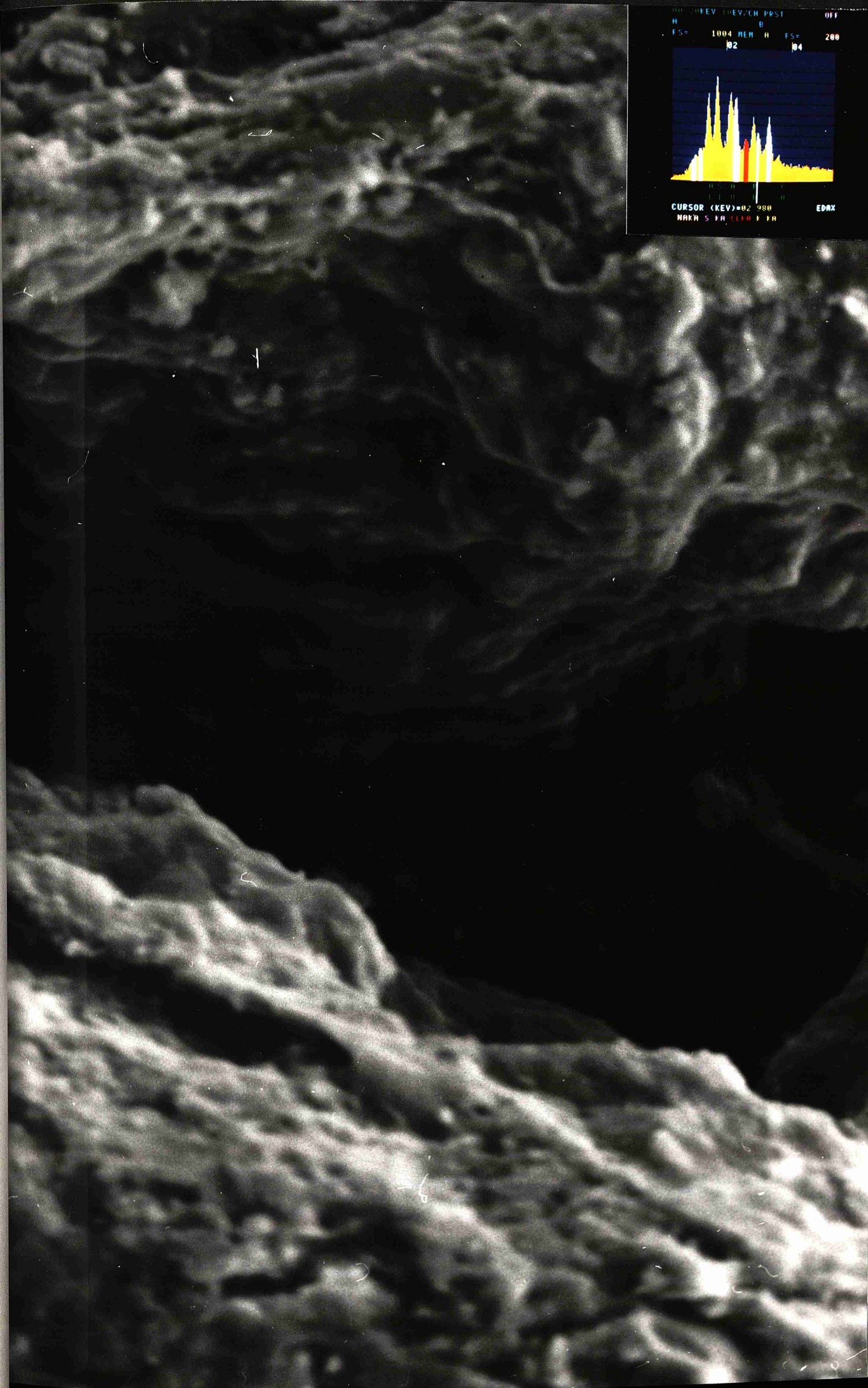


PLATE 41

SEM of Reacted Feed Coke.

Magnification = X 2160



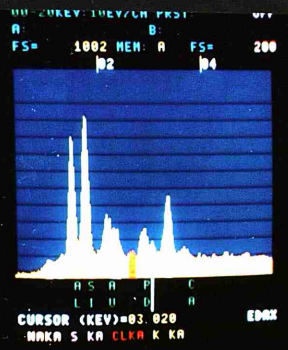
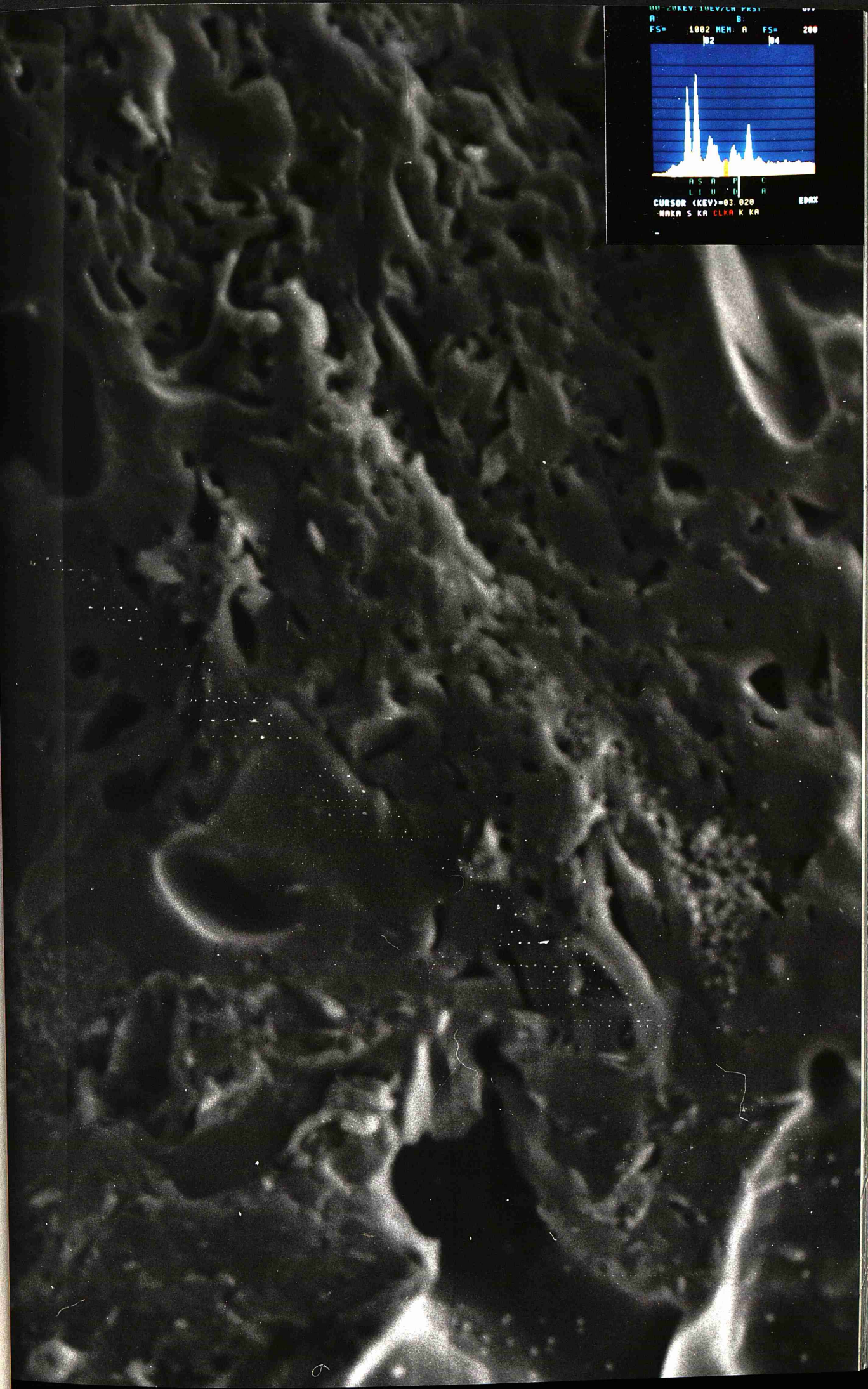


PLATE 42

SEM of Reacted Feed Coke.

Magnification = X 1584

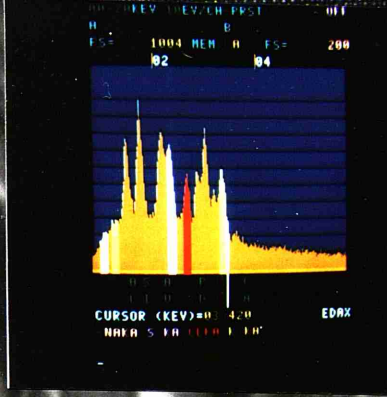
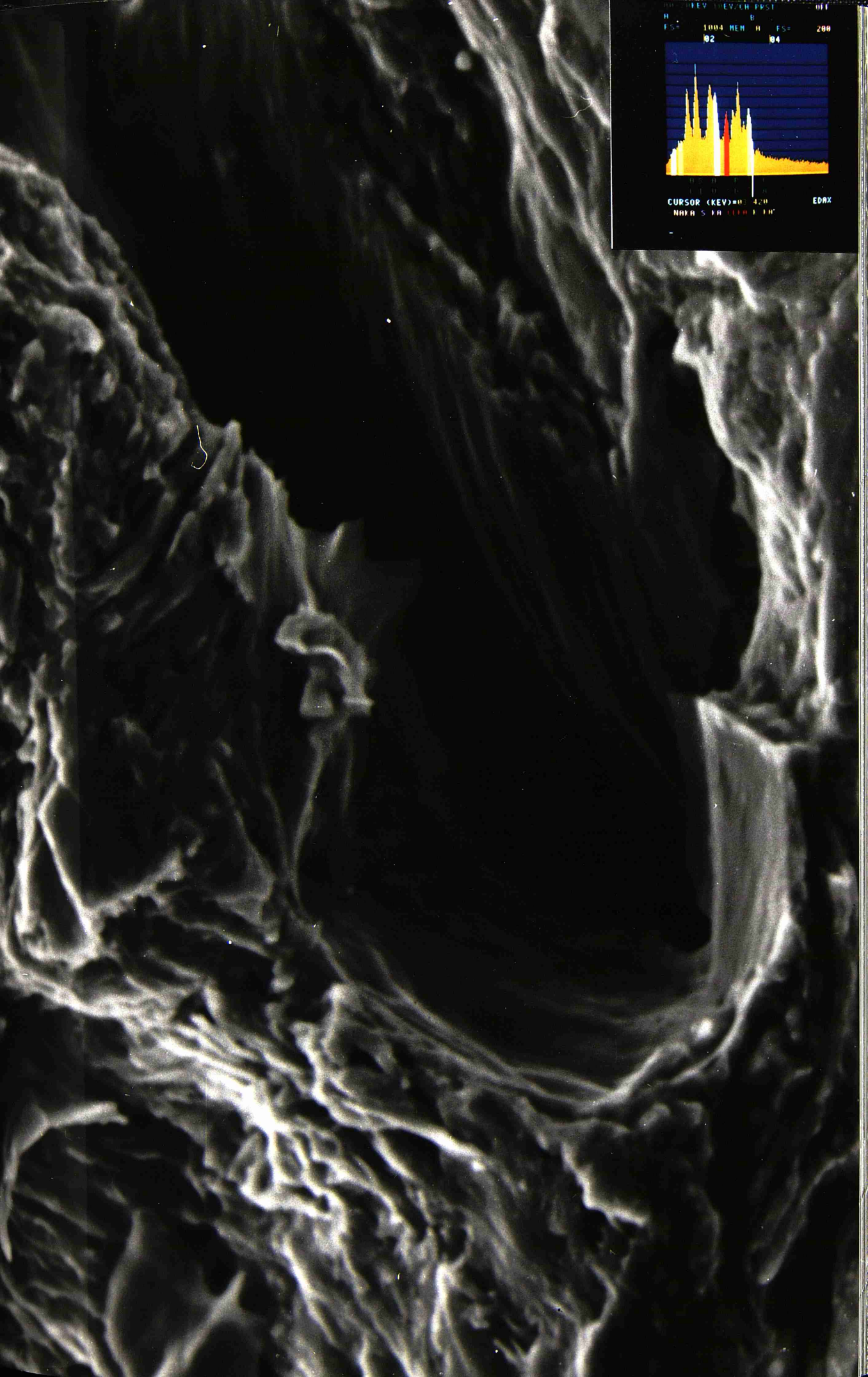


PLATE 43

LREM of Reacted Feed Coke.

Magnification = X 450000

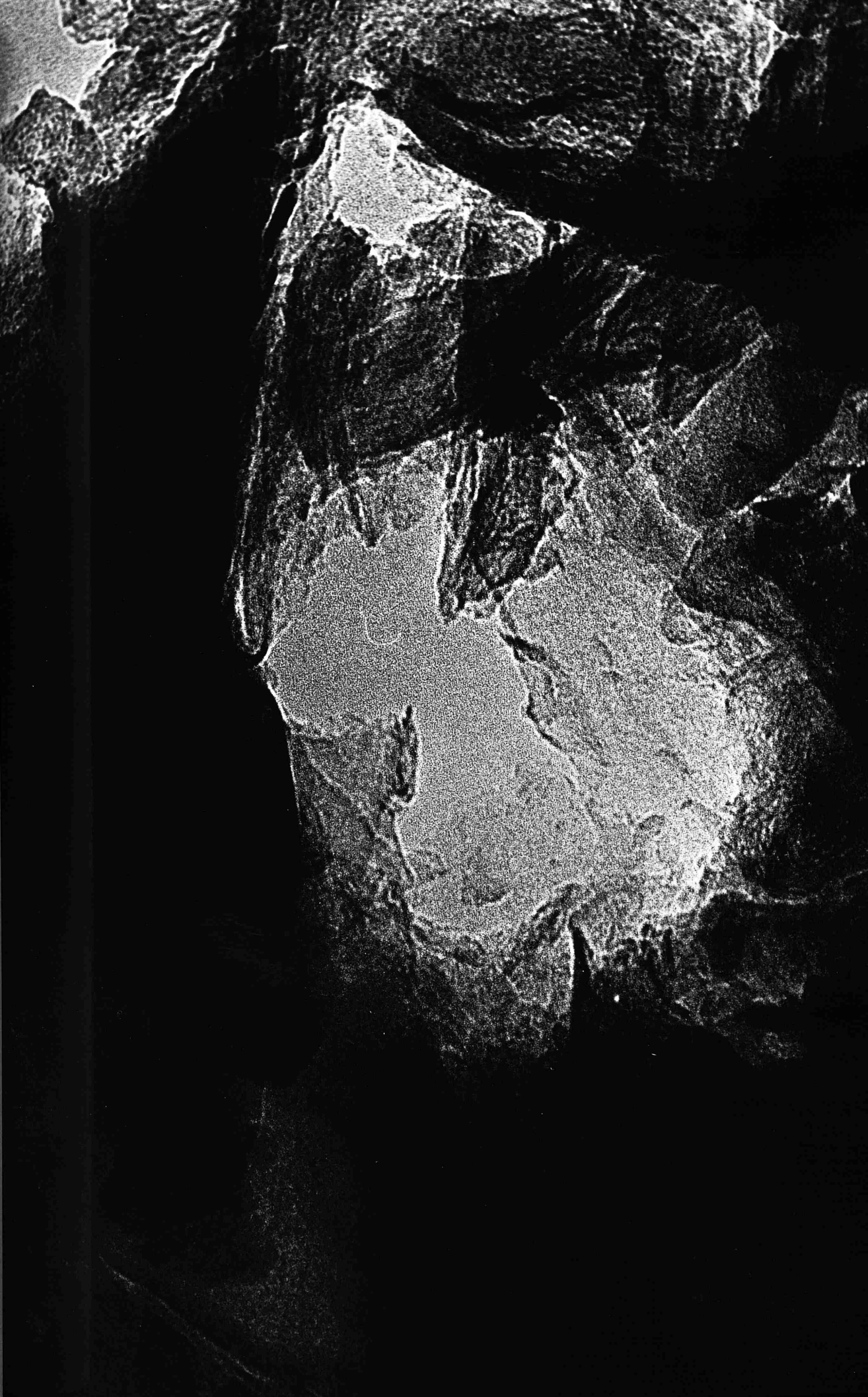


PLATE 44

LREM of Reacted Feed Coke.

Magnification = X 696000

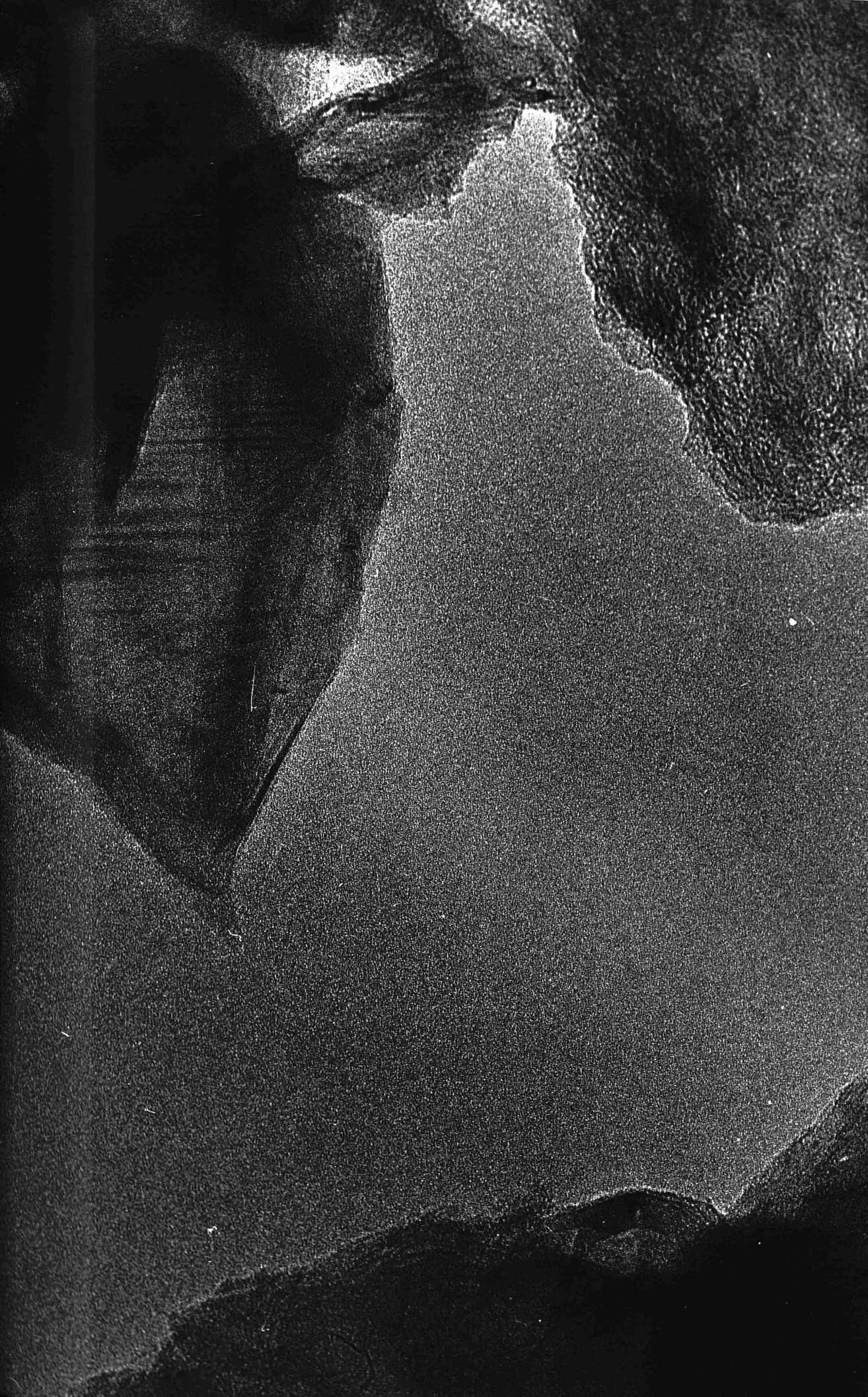


PLATE 45

HREM of Reacted Feed Coke Showing Original Feed Coke Structure.

Magnification = X 2995000



PLATE 46

HREM of Reacted Feed Coke Showing Original Feed Coke
Structure.

Magnification = X 4920000

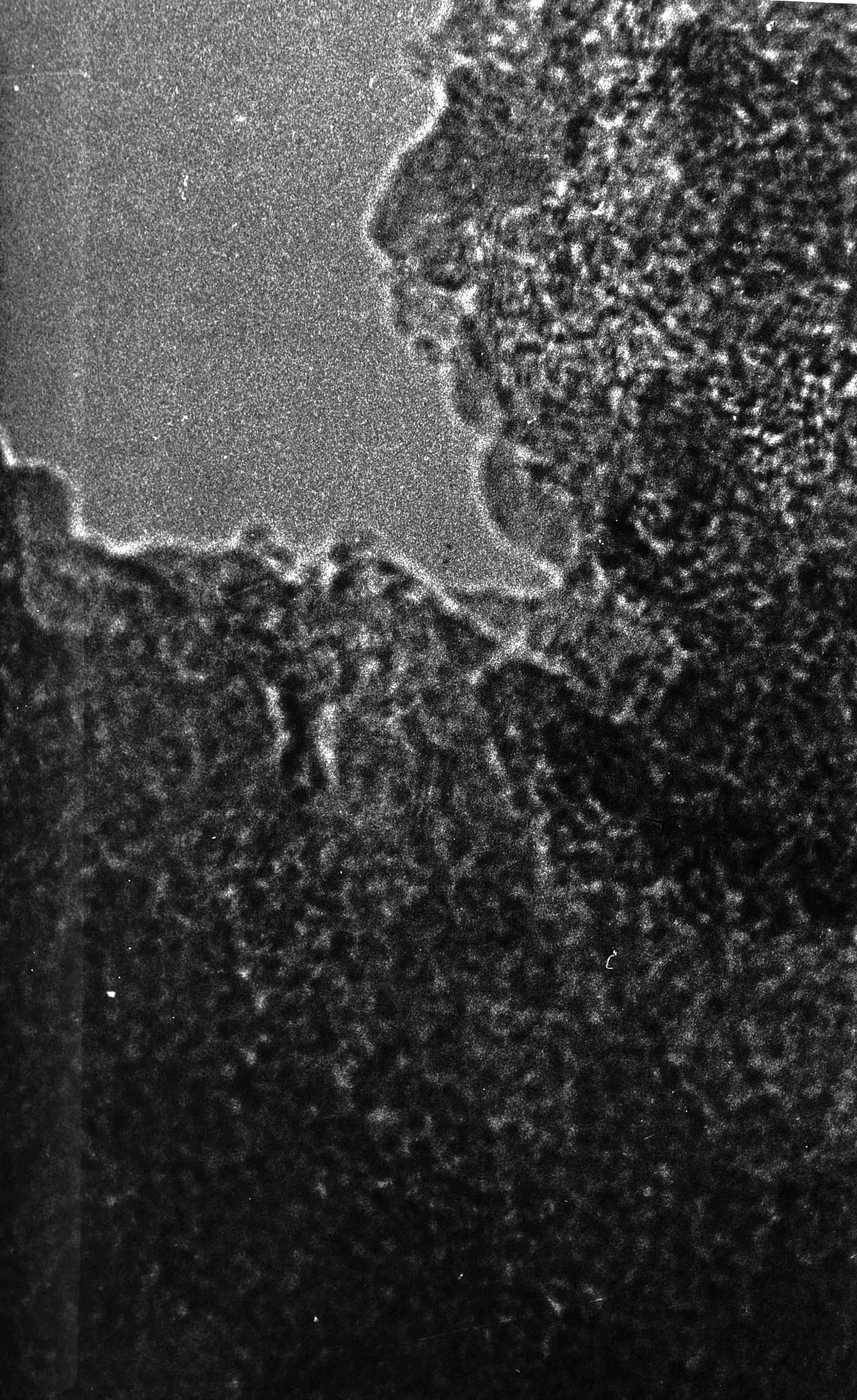


PLATE 47

HREM of Reacted Feed Coke Showing Original Feed Coke
Structure.

Magnification = X 4470000

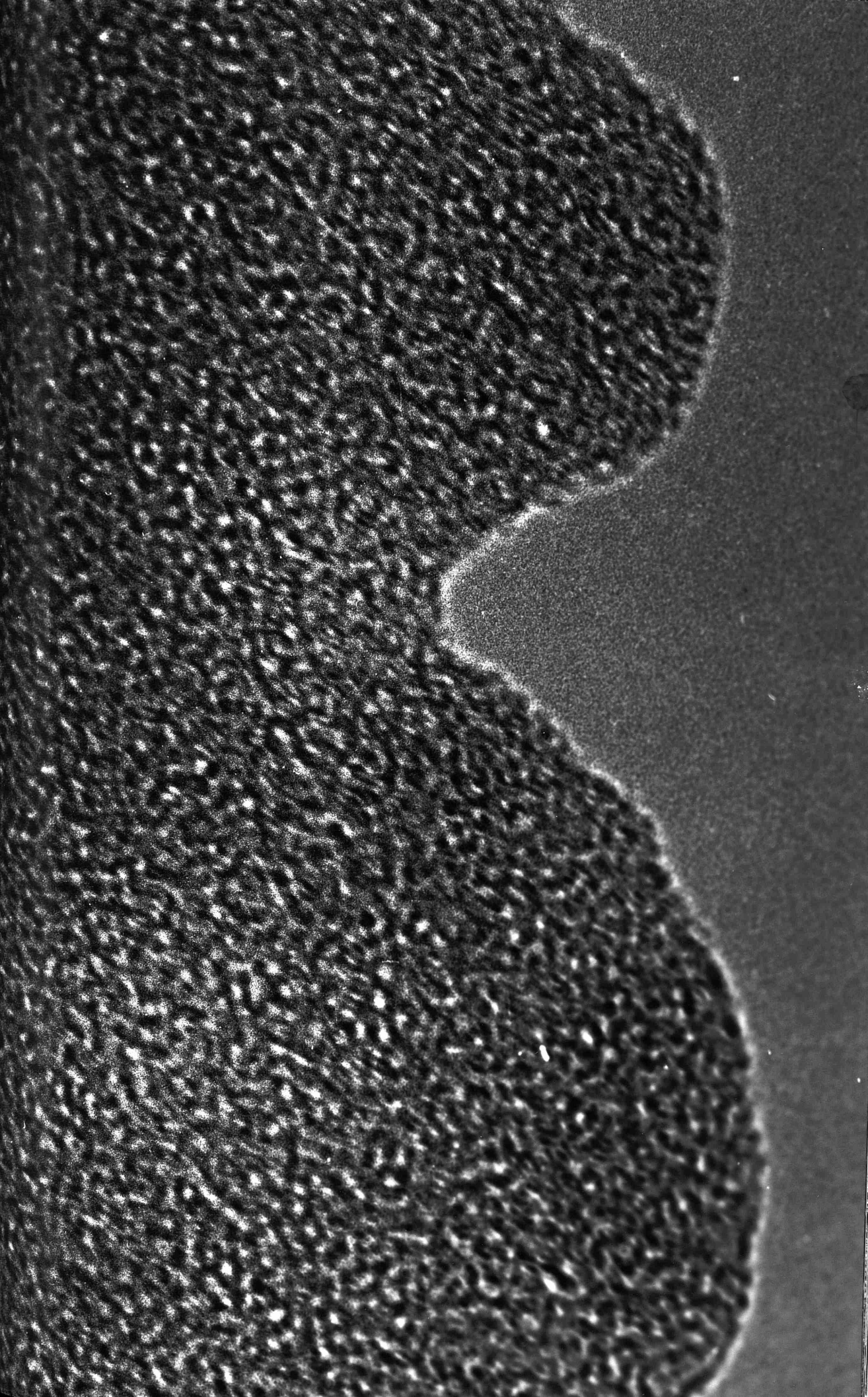


PLATE 48

HREM of Reacted Feed Coke Showing Expansion of Carbon Structure.

Magnification = X 4443600

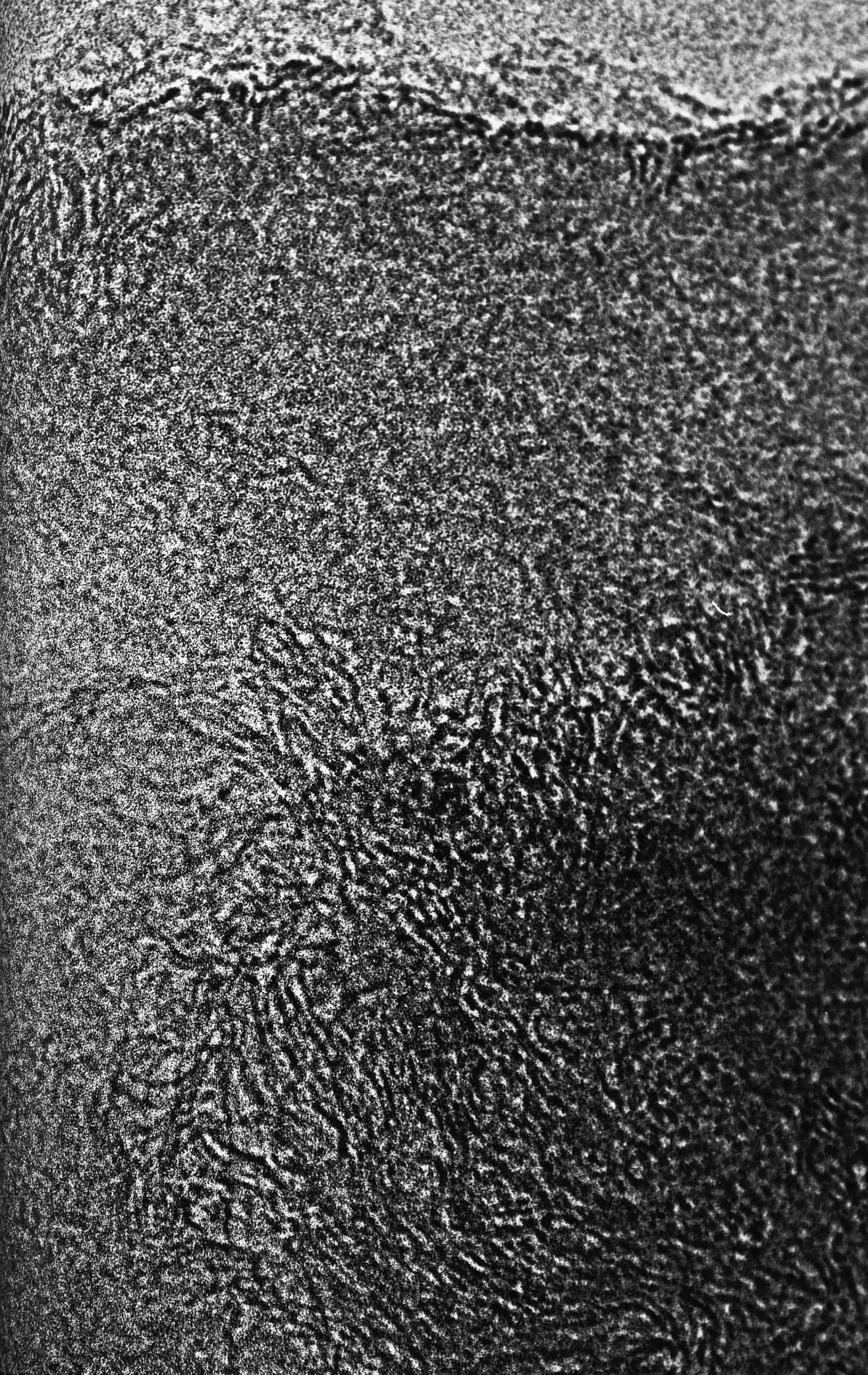


PLATE 49

HREM of Reacted Feed Coke Morphology Showing Expanded
Carbon Lattices.

Magnification = X 4443600



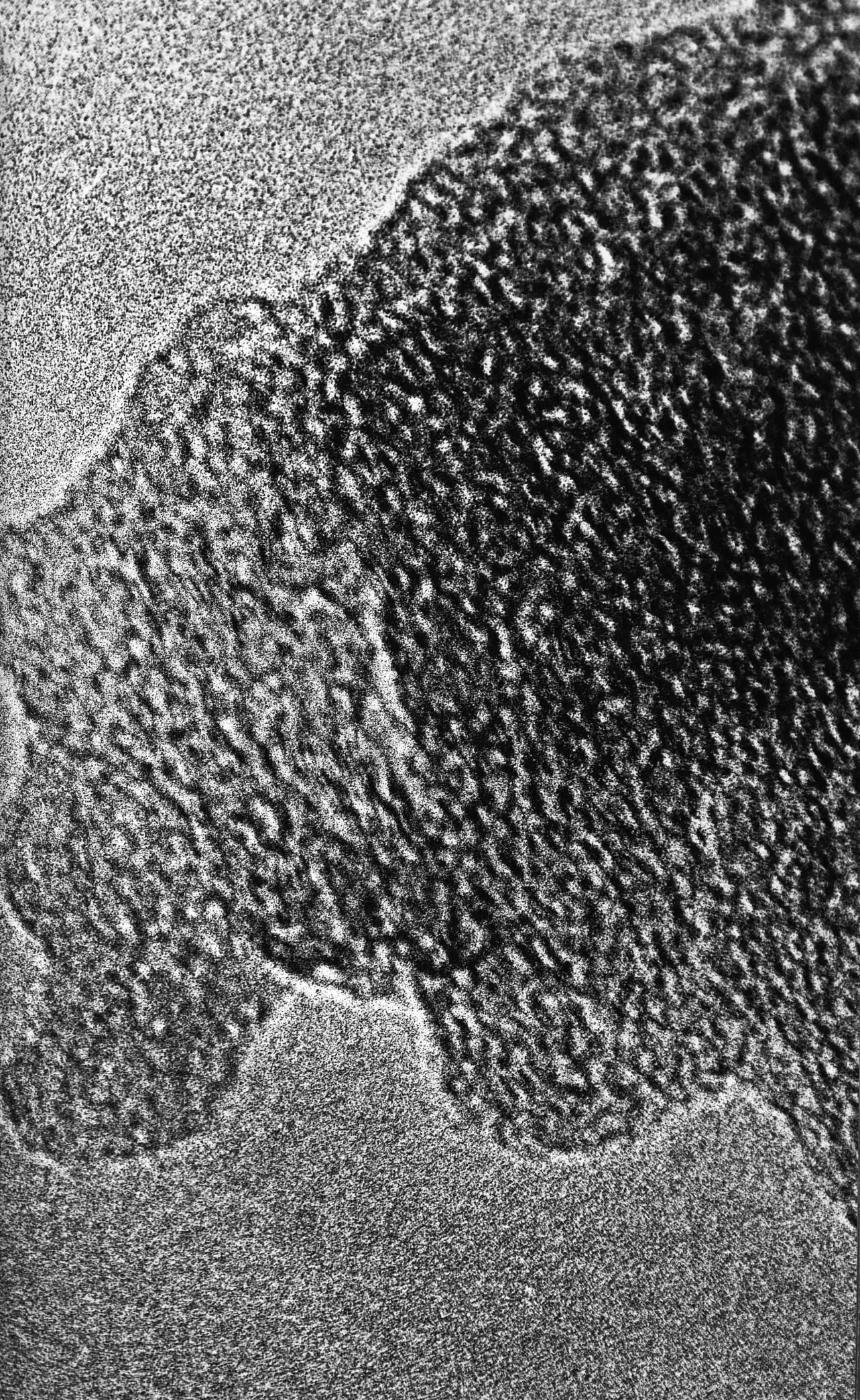


PLATE 50

HREM of Expanded Carbon Structure Found in Reacted Feed
Cokes.

Magnification = X 1776000



PLATE 51

HREM of Ordered Carbon Structure Observed in Reacted Feed
Cokes.

Magnification = X 2985000

PLATE 52

HREM of Observed Ordered Regions in Reacted Feed Cokes.

Magnification = X 2995000

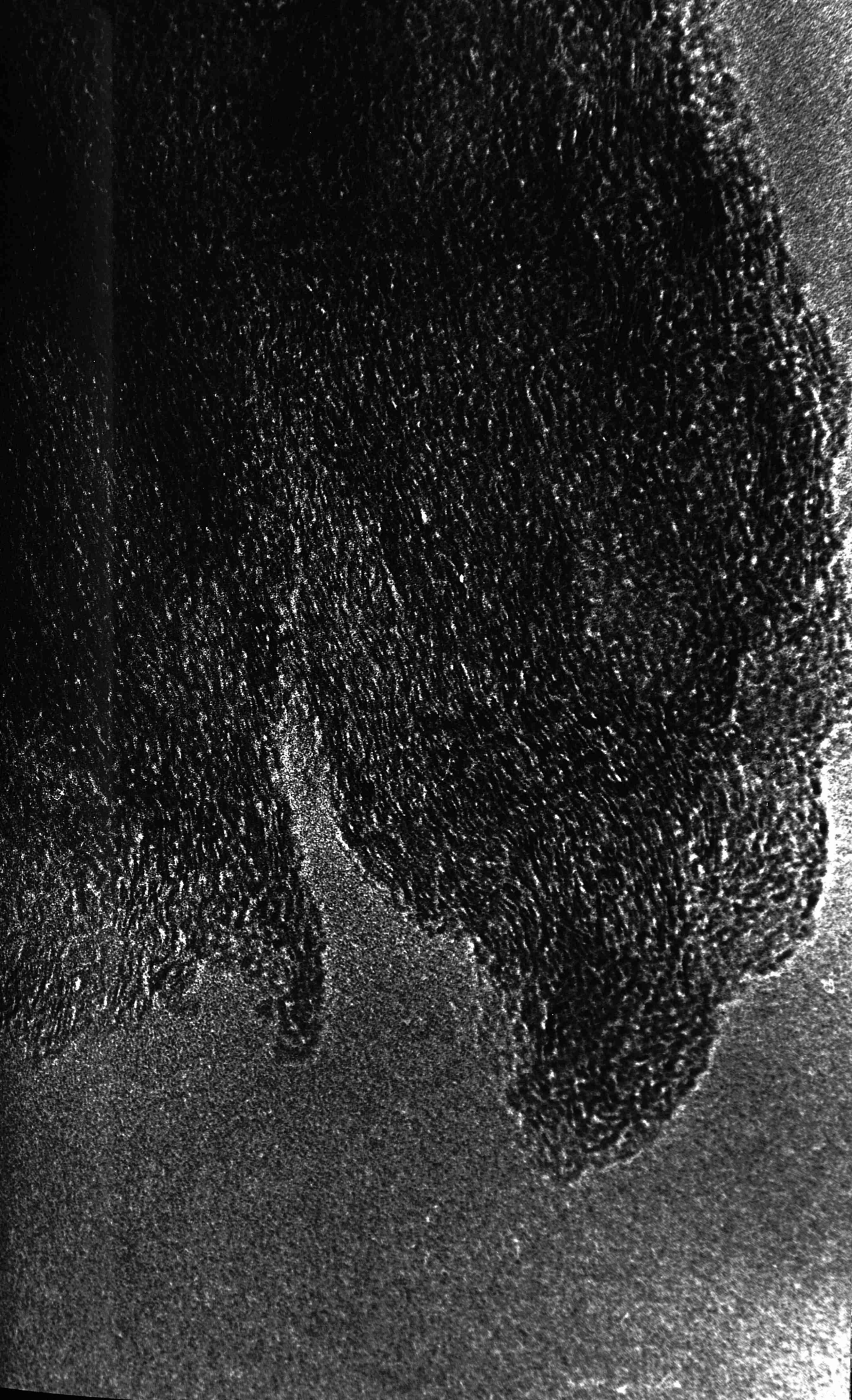


PLATE 53

HREM Showing Area of Structural Ordering in Reacted Feed
Coke.

Magnification = X 5100000



PLATE 54

SEM of Heat Treated Feed Cokes.

Magnification = X 140



PLATE 55

SEM of Heat Treated Feed Cokes.

Magnification = X 1664

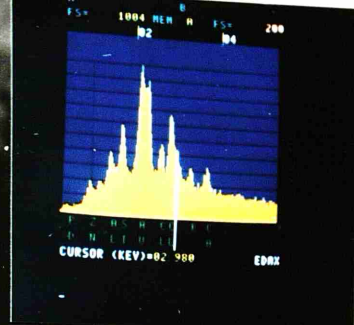
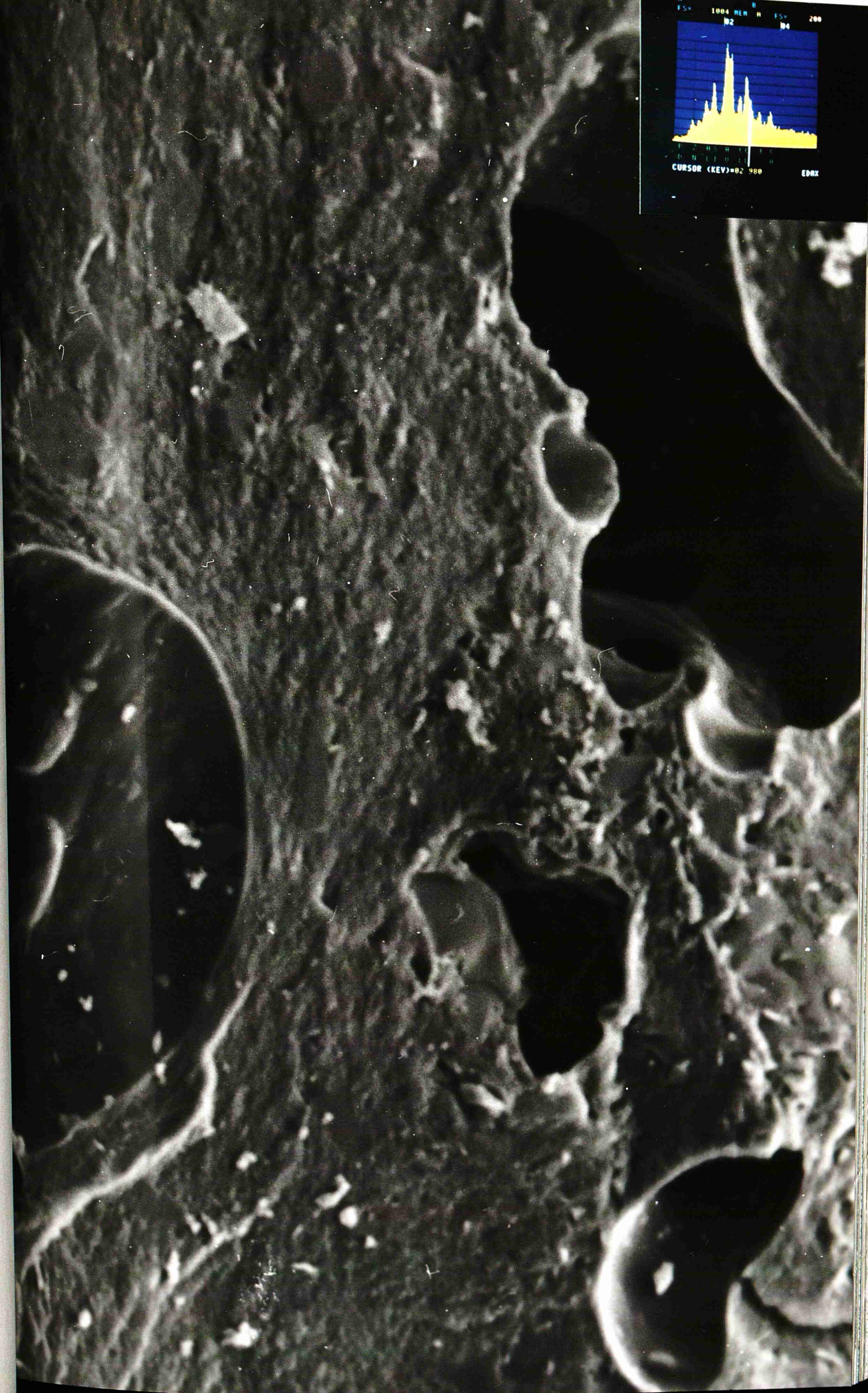


PLATE 56

SEM of Heat Treated Feed Cokes.

Magnification = X 824

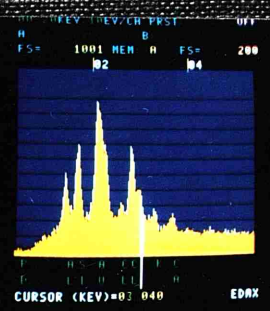


PLATE 57

LREM of Heat Treated Feed Cokes.

Magnification = X 1627500

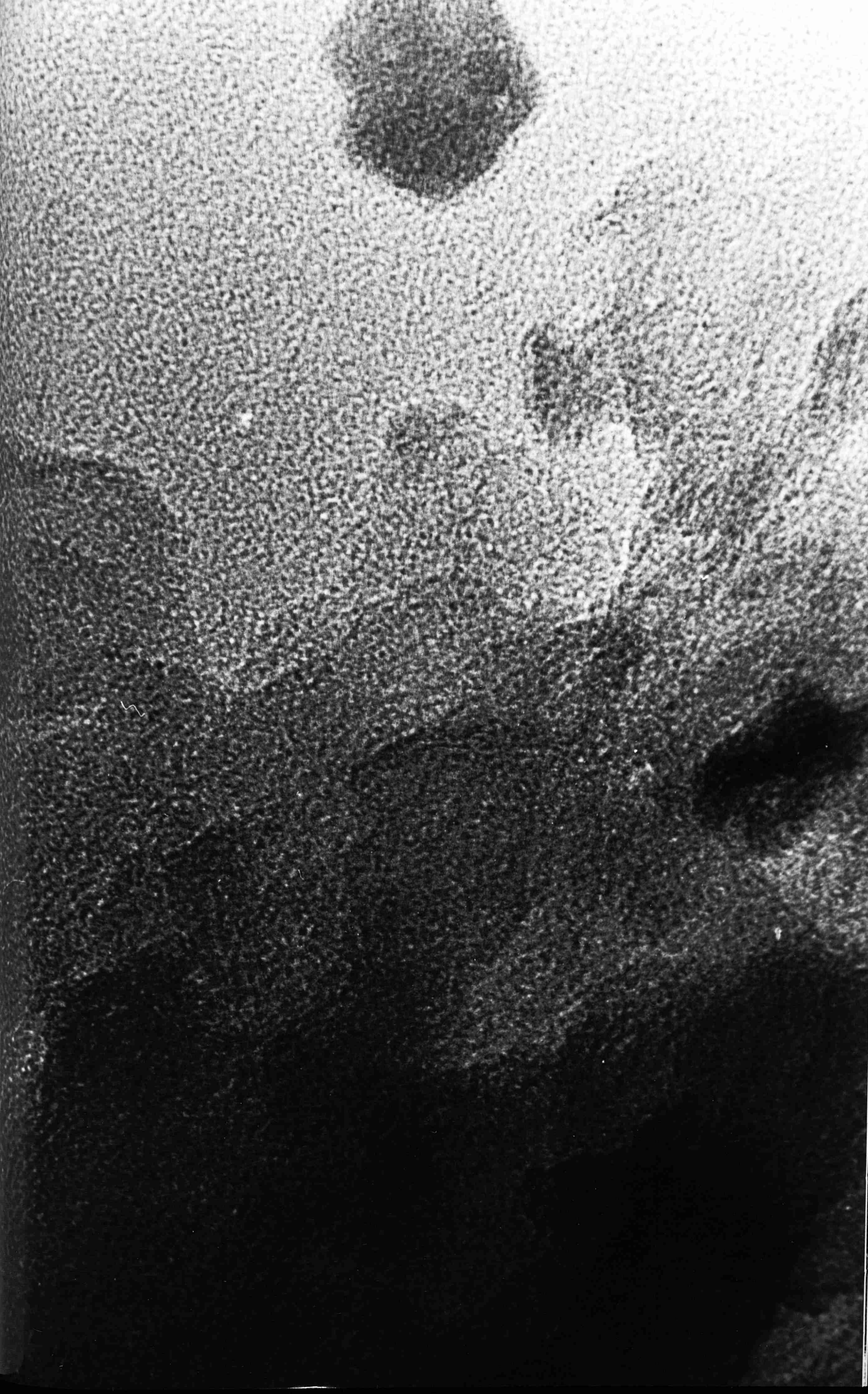


PLATE 58

HREM Showing Ordering of Carbon Structure.

Magnification = X 1560000



PLATE 59

HREM of Ordered Carbon Structure in Heat Treated Feed
Cokes.

Magnification = X 4440000

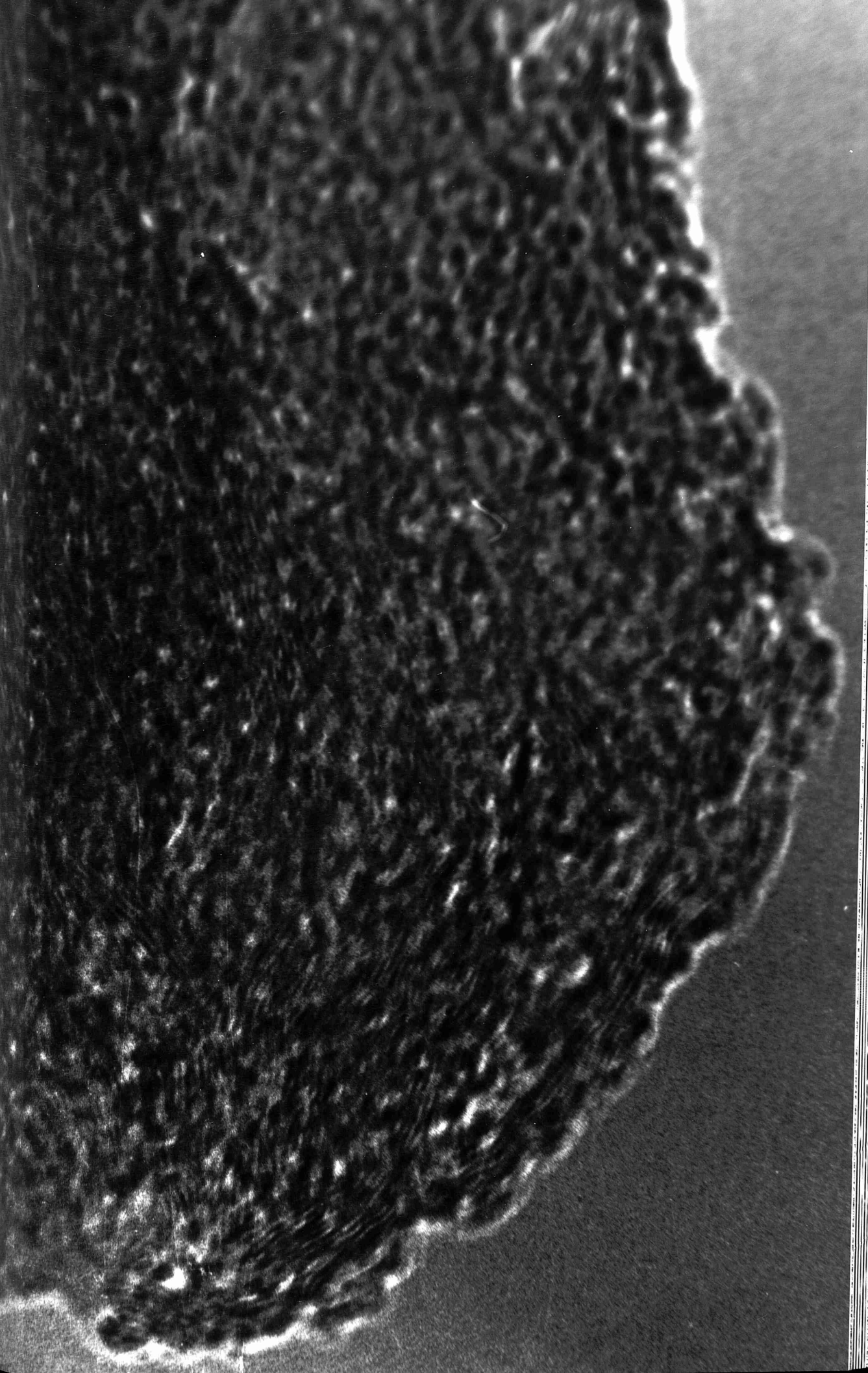


PLATE 60

Ordering of Carbon Structure in Heat Treated Feed Cokes.

Magnification = X 5070000

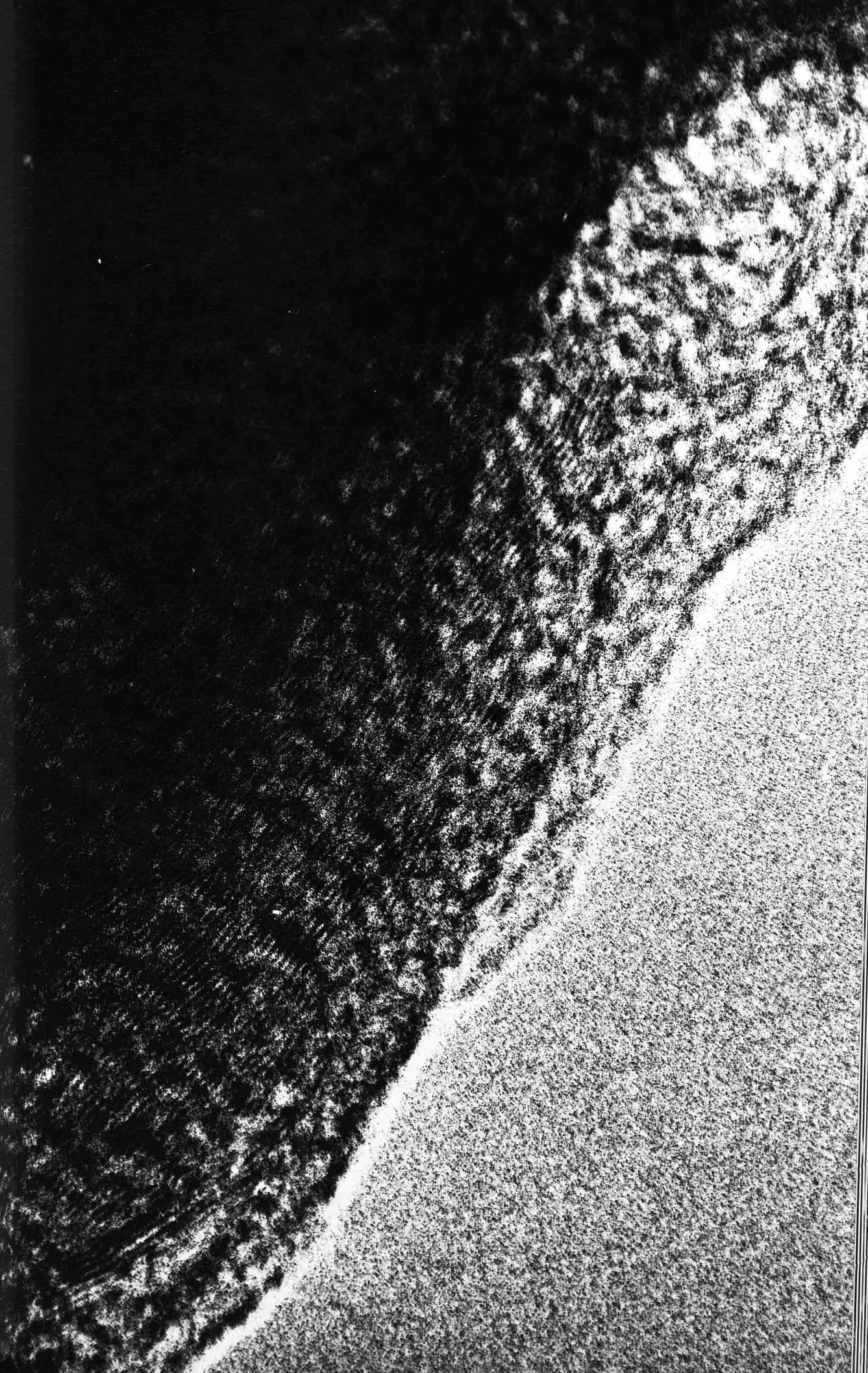


PLATE 61

SEM of Feed Coke Reacted Below Carbonisation Temperature.

Magnification = X 1984

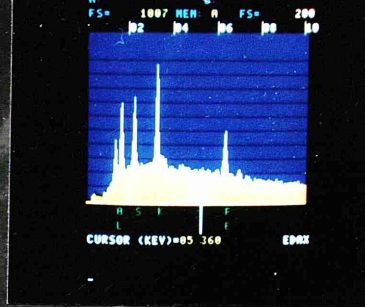
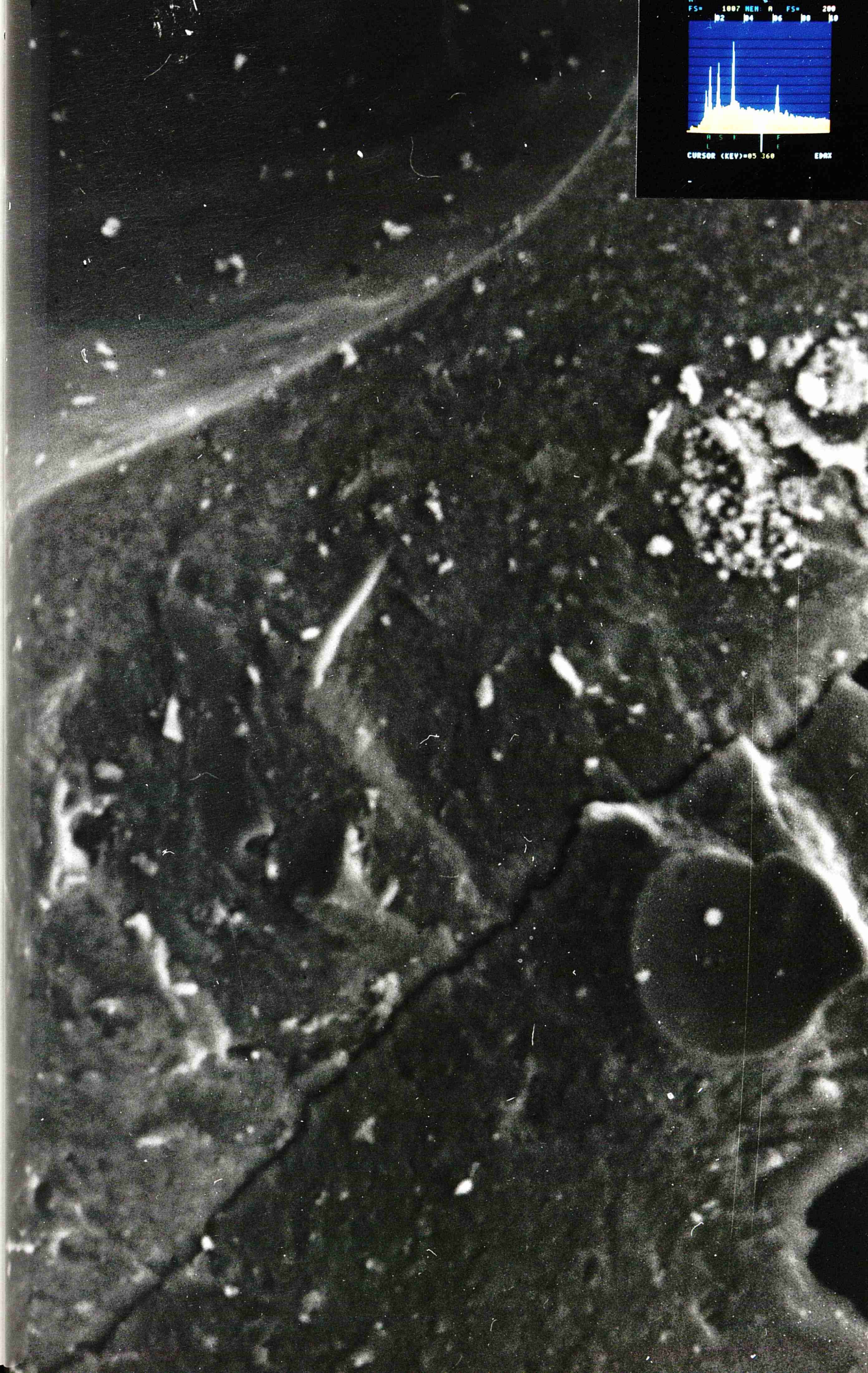


PLATE 62

SEM of Feed Coke Reacted Below Carbonisation Temperature.

Magnification = X 1008

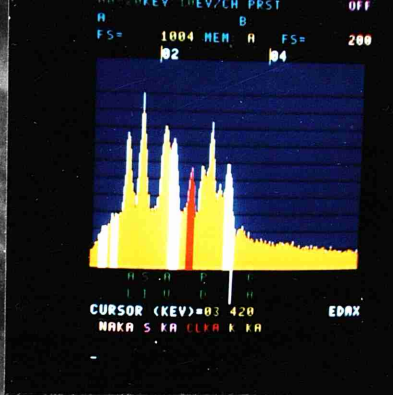
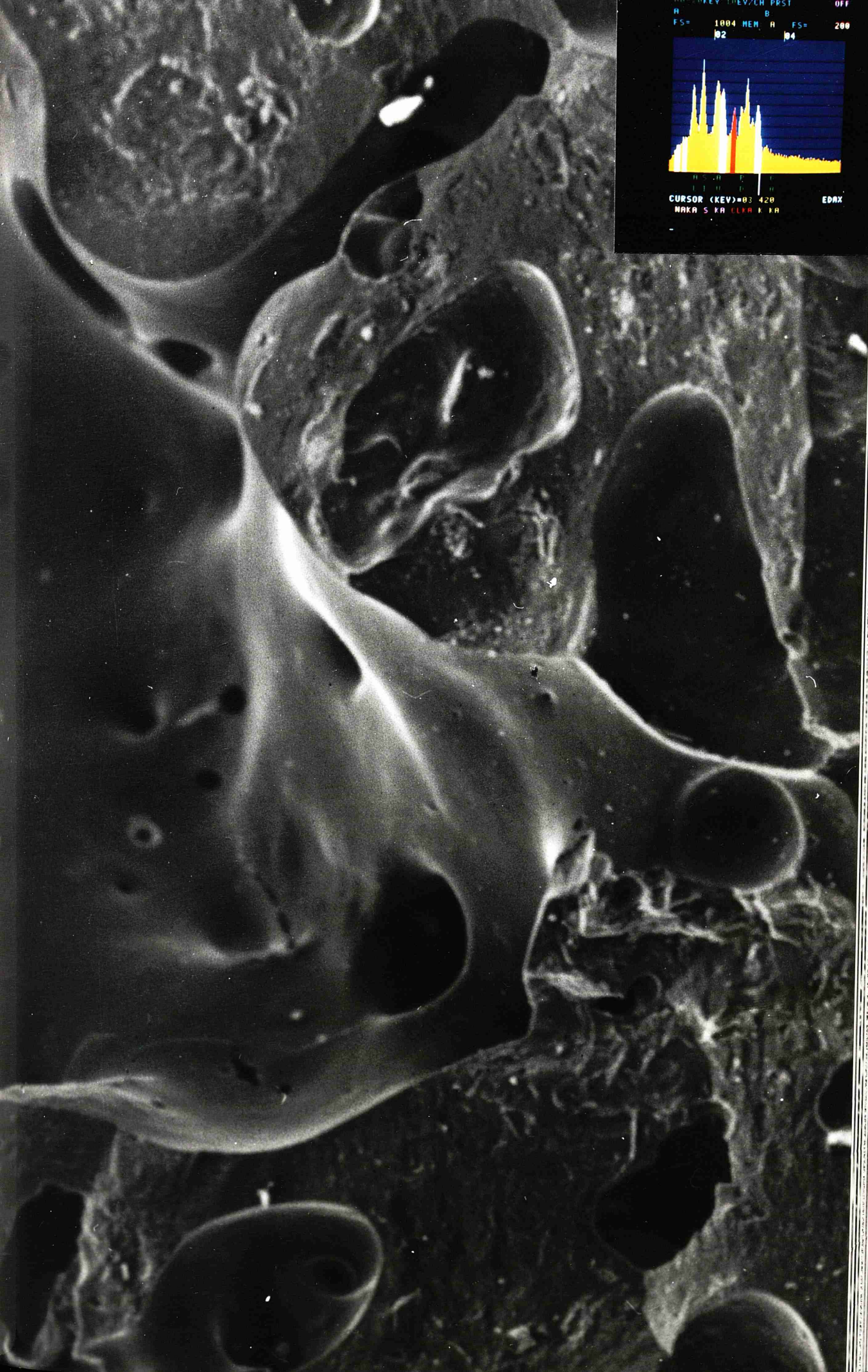


PLATE 63

SEM of Feed Coke Reacted Below Carbonisation Temperature.

Magnification = X 1000

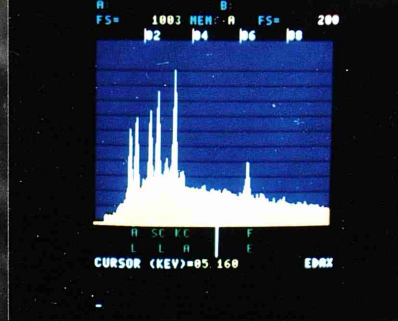
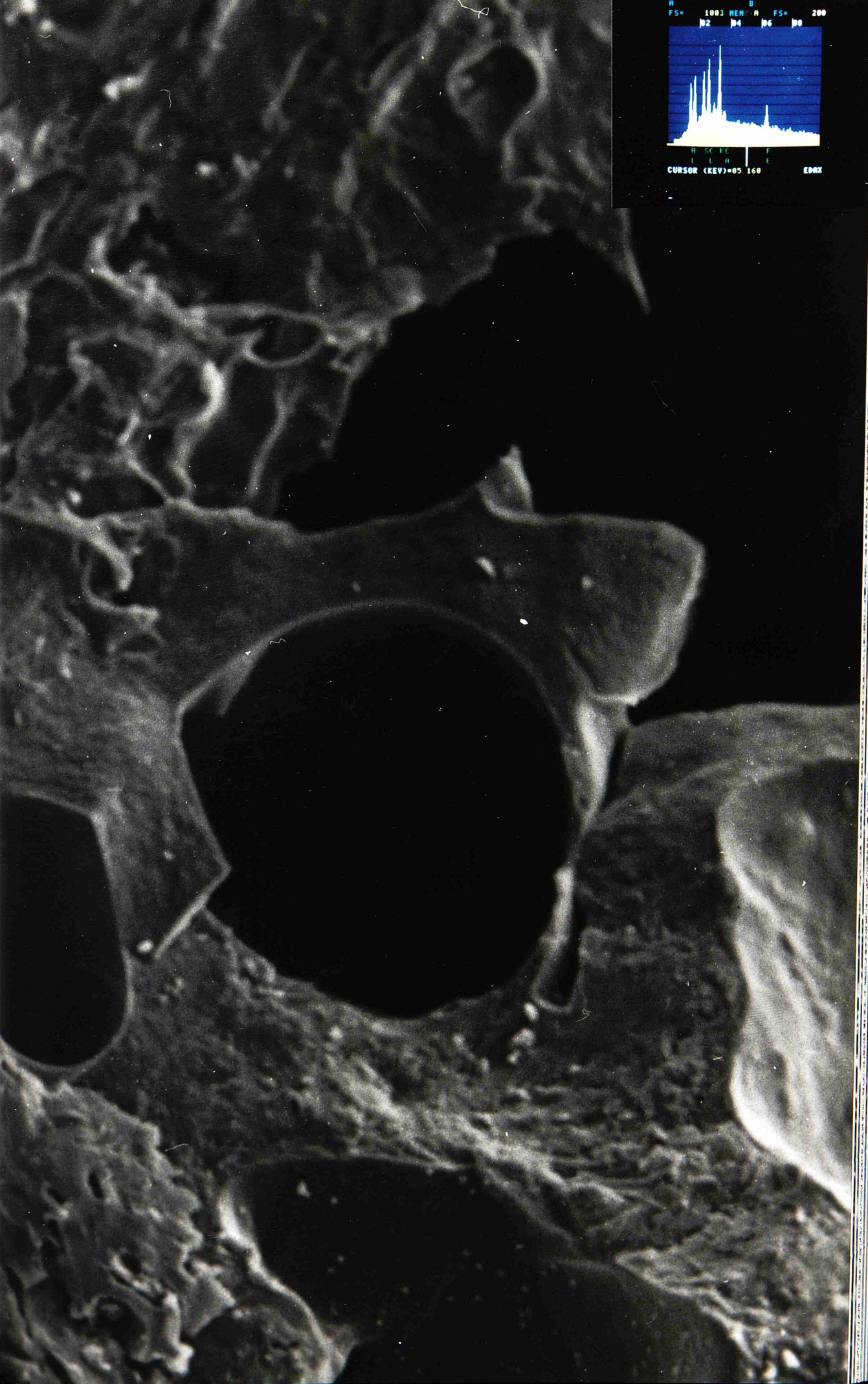
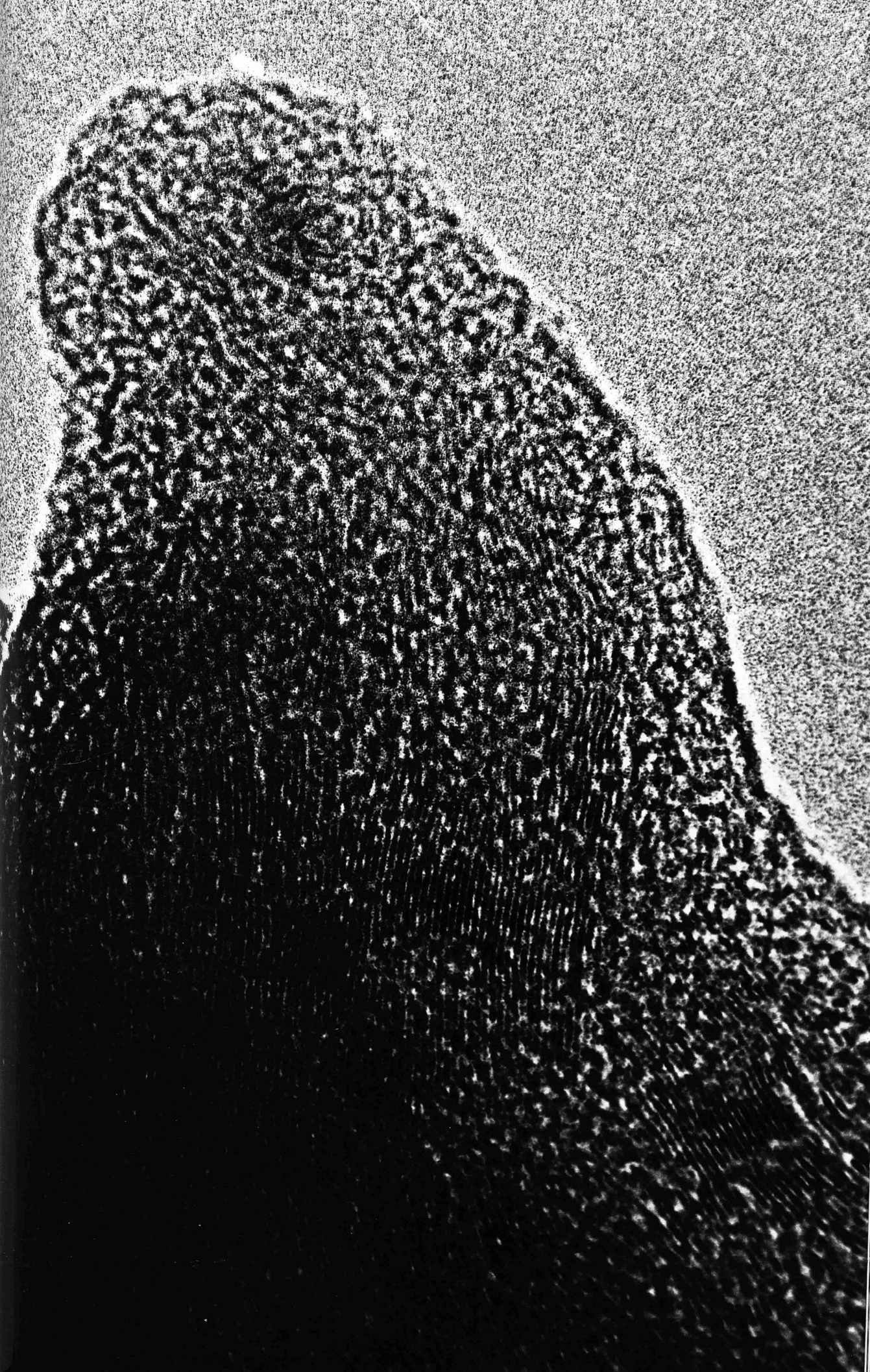


PLATE 64

HREM of Feed Coke Reacted Below Carbonisation Temperature
Showing Ordering of Carbon Structure.

Magnification = X 4875000



, PLATE 65

HREM Showing Ordering of Carbon Structure in Feed Cokes
Reacted Below Carbonisation Temperature.

Magnification = X 4890000

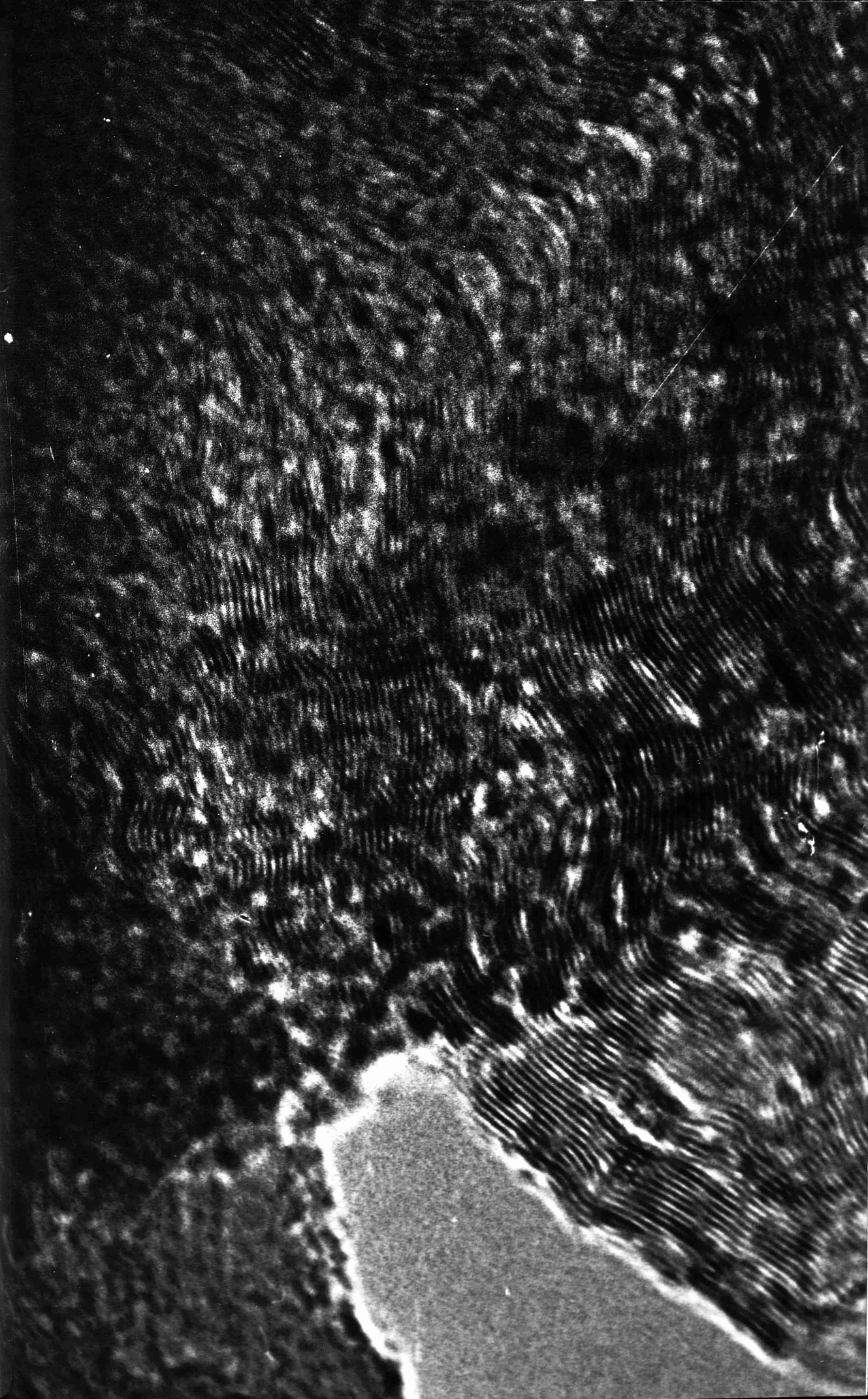


PLATE 66

HREM of Feed Coke Reacted Below Carbonisation Temperature.

Magnification = X 4890000

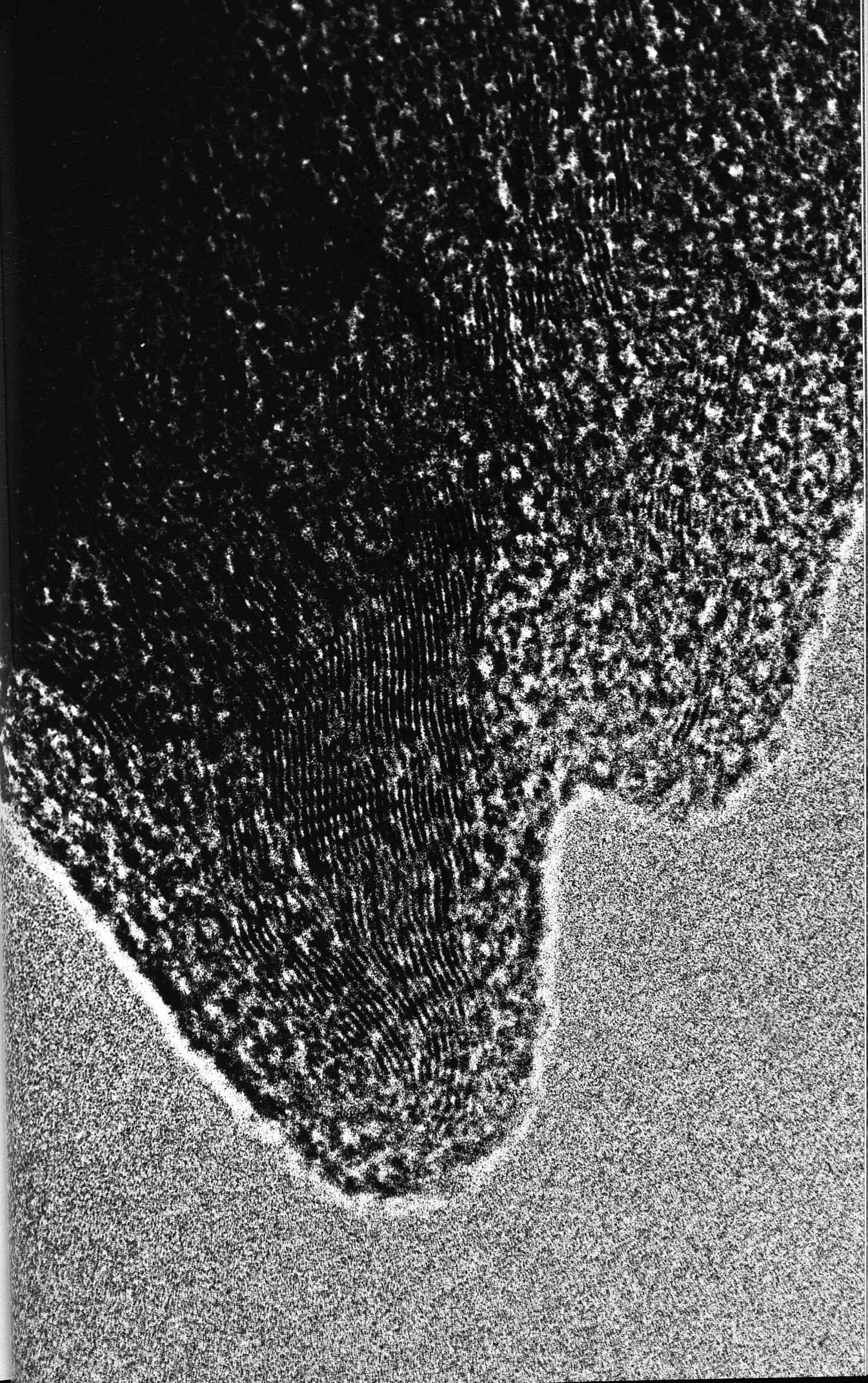


PLATE 67

HREM of Feed Coke Reacted Below Carbonisation Temperature
Showing Expanded Carbon Structure.

Magnification = X 3330600

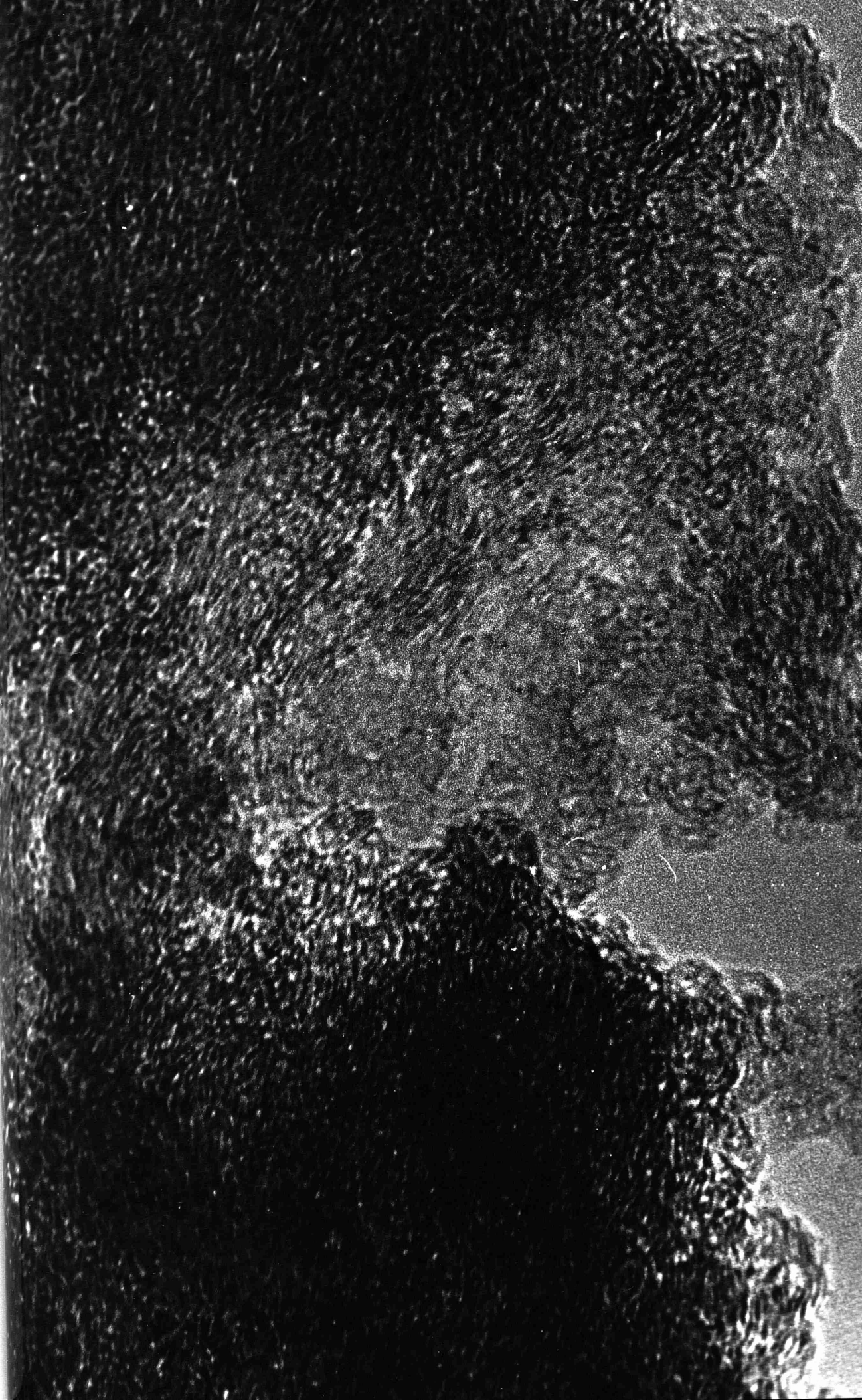


PLATE 68

Expanded Carbon Structure in Feed Cokes Reacted Below
Carbonisation Temperature.

Magnification = X 4444444

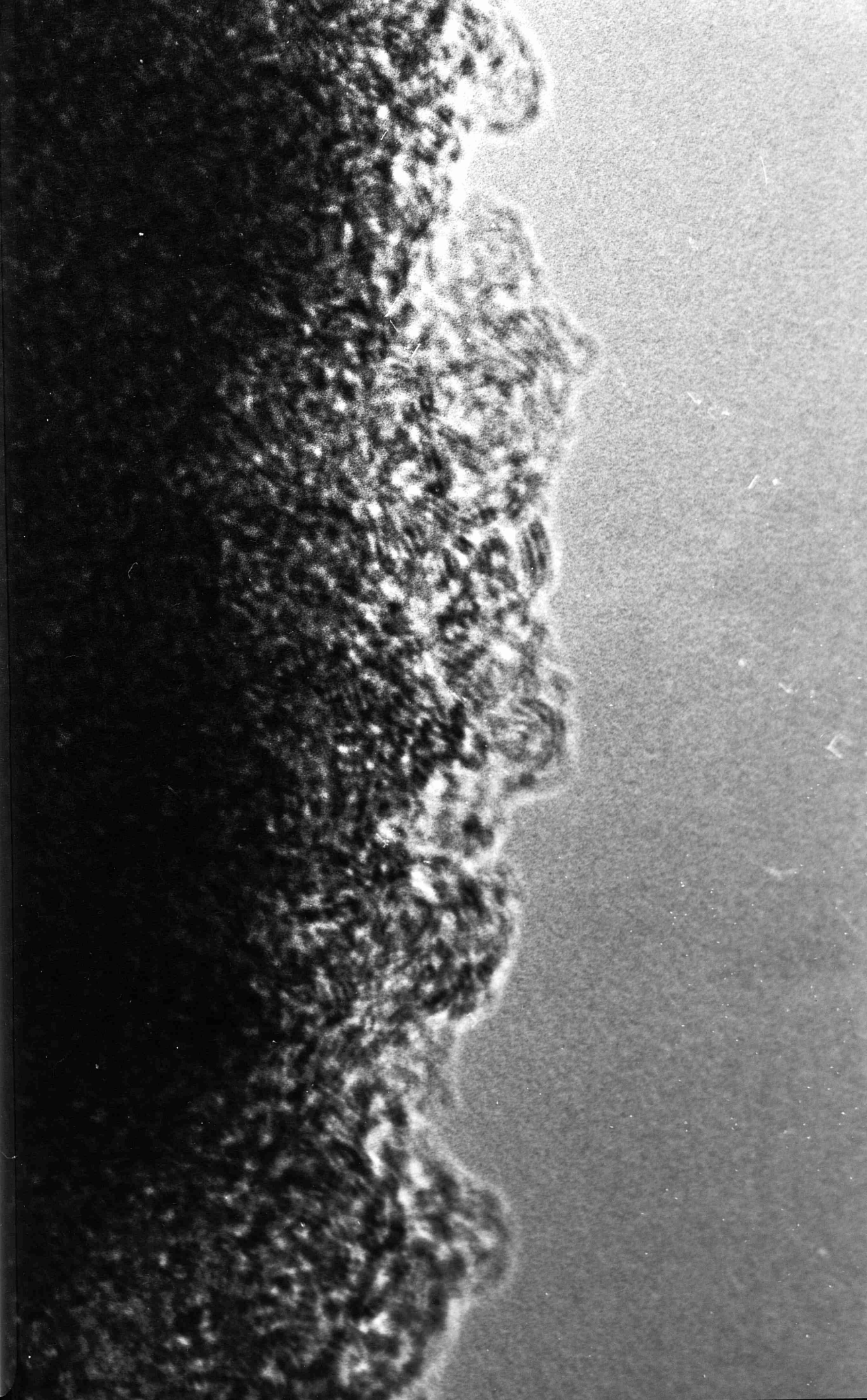


PLATE 69

Expanded Carbon Structure Observed in Feed Cokes Reacted
Below Carbonisation Temperature.

Magnification = X 4443600



PLATE 70

SEM of Reacted Ex-tuyere Cokes.

Magnification = X 1408

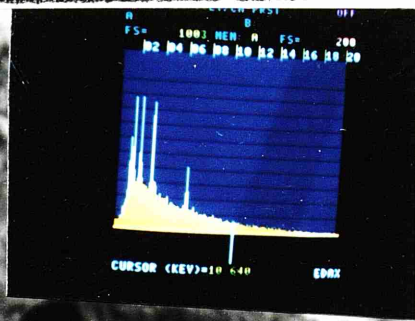
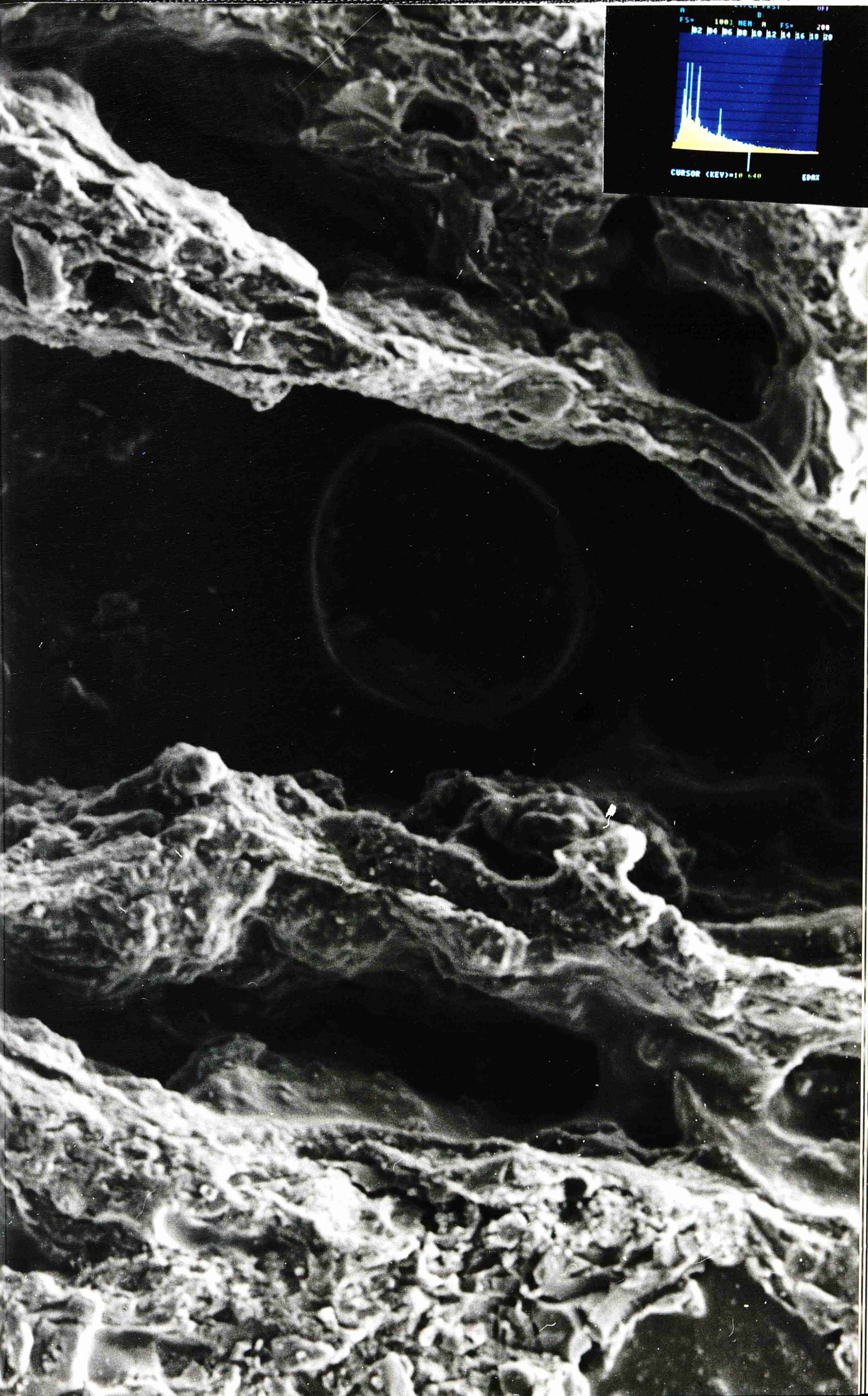


PLATE 71

SEM of Reacted Ex-tuyere Coke.

Magnification = X 768

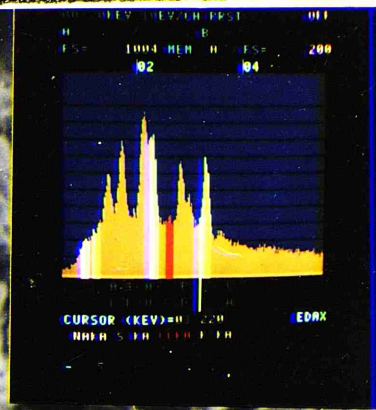
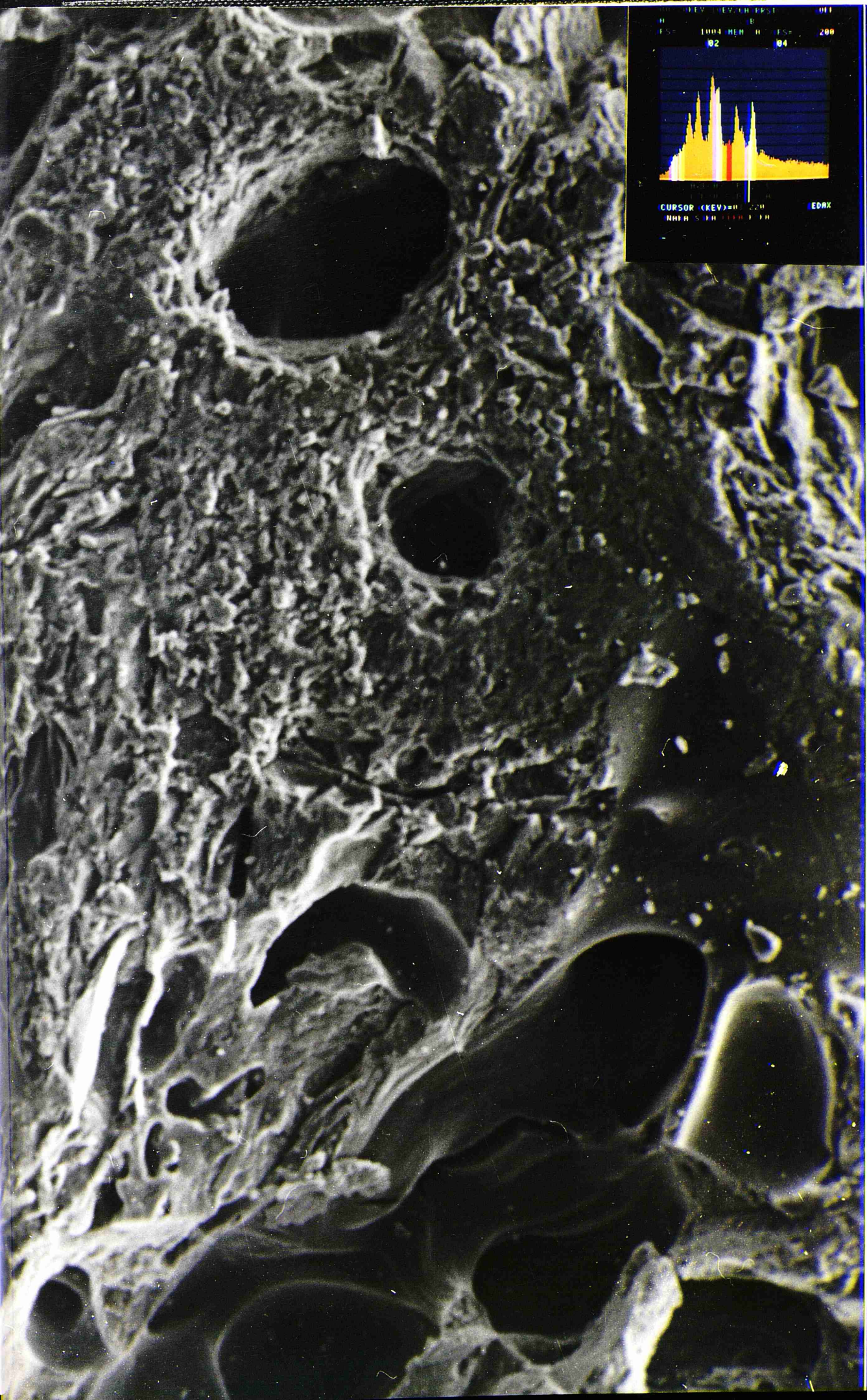


PLATE 72

SEM of Reacted Ex-tuyere Coke.

Magnification = X 1536

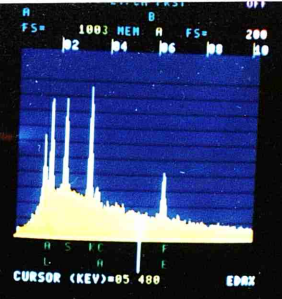
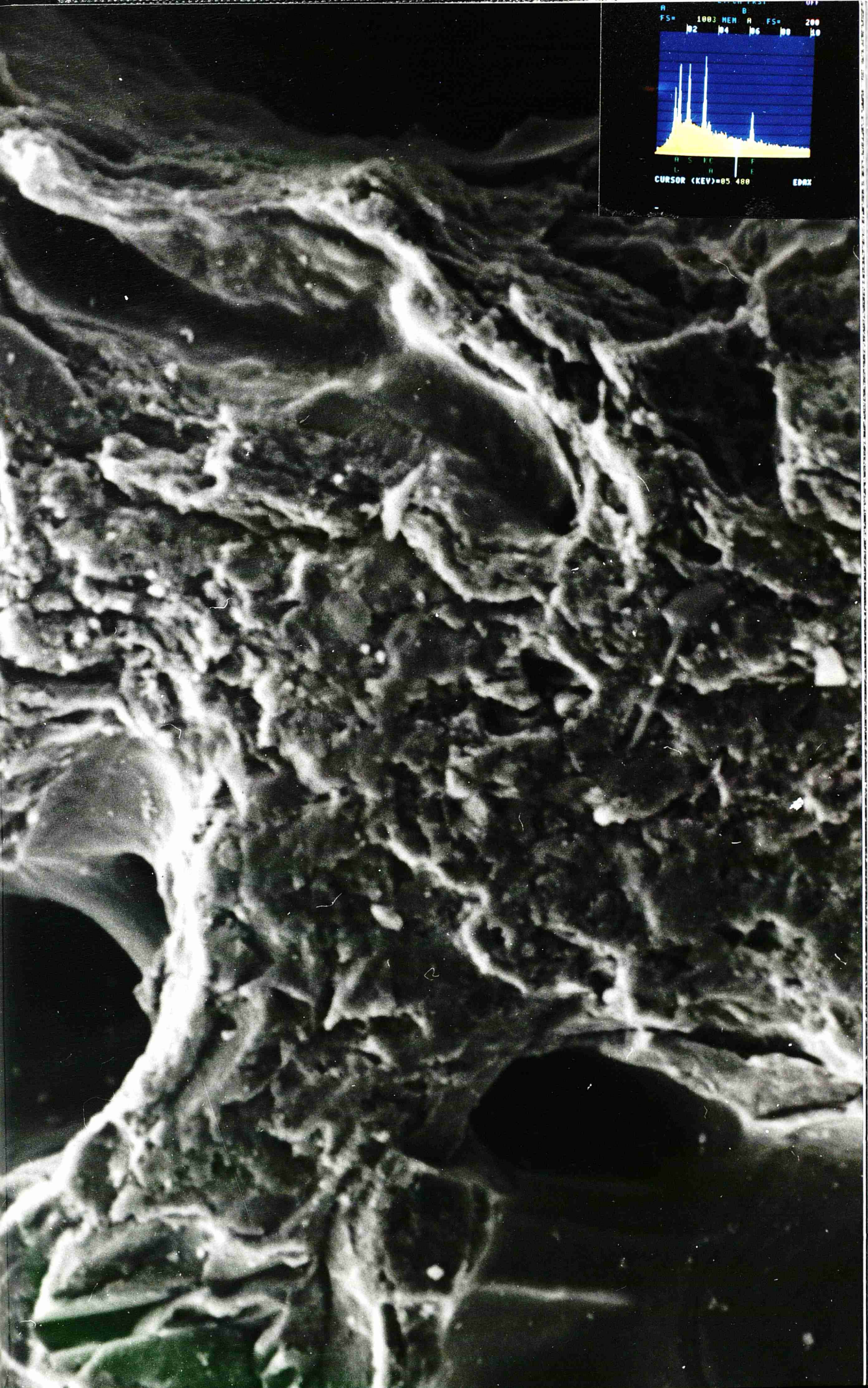


PLATE 73

HREM of Reacted Ex-tuyere Coke.

Magnification = X 3200000



PLATE 74

HREM of Reacted Ex-tuyere Coke Showing Extensive Ordering
of Carbon Structure

Magnification = X 3090000



PLATE 75

HREM of Reacted Ex-tuyere Coke Showing Expanded Carbon
Structure.

Magnification = X 2130000



PLATE 76

BEI of Feed Coke

Magnification = X 2000

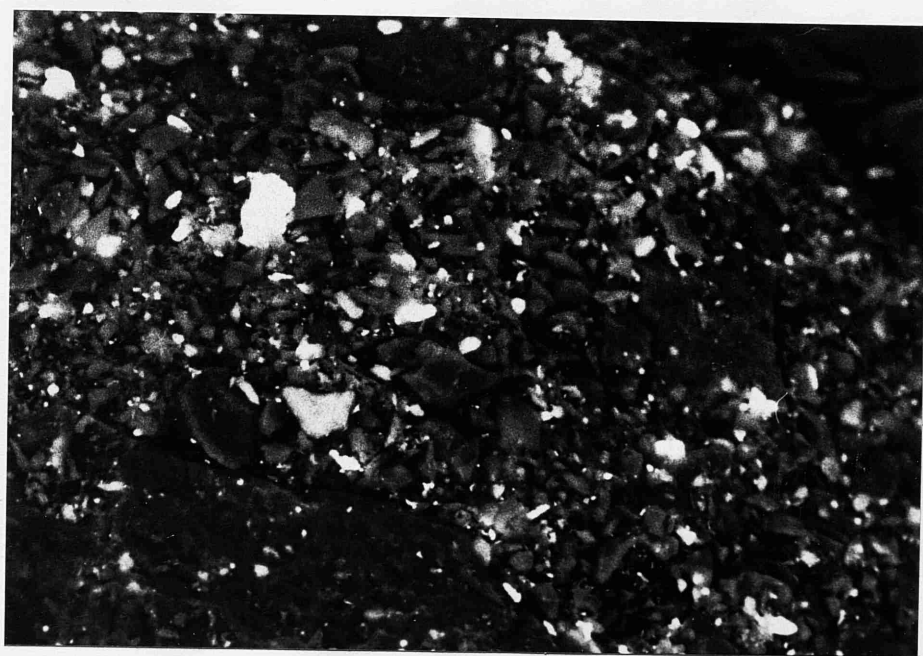


PLATE 77

BEI of Ex-tuyere Coke

Magnification = X 2000



GLASGOW
UNIVERSITY
LIBRARY: